# BERICHTE

## aus dem Fachbereich Geowissenschaften der Universität Bremen

No. 129

Pätzold, J., S. Becker, K. Fabian, T. Frederichs, J. Funk, P. Hebbeln, R. Höppner, B. Jahn, J. Jungclaus, B. Kottke, H. Kuhlmann, B. Laser, R. Link, T. Lützeler, A. Meyer, C. Moos, S. Niebler, S. Rath, C. Rüth, F. Schewe, S. Schulz, A. Vink, T. Westerhold, W. Zenk

# REPORT AND PRELIMINARY RESULTS OF METEOR-CRUISE M 41/3 VITÓRIA - SALVADOR , 18.4. - 15.5.1998

Berichte, Fachbereich Geowissenschaften, Universität Bremen, No. 129, 160 pages, Bremen 1999

ISSN 0931-0800

The "Berichte aus dem Fachbereich Geowissenschaften" are produced at irregular intervals by the Department of Geosciences, Bremen University.

They serve for the publication of experimental works, Ph.D.-theses and scientific contributions made by members of the department.

Reports can be ordered from:

Gisela Boelen

Sonderforschungsbereich 261

Universität Bremen

Postfach 330 440

**D 28334 BREMEN**

Phone: (49) 421 218-4124

Fax: (49) 421 218-3116

e-mail: eggerich@uni-bremen.de

Citation:

Pätzold, J. and cruise participants

Report and preliminary results of METEOR-Cruise M 41/3, Vitória – Salvador, 18.4. - 15.5.1998.

Berichte, Fachbereich Geowissenschaften, Universität Bremen, No. 129, 160 pages, Bremen, 1999.

ISSN 0931-0800

## Content

## 1 Participants

| Name | Discipline | Institution |
|---|---|---|
| Pätzold, Jürgen, Dr. (Chief Scientist) | Marine Geology | GeoB |
| Bassek, Dieter, Technician | Meteorolgy | DWD |
| Becker, Sylvia, Dipl.-Oceanogr. | Oceanography | IfMK |
| Fabian, Karl, Dr. | Geophysics | GeoB |
| Frederichs, Thomas, Dr. | Geophysics | GeoB |
| Funk, Jens, Dipl.-Geophys. | Geophysics | GeoB |
| Hebbeln, Peter, cand. geol. | Tracer-Oceanography | IUP |
| Höppner, René, Dipl.-Geol. | Sedimentology | GeoB |
| Jahn, Britta, Dipl.-Geol. | Marine Geology | GeoB |
| Jungclaus, Johann, Dr. | Oceanography | IfMK |
| Knaack, Christian, Dr. | Meteorology | DWD |
| Kottke, Bernd, Cand. Geol. | Sedimentology | GeoB |
| Kuhlmann, Holger, Cand. Geol. | Marine Geology | GeoB |
| Laser, Bernd, Dipl.-Geophys. | Geophysics | GeoB |
| Link, Rudolf, Technician | Oceanography | IfMK |
| Lützeler, Thurid, Cand Geol. | Marine Geology | GeoB |
| Meyer, Anja, Technician | Paleobiology | GeoB |
| Moos, Christopher, Dipl.-Geol. | Marine Geology | GeoB |
| Niebler, Stefan, Dr. | Marine Geology | GeoB |
| Rath, Stefanie, Dipl.-Geol. | Sedimentology | GeoB |
| Rüth, Christine, Dipl.-Phys. | Tracer-Oceanography | IUP |
| Schewe, Felix, Technician | Marine Geology | GeoB |
| Schulz, Sigrid, Cand. Geol. | Paleobiology | GeoB |
| Vink, Annemiek, Dipl.-Geol. | Paleobiology | GeoB |
| Westerhold, Thomas, Cand. Geol. | Marine Geology | GeoB |
| Zenk, Walter, Dr. | Oceanography | IfMK |

| | |
|---|---|
| DWD | Deutscher Wetterdienst, Geschäftsfeld Seeschiffahrt<br>Bordwetterwarte FS Meteor<br>Bernhard Nocht-Straße 76, D 20359 Hamburg |
| IfMK | Institut für Meereskunde an der Universität Kiel<br>Abteilung Meeresphysik, Düsternbrooker Weg 20<br>D 24105 Kiel |
| IUP | Fachbereich 1 - Physik, Institut für Umweltphysik<br>Abteilung Tracer-Ozeanographie<br>Universität Bremen, Kufsteiner Strasse<br>D 28359 Bremen |
| GeoB | Fachbereich 5 - Geowissenschaften<br>Universität Bremen, Klagenfurter Strasse<br>D 28359 Bremen |

## 2 Research Program

*Physical Oceanography*

The bottom water flow in the South Atlantic across the Rio Grande Rise is part of the global circulation (conveyor belt) together with Intermediate and North Atlantic Deep Water transports. The Vema Channel represents the deepest conduit of the Rio Grande Rise. Accordingly, Antarctic Bottom Water flows on its northward path across the Vema Sill (depth 4660 m). Estimates based on earlier RV METEOR cruises with moored current meters as part of the World Ocean Circulation Experiment (WOCE) have demonstrated that about half of the export from the Argentine into the Brazil Basin is achieved through the deep Vema Channel. According to these long-term observations the equatorward transport amounts to 6.4 ± 3.0 Mio $m^3s^{-1}$.

In addition WOCE observations have shown a tendency towards increased bottom water temperatures. In fact, a systematic temperature increase of 30 mK was observed in the Vema Channel near the sill between January 1991 and December 1992. Comparable changes have never been observed in the Vema Channel since the availability of the first highly accurate CTD records in 1972. The trend towards higher temperatures has also been documented in newer WOCE observations by Brazilian and English parties. Nevertheless, according to the latest RV METEOR observations in the spring of 1996 the upward trend appears to have stopped.

During RV METEOR leg M 41/3 the oceanographic working group aimed at two related subjects: The long-term (> 1 year) recording of temporal variability of bottom water properties with great accuracy and the mapping of their significant spatial differences due to the bottom topography in the southern Brazil Basin.

The deployment of a near-bottom mooring in the Vema Channel was performed during the cruise. It has been equipped with a precision temperature and salinity recorder for the core of Antarctic Bottom Water (AABW). Furthermore, two thermistor chains and two current meters were added to observe the vertical temperature stratification and current shear below 3000 m depth. Supplementary hydrographic observations with CTD and rosette sampler were conducted. They will help to further reveal the structure of the import channels for the bottom water. Water samples were jointly used by the tracer group on board.

*Tracer-Oceanography*

The tracers CFCs, helium-isotopes, and tritium are of anthropogenic origin and provide together with the classical hydrographic parameters additional information for water mass analysis. They are particularly important for the determination of water mass transports and mixing processes making use of their well-known time-dependent input history at the ocean surface. After the zonal sections on 19°S (1991) and 30°S (1993) which were examined during WOCE (World Ocean Circulation Experiment) additional sampling for tritium, helium and CFCs were planned. Sampling for bottom water in the region of the Vema Channel was of particular interest and thereafter small sections in the region of the Mid-Atlantic Ridge at 24°S (zonal) and meridional at about 9°W up to 19°S. Special focus was placed on the pathways of the North Atlantic Deep Water (NADW) over the Mid-Atlantic Ridge and in the Angola Basin, the deep boundary current which has been observed earlier.

*Marine Geology / Sedimentology*

The geological program of the cruise aimed to continue and extend previous investigations on pelagic sediments in the region of the Mid-Atlantic Ridge by the long-term research project SFB 261 which aims at the reconstruction of the mass budget and current systems of the South Atlantic during the Late Quaternary. Earlier studies across the Mid-Atlantic Ridge were carried out further north and south during RV METEOR cruises M 16/1 and M 34/4. For the reconstruction of variations in surface, deep and bottom water circulation in the central South Atlantic a geological survey was scheduled along two transects at about 24°S and 19°S across the Mid-Atlantic Ridge. Sediment surface samples had to be recovered with a multicorer and a large box corer, longer sediment cores were planned with a gravity corer mainly from water depths between 2500 and 4200 m. The sampling of these two profiles located within the central gyre of the South Atlantic were performed to enlarge the data set for mapping paleoceanographic changes in the circulation patterns within the South Atlantic and contribute to the reconstruction of the biological productivity in this oligotrophic area.

The focus of sedimentological research interest during RV METEOR cruise M 41/3 concentrated on sampling the near surface sediments from the southeastern Brazil Basin and along two zonal sediment core transects over the Mid-Atlantic Ridge. Investigations of grain size spectra performed on surface sediments and Late Quaternary deposits from the northern Vema Channel and the adjacent southern Brazil Basin reveal important information for the reconstruction of the flow of Antarctic Bottom Water (AABW) and the North Atlantic Deep Water (NADW). Grain size studies of surface sediments correlate to current conditions, transport mechanics and accumulation patterns hence documenting the recent hydrography in the ocean.

*Paleobiology*

Oceanic surface sediments were sampled using the multicorer and large box corer in as many different locations as possible, to obtain information on the recent and sub-recent distribution of organic walled and calcareous dinoflagellate cysts. These distributions are of great importance as they substantially improve interpretation possibilities of changing dinoflagellate cyst assemblages through glacial and interglacial periods and can provide more insight into the changing current systems of the South Atlantic during the Late Quaternary. In addition, plankton was extracted from the upper water column by filtration. For these purposes, water samples were collected with the rosette at various depths within the photic zone and by the daily sampling of surface waters using the ship's membrane pump. The aim of this was to isolate living dinoflagellates for culture studies, with emphasis on those dinoflagellates producing calcareous cysts which are not yet in culture at the University of Bremen. The remaining plankton material was conserved for later, more detailed investigations.

*Geophysics*

The sediment cores from the central South Atlantic were expected to provide useful magnetic data sets about glacial and interglacial fluctuations to document the particular variations in eolian influx. The chronostratigraphic core network SUSAS based on orbitally tuned high-resolution records of magnetic susceptibility presently covers latitudes from 40° to 30°S. It will be extended into the adjacent northern region permitting continuous time slice analysis of depositional processes within the entire subtropical South Atlantic.

During the entire cruise the shipboard echosounder systems HYDROSWEEP and PARASOUND were continuously operated to record the bathymetry of the ocean floor and shallow sediment structures. In accordance with past experience, the geological sampling sites were selected very efficiently based on these surveys. In particular, the coring profiles across the Mid-Atlantic Ridge at about 24°S and 19°S are situated in a region of exceptionally rough morphology and therefore required thorough acoustic pre-site profiling. Special interest was placed on recording the sediment structures in the central Vema Channel and in its northern vicinity in the southern Brazil Basin. Multiple frequency tests at all coring stations are a prerequisite for a detailed correlation of PARASOUND records with on board physical property logs.

## 3 Narrative of the Cruise

After three days in port, RV METEOR left Vitória (Brazil) on Saturday, April 18, 1998 at 08:15 p.m. local time beginning the third leg of M 44. The scientific shipboard party included 17 colleagues from the Geoscience Department of Bremen University, two from the Institute of Environmental Physics of Bremen University, four from the Institut für Meereskunde Universität Kiel, and two meteorologists from the Deutscher Wetterdienst in Hamburg. The scientific program of the cruise included oceanographical, tracer-oceanographical, marine geological, and geophysical studies in the central area of the South Atlantic.

The vessel sailed southward towards the first working area in the Vema Channel. On Monday morning, April 20, the scientific program began with profiling measurements of HYDROSWEEP and PARASOUND, water pumping for plankton and thermosalinograph recordings at 27°33′S/40°40′W. On the same day we performed a test station with a CTD/rosette and another rosette system at a deep station of about 4390 m in a gap in the eastern Santos Plateau.

On April 21, we successfully deployed a near bottom mooring in the central Vema Channel. It was equipped with a precision temperature and salinity recorder for the core of the Antarctic Bottom Water (AABW). Furthermore, two thermistor chains and two current meters were added to observe the vertical temperature stratification and current shear below 3800 m depth. Four CTD/rosette stations and another shallow rosette cast for plankton across the Vema Channel supplemented the hydrographic surveys in this southernmost working area of the cruise. We then steamed northwestward to the northern extension of the Vema Channel into the southern Brazil Basin. Here, a second hydrographic profile with different CTD/rosette stations and the first sediment stations with multicorer, box corer and gravity corer were performed. A 9.6 m long sediment core at the end of the profile was retrieved to study the sedimentological history of bottom flow conditions in the southern Brazil Basin during the Late Quaternary.

We left this area in the early morning of April 25 and sailed 3.5 days eastward towards a profile crossing the Mid-Atlantic Ridge (MAR) from the Brazil Basin to the Angola Basin at about 24°S between 20°W and 9°W. From April 28 to May 3 we carried out nine hydrographic casts with CTD/rosette and searched for suitable sediment stations on the flanks of the Mid-Atlantic Ridge. Sediment sampling on the flanks of the Mid Atlantic Ridge required detailed geophysical surveys by HYDROSWEEP and PARASOUND. However, local sediment basins on the slopes of the basaltic MAR revealed suitable coring sites. We successfully covered six sediment stations with multicorer, box corer and gravity corer at 19°S with four stations located in the Brazil Basin and two in the Angola Basin.

On May 3 and 4 we continued research with a hydrographic section on a S-N directed profile at 9°W with three CTD/rosette casts. At most hydrographic stations of the cruise, water samples were collected for the tracers tritium, helium and CFC's in addition to the classical hydrographic measurements for water mass analysis. A total of 240 helium- 144 tritium- and 400 CFC-samples were drawn from standard Niskin bottles. At 21 stations, water samples from the whole water column were also taken for analysis of stable carbon and oxygen isotopes and nutrients. The main interests of this research were to sample the flow of Antarctic Bottom Water through the Vema Channel into the Brazil Basin and the pathways of North Atlantic Deep Water (NADW) across the Mid Atlantic Ridge (MAR) into the Angola Basin. The L-shaped section across the MAR at 24°S and along its eastern flank at 9°W intersects the WOCE A9 cruise at both ends and thus closes a box within which NADW presumably crosses the MAR.

On May 4, we started a second profile across the Mid-Atlantic Ridge at about 19°S beginning in the Angola Basin and leading back to the Brazil Basin. This last profile of the cruise concentrated on geoscientific studies. Along this northern transect across the Mid-Atlantic Ridge we covered six sedimentological stations in the Angola Basin and six in the Brazil Basin. The last sediment station was carried out in the night from May 9 to 10, at 19°05'S/17°09'W. During the whole cruise in total 21 sediment sampling stations were covered including 21 multicorer, two box corer and 22 gravity corer deployments. Recoveries of sediment cores ranged between 0.3 and 9.6 m. Initial results indicate that the up to 5.6 m long sediment cores from the Mid-Atlantic Ridge in water depths between 2550 and 3950 m were collected with very little disturbance of the recovered material. Core descriptions and initial stratigraphic analyses reveal continuous sediment records in many areas of the Mid-Atlantic Ridge with sedimentation rates ranging between 0.5 and 1.0 cm/1000 years.

Surface water pumping during the cruise was carried out for chlorophyll samples and the collection of dinoflagellates, coccolithophorids and foraminifera. In addition, at seven stations, coccolithophorid and dinoflagellate samples were taken from Niskin bottles from up to six depth horizons down to 200 m. The samples are important to study the distribution of the different groups of planktic organisms and will be used for calibration of the paleorecords from sediment cores. Geophysical surveys with the shipboard echosounder PARASOUND and the multibeam echosounder HYDROSWEEP were continuously carried out during the cruise to record and study high resolution bathymetric and sediment echosounding profiles.

The completion of water sampling and all profiling measurements concluded the scientific work of the cruise on May 14, 06:00 p.m. at 14°16′S/34°30′W before entering the 200 n.m. economic zone of Brazil. RV METEOR sailed west towards Salvador, where the third leg of cruise M 44 ended safely on the morning of May 15, 1998.

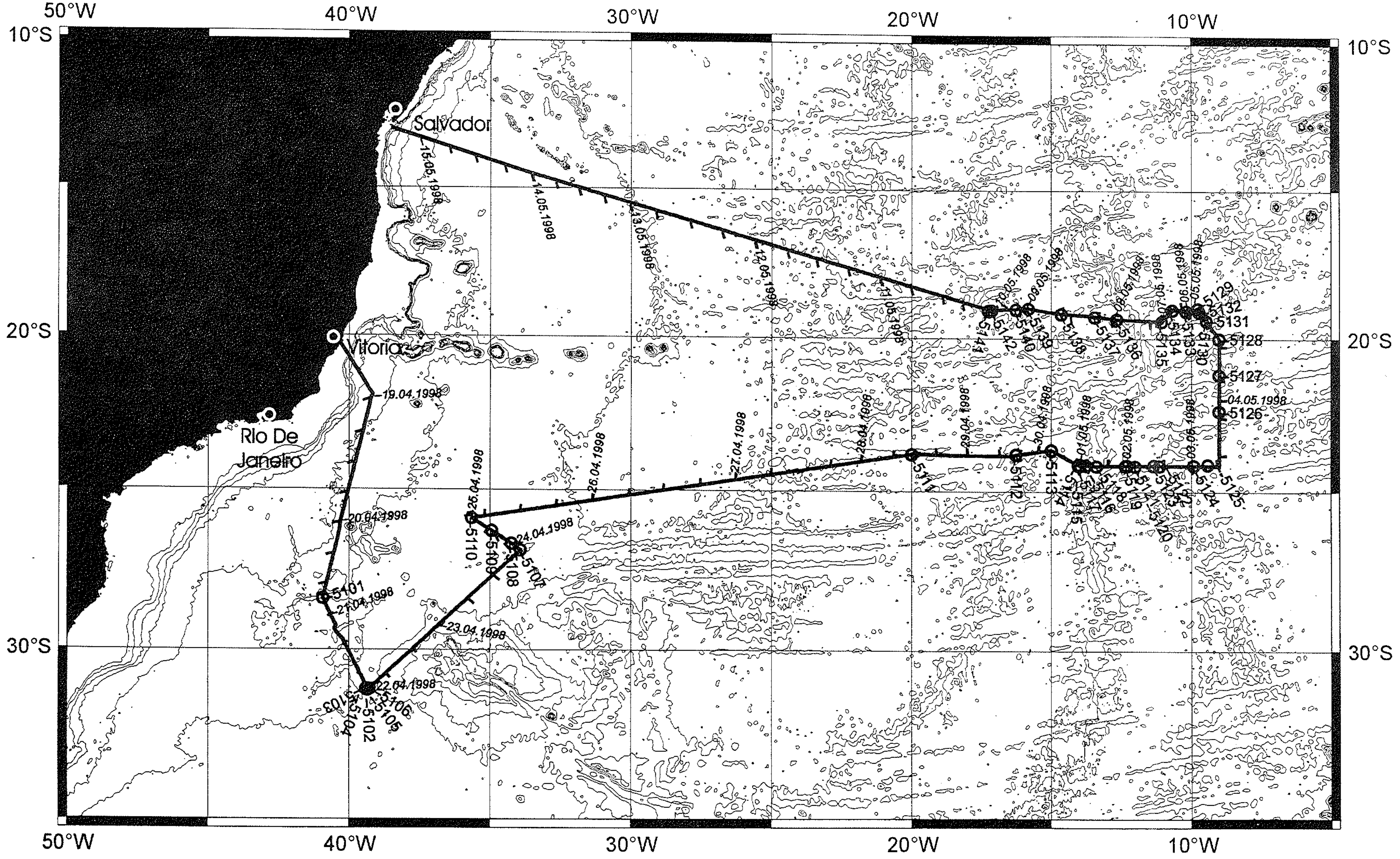


Fig. 1 RV METEOR Cruise M 41/3. Track annotation interval is 6 hours, dates are set at 0 hours. Sampling locations (GeoB) are indicated

# 4 Preliminary Results

## 4.1 Physical Oceanography

(W. Zenk, S. Becker, J. Jungclaus, R. Link)

*Introduction*

The World Ocean Circulation Experiment (WOCE) will terminate its observational phase by the end of 1998. This unique oceanographic campaign compassed planning, implementation and coordination of a global network of hydrographic observations and now aims at extensive modeling studies during its analysis, interpretation and synthesis phase in the years to come. The hydrographic work during M 41/3 was part of the Deep Basin Experiment (Hogg et al. 1996), a subprogram in Core Project 3 of WOCE. Furthermore, the physical oceanography group on board assisted in collecting water samples for other parties on the METEOR, including supplements to the WOCE Hydrographic Program (WHP) tracer network.

The equatorward flow of Antarctic Bottom Water (AABW) in the South Atlantic is part of the global thermohaline circulation, together with fluxes of Antarctic Intermediate Water (AAIW) and North Atlantic Deep Water (NADW). The Rio Grande Rise at a nominal latitude of 30°S represents a natural barrier for the spreading of Antarctic Bottom Water between the Argentine and the Brazil Basin. It is intersected by two deep channels: The Vema Channel (originally called Rio Grande Gap) and the Hunter Channel (Zenk et al. 1993; Zenk et al. 1998). Estimates based on geostrophy and results from moored current meters have demonstrated that more than half of the bottom water export between the two neighbouring basins is achieved through the deep Vema Channel (Speer and Zenk 1993; Hogg et al. 1998). According to these long-term observations the total northward transport of Antarctic Bottom Water amounts to $6.9 \times 10^6\ m^3s^{-1}$. The contribution of the Hunter Channel ($2.3 \times 10^6\ m^3s^{-1}$) is not insignificant (Zenk et al. 1998) but was beyond the scope of this cruise.

At a number of locations, WOCE observations demonstrated a tendency towards increasing bottom water temperatures. In fact, a systematic temperature increase of 30 mK was observed by the METEOR in the Vema Channel near the sill between January 1991 and December 1992. Comparable changes of bottom water properties had never before been observed in the Vema Channel since the availability of the first highly accurate CTD records in 1972. The trend towards higher bottom water temperatures has also been documented in comparable, yet unpublished WOCE observations by Brazilian and English groups. According to the latest visit in the spring of 1996 the upward trend appeared to have stopped, however we had to revise this view at the end of our cruise.

During M 41/3 the physical oceanography group aimed at a new survey of the bottom water properties and distribution by (i) starting a long-term record of the variability of water mass characteristics at the sill of the Vema Channel with moored instruments and (ii) enlarging the set of highly accurate hydrographic data during cruises. The latter is also expected to serve as an improved input for modeling efforts. Monitoring of bottom water properties will provide more insight into its fluctuations which for a long time have been assumed to be negligible.

*Methods, data acquisition and reduction*

A number of observational tools were applied during the cruise. The backbone for hydrographic observations was a CTD (conductivity, temperature, depth (pressure)) recorder in combination with a rosette sampler carrying 21 bottles. An inventory of all CTD stations is given in Table 1. Locations of CTD stations are displayed in Figs. 1 and 2. The bottle set was used on 25 stations yielding over 500 water samples. Because of the application of a lowered Acoustic Doppler Profiler (lADCP), to be described later, no mechanical bottom finder was used. Instead, bottom approaches were monitored by a pinger.

Our CTD system (Neil Brown MKIIIB, IfM no. NB3) was provided by the IfM based *Zentral-labor für Meßtechnik*, a German WOCE unit maintaining high quality instruments as well as their reliable calibration. The CTD probe was last calibrated in temperature immediately prior to cruise M 41/3 on 11/12 March 1998. A post-cruise calibration was performed in summer 1998.

We made every effort to calibrate all CTD stations while still on board. 42 salinity twin samples, a subtotal of all the rosette samples, were analyzed by an Autosal salinometer (IfM no AS6). For standardizing we used batch No P129. The resulting 21 pairs of check values were systematically taken from the deepest part of the profiles, i.e. about 25 m above the ground (near-bottom, NB), and from the mixed layer (ML) at the 10 m level. The inter-twin standard deviations of salinity amount to $\pm\{0.0009, 0.0019, 0.0015\}$ for {NB, ML, all} levels. Comparable sampling noise during the CTD data acquisition at constant depth while firing bottles is of a similar order $\pm\{0.0007, 0.0027, 0.0017\}$. Quasi-time series of salinity corrections are shown in Fig. 4. Mean salinity corrections for {NB, ML, all} levels ({+1.8,

+9.3, +5.5} × $10^{-3}$) are included. No systematic calibration drift could be recognized. Fig. 5 contains corrections as a function of salinity readings. Here, we found a dependence on salinity (conductivity) which needs to be considered in the final calibration. Assuming all ML values taken at the surface, all NB values sampled at 4000 dbar and salinity decreasing linearly with pressure $P_{CTD}$ we can infer a crude preliminary correction for raw salinities $S_{CTD}$:

$$S_{corrected} = S_{CTD} + (B \times P_{CTD} + A) \qquad (1)$$

with $B = -1.85 \times 10^{-6}$ dbar$^{-1}$ and $A = 9.2 \times 10^{-3}$. In the following text and figures no salinity correction is applied. Since corrections are relatively tiny, they would not be recognizable in the majority of the salinity graphs shown in this document. Final salinity values are subject to a more careful post-cruise CTD calibration.

Lists of all CTD casts with observed *in situ* temperatures, potential temperatures and salinities at standard depth/pressure values are given in Chapter 8.2. Here, preliminary salinity corrections according to (1) have been taken into account.

The latest version of the processing and data reduction software package CTDOK, administered by Thomas Müller of IfM, was used on a Personal Computer. The processing includes the following sequential software modules: Inspection and graphic editing by hand, maximum lowering speed check to detect pressure spikes, dynamic pressure correction, despiking by a median argument, monotonizing with respect to pressure, minimum lowering speed check, low pass filter run with 19 weights, pre-cruise fine-tune calibration, static pressure-offset correction, interpolation on 2 dbar steps and storage for plotting and export in MATLAB® binary files (*.mat).

During earlier WOCE cruises the same CTD probe was used repeatedly in the Vema Channel and for WHP section work. According to our earlier experiences and after the application of all corrections and the post-cruise calibration, an absolute accuracy of better than ±2 mK in temperature, ±0.003 practical salinity units (PSU), and ±3 dbar in pressure can be expected.

The refurbished on-track observational system *DVS* of the METEOR was used to collect quasi-continuous near-surface temperature from two sensors of the ship's meteorological station. It was found that the portside thermometer reading lies systematically {0.149 ± 0.050} K below the starboard thermometer of the ship (Fig. 6). Both sensors are mounted 4 m below the surface. An *ad-hoc* comparison with CTD data from the surface (according to Table 1) indicates the portside *DVS* temperature to be systematically lower by ~ 0.3 K (see Fig. 12b).

Between 21 April and 5 May we collected 34 twin water samples for a calibration check of the ship's thermosalinograph, the data of which are also fed to the *DVS* system. From the resulting 17 salinity check values we inferred a calibration equation that is valid for April / May 1998:

$$S_{corrected} = D \times S_{ThermosalinographDisplay} + C \qquad (2)$$

with D = 1.0054 and C = -0.0211. Four samples of these were collected on passage. Although the latter are supposed to be of slightly lower quality, all samples were treated equally by the indicated least square linear fit (Fig. 7).

Preliminary depth profiles for sections were exported from the *DVS* data bank as well. Due to varying numbers of outliers, depth values were clipped by plausible extrema and subsequently low pass filtered.

Until Sta. 229, the CTD/rosette sampler was supplemented by a *lowered* broad-band Acoustic Doppler Current Profiler (BB lADCP) which was kindly provided by Jürgen Fischer from IfM Kiel. We expect the obtained vertical current profiles to deliver valuable information on shear as an indicator for enhanced mixing in the benthic boundary layer of the Vema Channel and its northward extension. Due to a technical problem, the last lADCP station (no 229) failed to deliver currents. After successful repair, the instrument was not remounted on the rosette sampler. The lADCP log is given in Table 4.

In addition to the well known problem of the near bottom interference layer, our lADCP measurements suffered from a lack of scattering particles in the intermediate depth ranges of this 'blue water' environment. The dramatic decrease of the received signal amplitude can be seen in the vertical profile of target strength (Fig. 8a, profile 212) below 1000 m. However, the signal strength recovers over the deepest 600 m of the profile, apparently owing to an increase of sediment particle concentration on the Vema Sill.

Fig. 8b depicts the raw vertical velocity component (bin 3) over the total duration of the cast. The lowering speeds of 1 $ms^{-1}$ during downtrace and 1.2 $ms^{-1}$ during uptrace are generally recovered. However, there is a large data gap between, say, ensemble 700 and 1100 (the bottom-nearest point was approached around ensemble 1300). During uptrace a similar behaviour is observed and there are additional periods of near-zero vertical velocities during water sampling stops. These data gaps are also visible in the raw data northward velocity component (Fig. 8c). Near the bottom (around ensemble 1300) the (earth) velocities are predominantly northwards as expected in the deep trough of the Vema Channel.

The standard procedure to derive relative velocities is to differentiate individual lADCP profiles vertically, then to average overlapping profiles in depth cells and integrate the resulting mean shear profile from a reference level (Fischer and Visbeck 1993).

The lADCP is a self-contained instrument without pressure sensor. Its depth is determined by integrating the measured vertical velocity in time. The large data gaps prevented us from calculating reference velocities from time integrals of the baroclinic velocities by our software package so that the data require additional post-cruise processing. (The set of processing programs had been kindly provided by J. Fischer.)

Relative northward velocities (referenced to the deepest point at 4362 m) are displayed for the deep part of the profile in Fig. 8d (downtrace), and 8e (uptrace). Northward velocities show maximum values between 100 to 200 m above the bottom. They are consistent with earlier findings from moored current meters in the Vema Channel and from numerical modeling. This nose-shaped velocity profile with pronounced shear layers above and below the maximum is typical for bottom boundary currents (Mercier and Speer 1997; Zenk et al. 1998).

The *vessel mounted* Acoustic Doppler Current Profiler (VM ADCP) operated routinely. It covered approximately the upper 250 m layer. Unfortunately its data flow is still not yet integrated by the ship's own *DVS* data bank.

For topographic surveys we used the multi-beam echosounder HYDROSWEEP® of the METEOR. In the subsequent data processing we were kindly supported by the ship's system operator V. Gebhardt. Of special interest were details of the topography of the Vema Sill where IfM mooring V389 was deployed (see Table 2, Fig. 9). This area had already been surveyed with HYDROSWEEP in 1991 during METEOR cruise 15. Fig. 10 shows blow-ups on identical scales of both independent observations from the eastern side of the Vema Sill. They were obtained with the same hardware but with significantly different HYDROMAP® software versions. As expected, both maps agree excellently in regions with steep topography. In fact, the slope of the eastern wall (as depicted) can exceed 25 %. Less agreement in the details can be found on the ground plateau with its minimal slopes. Inaccuracies in depth estimates can shift isobaths horizontally by a few kilometers.

At the beginning of the cruise, on Sta. 209 we deployed a current meter mooring (IfM no V389) on the sill of the Vema Channel. Logistical and operational details are given in Fig. 9 and Table 2. The current meter rig is designed for a two-year record of temperature and speed fluctuations. The moored CTD recorder (MicroCat® by Sea Bird, Inc.) has a sampling capacity of over three years. A major goal of the physical oceanography group on board was to start a long-term record of temperature variability of Antarctic Bottom Water with great accuracy.

*Hydrographic conditions in the central South Atlantic*

Here we discuss the water mass stratification on two orthogonal sections at 9°W and 24°S. We assume that the hydrographic stations selected are representative for the central subtropical South Atlantic. The sections (see Fig. 2) are short in comparison with the WHP network (Siedler et al. 1996). Related WOCE sections A9 and A14 are located on 19°S and 9°W. They were occupied in 1991 and 1995 by METEOR (M 15) (Siedler and Zenk 1992) and the French research vessel L'ATALANTE.

For the general descriptions of distinctive water masses we depict their characteristic potential temperature salinity ($\theta$/S) properties in Fig. 11. For this purpose we have plotted all interpolated ($\Delta p$ = 2 dbar) CTD data from the two sections in one diagram.

Tropical surface water (TW) with $\theta$ >20°C at the top of Fig. 11 shows a tendency to split. Colder, more fresher water was encountered on and to the East of the Middle Atlantic Ridge in the Angola Basin. Its counterpart with warmer and saltier surface conditions in the Brazil Basin can be better recognized in Fig. 12. This figure shows the near-surface T/S record from the thermosalinograph ($\Delta t$ = 10 min) on four sections. The higher variability in T/S in the western (Fig. 12b) and the southern (Fig. 12a) regions reflects a number of fronts, more frequently encountered in the open Brazil Basin than in the Angola Basin (Fig. 12b). The frontal structure of surface parameters appears to be caused by the Brazil Current Front (BCF) as part of the inner recirculation in the Brazil Basin.

The colder surface waters (< 25°C) on 9°W and on its cross point with the 24°S section can be interpreted as a signal of the far reaching Benguela Current southwest of the Benguela Angola Front (Fig. 13). Densities, i.e. $\sigma_t$ values, at the surface of the central South Atlantic of {(24.3 - 24.5), (24.7 - 24.9)} kgm$^{-3}$ are typical ranges for the {Brazil, Angola} Current regime in May 1998. Here we note that two subtropical surface water types are separated by a line west of the Middle Atlantic Ridge. The crest region itself has the same T/S properties as the eastern side of the Ridge.

We return to the CTD derived θ/S diagram in Fig. 11. At temperatures between approximately 10° and 16°C we find a tight θ/S relation which in our case is characteristic for South Atlantic Central Water (SACW) of the main thermocline. Farther down in the water column it is replaced by Antarctic Intermediate Water (AAIW) with its salinity low at < 34.5 (Boebel et al. 1997). The next salinity extremum (> 34.86) belongs to the North Atlantic Deep Water (NADW) (Zangenberg and Siedler, 1998). After crossing the equator it erodes Circumpolar Deep Water (CDW), splitting this lower saline water mass into an upper CDW and a lower CDW type (Reid et al. 1977). Towards the West of our 24°S section, the deepest part of the water column (θ < 2.0°C) is occupied by the Antarctic Bottom Water (AABW) (Speer and Zenk 1993). Its properties will be discussed in more detail in the next paragraph on observations in the Vema Channel.

Our presentation of the water mass structure in the θ/S diagram (Fig. 11) is paralleled by figures of vertical sections of potential temperature (θ) and salinity (S) from the adjunct sections on 9°W and 24°S (Figs. 14, 15). The low saline tongue of Intermediate Water at 750 m remains unchanged at $S_{min}$~34.40 on the zonal section (Fig. 15) while we recognize a well expressed meridional gradient with equatorward increasing salinities on the meridional section (Fig. 14).

The thick tongue of North Atlantic Deep Water (S > 34.90) appears to be blocked by the topography of the Middle Atlantic Ridge (Fig. 15). However, at the northern side of the 9°W section we cut through a salty tongue of Deep Water (S > 34.90) which we interpret as being deflected eastwards across the Ridge into the Angola Basin by the change of its potential vorticity in the presence of the zonal Vitoria Trindade Ridge at 19°S (Zangenberg and Siedler 1998) and being one source of the Namib Col current (Speer et al. 1995).

Farther south we have traversed the deep Rio de Janeiro Fracture Zone at 23.7°S. It allows lower Circumpolar Deep Water with θ ≥ 2.0°C to be exchanged across the Ridge. Its role in the deep circulation of the Angola Basin remains unclear and deserves further efforts. As expected, a distinct near-bottom temperature step in vertical profiles as seen so clearly in the Brazil Basin was found nowhere in the Angola Basin. This observation agrees with the known absence of Antarctic Bottom Water in the Angola Basin (Siedler et al. 1996).

*Flow of Antarctic Bottom Water through the Vema Channel*

The Vema Channel represents the deepest conduit for bottom water of the Rio Grande Rise (Hogg et al. 1982). According to our newest bathymetric survey (Fig. 10b) its depth varies between 4620 and 4640 m. Its northern extension can easily be followed by tracking the 4000 m isobath on the digital topographic map by Smith and Sandwell (1997) displayed in Fig. 16.

We have included positions of the two hydrographic sections: 'Vema Channel' (VC) across the Vema Sill and the section 'Vema Extension' (VE) at the northeastern corner. Both sections are shown on different horizontal scales (section VC in Fig. 17, section VE in Fig. 18). Mooring V389, deployed 21 May 1998 (Fig. 9; Table 2), lies 4 km upstream between CTD Sta. 210 and 211 (Fig. 17). Its projection can be seen in the temperature sections of Fig. 17. Results from the self-recording instruments are not expected before the year 2000.

Water masses found in the Vema Channel (Speer and Zenk 1993) resemble those described in the last paragraph for the central South Atlantic. They are stacked in the well known fashion from the top to the bottom: Tropical surface Water and South Atlantic Central Water of the main thermocline, low saline Antarctic Intermediate Water at 900 m, upper and lower Circumpolar Deep Water penetrated by more saline North Atlantic Deep Water (1500 - 3500 m) and closest to the ground Antarctic Bottom Water with $\theta < 2°C$ including its coldest compound Weddell Sea Deep Water ($\theta < 0.2°C$, see Figs. 17, 18 for pressures larger than 2500 dbar).

Water properties of the Vema Channel and in the Vema Extension below approximately 4100 m can be studied in more detail in the blown-up θ/S diagram of the deepest stations (Stat. no. 212 and 215) in Fig. 19. The form of the vertical profile (Fig. 20) demonstrates the well mixed bottom boundary layer in the channel. Its thickness is of O(140 - 180) m.

Thick bottom boundary layers are a unique feature of narrow oceanic passages with bottom water flow (Hogg et al. 1982; Jungclaus and Vanicek 1998). Frictionally driven secondary circulation drive relatively warm waters down the (here western) channel wall leading to hydrostatic unstable conditions and intense vertical mixing. On the eastern side of the Vema Sill relatively cold water is transported upslope enhancing the stratification there. Thus, the coldest waters are trapped and shielded on the eastern side of the channel (Fig. 17) by both a pronounced thermocline and the channel wall (Fig. 10).

*Summary and concluding remarks*

We summarize our preliminary results as follows:

- Earlier observations (Fig. 21; Zenk and Hogg 1996; Hogg and Zenk 1997) showing increasing bottom temperatures and salinities in the Vema Channel were confirmed. Compared with 1996, the lowest potential temperature in the Vema Sill rose again by 20 mK (Table 3). A pertinent salinity increase of 0.007 was directly observed from salinity samples taken by the rosette sampler closest to the bottom from two METEOR expeditions (M 36 in 1996 and M 41). No change in the density stratification appears to be associated with this change in $\theta$/S properties. However, final salinity calibration of the CTD records remains subject to the post-cruise calibration.
- Between the Vema Sill and the Vema Extension (~ 27°S, 34°W, see Fig. 16) Weddell Sea Bottom Water with $\theta \leq 0.2$°C is guided and isolated from mixing with warmer Lower Circumpolar Deep Water for over 700 km by the cañon-dominated topography. Its temperature rises from $\theta = -0.136$ to -0.098, i.e. by only 38 mK, salinity increases by barely 0.005 practical salinity units (34.670 $\Rightarrow$ 34.675). The question of how far these temperature and salinity increases are caused by turbulent diffusion and/or by advected modulations of the source waters must remain open, since they can both be of the same order.
- Further mixing takes place northeast of the funnel-shaped end of the Vema Extension in the deep Brazil Basin with depths > 4800 m (upper right hand corner in Fig. 16). Some additional 1300 km downstream at Sta. 218 (see Fig. 2), the tongue of Weddell Sea Deep Water, the coldest subtype of Antarctic Bottom Water, has been totally eroded. There we found bottom values of $\theta = 0.440$°C and S = 34.716. Hence, the horizontal bottom temperature and salinity gradients between the exit of the Vema Extension and the inner Brazil Basin increase significantly due to turbulent mixing in the absence of a shielding cañon. They are one order of magnitude larger, {550 mK, 0.04}/1300 km in {$\theta$, S} than in the Vema Channel itself.
- A long-term mooring carrying current meters (Fig. 9; Table 2), thermistor chains and a CTD recorder for the observation of property fluctuations was deployed without any problems.

Table 1 Inventory of CTD stations

| Station No/ Profile No | GeoB No | Date 1998 | Time UTC | Lat °S | Long °W | z(m) Bridge Log | near surface T(°C) | at depth (m) T(°C) | at depth (m) $p_{max}$(dbar) | lADCP y/n | Remarks |
|---|---|---|---|---|---|---|---|---|---|---|---|
| 208 / 01 | 5101-1 | 20/04 | 16:44 | 28 26.25 | 40 54.59 | 4388 | 23.94 | 0.36 | 4421 | y | Test station |
| 210 / 02 | 5103-1 | 21/04 | 17:42 | 31 11.84 | 39 23.86 | 4614 | 21.04 | 0.22 | 4666 | y | Vema Channel |
| 211 / 03 | 5104-1 | 21/04 | 21:59 | 31 12.04 | 39 21.02 | 4574 | 21.15 | 0.22 | 4630 | y | |
| 212 / 04 | 5105-1 | 22/04 | 01:42 | 31 12.02 | 39 18.90 | 4475 | 21.16 | 0.20 | 4510 | y | |
| 213 / 05 | 5106-1 | 22/04 | 05:56 | 31 12.03 | 39 16.02 | 4066 | 21.44 | 1.20 | 4098 | y | |
| 214 / 06 | 5107-1 | 23/04 | 19:16 | 26 53.99 | 33 54.96 | 3798 | 23.59 | 1.60 | 3812 | y | Vema Extension |
| 215 / 07 | 5108-1 | 23/04 | 23:53 | 26 41.97 | 34 14.02 | 4783 | 23.65 | 0.28 | 4862 | y | |
| 216 / 08 | 5109-1 | 24/04 | 07:06 | 26 17.99 | 34 56.16 | 4341 | 24.35 | 0.30 | 4388 | y | |
| 217 / 09 | 5110-1 | 24/04 | 16:45 | 25 53.88 | 35 38.89 | 4215 | 25.03 | 0.41 | 4241 | y | |
| 218 / 10 | 5111-1 | 28/04 | 10:14 | 23 48.81 | 20 00.03 | 5215 | 25.71 | 0.90 | 5284 | y | 24°S |
| 219 / 11 | 5112-1 | 29/04 | 10:07 | 23 49.59 | 16 16.34 | 3874 | 25.19 | 1.50 | 3901 | y | |
| 220 / 12 | 5113-1 | 30/04 | 02:58 | 23 40.12 | 15 00.02 | 3853 | 25.01 | 2.14 | 3885 | y | |
| 221 / 13 | 5114-1 | 30/04 | 11:46 | 24 09.95 | 13 59.86 | 3171 | 24.75 | 2.61 | 3204 | y | |
| 225 / 14 | 5118-1 | 01/05 | 08:17 | 24 10.81 | 13 23.07 | 2741 | 24.61 | 2.71 | 2778 | y | |
| 226 / 15 | 5119-1 | 01/05 | 15:57 | 24 10.08 | 12 18.11 | 3910 | 24.46 | 2.49 | 4008 | y | |
| 229 / 16 | 5122-1 | 02/05 | 10:56 | 24 10.25 | 11 07.95 | 3737 | 24.31 | 2.41 | 3760 | y | |
| 231 / 17 | 5124-1 | 02/05 | 23:35 | 24 09.96 | 09 53.92 | 4322 | 23.91 | 2.43 | 4375 | n | |
| 232 / 18 | 5125-1 | 03/05 | 06:55 | 24 09.91 | 09 00.19 | 4462 | 23.68 | 2.44 | 4523 | n | 9°W |
| 233 / 19 | 5126-1 | 03/05 | 19:00 | 22 23.96 | 08 59.96 | 4192 | 24.04 | 2.40 | 4231 | n | |
| 234 / 20 | 5127-1 | 04/05 | 03:51 | 21 12.10 | 09 00.15 | 3941 | 24.34 | 2.38 | 3878 | n | |
| 235 / 21 | 5128-1 | 04/05 | 13:03 | 20 00.03 | 09 00.09 | 3959 | 23.93 | 2.40 | 3951 | n | |
| 236 / 22 | 5129-1 | 04/05 | 21:48 | 18 59.98 | 09 46.23 | 3838 | 24.46 | 2.43 | 3857 | n | 19°S |
| 236 / 23 | 5129-2 | 05/05 | 00:57 | 18 59.98 | 09 46.20 | 3840 | 24.45 | 13.14 | 250 | n | |
| 243 / 24 | 5136-3 | 07/05 | 22:22 | 19 22.00 | 12 42.67 | 4536 | 24.69 | 3.48 | 1500 | n | |
| 248 / 25 | 5141-1 | 09/05 | 18:30 | 19 05.75 | 17 15.12 | 3453 | 25.62 | 3.65 | 1502 | n | |

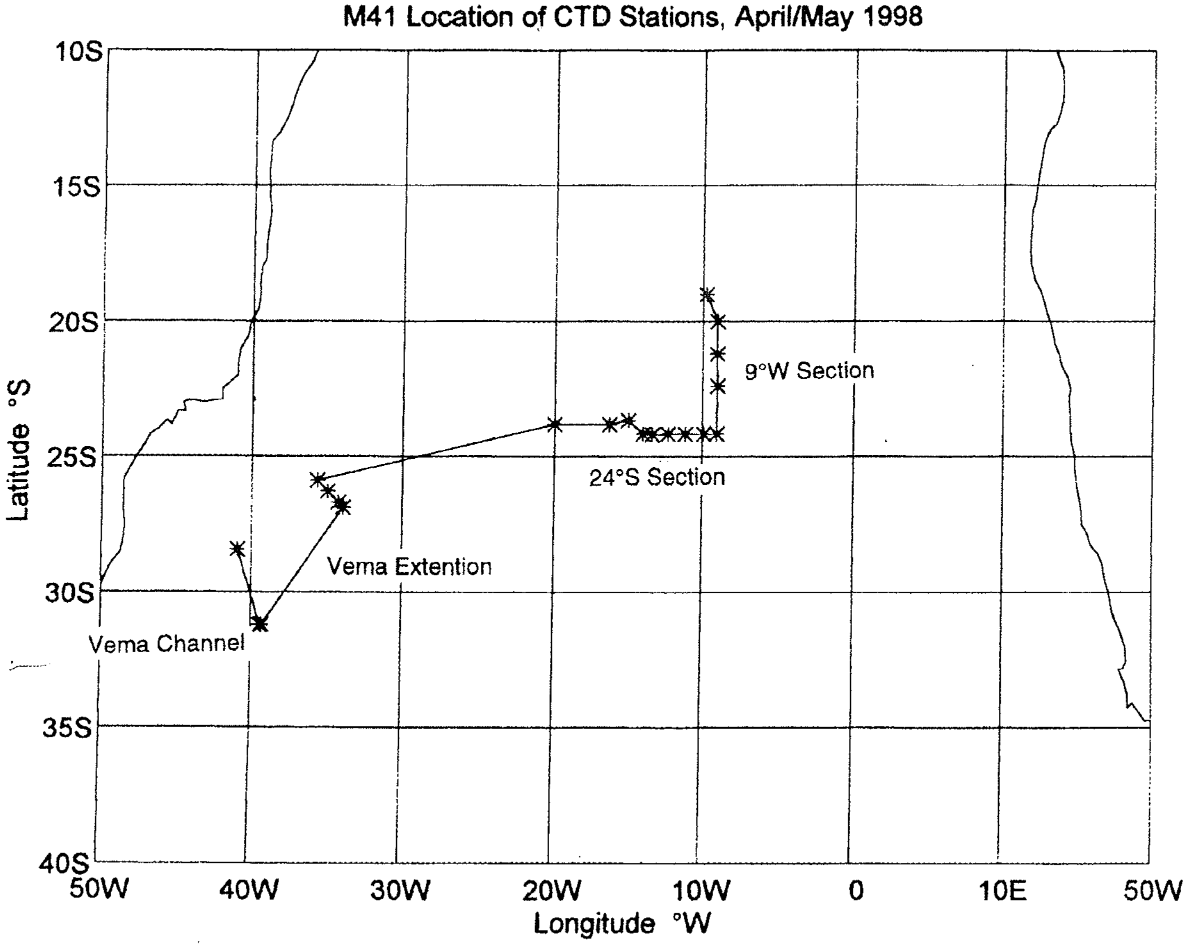


Fig. 2 Location of all CTD stations (*). Hydrographic work was equally split between Vema Channel, Vema Extension, and sections on 24°S and 9°W. For details see Table 1

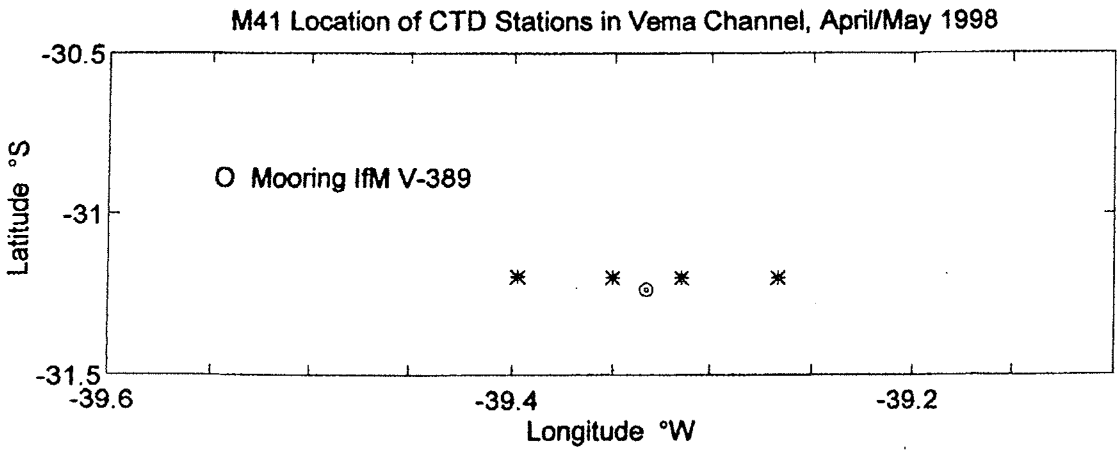


Fig. 3 CTD station (*) distribution in the area of the Vema Sill. Location (0) denotes the position of IfM mooring V-289. For details see Table 1 and 2

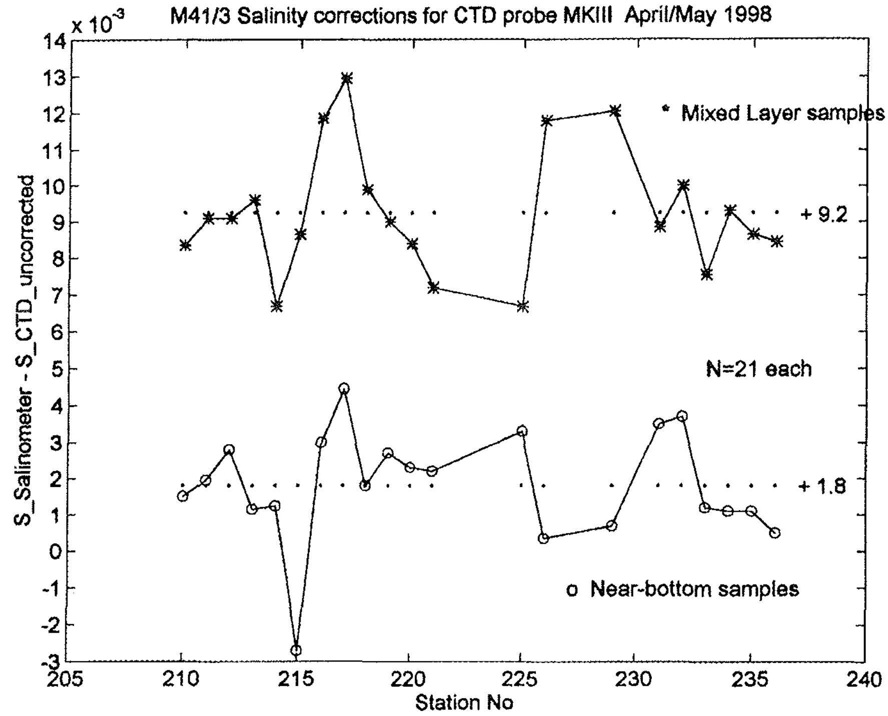


Fig. 4 Comparison of displayed CTD data and their bottle check values as a function of station number or time. The upper curve (*) contains all cases from the mixed layer at 10 m depth. The lower curve (o) denote check values from the deepest level, i.e.~ 20 m above the sea bed. No drift or calibration shifts are visible

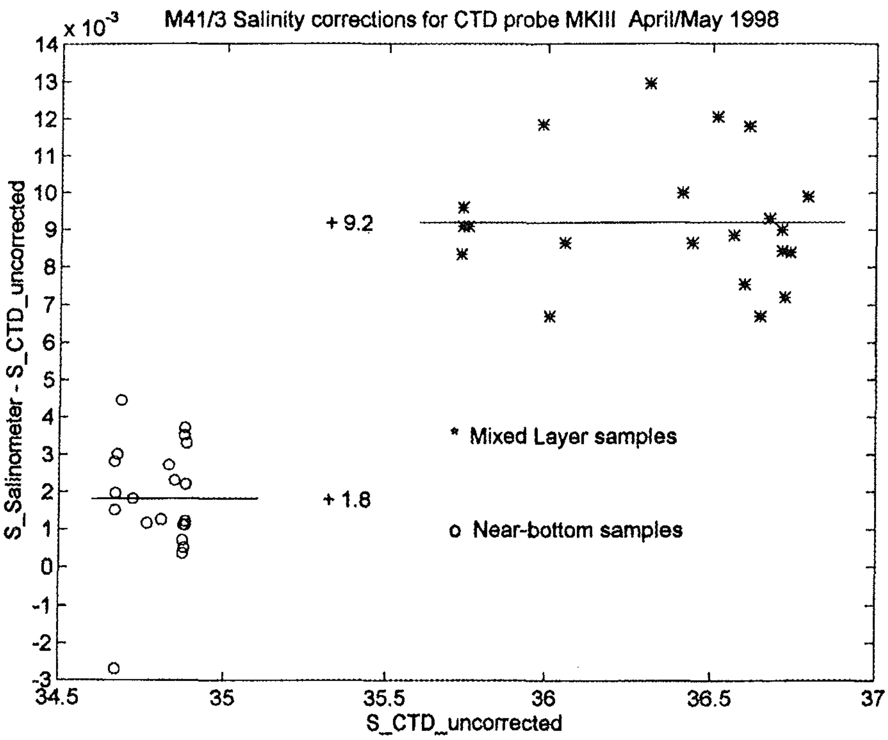


Fig. 5 Comparison of displayed CTD data and their bottle check values as a function of salinity. For symbols see Fig. 4

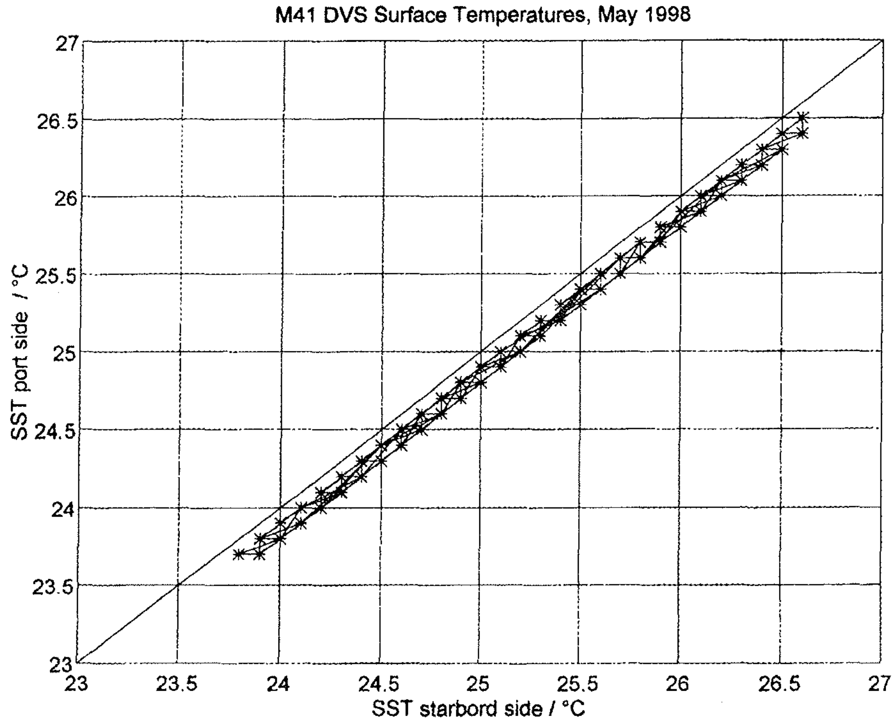


Fig. 6 Comparison of the two sea surface thermometers of the meteorological station METEOR. Data were recorded by the *DVS* system. Sensors show a bias of O(0.15°C)

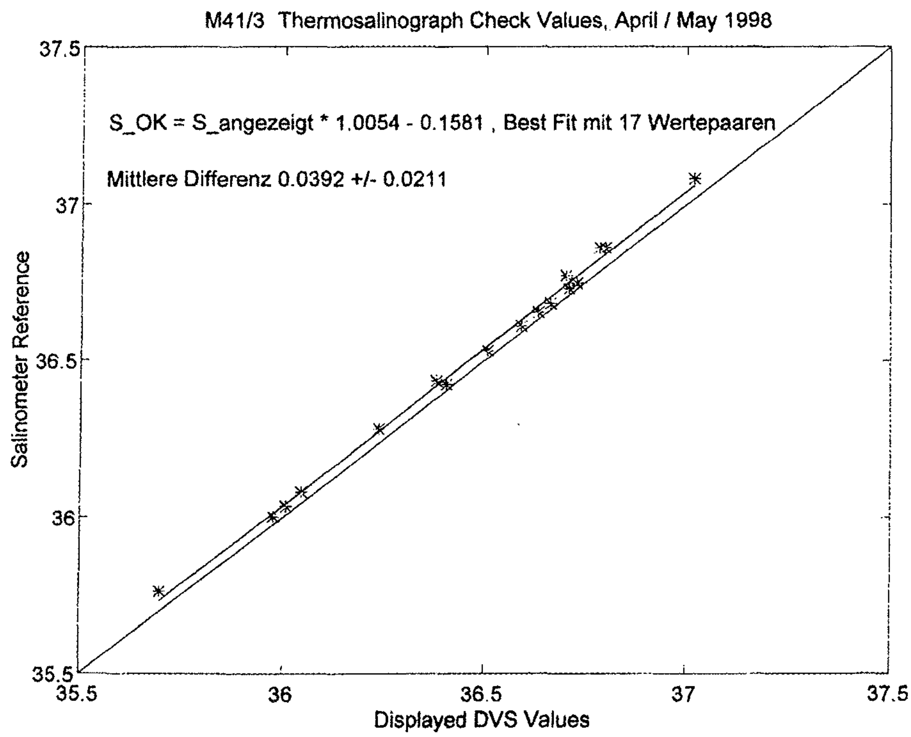


Fig. 7 Comparison of surface salinities displayed by the *DVS* system with salinity check values from water samples taken immediately behind the thermosalinograph chamber in the bow of METEOR

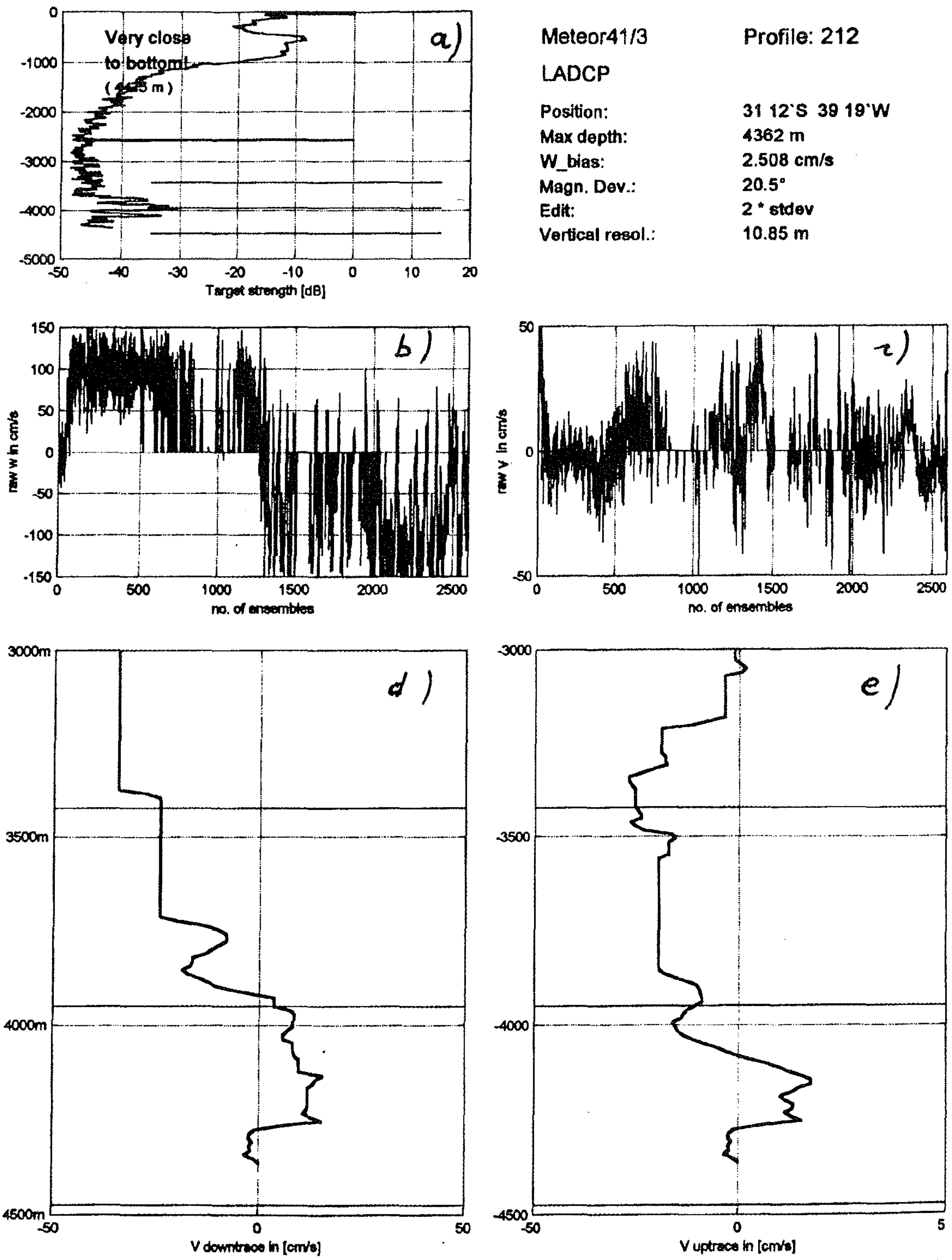


Fig. 8 Sample plots of the lowered Acoustic Doppler Current Profiler (lADCP) from CTD Sta. 212 in the Vema Channel. Note the bottom intensified current profiles (d and e) which indicate the northward transport of Antarctic Bottom Water (AABW) across the Vema Sill. For further details see text

Table 2 Mooring activities in the Vema Channel

| Sta. No | IfM VNo | CTD Sta/Prof | Date 1998 | Latitude S | Longitude W | Depth (m) | Ref No | Instr. Type | Instr. S/N | Remarks |
|---|---|---|---|---|---|---|---|---|---|---|
| 209 | 389 | {210/2- 212/4} | 21APR | 31°14.30' | 39°20.00' | 4580 | - | WD | 2266 | ARGOS, no recept. d. deploym. |
| | | | | | | | 389101 | ThCh | 1295/ 1960 | nom recorder depth 4090 m i.e. 490 m above ground 11 sensors, 20 m apart |
| | | | | | | | 389102 | AVTP | 11442 | nominal depth 4310 m i.e. 270 m above ground |
| | | | | | | | 389103 | ThCh | 1296/ 1961 | nom recorder depth 4312 m i.e. 268 m above ground 11 sensors, 20 m apart |
| | | | | | | | 389104 | AVTP | 11348 | nominal depth 4528 m i.e. 52 m above ground |
| | | | | | | | 389105 | MiCat | 206 | nominal depth 4529 m i.e. 51 m above ground |
| | | | | | | | - | AR | 428 | 48 m above ground |

Abbreviations

| | |
|---|---|
| AVTP | Anderaa Current Meter incl. pressure sensor |
| ThCh | Aanderaa Thermistor Chain, recorder / chain |
| MiCat | MicroCat moored CTD by SeaBird, Inc. |
| WD | WatchDog bouy built at IfM Kiel |
| AR | Acoustic Release by MORS |

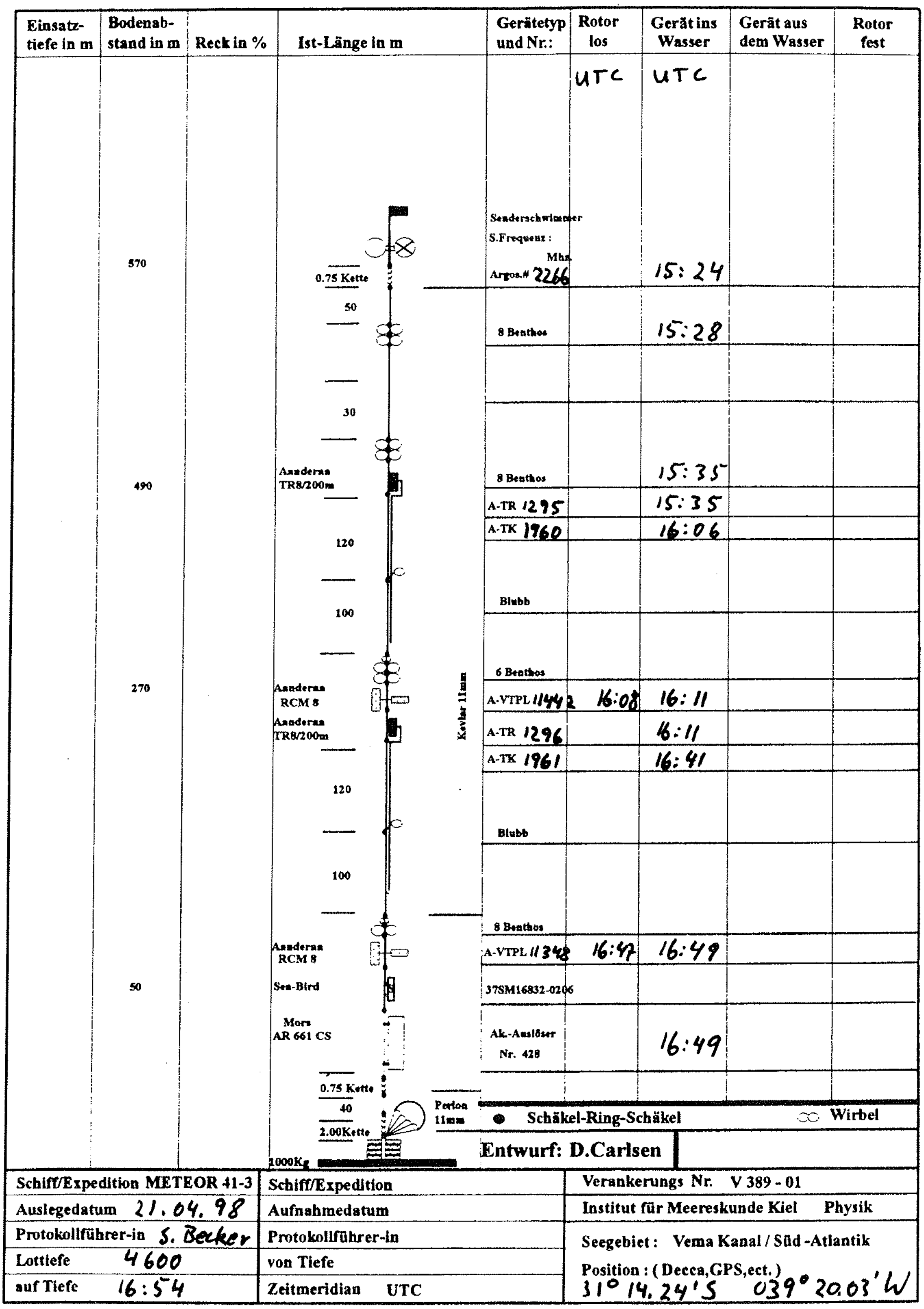


Fig. 9 Design of IfM mooring V-389 which was moored in the Vema Channel. For details see Table 2

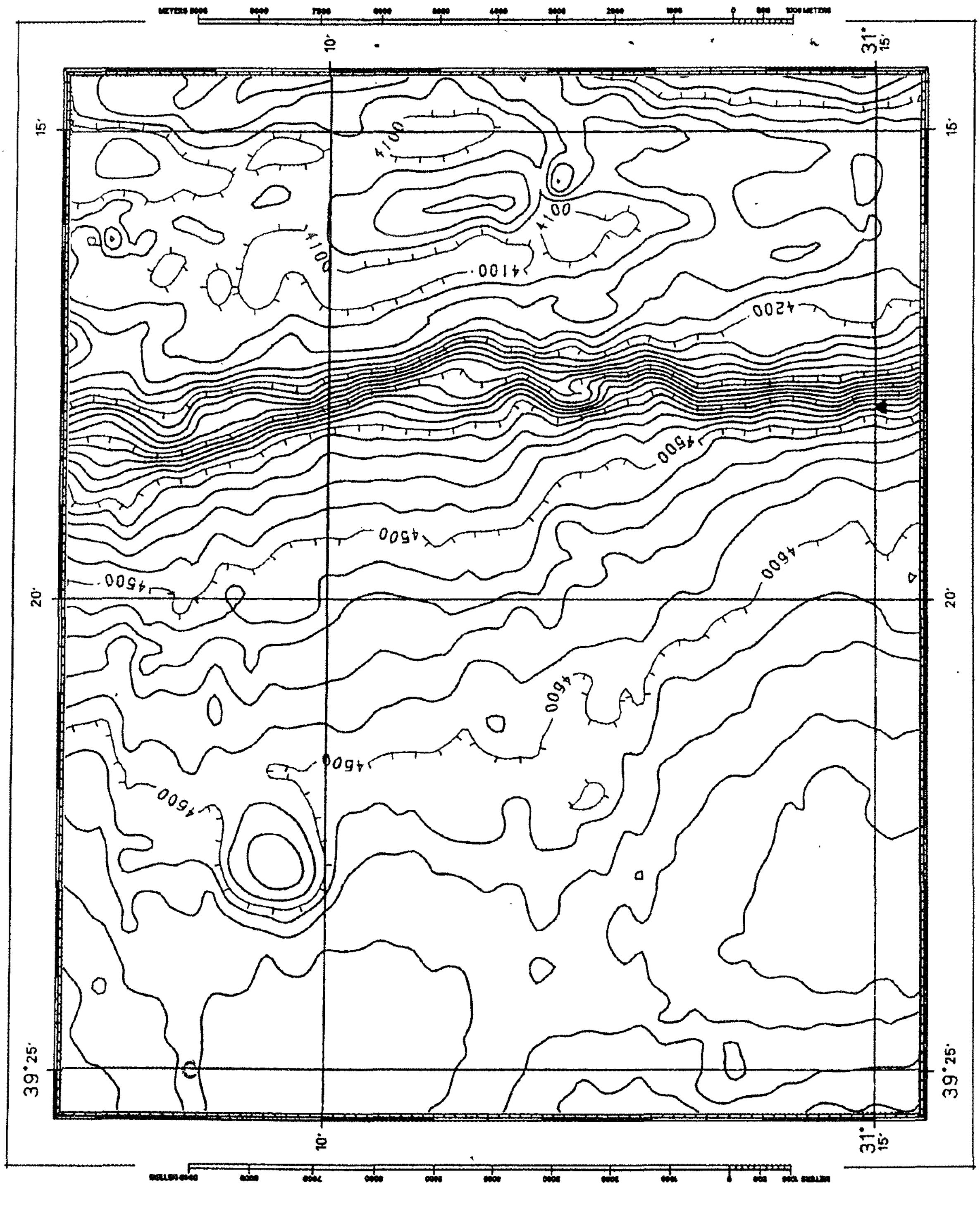

Fig. 10 Topographic charts from the eastern side of the Vema Channel taken in January 1991 during METEOR cruise M 15 (a, top) and during METEOR cruise M 41/3 (b, see right page) in April 1998

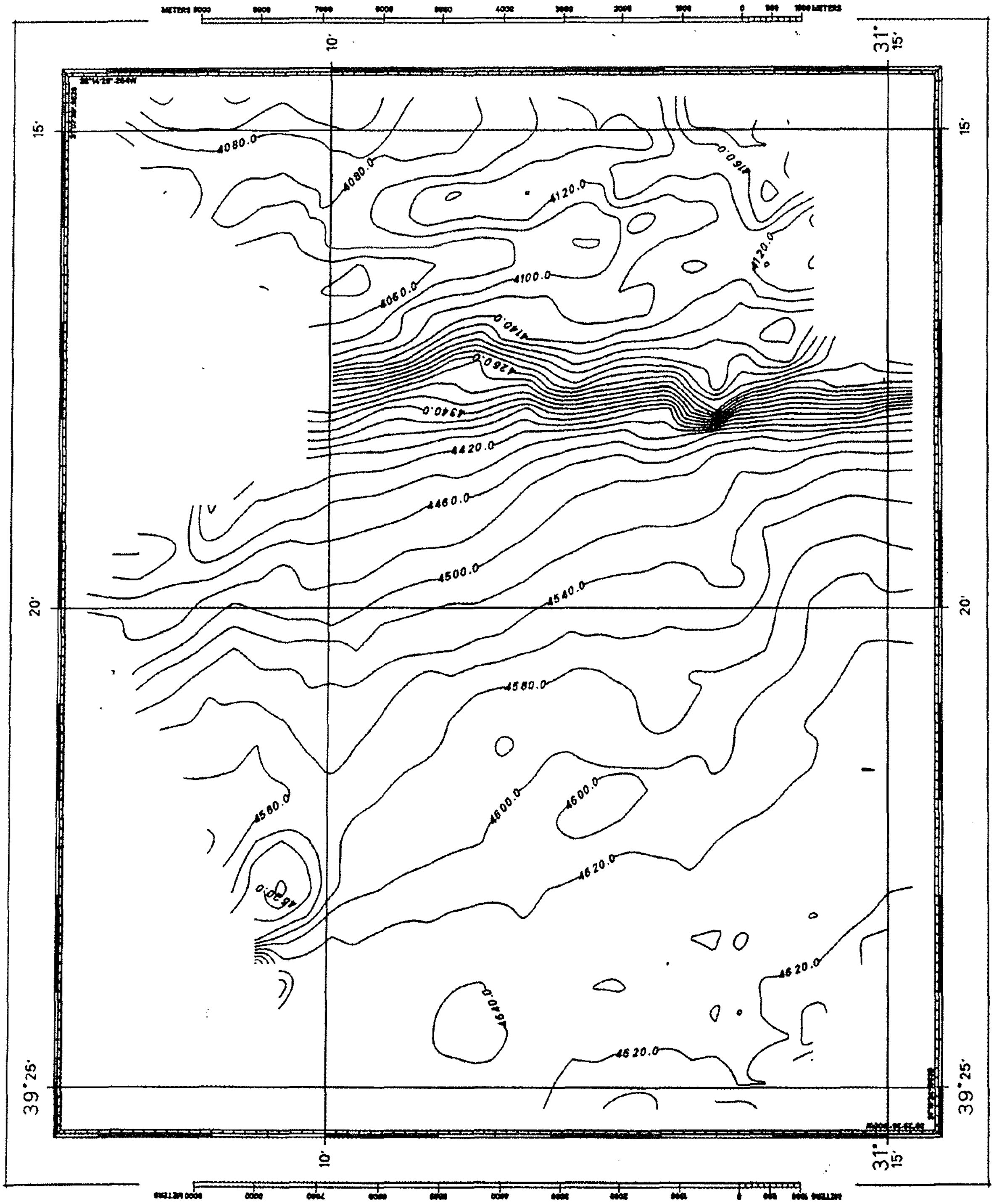
10'
31°
15'
15'
20'
39°25'
4080.0
4120.0
4100.0
4060.0
4140.0
4260.0
4340.0
4420.0
4460.0
4500.0
4540.0
4580.0
4600.0
4620.0
4640.0

Fig. 10 b

Table 3 Near-bottom CTD and salinometer values from the Vema Sill, 1972 - 1998 (acc. to Zenk and Hogg 1996; Hogg and Zenk 1997)

| Expedition<br>mm/yy | Sta.<br>No | Pro.<br>No | θ<br>°C | Acc.T<br>mK | $S_{CTD}$<br>raw | $S_{CTD}$<br>corr | $S_{Sali}$<br>No 1 | <br>2 | <br>3 | Acc.S |
|---|---|---|---|---|---|---|---|---|---|---|
| Cato<br>11/72 | 14 | | **-0.175** | | | | | | | |
| Geosecs<br>11/72 | 59 | | **-0.180** | | | | | | | |
| CHAIN<br>4/74 | 4 | | **-0.188** | | | | | | | |
| ATLANTIS II<br>10/79 | 76 | | **-0.192** | | | | | | | |
| ATLANTIS II<br>5/80 | 112 | | **-0.181** | | | | | | | |
| METEOR 15<br>1/91 | 49 | 47 | **-0.185** | ±2 | | | | | | |
| METEOR 22<br>12/92 | 43 | | **-0.155** | | | | | | | |
| COROAS I [§]<br>3/93 | 24 | | **-0.140** | | | | | | | |
| COROAS II [§]<br>3/94 | | | **-0.134** | | | | | | | |
| POLAR-<br>STERN<br>10/94 | 128 | 31 | **-0.158** | ±2 | 34.655 | | 34.683 | 34.683 | ./. | |
| METEOR 34<br>3/96 | 49 | 5 | **-0.156** | ±2 | 34.657 | **34.665** | $34.664_9$ | $34.665_1$ | $34.663_7$ | ±0.003 |
| METEOR 41<br>4/98 | 212 | 4 | **-0.136** | ±2 | 34.670 | **$34.671_8$** | $34.673_0$ | $34.672_4$ | ./. | ±0.003 |

[§] Kindly provided by Y. Ikeda, University of Sao Paulo.

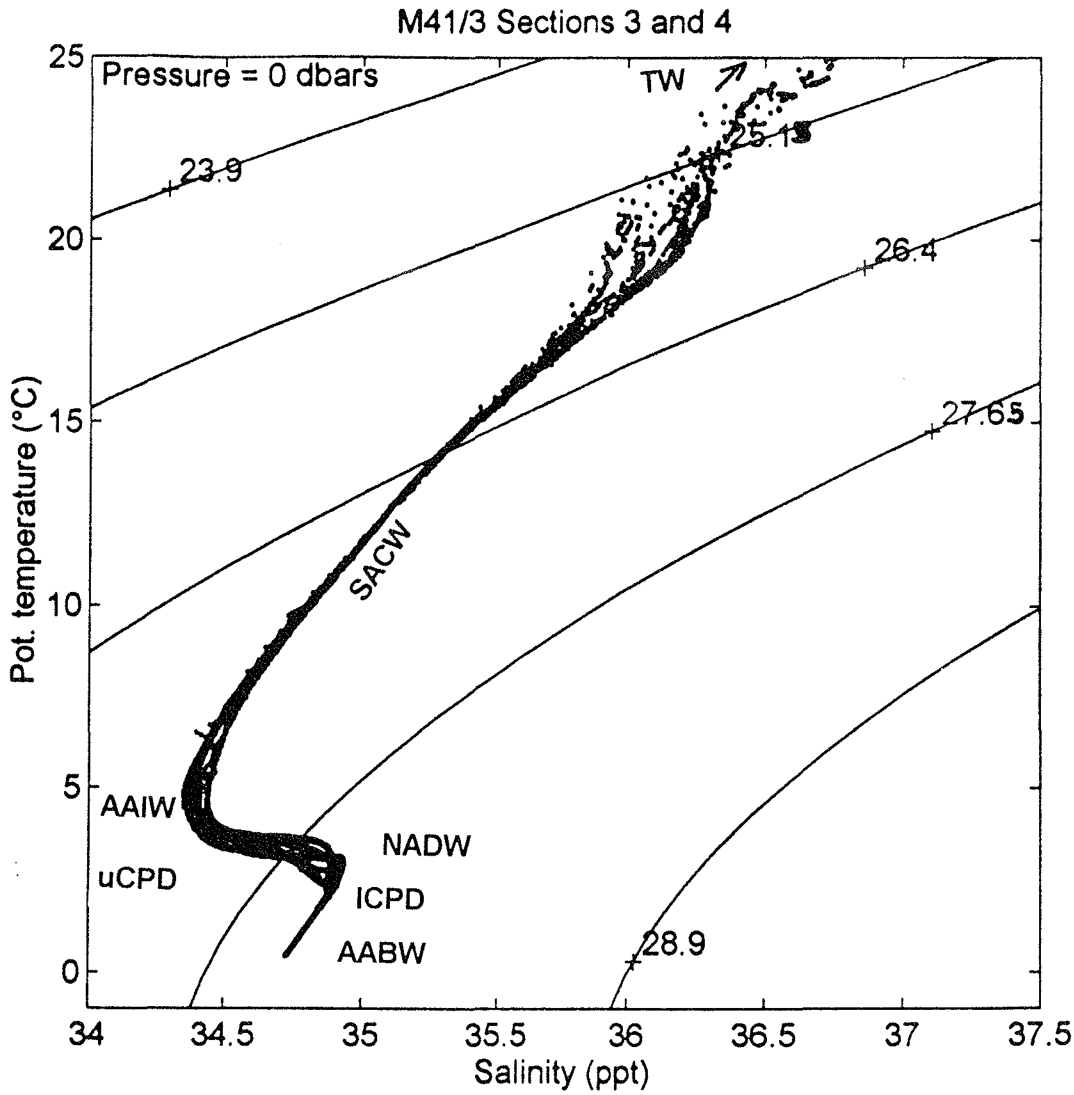


Fig. 11 Diagram of all pairs of salinity (S) and potential temperature (θ) from Sections at 24°S and 9°W. Data were interpolated in 2 dbar steps prior to plotting. Abbreviations: TW - Tropical Surface Water, SACW - South Atlantic Central Water, AAIW - Antarctic Intermediate Water, NADW - North Atlantic Deep Water, CDW - Circumpolar Deep Water (u - upper, l - lower), AABW - Antarctic Bottom Water. Diagonal lines of equal densities are referenced to the surface ($\sigma_\theta$ / kg $m^{-3}$)

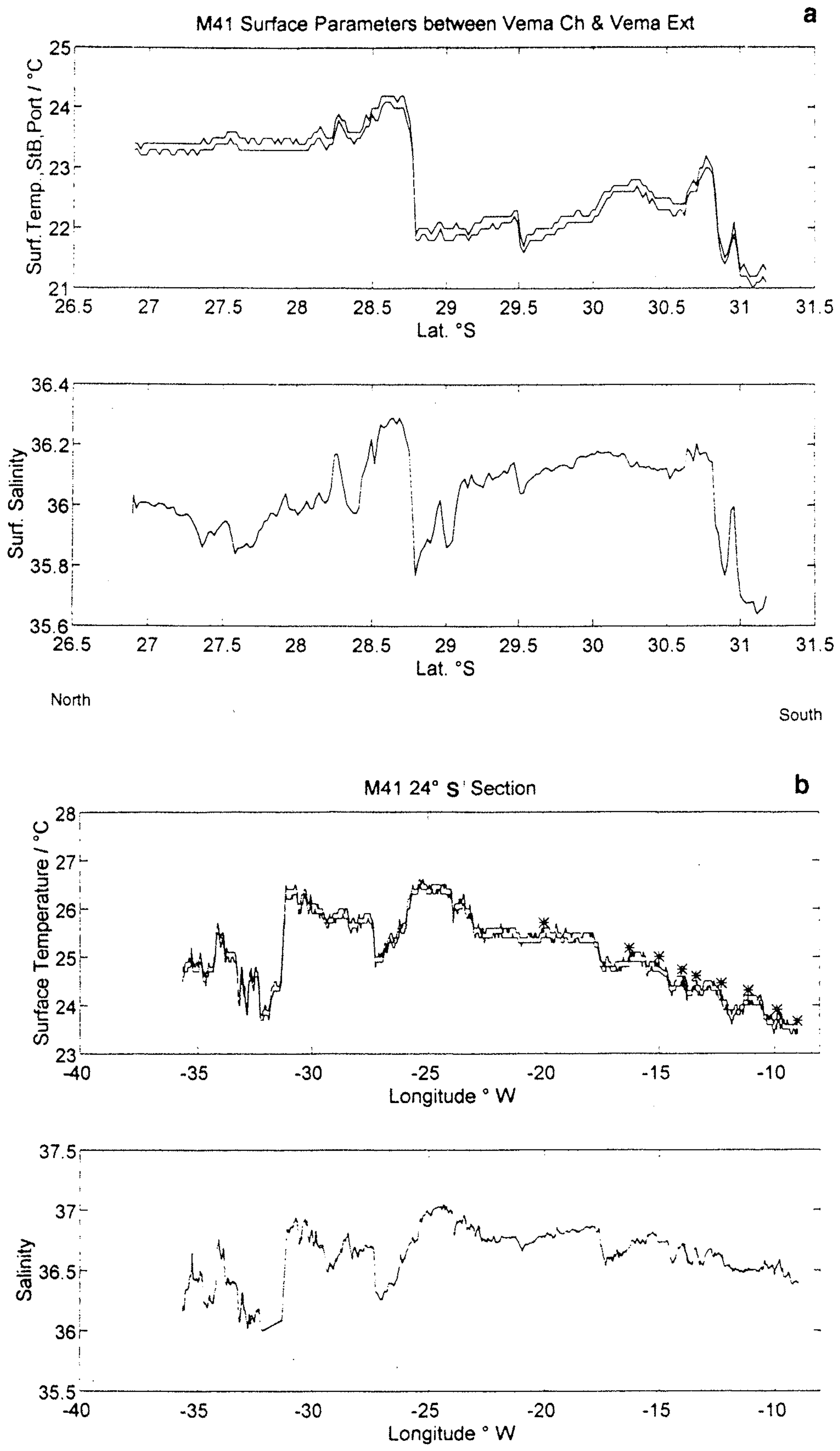


Fig. 12 *DVS* plots of surface temperatures and salinities on various track lines (see top of graphs). In (a) we have included 10 m CTD temperature values. They appear to ly systematically above the two ship's own surface thermometer readings. See also Fig. 6

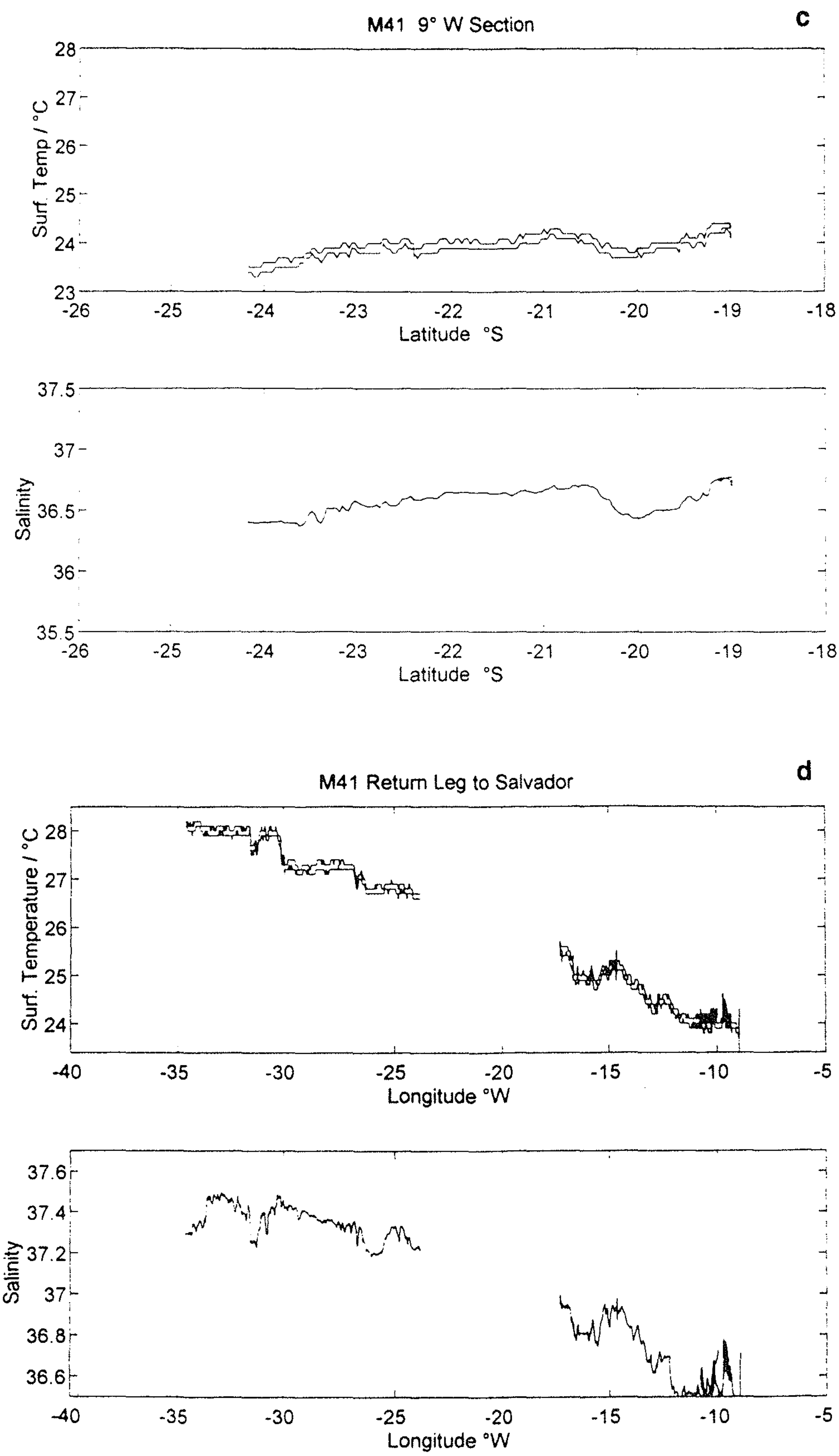


Fig. 12 continued

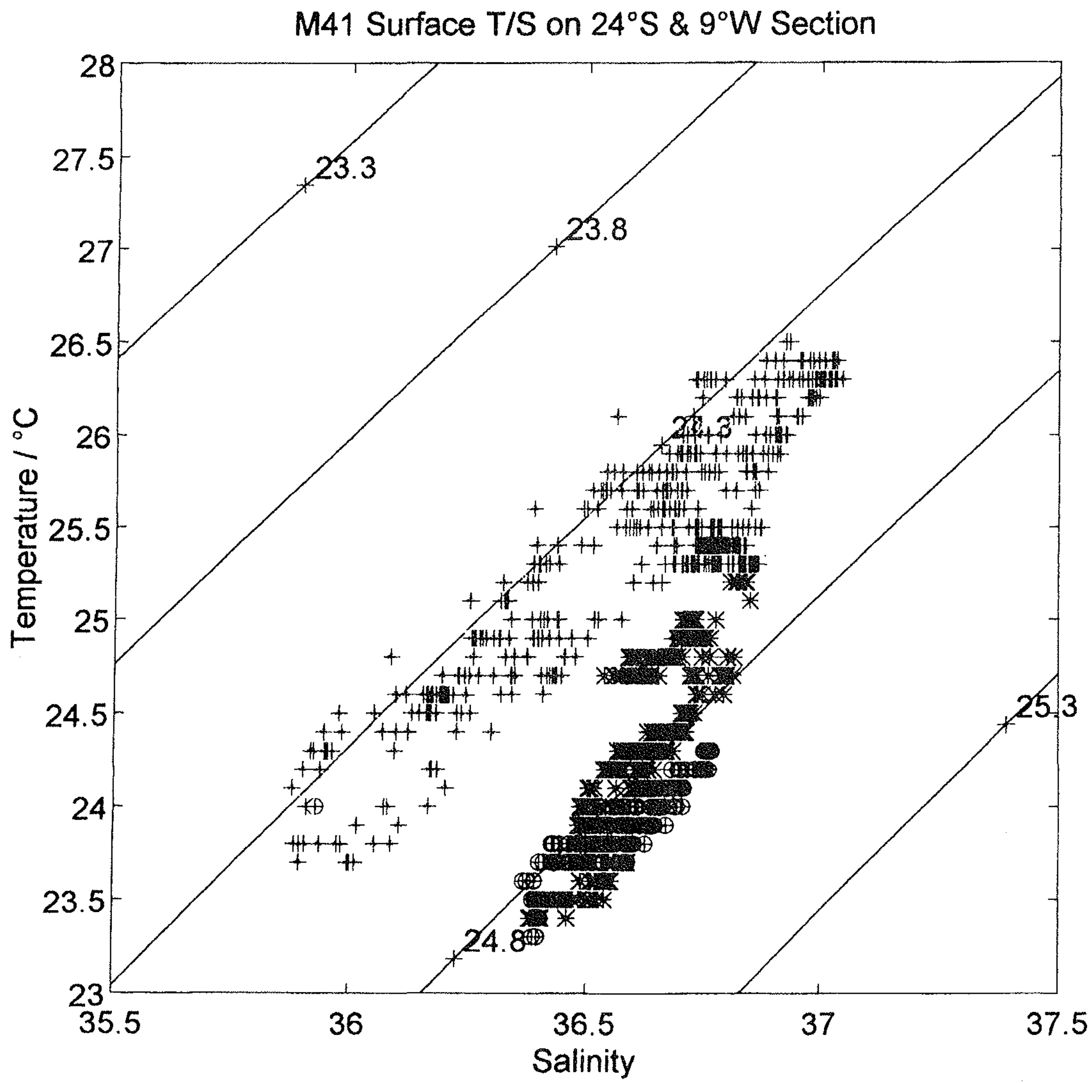


Fig. 13 Diagram of all pairs of salinity and temperature from the surface of sections at 24°S (+ and *) and 9°W (+ with o) recorded by the *DVS* system. Values * and + differ by their location east or west of 18°W. Note that data feature two clusters. $\sigma_t$ lines ($kgm^{-3}$) are overlaid

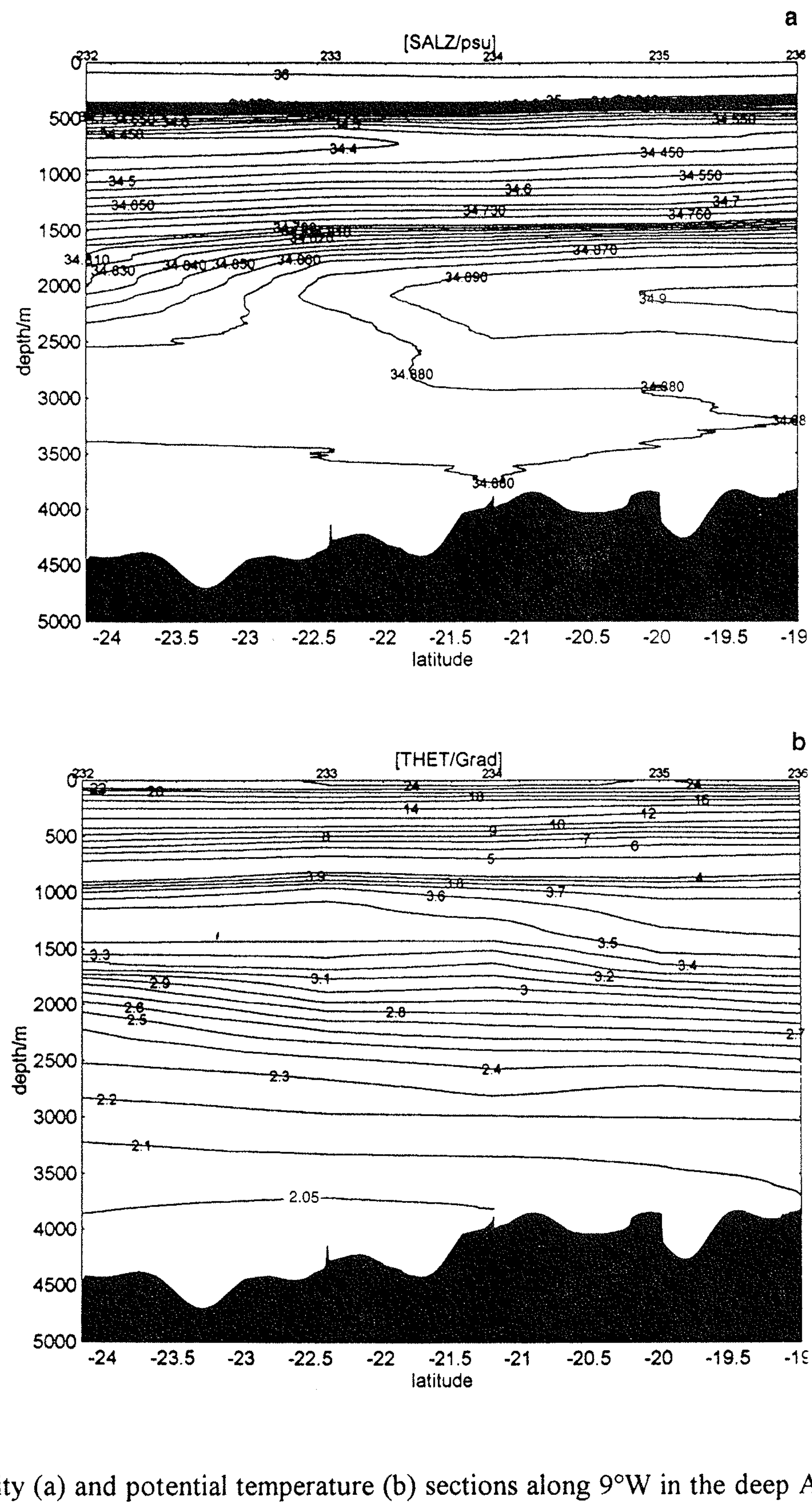


Fig. 14 Salinity (a) and potential temperature (b) sections along 9°W in the deep Angola Basin east of the Middle Atlantic Ridge. The distribution of water masses is discussed in the text. Note that no water with $\theta$ < 2.0°C reaches the Angola Basin, i.e. Antarctic Bottom Water is absent

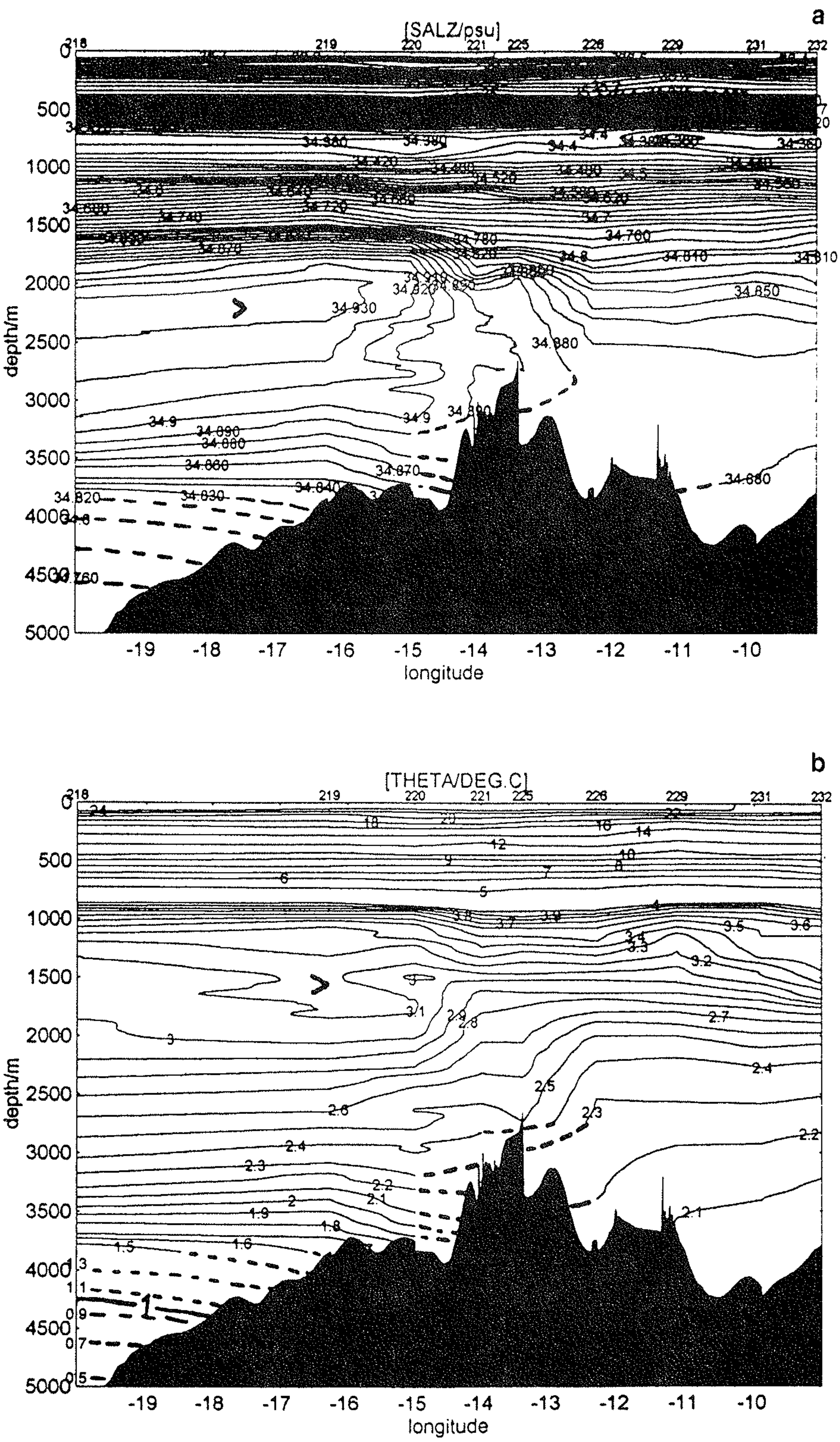


Fig. 15 Salinity (a) and potential temperature (b) sections along 24°S. The center of the Middle Atlantic Ridge (MAR) is situated at ~ 13.5°W. Note the drastic differences between the stratification on the eastern side, i.e. in the Angola Basin and in the Brazil Basin on the western side of the MAR. North Atlantic Deep Water features a deep front preventing this water mass from penetrating into the Angola Basin. The western abyssal is filled with Antarctic Bottom Water ($\theta < 2°C$). No such water is present in the eastern abyssal

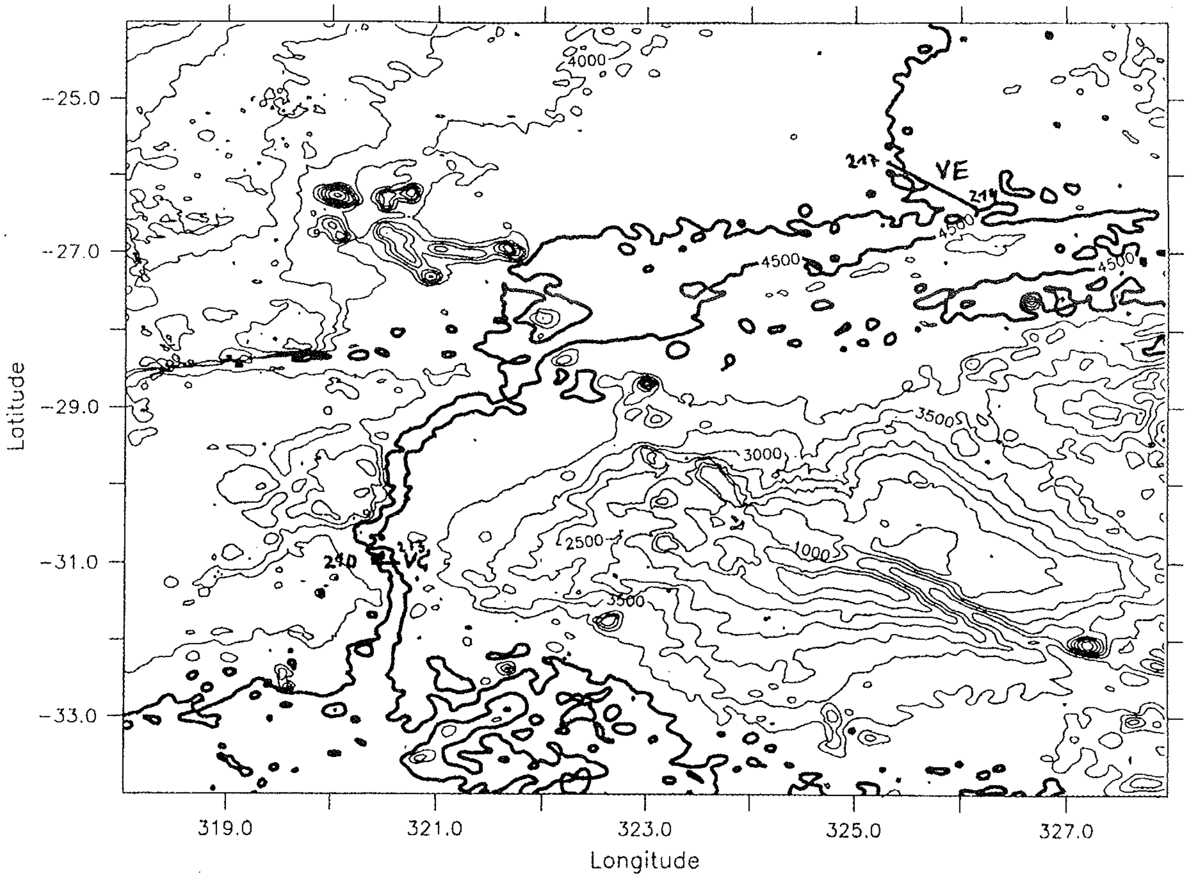


Fig. 16 Topographic map of the Vema Channel and its northeastern extension. The 4000 m isobath is an optimal indicator for the channelized spreading of Antarctic Bottom Water ($\theta$ > 2°C) while filling the deep Brazil Basin

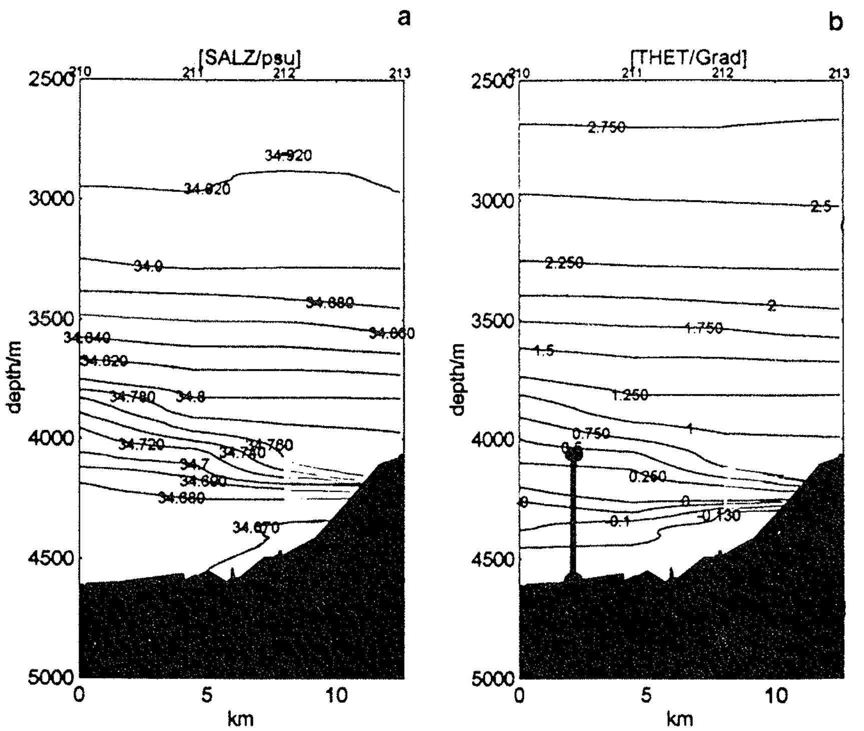


Fig. 17 Salinity (a) and potential temperature (b) sections from the Vema Sill below 2500 m. In the right subfigure we have included the position and length of IfM mooring V-389 (see Table 2). Note the asymmetric horizontal property distribution in the range below ~3800 m. For details see text

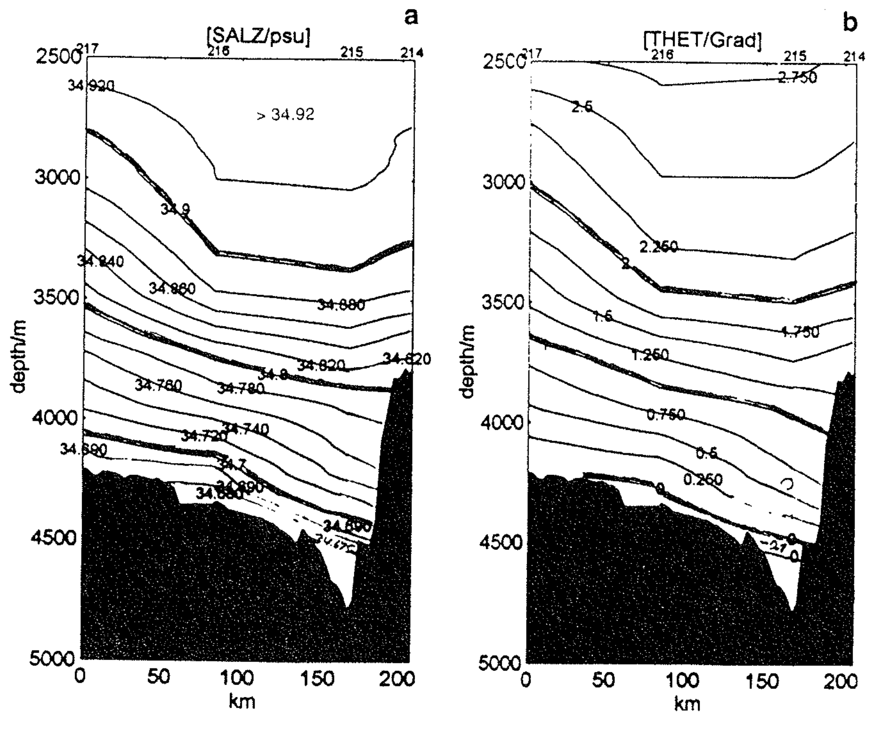


Fig. 18 Sections as in Fig. 15, however from the Vema Extension. Note the isolated deep channel that prevents Antarctic Bottom Water to be mixed more rapidly with its surrounding water masses then farther north in the inner Brazil Basin

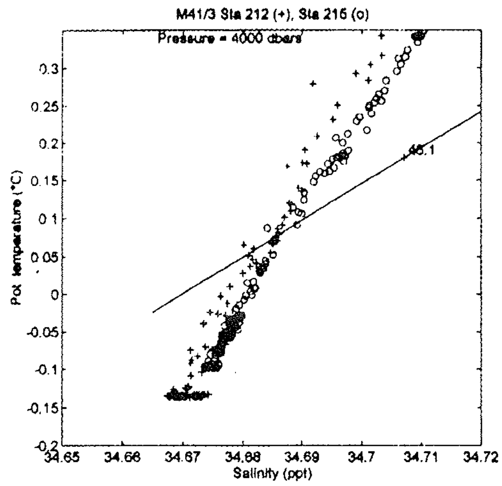


Fig. 19 Diagram of potential temperature vs. salinity (θ/S) from Sta. 212 (+) and 215 (o) from the Vema Sill (see Figs. 2 and 3) and from the Vema Extension (see Fig. 2)

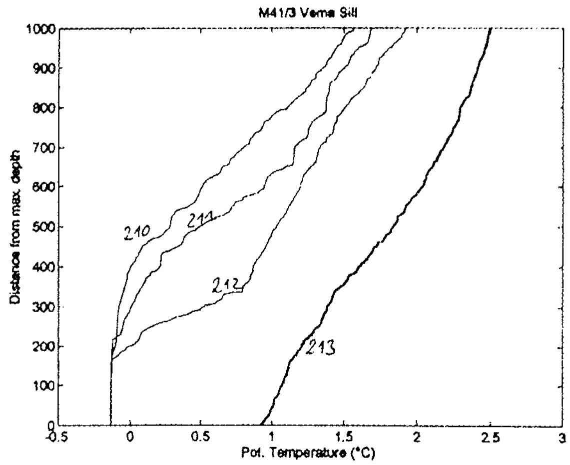


Fig. 20 Bottom oriented profiles of potential temperature from section (a) at the Vema Channel and (b) the Vema Extension. Note the homogenized temperature on the sill also seen in Fig. 18

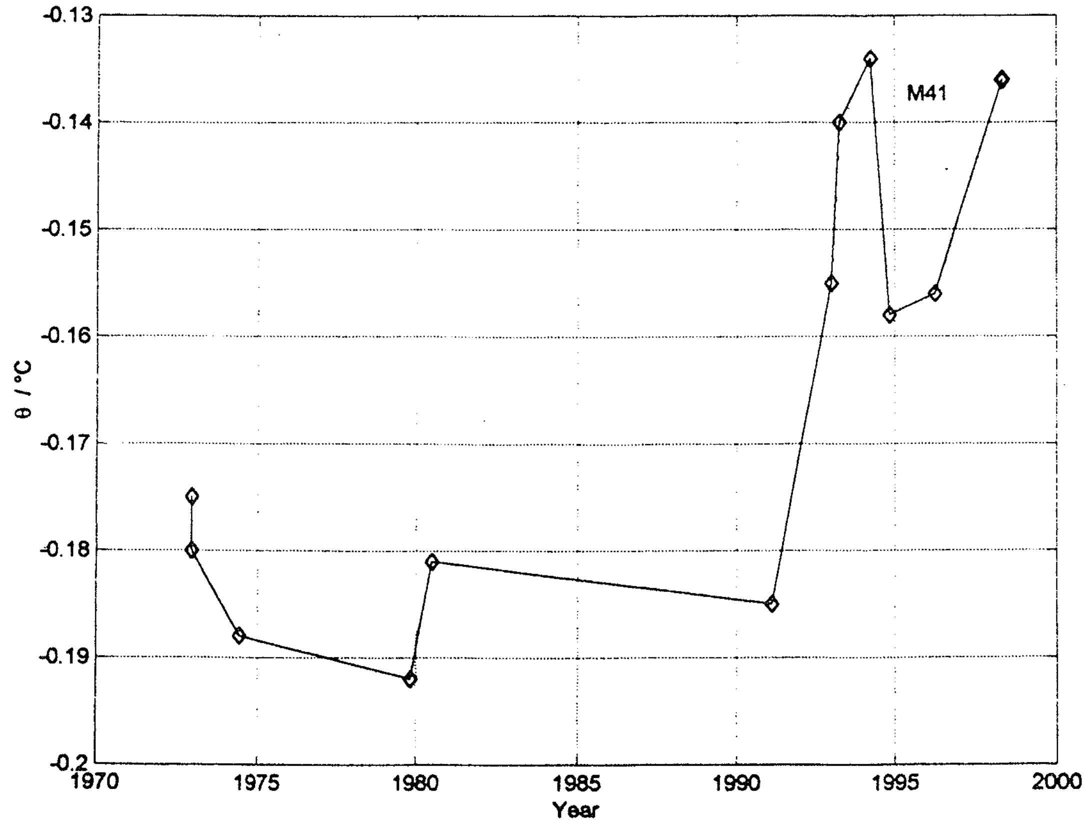


Fig. 21 Long-term CTD temperature time series from the Vema Channel. The newest data point from M 41 shows again increased temperatures. In fact, the latest value of $\theta_{min}$ = -0.136°C measured on Sta. 212 (see Figs. 3 and 10) is among the highest in the total time series from the sill region in the Vema Channel

Table 4a LADCP Log

| Pr. No. | Stat No. | LADCP Start (UTC) | Tiefe (m) | Date (Start, End) yyyy,mm,dd yyyy,mm,dd | Time, down 10m (CTD Prot) hh,mm,ss (UTC) | Posi., down 10m (CTD Prot) gg,mm.mm gg,mm.mm | Posi., down 10m (DVS Stream ) gg,mm.mmm gg,mm.mmm | Time, up 10m. Start hh,mm,ss | Posi, up 10m (CTD Prot) gg,mm.mm gg,mm.mm | Posi, up 10m (DVS Stream ) gg,mm.mmm S gg,mm.mmm | Time, up 10m End (DVS) hh,mm,ss | Posi, up 10m (DVS,End ) gg,mm.mmm S gg,mm.mmm |
|---|---|---|---|---|---|---|---|---|---|---|---|---|
| 1 | 208 | 15,37 | 4387 | 1998,04,20 | 16,46,35 | 28,26.34 S 40,54.60 W | Wrong time in protocol | 19,43,35 | 28,26.48 S 40,54.69 W | | | |
| 2 | 210 | 17,24,48 | 4611 | 1998,04,21 | 17,45,05 | 31,11.99 S 39,23.93 W | 31,11.987 S 39,23.928 W | 20,38,40 | 31,12.11 S 39,23.79 W | 31,12.108 S 39,23.784 W | 20,41,40 | 31,12.152 S 39,23.812 W |
| 3 | 211 | 21,36,54 | 4574 | 1998,04,21 1998,04,22 | 22,02,13 | 31,12.04 S 39,21.01 W | 31,12.003 S 39,21.055 W | 00,43,45 | 31,12.27 S 39,21.02 W (End) | 31,12.258 S 39,20.989 W | 00,47,45 | 31,12.263 S 39,21.019 |
| 4 | 212 | -"- | 4475 | 1998,04,22 | 01,47,12 | 31,12.06 S 39,18.88 W | 31,12.057 S 39,18.872 W | 04,40,54 | 31,12.05 S 39,19.13 W (End) | 31,12.027 S 39,19.121 W | 04,43,45 | 31,12.046 S 39,19.132 W |
| 5 | 213 | -"- | 4065 | 1998,04,22 | 05,58,37 | 31,12.02 S 39,16.00 W | 31,12.019 S 39,16.008 W | 08,20,00 | 31,11.98 S 39,15.98 W (Start) | 31,11.985 S 39,15.978 W | 08,23,15 | 31,12.000 39,15.968 |
| 6 | 214 | 19,09,19 | 3784 | 1998,04,23 | 19,21,38 | 26,53.99 S 33,54.96 W | 26,53.943 S 33,54.934 W | 21,48,03 | 26,53.97 S (S) 33,55.00 W 26,53.95 S (E) 33,54.99 W | 26,53.972 S 33,55.007 W | 21,51,07 | 26,53.949 S 33,54.994 W |
| 7 | 215 | ? | 4785 | 1998,04,23 1998,04,24 | 23,56,07 | 26,41.96 S 34,14.01 W | 26,41.956 S 34,14.005 W | 02,59,19 | 26,41.98 S (S) 34,14.00 W 26,42.00 S (E) 34,14.02 W | 26,41.978 S 34,14.001 W | 03,02,21 | 26,41.996 S 33,14.019 W |
| 8 | 216 | 06,55,41 | 4350 | 1998,04,24 | 07,09,27 | 26,18.00 S 34,56.17 W | 26,17.995 S 34,56.165 W | 09,50,40 | 26,18.00 S (A) 34,55.99 W 26,18.03 S (E) 34,55.95 | 26,18.001 S 34,55.988 W | 09,53,41 | 26,18.030 S 34,55.950 W |

Table 4b LADCP Log (continued)

| Pr. No. | Stat No. | LADCP Start (UTC) | Tiefe (m) | Date (Start, End) yyyy,mm,dd yyyy,mm,dd | Time, down 10m. (CTD Prot) hh,mm,ss (UTC) | Posi., down 10m (CTD Prot) gg,mm.mm gg,mm.mm | Posi., down 10m (DVS Stream ) gg,mm.mmm gg,mm.mmm | Time, up 10m. Start hh,mm,ss | Posi, up 10m (CTD Prot) gg,mm.mm gg,mm.mm | Posi, up 10m (DVS Stream ) gg,mm.mmm S gg,mm.mmm | Time, up 10m End (DVS) hh,mm,ss | Posi, up 10m (DVS,End ) gg,mm.mmm S gg,mm.mmm |
|---|---|---|---|---|---|---|---|---|---|---|---|---|
| 9 | 217 | ? | 4190 | 1998,04,24 | 16,47,49 | 25,53.97 S 35.38.88 W | 25,53.965 S 35,38.881 W | 19,26,15 | 25,54.00 S (A) 35,39.01 W 25,53.99 S (E) 35,39.01 W | 25,53.996 S 35,39.005 W | 19,29,15 | 25,53.986 S 35,39.014 W |
| 10 | 218 | 09,58,05 | 5215 | 1998,04,28 | 10,17,19 | 23,48.93S 20,00.01W | 23,48.904 S 20,00.009 W | 13,31,27 | 23,48.95 S 19,59.78W(A) 23,48.96S 19,59.75W(E) | 23,48.950 S 19,59.774 W | 13,34,29 | 23,48,962 19,59.756 |
| 11 | 219 | 09,57,43 | 3860 | 1998,04,29 | 10,09,49 | 23,49.57 S 16,16.34 W | 23,49.570 S 16,16.333 W | 12,38,38 | 23,49.57 S 16,16.34 W(A) 23,49.57 S 16,16.33 W (E) | 23,49.571 S 16,16,339 W | 12,41,42 | 23,49.580S 16,16.320W |
| 12 | 220 | 02,43,28 | 3850 | 1998,04,30 | 03,01,14 | 23,40.18 S 15,00.09 W | 23,40.180 S 15,00.090 W | 05,20,38 | 23,40.21 S 14,59.94 W(A) 23,40.21 14.59.94W (E) | kein DVS! | 05,30,55 | kein DVS |
| 13 | 221 | 11,23,09 | 3130 | 1998,04,30 | 11,49,45 | 24,09.97 S 13,59.81 W | 24,09.972 S 13.59.817 W | 13,54,48 | 24,09,88 S 13,59.56 W 24,09,88 S 13,59,55 W | 24,09,876 S 13,59.559 W | 13,57,56 | 24,09.881 S 13,59.546 W |
| 14 | 225 | 08,05,08 | 2740 | 1998,05,01 | 08,19,59 | 24,10.83 S 13,23.07 W | 24,10.827 S 13,23.074 W | 10,13,18 | 24,10.77 S 13,23.01 W 24,10.78 S 13,23,07 W | 24,10.767 S 13,23.005 W | 10,16,27 | 24,10.777 S 13,23.036 W |
| 15 | 226 | 15,25,02 | 3865 | 1998,05,01 | 16,02,21 | 24,10,05 S 12,18.01 W | 24,10.045 S 12,18.014 W | 18,30,38 | 24,10.05 S 12,17.86 W 24,10.04 S 12,17.85 W | 24,10.767 S 13,23.005 W | 18,33,38 | 24,10.041 S 12,17.852 W |

## 4.2 Tracer-Oceanography

(C. Rüth, P. Hebbeln)

The main interests of this cruise were the flow of Antarctic Bottom Water (AABW) through the Vema Channel into the Brazil Basin and the pathways of North Atlantic Deep Water (NADW) across the Mid Atlantic Ridge (MAR) into the Angola Basin. An L-shaped section across the MAR at 24°S and along its eastern flank at 9°W intersects the WOCE A9 cruise at both ends and thus closes a box within which NADW presumably crosses the MAR (see Speer et al. 1995). Helium measurements in the MAR-region are also expected to provide more information about helium-input along the MAR-crest, which is indicated by data aquired during the WOCE cruises A8, A9, and A10.

The tracers CFC's and tritium are of anthropogenic origin and have a well known time-dependent input history at the ocean surface. Thus they are used not only to trace newly formed water masses but also to study the timescale of their spreading into the oceans. Both, AABW and NADW show enhanced CFC and tritium concentrations.

Helium-Isotope measurements are used to trace terrigenic helium wich enters the ocean at Mid Ocean Ridges. Because of its slow spreading rate the MAR is thought to be a weak or insignificant source of helium regarding the ocean interior. Helium detected in the South Atlantic is of Pacific origin and reaches the South Atlantic with the Antarctic Circumpolar Current (ACC). Thus, helium in the South Atlantic is used as a tracer for circumpolar water masses. AABW and CDW (Circumpolar Deep Water) show high helium-isotope ratios, whereas NADW is characterised by relatively low values. Helium is therefore a valuable tracer to study the pathways and the mixing processes of these water masses. Recent data however, did indicate some helium input along the MAR-crest, which is investigated further on the MAR-transect of this cruise.

A total of 240 helium-, 144 tritium-, and 400 CFC-samples were drawn at most hydrographic stations from standard niskin bottles (Table 5). The distribution with depth was mainly chosen with respect to AABW and NADW and is given in the table below. For each CFC-sample 100 ml water is filled into a glass ampoule, which is then flame-sealed and shipped to our laboratory in Bremen. There, the CFC-11, CFC-12, CFC-113, and CCL4 concentrations are measured with a gaschromatographic system. For the helium-analysis, 40 ml of seawater are filled into a copper tube which is then pinched off at both ends. For tritium, 1 l of water is sampled into glass bottles. Both, helium and tritium are measured in Bremen in a dedicated helium-isotope mass-spectrometric system. For the helium-data, the concentrations of $^4$He, $^3$He and Neon as well as the helium-isotope ratio are measured. Rather than measuring tritium directly, all the gas is extracted from the water sample and $^3$He is detected as a result of the tritium decay. The tritium content of the water sample is then determined using the $^3$He concentration together with the storage time of the extracted sample.

Table 5 Sample collection for tritium, helium and CFC's

| Station/ Profile | Bottle | Depth [m] | CFC-ampoule # | Helium-sample # | Tritium-sample # |
|---|---|---|---|---|---|
| 210/2 | 1 | 4660 | 2714 | 1 | 1 |
| 210/2 | 2 | 4610 | 2704 | 2 | --- |
| 210/2 | 3 | 4500 | 2707 | 3 | 2 |
| 210/2 | 4 | 4250 | 2718 | 4 | 3 |
| 210/2 | 5 | 4000 | 2724 | 5 | 4 |
| 210/2 | 6 | 3750 | 2717 | 6 | 5 |
| 210/2 | 7 | 3500 | 2706 | 7 | 6 |
| 210/2 | 8 | 3250 | 2705 | 8 | 7 |
| 210/2 | 9 | 3000 | 2713 | 9 | 8 |
| 210/2 | 10 | 2600 | 2709 | 10 | 9 |
| 210/2 | 11 | 2300 | 2708 | 11 | 10 |
| 210/2 | 12 | 2000 | 2715 | 12 | --- |
| 210/2 | 13 | 1500 | 2730 | 13 | 11 |
| 210/2 | 14 | 1000 | 2723 | 14 | 12 |
| 210/2 | 15 | 750 | 2728 | 15 | --- |
| 210/2 | 16 | 500 | 2721 | 16 | 13 |
| 210/2 | 17 | 300 | 2710 | 17 | --- |
| 210/2 | 18 | 200 | 2719 | 18 | 14 |
| 210/2 | 19 | 100 | 2729 | 19 | 15 |
| 210/2 | 21 | 100 | 2722 | 20 | 16 |
| 211/3 | 1 | 4590 | 2754 | 21 | --- |
| 211/3 | 2 | 4520 | 2741 | 22 | --- |
| 211/3 | 3 | 4500 | 2744 | 23 | --- |
| 211/3 | 4 | 4250 | 2742 | 24 | --- |
| 211/3 | 5 | 4000 | 2743 | 25 | --- |
| 212/4 | 1 | 4480 | 2731 | 26 | 17 |
| 212/4 | 2 | 4430 | 2732 | 27 | --- |
| 212/4 | 3 | 4400 | 2733 | 28 | 18 |
| 212/4 | 4 | 4250 | 2735 | 29 | 19 |
| 212/4 | 5 | 4000 | 2727 | 30 | 20 |
| 212/4 | 6 | 3750 | 2726 | 31 | 21 |
| 212/4 | 7 | 3500 | 2738 | 32 | 22 |
| 212/4 | 8 | 3250 | 2737 | 33 | 23 |
| 212/4 | 9 | 3000 | 2734 | 34 | 24 |
| 212/4 | 10 | 2600 | 2736 | 35 | 25 |
| 212/4 | 11 | 2300 | 2720 | 36 | 26 |
| 212/4 | 12 | 2000 | 2725 | 37 | --- |
| 212/4 | 13 | 1500 | 2739 | 38 | 27 |
| 212/4 | 14 | 1000 | 2747 | 39 | 28 |
| 212/4 | 15 | 750 | 2740 | 40 | 29 |
| 212/4 | 16 | 500 | 2748 | 41 | 30 |
| 212/4 | 17 | 300 | 2764 | 42 | --- |
| 212/4 | 18 | 200 | 2752 | 43 | 31 |
| 212/4 | 19 | 100 | 2751 | --- | --- |
| 212/4 | 21 | 100 | 2750 | 44 | 32 |
| 213/5 | 1 | 4070 | 2753 | 45 | --- |
| 213/5 | 2 | 4020 | 2756 | --- | --- |
| 213/5 | 3 | 4000 | 2772 | 46 | --- |
| 213/5 | 4 | 3800 | 2745 | 47 | --- |
| 213/5 | 5 | 3600 | 2765 | 48 | --- |
| 214/6 | 1 | 3812 | 2774 | 49 | --- |
| 214/6 | 2 | 3750 | 2773 | 50 | --- |
| 214/6 | 3 | 3600 | 2771 | 51 | --- |
| 214/6 | 5 | 3200 | 2768 | 52 | --- |
| 214/6 | 5 | 3200 | 2770,2768 | 53 | --- |
| 214/6 | 6 | 3000 | 2775 | 54 | --- |
| 214/6 | 7 | 2750 | 2755 | 55 | --- |
| 214/6 | 8 | 2500 | 2759 | 55 | --- |
| 214/6 | 9 | 2250 | 2760 | 56 | --- |
| 214/6 | 10 | 2000 | 2758 | 57 | --- |
| 214/6 | 11 | 1600 | 2761 | 58 | --- |
| 214/6 | 12 | 1300 | 2757 | 59 | --- |
| 214/6 | 13 | 1000 | 2782 | 59 | --- |
| 214/6 | 14 | 800 | 2783 | 60 | --- |
| 214/6 | 16 | 500 | 2746,2781 | 61 | --- |
| 214/6 | 17 | 350 | 2766 | 62 | --- |
| 214/6 | 18 | 250 | 2767 | 63 | --- |
| 214/6 | 19 | 150 | 2769 | 64 | --- |
| 214/6 | 21 | 100 | 2763 | 65 | --- |
| 215/7 | 1 | 4853 | 2787 | 66 | 33 |
| 215/7 | 2 | 4800 | 2791 | 67 | 34 |
| 215/7 | 3 | 4500 | 2792 | 68 | 35 |
| 215/7 | 4 | 4250 | 2788 | 69 | 36 |
| 215/7 | 5 | 4000 | 2798 | 70 | --- |
| 215/7 | 6 | 3750 | 2789 | 71 | 37 |
| 215/7 | 7 | 3500 | 2780 | 72 | --- |
| 215/7 | 8 | 3250 | 2779 | 73 | 38 |
| 215/7 | 9 | 3000 | 2790 | 74 | --- |
| 215/7 | 10 | 2600 | 2762 | 75 | 39 |
| 215/7 | 11 | 2300 | 2778 | 76 | --- |
| 215/7 | 12 | 2000 | 2777 | 77 | 40 |
| 215/7 | 13 | 1500 | 2801 | 78 | 41 |
| 215/7 | 14 | 1000 | 2802 | 79 | 42 |
| 215/7 | 15 | 750 | 2784 | 80 | --- |
| 215/7 | 16 | 500 | 2785 | 81 | 43 |
| 215/7 | 17 | 300 | 2793 | 82 | 44 |
| 215/7 | 18 | 200 | 2786 | 83 | 45 |
| 215/7 | 19 | 100 | 2803 | 84 | 46 |
| 215/7 | 21 | 100 | 2800 | 85 | 47 |
| 216/8 | 1 | 4380 | 2611 | 86 | 48 |
| 216/8 | 2 | 4350 | 2606 | 87 | 49 |
| 216/8 | 3 | 4300 | 2629 | 88 | 50 |
| 216/8 | 4 | 4150 | 2607 | 89 | 51 |
| 216/8 | 5 | 4000 | 2609 | 90 | --- |
| 216/8 | 6 | 3800 | 2608 | 91 | --- |
| 216/8 | 7 | 3500 | 2797,2612 | 92 | --- |
| 216/8 | 8 | 325 | 2605 | 93 | --- |
| 216/8 | 9 | 3000 | 2621 | 94 | --- |

Table 5 continued

| Station/ Profile | Bottle | Depth [m] | CFC-ampoule # | Helium-sample # | Tritium-sample # |
|---|---|---|---|---|---|
| 216/8 | 10 | 2600 | 2610 | 95 | --- |
| 216/8 | 11 | 2300 | 2609 | 96 | --- |
| 216/8 | 12 | 2000 | 2604 | 97 | --- |
| 216/8 | 13 | 1500 | 2619 | 98 | --- |
| 216/8 | 14 | 1000 | 2616 | 99 | --- |
| 216/8 | 15 | 750 | 2615 | 100 | --- |
| 216/8 | 16 | 500 | 2618 | 101 | --- |
| 216/8 | 17 | 500 | 2617 | 102 | --- |
| 216/8 | 18 | 200 | 2620 | 103 | --- |
| 216/8 | 19 | 100 | 2613 | 104 | --- |
| 216/8 | 20 | 500 | 2614 | 105 | --- |
| 216/8 | 21 | 100 | 2628 | 105 | --- |
| 217/9 | 1 | 4215 | 2626 | 106 | 52 |
| 217/9 | 2 | 4100 | 2627 | 107 | --- |
| 217/9 | 3 | 4000 | 2794 | 108 | 53 |
| 217/9 | 4 | 3750 | 2799 | 109 | 54 |
| 217/9 | 5 | 3500 | 2795 | 110 | 55 |
| 217/9 | 6 | 3250 | 2796 | 111 | --- |
| 217/9 | 7 | 3000 | 2625 | 112 | 56 |
| 217/9 | 8 | 2600 | 2624 | 113 | 57 |
| 217/9 | 9 | 2300 | 2623 | 114 | --- |
| 217/9 | 10 | 2000 | 2630 | 115 | 58 |
| 217/9 | 11 | 1600 | 2631 | 116 | --- |
| 217/9 | 12 | 1300 | 2632 | 117 | 59 |
| 217/9 | 13 | 1000 | 2636 | 118 | --- |
| 217/9 | 14 | 800 | 2639 | 119 | 60 |
| 217/9 | 15 | 600 | 2640 | 120 | --- |
| 217/9 | 16 | 400 | 2637 | --- | 61 |
| 217/9 | 17 | 300 | 2638 | 121 | --- |
| 217/9 | 18 | 200 | 2649 | --- | 62 |
| 217/9 | 19 | 100 | 2642 | 122 | 63 |
| 217/9 | 20 | 500 | --- | --- | 64 |
| 217/9 | 21 | 100 | 2634 | 123 | 65 |
| 218/10 | 1 | 5150 | 2657 | 124 | 66 |
| 218/10 | 2 | 5100 | 2654 | 125 | --- |
| 218/10 | 3 | 5000 | 2646 | 126 | 67 |
| 218/10 | 4 | 4750 | 2648 | 127 | --- |
| 218/10 | 5 | 4500 | 2644 | 128 | 68 |
| 218/10 | 6 | 4250 | 2643 | 129 | --- |
| 218/10 | 7 | 4000 | 2650 | 130 | 69 |
| 218/10 | 8 | 3600 | 2655 | 131 | --- |
| 218/10 | 9 | 3300 | 2653 | 132 | 70 |
| 218/10 | 10 | 3000 | 2666 | 133 | --- |
| 218/10 | 11 | 2600 | 2673 | 143 | 71 |
| 218/10 | 12 | 2300 | 2671 | 135 | --- |
| 218/10 | 13 | 2000 | 2659 | 136 | 72 |
| 218/10 | 14 | 1500 | 2658 | 137 | 73 |
| 218/10 | 15 | 1000 | 2656 | 138 | 74 |
| 218/10 | 16 | 750 | 2661 | 139 | 75 |
| 218/10 | 16 | 750 | --- | 144 | --- |
| 218/10 | 17 | 500 | 2652 | 140 | --- |
| 218/10 | 18 | 300 | 2645 | 141 | 76 |
| 218/10 | 18 | 300 | --- | --- | 78 |
| 218/10 | 19 | 200 | 2651 | 142 | 79 |
| 218/10 | 20 | 500 | 2668 | --- | 80 |
| 218/10 | 21 | 100 | 2670 | 143 | 81 |
| 219/11 | 1 | 3890 | 2663 | 145 | 82 |
| 219/11 | 2 | 3750 | 2664 | 146 | --- |
| 219/11 | 3 | 3600 | 2667 | 147 | --- |
| 219/11 | 4 | 3400 | 2666 | 148 | 83 |
| 219/11 | 5 | 3200 | 2669 | 149 | --- |
| 219/11 | 6 | 3000 | 2662 | 150 | 84 |
| 219/11 | 7 | 2750 | 2676 | 151 | --- |
| 219/11 | 8 | 2500 | 2680 | --- | 85 |
| 219/11 | 9 | 2250 | 2681 | 152 | --- |
| 219/11 | 10 | 2000 | 2682 | 153 | 86 |
| 219/11 | 11 | 1600 | 2665 | 154 | --- |
| 219/11 | 12 | 1300 | 2674 | 155 | 87 |
| 219/11 | 13 | 1000 | 2690 | --- | --- |
| 219/11 | 14 | 800 | 2691 | 156 | 88 |
| 219/11 | 15 | 600 | 2692 | --- | --- |
| 219/11 | 16 | 500 | 2693,2676 | 157 | 89 |
| 219/11 | 17 | 300 | 2677 | --- | --- |
| 219/11 | 18 | 200 | 2678 | 158 | 90 |
| 219/11 | 19 | 100 | 2675 | 159 | --- |
| 219/11 | 20 | 500 | 2689 | --- | --- |
| 219/11 | 21 | 100 | 2687 | 160 | 91 |
| 220/12 | 1 | 3890 | 2688 | 161 | --- |
| 220/12 | 2 | 3750 | 2699 | --- | --- |
| 220/12 | 3 | 3600 | 2696 | 162 | --- |
| 220/12 | 4 | 3400 | 2694 | --- | --- |
| 220/12 | 5 | 3200 | 2697 | --- | --- |
| 220/12 | 6 | 3000 | 2683 | 163 | --- |
| 220/12 | 7 | 2750 | 2698 | --- | --- |
| 220/12 | 8 | 2500 | 2686 | 164 | --- |
| 220/12 | 9 | 2250 | 2701 | --- | --- |
| 220/12 | 10 | 2000 | 2685 | 165 | --- |
| 220/12 | 11 | 1600 | 2700 | --- | --- |
| 220/12 | 12 | 1300 | 2703 | --- | --- |
| 220/12 | 13 | 1000 | 2508 | 166 | --- |
| 220/12 | 14 | 800 | 2506 | --- | --- |
| 220/12 | 15 | 600 | 2505 | ---- | --- |
| 220/12 | 16 | 500 | 2504 | 167 | --- |
| 220/12 | 17 | 300 | 2511,2684 | --- | --- |
| 220/12 | 18 | 200 | 2702 | --- | --- |
| 220/12 | 19 | 100 | 2509 | ---- | --- |
| 220/12 | 20 | 500 | 2507 | ---- | --- |
| 220/12 | 21 | 100 | 2510 | 168 | --- |
| 221/13 | 1 | 3170 | 2522 | 169 | --- |
| 221/13 | 2 | 3100 | 2521 | --- | --- |
| 221/13 | 3 | 3000 | 2520 | 170 | --- |
| 221/13 | 4 | 2750 | 2523 | 171 | --- |
| 221/13 | 5 | 2500 | 2513 | 172 | --- |
| 221/13 | 6 | 2250 | 2512 | 173 | --- |
| 221/13 | 7 | 2000 | 2518 | 174 | --- |
| 221/13 | 8 | 1750 | 2516 | 175 | --- |
| 221/13 | 8 | 1750 | --- | 176 | --- |
| 221/13 | 9 | 1500 | 2514 | --- | --- |
| 221/13 | 10 | 1250 | 2515 | --- | --- |
| 221/13 | 11 | 1000 | 2525 | --- | --- |
| 221/13 | 12 | 800 | 2527,2530 | --- | --- |
| 221/13 | 13 | 700 | 2528 | --- | --- |
| 221/13 | 14 | 600 | 2526 | --- | --- |
| 221/13 | 15 | 500 | 2524 | --- | --- |
| 221/13 | 16 | 400 | 2517 | --- | --- |
| 221/13 | 17 | 300 | 2519 | --- | --- |
| 221/13 | 18 | 200 | 2529 | --- | --- |
| 221/13 | 19 | 100 | 2531 | --- | --- |
| 221/13 | 20 | 50 | 2532 | --- | --- |
| 221/13 | 21 | 10 | 2533 | --- | --- |
| 225/14 | 1 | 2750 | 2537 | 177 | 92 |
| 225/14 | 2 | 2700 | 2540 | 178 | --- |
| 225/14 | 3 | 2500 | 2539 | 179 | 93 |
| 225/14 | 4 | 2250 | 2541 | 180 | --- |
| 225/14 | 5 | 2000 | 2543 | 181 | 94 |
| 225/14 | 6 | 1750 | 2542 | 182 | --- |
| 225/14 | 7 | 1500 | 2538 | 183 | 95 |
| 225/14 | 8 | 1250 | 2535 | 184 | --- |
| 225/14 | 9 | 1000 | 2536 | 185 | 96 |
| 225/14 | 10 | 1000 | 2534 | 186 | --- |
| 225/14 | 10 | 1000 | --- | --- | --- |
| 225/14 | 11 | 900 | 2544 | --- | --- |
| 225/14 | 12 | 800 | 2545 | --- | 97 |
| 225/14 | 13 | 700 | 2551 | 187 | --- |
| 225/14 | 14 | 600 | 2560 | --- | 98 |
| 225/14 | 15 | 500 | 2549 | --- | 98 |
| 225/14 | 16 | 400 | 2548 | --- | 99 |
| 225/14 | 17 | 300 | 2547 | 189 | --- |

Table 5 continued

| Station/ Profile | Bottle | Depth [m] | CFC-ampoule # | Helium-sample # | Tritium-sample # |
|---|---|---|---|---|---|
| 225/14 | 18 | 200 | 2546 | --- | 100 |
| 225/14 | 19 | 100 | 2552 | 190 | 101 |
| 225/14 | 20 | 50 | 2553 | --- | --- |
| 225/14 | 21 | 10 | 2563 | 191 | 102 |
| 226/15 | 1 | 3997 | 2571 | 192 | --- |
| 226/15 | 2 | 3900 | --- | 193 | --- |
| 226/15 | 3 | 2600 | 2572 | 194 | --- |
| 226/15 | 4 | 3400 | 2573 | 195 | --- |
| 226/15 | 5 | 3200 | --- | 196 | --- |
| 226/15 | 6 | 3000 | 2555 | 197 | --- |
| 226/15 | 7 | 2750 | 2554 | --- | --- |
| 226/15 | 8 | 2500 | 2557 | 198 | --- |
| 226/15 | 8 | 2500 | --- | 199 | --- |
| 226/15 | 9 | 2250 | 2550 | --- | --- |
| 226/15 | 10 | 2000 | 2563 | --- | --- |
| 226/15 | 11 | 1600 | 2561 | --- | --- |
| 226/15 | 12 | 1300 | 2558 | --- | --- |
| 226/15 | 13 | 1000 | 2559 | --- | --- |
| 226/15 | 14 | 750 | 2556 | --- | --- |
| 226/15 | 15 | 750 | 2565 | --- | --- |
| 226/15 | 16 | 500 | 2566,2567 | --- | --- |
| 226/15 | 17 | 300 | 2568 | --- | --- |
| 226/15 | 18 | 200 | 2569 | ---- | --- |
| 226/15 | 19 | 100 | 2570 | --- | --- |
| 226/15 | 20 | 50 | 2575 | --- | --- |
| 226/15 | 21 | 10 | 2574 | | |
| 229/16 | 1 | 3790 | 2588 | 200 | --- |
| 229/16 | 3 | 3400 | 2596 | 201 | --- |
| 229/16 | 3 | 3400 | --- | 202 | --- |
| 229/16 | 4 | 3200 | 2590 | 203 | --- |
| 229/16 | 5 | 3000 | 2591 | 204 | --- |
| 229/16 | 6 | 2700 | 2593 | --- | --- |
| 229/16 | 7 | 2500 | 2592 | --- | --- |
| 229/16 | 8 | 2250 | 2564 | --- | --- |
| 229/16 | 9 | 2000 | 2579 | --- | --- |
| 229/16 | 10 | 1600 | 2578 | --- | --- |
| 229/16 | 11 | 1300 | 2581 | --- | --- |
| 229/16 | 12 | 1000 | 2580 | --- | --- |
| 229/16 | 13 | 750 | 2583 | 205 | --- |
| 229/16 | 15 | 500 | 2584 | 204 | --- |
| 229/16 | 16 | 300 | 2585 | 204 | --- |
| 229/16 | 17 | 200 | 2586,2587 | 204 | --- |
| 229/16 | 18 | 100 | 2577 | 204 | --- |
| 229/16 | 19 | 50 | 2576 | 204 | --- |
| 229/16 | 20 | 10 | 2594 | 204 | --- |
| 231/17 | 1 | 4375 | 2603 | --- | --- |
| 231/17 | 2 | 4300 | 2598 | --- | --- |
| 231/17 | 3 | 4200 | 2595 | --- | --- |
| 231/17 | 5 | 4000 | 2601 | --- | --- |
| 231/17 | 6 | 3800 | 2600 | --- | --- |
| 231/17 | 7 | 3500 | 2808 | --- | --- |
| 231/17 | 8 | 3250 | 2807 | --- | --- |
| 231/17 | 9 | 3000 | 2806 | --- | --- |
| 231/17 | 10 | 2600 | 2805 | --- | --- |
| 231/17 | 11 | 2300 | 2804 | --- | --- |
| 231/17 | 12 | 2000 | 2811 | --- | --- |
| 231/17 | 13 | 1500 | 2602 | --- | --- |
| 231/17 | 14 | 1000 | 2597 | --- | --- |
| 231/17 | 15 | 750 | 2599 | --- | --- |
| 231/17 | 16 | 500 | 2809 | --- | --- |
| 231/17 | 17 | 300 | 2810 | --- | --- |
| 231/17 | 18 | 200 | 2812 | --- | --- |
| 231/17 | 19 | 100 | 2813 | --- | --- |
| 231/17 | 20 | 50 | 2815,2819 | --- | --- |
| 231/17 | 21 | 10 | 2814 | --- | --- |
| 232/18 | 1 | 4523 | 2839,2825 | 206 | 103 |
| 232/18 | 2 | 4300 | 2824 | 207 | 104 |
| 232/18 | 3 | 4000 | 2836 | 208 | 105 |

| Station/ Profile | Bottle | Depth [m] | CFC-ampoule # | Helium-sample # | Tritium-sample # |
|---|---|---|---|---|---|
| 232/18 | 4 | 3500 | 2835 | 209 | 106 |
| 232/18 | 5 | 3000 | 2832 | 210 | 107 |
| 232/18 | 6 | 2500 | 2830 | 211 | 108 |
| 232/18 | 7 | 2000 | 2816 | 212 | 109 |
| 232/18 | 8 | 1500 | 2817 | 213 | --- |
| 232/18 | 9 | 1250 | 2820 | 214 | --- |
| 232/18 | 10 | 1000 | 2822 | 215 | 110 |
| 232/18 | 11 | 750 | 2832 | 216 | --- |
| 232/18 | 12 | 500 | 2829 | 217 | --- |
| 232/18 | 13 | 300 | 2818 | 218 | 112 |
| 232/18 | 13 | 300 | --- | 219 | --- |
| 232/18 | 14 | 200 | 2821 | 220 | 113 |
| 232/18 | 15 | 150 | 2833 | --- | --- |
| 232/18 | 17 | 100 | 2831 | 221 | 115 |
| 232/18 | 17 | 100 | --- | --- | 114 |
| 232/18 | 19 | 50 | 2834 | --- | --- |
| 232/18 | 21 | 10 | 2827 | 222 | 116 |
| 233/19 | 1 | 4200 | 2856 | 223 | 117 |
| 233/19 | 2 | 4100 | 2860 | 224 | 118 |
| 233/19 | 3 | 4000 | 2854 | 225 | 119 |
| 233/19 | 4 | 3750 | 2855 | 226 | 227 |
| 233/19 | 5 | 3500 | 2837 | 227 | 121 |
| 233/19 | 6 | 3250 | 2838 | --- | --- |
| 233/19 | 7 | 3000 | 2841 | --- | --- |
| 233/19 | 8 | 2600 | 2826 | --- | --- |
| 233/19 | 9 | 2300 | 2840 | --- | --- |
| 233/19 | 10 | 2000 | 2828 | --- | --- |
| 233/19 | 11 | 1600 | 2842 | --- | --- |
| 233/19 | 12 | 1300 | 2843 | --- | --- |
| 233/19 | 13 | 1000 | 2857 | --- | --- |
| 233/19 | 14 | 800 | 2853 | --- | --- |
| 233/19 | 15 | 600 | 2858 | --- | --- |
| 233/19 | 16 | 400 | 2880 | --- | --- |
| 233/19 | 17 | 300 | 2852 | --- | --- |
| 233/19 | 18 | 200 | 2845 | --- | --- |
| 233/19 | 19 | 100 | 2851 | --- | --- |
| 233/19 | 20 | 50 | 2876 | --- | --- |
| 233/19 | 21 | 10 | 2859 | --- | --- |
| 234/20 | 1 | 3866 | 2850 | --- | --- |
| 234/20 | 2 | 3790 | 2847 | --- | --- |
| 234/20 | 3 | 3600 | 2874 | --- | --- |
| 234/20 | 4 | 3400 | 2873 | --- | --- |
| 234/20 | 5 | 3200 | 2877 | --- | --- |
| 234/20 | 6 | 3000 | 2864 | --- | --- |
| 234/20 | 7 | 2750 | 2849 | --- | --- |
| 234/20 | 8 | 2500 | 2848 | --- | --- |
| 234/20 | 9 | 2250 | 2846 | --- | --- |
| 234/20 | 10 | 2000 | 2844 | --- | --- |
| 234/20 | 11 | 1600 | 2862 | --- | --- |
| 234/20 | 12 | 1300 | 2861 | --- | --- |
| 234/20 | 13 | 1000 | 2863 | --- | --- |
| 234/20 | 14 | 800 | 2882 | --- | --- |
| 234/20 | 15 | 600 | 2865 | --- | --- |
| 234/20 | 16 | 500 | 2866 | --- | --- |
| 234/20 | 17 | 300 | 2878 | --- | --- |
| 234/20 | 18 | 200 | 2883 | --- | --- |
| 234/20 | 19 | 100 | 2884 | --- | --- |
| 234/20 | 20 | 50 | 2867 | --- | --- |
| 234/20 | 21 | 10 | 2875 | --- | --- |
| 235/21 | 1 | 3950 | 2885 | 228 | 122 |
| 235/21 | 2 | 3900 | 2886 | 229 | --- |
| 235/21 | 3 | 3600 | 2888 | 230 | 123 |
| 235/21 | 3 | 3600 | --- | 231 | --- |
| 235/21 | 4 | 3400 | 2889 | 232 | 124 |
| 235/21 | 5 | 3200 | 2892 | 233 | 125 |
| 235/21 | 6 | 3000 | 2891 | 234 | --- |
| 235/21 | 7 | 2750 | 2869 | 235 | 126 |
| 235/21 | 8 | 2500 | 2870 | 236 | --- |
| 235/21 | 9 | 2250 | 2871 | 237 | 127 |

Table 5 continued

| Station/ Profile | Bottle | Depth [m] | CFC-ampoule # | Helium-sample # | Tritium-sample # |
|---|---|---|---|---|---|
| 235/21 | 10 | 2000 | 2872 | --- | --- |
| 235/21 | 11 | 1600 | 2881 | 238 | 128 |
| 235/21 | 12 | 1300 | 2879 | --- | --- |
| 235/21 | 13 | 1000 | 2890 | --- | 129 |
| 235/21 | 14 | 750 | 2887 | 239 | 131 |
| 235/21 | 16 | 500 | 2903,2893 | 240 | 132 |
| 235/21 | 17 | 300 | 2895 | --- | --- |
| 235/21 | 18 | 200 | 2894 | 241 | 133 |
| 235/21 | 19 | 100 | 2896 | --- | --- |
| 235/21 | 20 | 50 | 2897 | 242 | 134 |
| 235/21 | 21 | 10 | 2898 | --- | --- |
| 236/22 | 1 | 3857 | 2407 | --- | 135 |
| 236/22 | 2 | 3750 | 2414 | --- | --- |
| 236/22 | 3 | 3600 | 2405 | --- | --- |
| 236/22 | 4 | 3400 | 2900 | --- | 136 |
| 236/22 | 5 | 3200 | 2901 | --- | --- |

| Station/ Profile | Bottle | Depth [m] | CFC-ampoule # | Helium-sample # | Tritium-sample # |
|---|---|---|---|---|---|
| 236/2 | 6 | 3000 | 2902 | --- | 137 |
| 236/22 | 7 | 2750 | 2406 | --- | --- |
| 236/22 | 8 | 2500 | 2408 | --- | --- |
| 236/22 | 9 | 2250 | 2410 | --- | 138 |
| 236/22 | 10 | 2000 | 2412 | --- | --- |
| 236/22 | 11 | 1600 | 2411 | --- | --- |
| 236/22 | 12 | 1300 | 2414,2404 | --- | 139 |
| 236/22 | 13 | 1000 | 2413 | --- | --- |
| 236/22 | 14 | 800 | 2416 | --- | 140 |
| 236/22 | 15 | 600 | 2415 | --- | --- |
| 236/22 | 16 | 500 | 2418 | --- | --- |
| 236/22 | 17 | 300 | 2417 | --- | 141 |
| 236/22 | 18 | 200 | 2420 | --- | --- |
| 236/22 | 19 | 100 | 2419 | --- | --- |
| 236/22 | 20 | 50 | 2428 | --- | 142 |

## 4.3 Water Sampling for Analyses of Stable Isotopes and Nutrients

(B. Jahn, T. Lützeler, A. Meyer, C. Moos, T. Westerhold)

At 21 stations a rosette with 21 10 l Niskin bottles was used to obtain water samples from various depths of the water column. The rosette was always combined with a CTD-profiler for temperature and salinity measurements. At four stations a second rosette with 18 10 l Niskin bottles was additionally used for water sampling in the upper water column between 0 and 250 m. All sites and sampling depths are listed in detail in Table 6. All water samples will be used for the analysis of stable carbon and oxygen isotopes ($\delta^{13}C$, $\delta^{18}O$) and nutrients.

For carbon isotopes, 2 x 50 ml of sea water was carefully filled into brown bottles to minimise degassing of dissolved $CO_2$ and to avoid exchange between water and atmosphere and was poisoned with 1 ml saturated $HgCl_2$ solution. All samples were closed airtight with melted paraffin. Water samples for oxygen isotope measurements were handled similarly, but were not poisoned. For nutrient analyses, 150 ml of sea water were filled into lighttight NALGENE polycarbonate flasks and immediately frozen at -20°C. Measurements for stable isotopes and phosphate concentration will be carried out at Bremen University.

Each site was chosen to represent one of five different hydrographic conditions. The first site (GeoB 5101) was located near Geosecs stations 57 and 60. This site will be used to calibrate samples from the lower water column and to check anthropogenic increase of $^{12}C$ in surface waters. The five sites (GeoB 5103 to 5110) are located in the central and north-western Vema Channel to study the flow of AABW (Antarctic Bottom Water) from the Argentine into the Brazil Basin. A west-east transect of eight stations was chosen at 24°S from the Brazil Basin into the Angola Basin (GeoB 5111 to 5124). The overflow of deep and bottom water masses over the Mid-Atlantic Ridge into the Angola Basin between 24°S and 20°S will be studied at four sites at 9°W. Sampling depths of some sites, especially at 19°S, were taken to study the isotopic composition of Antarctic Intermediate Water. Site GeoB 5129 was chosen to get detailed information on the dependence of carbon isotope composition and nutrient supply to surface waters and into the thermocline. Water samples for tracer-oceanographic measurements were taken at most sites (see Chapter 4.2).

Table 6 Depths [dbar] of water samples for stable isotopes and nutrients

| | | **Brazil Basin Vema Channel** | | | | | | | **Brazil Basin Transect 24°S** | | | | | |
|---|---|---|---|---|---|---|---|---|---|---|---|---|---|---|
| **GeoB** | **5101-1** | **5103-1** | **5103-2** | **5105-1** | **5108-1** | **5109-1** | **5110-1** | **5110-4** | **5111-1** | **5112-1** | **5112-2** | **5113-1** | **5114-1** | **5118-1** |
| **Meteor #** | **208** | **210** | **210** | **212** | **215** | **216** | **217** | **217** | **218** | **219** | **219** | **220** | **221** | **225** |
| **bottle 1** | 4421 | 4659 | 200 | 4520 | 4853 | 4381 | 4231 | 200 | 5285 | 3893 | 200 | 3880 | 3195 | 2778 |
| **2** | 4301 | 4610 | 150 | 4501 | 4800 | 4351 | 4101 | 150 | 5202 | 3751 | 150 | 3801 | 3100 | 2731 |
| **3** | 4000 | 4500 | 100 | 4401 | 4499 | 4302 | 4001 | 100 | 5000 | 3602 | | 3601 | 3000 | 2499 |
| **4** | 3501 | 4250 | | 4300 | 4250 | 4151 | 3750 | | 4750 | 3401 | 120 | 3402 | 2750 | 2250 |
| **5** | 3001 | 4001 | | 4150 | 3999 | 3999 | 3501 | | 4502 | 3199 | | 3200 | 2500 | 2000 |
| **6** | 2501 | 3748 | | 4000 | 3751 | 3800 | 3250 | | 4252 | 3001 | | 3000 | 2249 | 1751 |
| **7** | 2001 | 3500 | 50 | 3745 | 3500 | 3501 | 3001 | 50 | 4002 | 2750 | 100 | 2750 | 2001 | 1500 |
| **8** | 1501 | 3250 | | 3500 | 3250 | 3251 | 2601 | | 3602 | 2501 | | 2501 | 1743 | 1249 |
| **9** | 1251 | 2999 | | 3250 | 3000 | 3001 | 2301 | | 3301 | 2250 | | 2251 | 1500 | 1002 |
| **10** | 1001 | 2600 | | 3000 | 2601 | 2601 | 2001 | | 3002 | 2001 | 50 | 2001 | 1250 | |
| **11** | 751 | 2300 | 20 | 2599 | 2300 | 2301 | 1601 | 20 | 2602 | 1599 | | 1601 | 1000 | 901 |
| **12** | 502 | 2001 | | 2299 | 2000 | 2000 | 1301 | | 2302 | 1300 | | 1300 | 799 | 800 |
| **13** | 301 | 1501 | | 2001 | 1500 | 1501 | 999 | | 2001 | 999 | 20 | 1000 | 701 | 699 |
| **14** | 201 | 999 | | 1500 | 1001 | 1000 | 801 | | 1501 | 800 | | 801 | 600 | 595 |
| **15** | 152 | 750 | | 999 | 749 | 750 | 601 | 10 | 1001 | 600 | | 600 | 501 | 400 |
| **16** | 127 | 501 | 10 | 749 | 500 | 500 | 400 | | 750 | 501 | 10 | 501 | 400 | 300 |
| **17** | 101 | 301 | | 499 | 300 | 300 | 301 | | 503 | 300 | | 299 | 300 | 199 |
| **18** | 76 | 202 | | 300 | 200 | 200 | 200 | | 301 | 200 | | 200 | 200 | 100 |
| **19** | 51 | 100 | | 199 | 100 | 101 | 100 | | 201 | 99 | | 101 | 100 | 50 |
| **20** | 26 | 10 | | 49 | 10 | 51 | 49 | | 50 | 49 | | 51 | 50 | 10 |
| **21** | 10 | | | 10 | | 10 | 11 | | 11 | 9 | | 10 | 10 | |

| | **Angola Basin Transect 24°S** | | | | **Angola Basin Transect 9°W** | | | | **Angola - Brazil Basin Transect 19°S** | | |
|---|---|---|---|---|---|---|---|---|---|---|---|
| **GeoB** | **5119-1** | **5119-2** | **5122-1** | **5124-4** | **5125-1** | **5126-1** | **5127-1** | **5128-1** | **5129-2** | **5136-3** | **5141-1** |
| **Meteor #** | **226** | **226** | **229** | **231** | **232** | **233** | **234** | **235** | **236** | **243** | **248** |
| **bottle 1** | 3997 | 200 | 3756 | 4375 | 4523 | 4231 | 3866 | 3954 | 250 | 1500 | 1200 |
| **2** | 3902 | 150 | 3699 | 4295 | 4301 | 4101 | 3800 | 3901 | 230 | 1250 | 900 |
| **3** | 3600 | 100 | 3400 | 4201 | 4000 | 4001 | 3600 | 3701 | 200 | 1000 | 700 |
| **4** | 3401 | | 3201 | | 3500 | 3749 | 3400 | 3400 | 170 | 750 | 500 |
| **5** | 3202 | | 3001 | 4000 | 3001 | 3500 | 3200 | 3201 | 150 | 200 | 200 |
| **6** | 3001 | | 2751 | 3800 | 2500 | 3252 | 3000 | 3001 | 120 | 150 | 150 |
| **7** | 2751 | 50 | 2500 | 3501 | 2001 | 3000 | 2751 | 2751 | 100 | 100 | 120 |
| **8** | 2501 | | 2250 | 3251 | 1500 | 2602 | 2499 | 2501 | | | |
| **9** | 2249 | | 2001 | 3000 | 1250 | 2302 | 2250 | 2250 | | | |
| **10** | 2002 | | 1602 | 2600 | 1000 | 1999 | 2001 | 2001 | 75 | 75 | 100 |
| **11** | 1601 | 20 | 1300 | 2300 | 750 | 1600 | 1601 | 1600 | | | |
| **12** | 1300 | | 1000 | 2000 | 500 | 1300 | 1301 | 1300 | | | |
| **13** | 1001 | | | 1499 | 300 | 1002 | 1001 | 1001 | 50 | 50 | 50 |
| **14** | 800 | | 749 | 1000 | 200 | 802 | 802 | 750 | | | |
| **15** | 600 | | 501 | 749 | 152 | 601 | 600 | 751 | | | |
| **16** | 500 | 10 | 300 | 500 | 126 | 400 | 501 | 500 | 20 | 20 | 20 |
| **17** | 300 | | 200 | 302 | 101 | 301 | 300 | 300 | | | |
| **18** | 201 | | 100 | 200 | 74 | 201 | 201 | 200 | | | |
| **19** | 100 | | 50 | 99 | 51 | 100 | 101 | 102 | 10 | 10 | 10 |
| **20** | 50 | | 12 | 50 | 26 | 50 | 51 | 54 | | | |
| **21** | 11 | | | 10 | 11 | 10 | 10 | 10 | | | |

## 4.4 Planktology

### 4.4.1 Chlorophyll (a)

(B. Jahn, T. Lützeler, H. Kuhlmann)

For the determination of chlorophyll (a) concentrations in the surface waters, 0,5 l of sea water was collected about three times a day from the ship's membrane pump and filtered onto glass fibre filters and frozen at -20°C. Unfortunalety, the first samples taken (no. 1 and 2) were contaminated by some pollution incurred whilst starting the pump. Chlorophyll (a) measurements by photometry will be done in the laboratory at the University of Bremen. 142 samples were taken during the cruise (Table 7). The chlorophyll (a) data will provide information about the seasonal and regional variations in biomass and will also be used to calibrate satellite-derived chlorophyll data.

Table 7 List of surface water samples for chlorophyll (a) measurements

| Sample No. | Date | Time [UTC] | Latitude (S) | Longitude (W) | Depth [m] | Salinity [‰] | Temp. [°C] |
|---|---|---|---|---|---|---|---|
| **1** | 20.04.98 | 10:56 | 40°45,18′ | 027°51,49′ | 3003 | 35,84 | 23,3 |
| **2** | 20.04.98 | 10:56 | 40°45,18′ | 027°51,49′ | 3003 | 35,84 | 23,3 |
| **3** | 20.04.98 | 14:58 | 40°53,88′ | 028°22,14′ | 3409 | 36,51 | 23,7 |
| **4** | 20.04.98 | 14:58 | 40°53,88′ | 028°22,14′ | 3409 | 36,51 | 23,7 |
| **5** | 20.04.98 | 20:59 | 40°51,48′ | 028°32,70′ | 4000 | 36,41 | 23,4 |
| **6** | 20.04.98 | 20:59 | 40°51,48′ | 028°32,70′ | 4000 | 36,41 | 23,4 |
| **7** | 21.04.98 | 10:55 | 39°37,76′ | 030°41,88′ | 4671 | 35,70 | 20,9 |
| **8** | 21.04.98 | 10:55 | 39°37,76′ | 030°41,88′ | 4671 | 35,70 | 20,9 |
| **9** | 21.04.98 | 14:59 | 39°19,70′ | 031°14,00′ | 4560 | 35,70 | 20,8 |
| **10** | 21.04.98 | 14:59 | 39°19,70′ | 031°14,00′ | 4560 | 35,70 | 20,8 |
| **11** | 21.04.98 | 20:58 | 39°23,72′ | 031°12,10′ | 4608 | 35,72 | 20,8 |
| **12** | 21.04.98 | 20:58 | 39°23,72′ | 031°12,10′ | 4608 | 35,72 | 20,8 |
| **13** | 22.04.98 | 10:55 | 38°53,18′ | 030°54,02′ | 3996 | 35,76 | 21,5 |
| **14** | 22.04.98 | 10:55 | 38°53,18′ | 030°54,02′ | 3996 | 35,76 | 21,5 |
| **15** | 22.04.98 | 15:04 | 38°14,09′ | 030°23,07′ | 3639 | 36,12 | 22,4 |
| **16** | 22.04.98 | 15:04 | 38°14,09′ | 030°23,07′ | 3639 | 36,12 | 22,4 |
| **17** | 22.04.98 | 20:55 | 37°19,90′ | 029°39,95′ | 3256 | 36,13 | 21,9 |
| **18** | 22.04.98 | 20:55 | 37°19,90′ | 029°39,95′ | 3256 | 36,13 | 21,9 |
| **19** | 23.04.98 | 10:53 | 35°09,47′ | 027°54,84′ | 4444 | 36,04 | 23,4 |
| **20** | 23.04.98 | 10:53 | 35°09,47′ | 027°54,84′ | 4444 | 36,04 | 23,4 |
| **21** | 23.04.98 | 14:56 | 34°33,20′ | 027°25,25′ | 4318 | 35,90 | 23,3 |
| **22** | 23.04.98 | 14:56 | 34°33,20′ | 027°25,25′ | 4318 | 35,90 | 23,3 |
| **23** | 23.04.98 | 20:53 | 33°55,00′ | 026°54,00′ | 3785 | 36,00 | 23,3 |
| **24** | 23.04.98 | 20:53 | 33°55,00′ | 026°54,00′ | 3785 | 36,00 | 23,3 |
| **25** | 24.04.98 | 10:55 | 34°56,04′ | 026°17,98′ | 4349 | 35,98 | 24,1 |
| **26** | 24.04.98 | 10:55 | 34°56,04′ | 026°17,98′ | 4349 | 35,98 | 24,1 |
| **27** | 24.04.98 | 14:43 | 35°19,11′ | 026°05,12′ | 4235 | 36,46 | 24,9 |
| **28** | 24.04.98 | 14:43 | 35°19,11′ | 026°05,12′ | 4235 | 36,46 | 24,9 |
| **29** | 24.04.98 | 20:58 | 35°38,40′ | 025°54,31′ | 4176 | 36,25 | 24,7 |

Table 7 continued

| Sample No. | Date | Time [UTC] | Latitude (S) | Longitude (W) | Depth [m] | Salinity [‰] | Temp. [°C] |
|---|---|---|---|---|---|---|---|
| **30** | 24.04.98 | 20:58 | 35°38,40′ | 025°54,31′ | 4176 | 36,25 | 24,7 |
| **31** | 25.04.98 | 10:55 | 34°14,81′ | 025°42,77′ | 4624 | 36,33 | 24,9 |
| **32** | 25.04.98 | 10:55 | 34°14,81′ | 025°42,77′ | 4624 | 36,33 | 24,9 |
| **33** | 25.04.98 | 14:44 | 33°26,42′ | 025°36,31′ | 4585 | 36,41 | 24,9 |
| **34** | 25.04.98 | 14:44 | 33°26,42′ | 025°36,31′ | 4585 | 36,41 | 24,9 |
| **35** | 25.04.98 | 20:56 | 32°07,50′ | 025°25,81′ | 4895 | 35,99 | 23,7 |
| **36** | 25.04.98 | 20:56 | 32°07,50′ | 025°25,81′ | 4895 | 35,99 | 23,7 |
| **37** | 26.04.98 | 09:59 | 29°22,09′ | 025°03,72′ | 4984 | 36,54 | 25,7 |
| **38** | 26.04.98 | 09:59 | 29°22,09′ | 025°03,72′ | 4984 | 36,54 | 25,7 |
| **39** | 26.04.98 | 13:46 | 28°33,67′ | 024°57,56′ | 5382 | 36,73 | 25,8 |
| **40** | 26.04.98 | 13:46 | 28°33,67′ | 024°57,56′ | 5382 | 36,73 | 25,8 |
| **41** | 26.04.98 | 19:56 | 27°13,67′ | 024°46,56′ | 6909 | 36,31 | 24,9 |
| **42** | 26.04.98 | 19:56 | 27°13,67′ | 024°46,56′ | 6909 | 36,31 | 24,9 |
| **43** | 27.04.98 | 09:24 | 24°23,85′ | 024°24,22′ | 4467 | 37,03 | 26,3 |
| **44** | 27.04.98 | 09:24 | 24°23,85′ | 024°24,22′ | 4467 | 37,03 | 26,3 |
| **45** | 27.04.98 | 12:55 | 24°21,44′ | 023°54,56′ | 4834 | 36,76 | 25,7 |
| **46** | 27.04.98 | 12:55 | 24°21,44′ | 023°54,56′ | 4834 | 36,76 | 25,7 |
| **47** | 27.04.98 | 18:55 | 24°11,61′ | 022°49,49′ | 4656 | 36,84 | 25,5 |
| **48** | 27.04.98 | 18:55 | 24°11,61′ | 022°49,49′ | 4656 | 36,84 | 25,5 |
| **49** | 28.04.98 | 08:53 | 20°11,79′ | 023°50,44′ | 6610 | 36,78 | 25,3 |
| **50** | 28.04.98 | 08:53 | 20°11,79′ | 023°50,44′ | 6610 | 36,78 | 25,3 |
| **51** | 28.04.98 | 12:53 | 19°59,82′ | 023°48,91′ | 5221 | 36,78 | 25,4 |
| **52** | 28.04.98 | 12:53 | 19°59,82′ | 023°48,91′ | 5221 | 36,78 | 25,4 |
| **53** | 28.04.98 | 19:10 | 18°59,70′ | 023°49,99′ | 6984 | 36,82 | 25,4 |
| **54** | 28.04.98 | 19:10 | 18°59,70′ | 023°49,99′ | 6984 | 36,82 | 25,4 |
| **55** | 29.04.98 | 08:52 | 16°24,17′ | 023°50,58′ | 4037 | 36,67 | 24,7 |
| **56** | 29.04.98 | 08:52 | 16°24,17′ | 023°50,58′ | 4037 | 36,67 | 24,7 |
| **57** | 29.04.98 | 12:55 | 16°16,31′ | 023°49,56′ | 3873 | 36,70 | 24,9 |
| **58** | 29.04.98 | 12:55 | 16°16,31′ | 023°49,56′ | 3873 | 36,70 | 24,9 |
| **59** | 29.04.98 | 18:59 | 16°15,51′ | 023°49,50′ | 3840 | 36,72 | 24,9 |
| **60** | 29.04.98 | 18:59 | 16°15,51′ | 023°49,50′ | 3840 | 36,72 | 24,9 |
| **61** | 30.04.98 | 08:55 | 14°27,04′ | 023°56,53′ | 3692 | 36,50 | 24,3 |
| **62** | 30.04.98 | 08:55 | 14°27,04′ | 023°56,53′ | 3692 | 36,50 | 24,3 |
| **63** | 30.04.98 | 12:54 | 24°09,96′ | 013°59,71′ | 4809 | 36,50 | 24,5 |
| **64** | 30.04.98 | 12:54 | 24°09,96′ | 013°59,71′ | 4809 | 36,50 | 24,5 |
| **65** | 30.04.98 | 18:51 | 13°59,68′ | 024°08,81′ | 3182 | 36,70 | 24,5 |
| **66** | 30.04.98 | 18:51 | 13°59,68′ | 024°08,81′ | 3182 | 36,70 | 24,5 |
| **67** | 01.05.98 | 08:00 | 13°23,03′ | 024°10,81′ | 2733 | 36,70 | 24,3 |
| **68** | 01.05.98 | 08:00 | 13°23,03′ | 024°10,81′ | 2733 | 36,70 | 24,3 |
| **69** | 01.05.98 | 12:51 | 12°54,34′ | 024°10,49′ | 5027 | 36,70 | 24,3 |
| **70** | 01.05.98 | 12:51 | 12°54,34′ | 024°10,49′ | 5027 | 36,70 | 24,3 |
| **71** | 01.05.98 | 19:00 | 12°17,84′ | 024°10,05′ | 3759 | 36,60 | 24,1 |
| **72** | 01.05.98 | 19:00 | 12°17,84′ | 024°10,05′ | 3759 | 36,60 | 24,1 |
| **73** | 02.05.98 | 12:52 | 11°08,16′ | 024°10,22′ | 3691 | 36,51 | 24,1 |
| **74** | 02.05.98 | 12:52 | 11°08,16′ | 024°10,22′ | 3691 | 36,51 | 24,1 |
| **75** | 02.05.98 | 18:48 | 10°53,33′ | 024°10,18′ | 4177 | 36,51 | 24,0 |
| **76** | 02.05.98 | 18:48 | 10°53,33′ | 024°10,18′ | 4177 | 36,51 | 24,0 |
| **77** | 03.05.98 | 08:54 | 09°00,05′ | 024°09,99′ | 4464 | 36,39 | 23,4 |
| **78** | 03.05.98 | 08:54 | 09°00,05′ | 024°09,99′ | 4464 | 36,39 | 23,4 |
| **79** | 03.05.98 | 12:50 | 08°59,99′ | 023°34,80′ | 4026 | 36,39 | 23,6 |
| **80** | 03.05.98 | 12:50 | 08°59,99′ | 023°34,80′ | 4026 | 36,39 | 23,6 |
| **81** | 03.05.98 | 19:11 | 08°59,96′ | 022°23,97′ | 4199 | 36,58 | 23,8 |
| **82** | 03.05.98 | 19:11 | 08°59,96′ | 022°23,97′ | 4199 | 36,58 | 23,8 |
| **83** | 04.05.98 | 08:50 | 09°00,00′ | 020°42,88′ | 3924 | 36,70 | 24,1 |

Table 7 continued

| Sample No. | Date | Time [UTC] | Latitude (S) | Longitude (W) | Depth [m] | Salinity [‰] | Temp. [°C] |
|---|---|---|---|---|---|---|---|
| **84** | 04.05.98 | 08:50 | 09°00,00′ | 020°42,88′ | 3924 | 36,70 | 24,1 |
| **85** | 04.05.98 | 12:50 | 09°00,09′ | 020°01,46′ | 3917 | 36,43 | 23,7 |
| **86** | 04.05.98 | 12:50 | 09°00,09′ | 020°01,46′ | 3917 | 36,43 | 23,7 |
| **87** | 04.05.98 | 18:55 | 09°25,22′ | 019°27,29′ | 3612 | 36,60 | 24,0 |
| **88** | 04.05.98 | 18:55 | 09°25,22′ | 019°27,29′ | 3612 | 36,60 | 24,0 |
| **89** | 05.05.98 | 08:54 | 09°27,52′ | 019°24,23′ | 4165 | 36,59 | 23,9 |
| **90** | 05.05.98 | 08:54 | 09°27,52′ | 019°24,23′ | 4165 | 36,59 | 23,9 |
| **91** | 05.05.98 | 12:50 | 09°45,23′ | 019°04,74′ | 3724 | 36,76 | 24,4 |
| **92** | 05.05.98 | 12:50 | 09°45,23′ | 019°04,74′ | 3724 | 36,76 | 24,4 |
| **93** | 05.05.98 | 18:59 | 09°43,17′ | 019°07,54′ | 3942 | 36,66 | 24,1 |
| **94** | 05.05.98 | 18:59 | 09°43,17′ | 019°07,54′ | 3942 | 36,66 | 24,1 |
| **95** | 06.05.98 | 08:50 | 10°06,03′ | 019°04,65′ | 3363 | 36,66 | 24,1 |
| **96** | 06.05.98 | 08:50 | 10°06,03′ | 019°04,65′ | 3363 | 36,66 | 24,1 |
| **97** | 06.05.98 | 12:50 | 10°11,58′ | 019°05,08′ | 3660 | 36,66 | 24,1 |
| **98** | 06.05.98 | 12:50 | 10°11,58′ | 019°05,08′ | 3660 | 36,66 | 24,1 |
| **99** | 06.05.98 | 18:56 | 10°41,00′ | 019°02,71′ | 3412 | 36,50 | 23,9 |
| **100** | 06.05.98 | 18:56 | 10°41,00′ | 019°02,71′ | 3412 | 36,50 | 23,9 |
| **101** | 07.05.98 | 08:52 | 11°03,76′ | 019°26,14′ | 3304 | 36,51 | 23,9 |
| **102** | 07.05.98 | 08:52 | 11°03,76′ | 019°26,14′ | 3304 | 36,51 | 23,9 |
| **103** | 07.05.98 | 12:36 | 11°31,79′ | 019°25,03′ | 2998 | 36,53 | 24,1 |
| **104** | 07.05.98 | 12:36 | 11°31,79′ | 019°25,03′ | 2998 | 36,53 | 24,1 |
| **105** | 07.05.98 | 18:55 | 12°40,23′ | 019°22,14′ | 3227 | 36,71 | 24,4 |
| **106** | 07.05.98 | 18:55 | 12°40,23′ | 019°22,14′ | 3227 | 36,71 | 24,4 |
| **107** | 08.05.98 | 08:46 | 13°33,88′ | 019°16,32′ | 3287 | 36,77 | 24,6 |
| **108** | 08.05.98 | 08:46 | 13°33,88′ | 019°16,32′ | 3287 | 36,77 | 24,6 |
| **109** | 08.05.98 | 12:46 | 14°23,62′ | 019°12,43′ | 4004 | 36,92 | 25,1 |
| **110** | 08.05.98 | 12:46 | 14°23,62′ | 019°12,43′ | 4004 | 36,92 | 25,1 |
| **111** | 08.05.98 | 18:49 | 14°41,98′ | 019°10,89′ | 3370 | 36,93 | 25,2 |
| **112** | 08.05.98 | 18:49 | 14°41,98′ | 019°10,89′ | 3370 | 36,93 | 25,2 |
| **113** | 09.05.98 | 08:45 | 16°39,26′ | 019°03,14′ | 3699 | 36,83 | 25,0 |
| **114** | 09.05.98 | 08:45 | 16°39,26′ | 019°03,14′ | 3699 | 36,83 | 25,0 |
| **115** | 09.05.98 | 12:43 | 16°36,76′ | 019°03,17′ | 3660 | 36,81 | 25,0 |
| **116** | 09.05.98 | 12:43 | 16°36,76′ | 019°03,17′ | 3660 | 36,81 | 25,0 |
| **117** | 09.05.98 | 19:00 | 17°15,05′ | 019°05,82′ | 3462 | 36,93 | 25,5 |
| **118** | 09.05.98 | 19:00 | 17°15,05′ | 019°05,82′ | 3462 | 36,93 | 25,5 |
| **119** | 10.05.98 | 09:53 | 18°43,12′ | 018°39,06′ | 4456 | 37,03 | 25,4 |
| **120** | 10.05.98 | 09:53 | 18°43,12′ | 018°39,06′ | 4456 | 37,03 | 25,4 |
| **121** | 10.05.98 | 13:02 | 19°01,76′ | 018°34,30′ | 4907 | 37,01 | 25,5 |
| **122** | 10.05.98 | 13:02 | 19°01,76′ | 018°34,30′ | 4907 | 37,01 | 25,5 |
| **123** | 10.05.98 | 19:48 | 19°23,45′ | 018°28,38′ | 4344 | 37,06 | 25,6 |
| **124** | 10.05.98 | 19:48 | 19°23,45′ | 018°28,38′ | 4344 | 37,06 | 25,6 |
| **125** | 11.05.98 | 09:55 | 22°55,42′ | 017°29,83′ | 4857 | 37,21 | 26,3 |
| **126** | 11.05.98 | 09:55 | 22°55,42′ | 017°29,83′ | 4857 | 37,21 | 26,3 |
| **127** | 11.05.98 | 13:44 | 23°31,20′ | 017°20,01′ | --- | 37,32 | 26,5 |
| **128** | 11.05.98 | 13:44 | 23°31,20′ | 017°20,01′ | --- | 37,32 | 26,5 |
| **129** | 11.05.98 | 19:50 | 24°44,98′ | 017°00,03′ | 5708 | 37,32 | 26,8 |
| **130** | 11.05.98 | 19:50 | 24°44,98′ | 017°00,03′ | 5708 | 37,32 | 26,8 |
| **131** | 12.05.98 | 09:57 | 27°26,47′ | 016°14,55′ | 5428 | 37,33 | 27,2 |
| **132** | 12.05.98 | 09:57 | 27°26,47′ | 016°14,55′ | 5428 | 37,33 | 27,2 |
| **133** | 12.05.98 | 14:15 | 28°18,02′ | 016°00,22′ | 5327 | 37,36 | 27,2 |
| **134** | 12.05.98 | 14:15 | 28°18,02′ | 016°00,22′ | 5327 | 37,36 | 27,2 |
| **135** | 12.05.98 | 19:57 | 29°22,16′ | 015°42,28′ | 5783 | 37,42 | 27,2 |
| **136** | 12.05.98 | 19:57 | 29°22,16′ | 015°42,28′ | 5783 | 37,42 | 27,2 |
| **137** | 13.05.98 | 10:50 | 31°36,10′ | 015°04,83′ | 4689 | 37,43 | 28,0 |

Table 7 continued

| Sample No. | Date | Time [UTC] | Latitude (S) | Longitude (W) | Depth [m] | Salinity [‰] | Temp. [°C] |
|---|---|---|---|---|---|---|---|
| **138** | 13.05.98 | 10:50 | 31°36,10′ | 015°04,83′ | 4689 | 37,43 | 28,0 |
| **139** | 13.05.98 | 14:47 | 32°6,72′ | 014°56,29′ | --- | 37,47 | 27,9 |
| **140** | 13.05.98 | 14:47 | 32°6,72′ | 014°56,29′ | --- | 37,47 | 27,9 |
| **141** | 13.05.98 | 20:55 | 33°01,94′ | 014°40,77′ | 4536 | 37,46 | 28,0 |
| **142** | 13.05.98 | 20:55 | 33°01,94′ | 014°40,77′ | 4536 | 37,46 | 28,0 |

### 4.4.2 Coccolithophorids

(R. Höppner, B. Kottke, S. Rath)

Coccolithophorids are biflagellate or coccoid unicells, whose longest dimensions rarely exceed 30 µm and are most often < 10 µm (Heimdal 1993). Over 150 known species of these minute unicellar, autotrophic, marine algae (Prymnesiophyceae) live in the present day oceans (Haq and Boersma 1978). They produce external plates of carbonate, named coccoliths. Coccoliths are a major component in almost all ocean sediments. Their distribution in the sediment is relatively well known, but information on their abundance, ecology and physiology in the surface water is rare. The occurrence and distribution of coccolithophores is directly dependent on the hydrography of the water masses.

With regard to these aspects, an investigation of the living coccolithophore communities in the South Atlantic was carried out in the uppermost water column. The water samples taken during the cruise will allow us a better understanding of the relationship between living communities and the assemblages in the sediments.

At 7 stations, 2 l water samples were taken from Niskin bottles of the rosette at 200 m, 150 m, 100 m, 50 m, 20 m and 10 m water depth (Table 8). In addition, 67 surface water samples were taken by the vessel's membrane pump system at about 5 m water depth during the whole cruise (Table 9) except in the territories off Brazil. Samples were taken about every second longitude plus every latitude, mostly at dawn, high noon and twilight. Generally, 2 liters of the water samples were immediately filtered through cellulose nitrate filters (25 mm diameter, 0,45 µm pore size) by a vacuum pump.

Without washing, rinsing or chemical conservation the filters were dried at 40°C for at least 24 h and then kept permanently dry with silica gel in transparent film to protect them from humidity. The filtered material will be used for studies on the distribution and composition of the coccolithophorid communities in the upper 200 m of the water column using a Scanning Electron Microscope (SEM). Species composition and abundance will be determined by identification and counting on measured filter transects. This is essential in order to broaden our knowledge of the paleoceanographic and climatic evolution of the coccolith assemblages.

Table 8 Phytoplankton water profile sampling (coccolithophores)

| No. | Date 1998 | Time [UTC] | GeoB No. | Water depth [m] | Sample depth [m] | Latitude | Longitude | Water temp. [°C] | Salinity uncorr. [psu] |
|---|---|---|---|---|---|---|---|---|---|
| I) 1 | 21.04. | 20:48-21:04 | 5103-2 | 4614 | 10 | 31°12.11'S | 39°23.75'W | 21.0 | 35.73 |
| I) 2 | | | | | 20 | | | 20.9 | 35.75 |
| I) 3 | | | | | 50 | | | 20.6 | 35.99 |
| I) 4 | | | | | 100 | | | 15.7 | 35.64 |
| I) 5 | | | | | 150 | | | 15.0 | 35.57 |
| I) 6 | | | | | 200 | | | 14.2 | 35.45 |
| II) 1 | 24.04. | 19:35-19:51 | 5110-2 | 4191 | --- | 25°53.99'S | 35°39.01'W | --- | --- |
| II) 2 | | | | | 20 | | | 24.9 | 36.34 |
| II) 3 | | | | | 50 | | | 22.3 | 36.37 |
| II) 4 | | | | | 100 | | | 19.7 | 36.21 |
| II) 5 | | | | | 150 | | | 18.2 | 35.9 |
| II) 6 | | | | | 200 | | | 16.7 | 35.72 |
| III) 1 | 29.04. | 12:48-13:03 | 5112-2 | 3873 | 10 | 23°49,58'S | 16°16,32'W | 25.2 | 36.70 |
| III) 2 | | | | | 20 | | | 25.1 | 36.72 |
| III) 3 | | | | | 50 | | | 25.0 | 36.67 |
| III) 4 | | | | | 100 | | | 19.9 | 36.17 |
| III) 5 | | | | | 150 | | | 18.3 | 35.97 |
| III) 6 | | | | | 200 | | | 16.1 | 35.60 |
| IV) 1 | 01.05. | 17:39-18:53 | 5119-2 | 3865 | 10 | 24°10.07'S | 12°18.03'W | 24.4 | 36.61 |
| IV) 2 | | | | | 20 | | | 24.4 | 36.63 |
| IV) 3 | | | | | 50 | | | 24.4 | 36.62 |
| IV) 4 | | | | | 100 | | | 20.1 | 36.17 |
| IV) 5 | | | | | 150 | | | 17.4 | 35.80 |
| IV) 6 | | | | | 200 | | | 15.9 | 35.56 |
| V) 1 | 05.05. | 0:59-1:31 | 5129-2 | 3840 | 10 | 18°59.98'S | 09°46.20'W | 24.4 | 36.71 |
| V) 2 | | | | | 20 | | | 24.4 | 36.71 |
| V) 3 | | | | | 50 | | | 24.4 | 36.70 |
| V) 4 | | | | | 100 | | | 19.3 | 36.02 |
| V) 5 | | | | | 150 | | | 16.8 | 35.68 |
| V) 6 | | | | | 200 | | | 14.5 | 35.34 |
| VI) 1 | 07.05. | 22:21-23:30 | 5136-3 | 3227 | 10 | 19°21.96'S | 12°42.69'W | 24.6 | 36.72 |
| VI) 2 | | | | | 20 | | | 24.6 | 36.71 |
| VI) 3 | | | | | 50 | | | 24.6 | 36.71 |
| VI) 4 | | | | | 100 | | | 20.4 | 36.23 |
| VI) 5 | | | | | 150 | | | 18.4 | 36.01 |
| VI) 6 | | | | | 200 | | | 15.8 | 35.56 |
| VII) 1 | 09.05. | 18:31-19:38 | 5141-1 | 3451 | 10 | 19°05.75'S | 17°15.12'W | 25.6 | 36.97 |
| VII) 2 | | | | | 20 | | | 25.5 | 36.96 |
| VII) 3 | | | | | 50 | | | 25.5 | 36.96 |
| VII) 4 | | | | | 100 | | | 21.4 | 36.40 |
| VII) 5 | | | | | 150 | | | 19.3 | 36.18 |
| VII) 6 | | | | | 200 | | | 16.3 | 35.64 |

Table 9 Phytoplankton surface water sampling (coccolithophores)

| No. | Date 1998 | Water depth [m] | Latitide | Longitude | Water temp. [°C] | Salinity [psu] |
|---|---|---|---|---|---|---|
| 1 | 20.04. | 3009 | 28°03.70'S | 40°48.43'W | 23,2 | 35,84 |
| 2 | 20.04. | 4388 | 28°27.19'S | 40°54.79'W | 23,6 | 36,51 |
| 3 | 20.04. | 3813 | 28°45.55'S | 40°44.78'W | 23,0 | 36,29 |
| 4 | 21.04. | 4669 | 30°41.67'S | 39°37,85'W | 20,9 | 35,76 |
| 5 | 21.04. | 4581 | 31°14.23'S | 39°19.96'W | 20,9 | 35.69 |
| 6 | 21.04. | 4575 | 31°12.04'S | 39°21.01'W | 20,9 | 35.70 |
| 7 | 22.04. | 3992 | 30°53.88'S | 38°52.93'W | 21,5 | 35.76 |
| 8 | 22.04. | 3618 | 30°10.22'S | 37°57.81'W | 22,6 | 36.16 |
| 9 | 22.04. | 3884 | 29°18.27'S | 36°53.03'W | 22,1 | 36.11 |
| 10 | 23.04. | 4441 | 27'47.93'S | 35°01,00'W | 23.3 | 35.95 |
| 11 | 23.04. | 4067 | 27°05.70'S | 34°09,30'W | 23.3 | 36.00 |
| 12 | 23.04. | 4042 | 26°48.62'S | 34°03.59'W | 23.1 | 36.09 |
| 13 | 24.04. | 4348 | 26°17.99'S | 34°56.03'W | 24.1 | 35.97 |
| 14 | 24.04. | 4232 | 25°55.45'S | 35°36.62'W | 24.8 | 36.32 |
| 15 | 24.04. | 4188 | 25°54.31'S | 35°38.37'W | 24.7 | 36.23 |
| 16 | 25.04. | 4696 | 25°38.08'S | 33°39,50'W | 24.9 | 36.43 |
| 17 | 25.04. | 4884 | 25°28.48'S | 32°27.27'W | 24.6 | 36.16 |
| 18 | 25.04. | 5055 | 25°92.26'S | 31°46.12'W | 24.2 | 35.88 |
| 19 | 26.04. | 6534? | 25°02.48'S | 29°13.00'W | 25.7 | 36.56 |
| 20 | 26.04. | 6840? | 24°53.10'S | 28°00.07'W | 25.6 | 36.60 |
| 21 | 26.04. | 5337 | 24°43.41'S | 26°47.11'W | 25.1 | 36.33 |
| 22 | 27.04. | 5072 | 24°24.18'S | 24°25.35'W | 26.3 | 37.03 |
| 23 | 27.04. | 5014 | 24°16.95'S | 23°28.98'W | 26.1 | 36.94 |
| 24 | 27.04. | 4583 | 24°09,54'S | 22°33,21'W | 25.4 | 36.75 |
| 25 | 28.04. | 6534? | 23°49,84'S | 20°06,89'W | 25.4 | 36.76 |
| 26 | 28.04. | 5157 | 23°49.29'S | 19°37.68'W | 25,3 | 36,77 |
| 27 | 28.04. | 4535 | 23°50.28'S | 18°45.49'W | 25,3 | 36,83 |
| 28 | 29.04. | 3547 | 23°50.43'S | 16°23.82'W | 24,8 | 36,67 |
| 29 | 29.04. | 3838 | 23°49.60'S | 16°15,52'W | 25,0 | 36,69 |
| 30 | 29.04. | 3906 | 23°49.41'S | 16°13.74'W | 24,9 | 36.72 |
| 31 | 30.04. | 3692 | 23°56.61'S | 14°26.85'W | 24,3 | 36.57 |
| 32 | 30.04. | 3291 | 24°08.64'S | 14°25.70'W | 24,5 | 36.48 |
| 33 | 30.04. | 2576 | 24°09.34'S | 13°46.19'W | 24,2 | 36.57 |
| 34 | 01.05. | 2734 | 24°10.80'S | 13°23.02'W | 24,3 | 36.63 |
| 35 | 01.05. | 3914 | 24'10.08'S | 12°18,51'W | 24.2 | 36.61 |
| 36 | 01.05. | 3844 | 24°10.18'S | 12°21.69'W | 24,1 | 36,62 |
| 37 | 02.05. | 3477 | 24°10.22'S | 11°13.68'W | 23,9 | 36,49 |
| 38 | 02.05. | 3197 | 24°09.89'S | 11°20.37'W | 24,1 | 36,52 |
| 39 | 03.05. | 4464 | 24°09.99'S | 09°00,02'W | 23,4 | 36,40 |
| 40 | 03.05. | 4667 | 23°12.36'S | 09°00.01'W | 23,8 | 36.53 |
| 41 | 03.05. | 4193 | 22°23.92'S | 08°59.98'W | 23,8 | 36.59 |
| 42 | 04.05. | 3971 | 20°39.21'S | 09°00.05'W | 24,0 | 36.68 |
| 43 | 04.05. | 4268 | 19°52.20'S | 09°06.11'W | 23,8 | 36.61 |
| 44 | 04.05. | 3885 | 19°07.19'S | 09°40.72'W | 24,2 | 36.74 |
| 45 | 05.05. | 4166 | 19°24.23'S | 09°27,57'W | 23.9 | 36.59 |
| 46 | 05.05. | 3890 | 19°02,52'S | 09°44,29'W | 24.5 | 36.77 |
| 47 | 05.05. | 3942 | 19°07,50'S | 09°43,13'W | 24.1 | 36.67 |
| 48 | 06.05. | 3660 | 19°05,14'S | 10°11,55'W | 24.1 | 36.66 |
| 49 | 06.05. | 3226 | 19°03,88'S | 10°27,16'W | 24.0 | 36.52 |
| 50 | 06.05. | 3411 | 19°02,71'S | 10°40,99'W | 23.9 | 36.48 |
| 51 | 07.05. | 3304 | 19°26,14'S | 11°03,77'W | 23.9 | 36.51 |
| 52 | 07.05. | 2584 | 19°23,74'S | 12°01,02'W | 24.3 | 36.50 |
| 53 | 07.05 | 3228 | 19°22,18'S | 12°40,15'W | 24.4 | 36.71 |
| 54 | 08.05. | 3502 | 19°17,50'S | 13°27,20'W | 24.6 | 36.76 |

Table 9 continued

| No. | Date<br>1998 | Water depth<br>[m] | Latitude | Longitude | Water temp.<br>[°C] | Salinity<br>[psu] |
|---|---|---|---|---|---|---|
| 55 | 08.05. | 3631 | 19°11,38'S | 14°39,21'W | 24.9 | 36.86 |
| 56 | 08.05. | 3859 | 19°06,64'S | 15°12,57'W | 25.0 | 36.94 |
| 57 | 09.05. | 3660 | 19°03,20'S | 16°36,80'W | 24.9 | 36.83 |
| 58 | 09.05. | 3820 | 19°04,15'S | 16°51,12'W | 25.4 | 36.94 |
| 59 | 09.05. | 3939 | 19°05,40'S | 17°09,14'W | 25.3 | 36.94 |
| 60 | 10.05. | 4513 | 18°37,66'S | 18°44,77'W | 25.5 | 37.01 |
| 61 | 10.05. | 4344 | 18°28,38'S | 19°23,45'W | 25.6 | 37.01 |
| 62 | 10.05. | 4471 | 18°11,63'S | 20°24,09'W | 25.8 | 37.08 |
| 63 | 11.05. | 4819 | 17°29,19'S | 22°57,84'W | 26.3 | 37.21 |
| 64 | 11.05. | 5081 | 17°14,99'S | 23°49,11'W | 26.5 | 37.22 |
| 65 | 12.05. | 5441 | 16°15,06'S | 27°24,75'W | 27.2 | 37.14 |
| 66 | 12.05. | 5264 | 15°53,24'S | 28°23,02'W | 27.1 | 37.38 |
| 67 | 12.05. | 5783 | 15°37,60'S | 29°38,98'W | 27.3 | 37.44 |

### 4.4.3 Dinoflagellates

(A. Meyer, S. Schulz, A. Vink)

Dinoflagellates are unicellular, biflagellated algae forming a major constituent of the marine phytoplankton, and are amongst the most important primary producers of the present oceans. All dinoflagellates have a motile cellulosic thecate stage as the active stage in their life cycle. Approximately 10% of all dinoflagellate species also undergo a resting cyst stage during sexual reproduction, in which the cysts formed are usually organic-walled but may, in a few species, be calcareous ('calcispheres'). As an exception within the group of calcareous dinoflagellates, the species *Thoracosphaera heimii* is subjected to a calcareous-walled vegetative coccoid stage rather than a calcareous cyst stage. Organic- and calcareous-walled cysts, including the vegetative coccoid *Th. heimii*, are generally extremely resistant to degradation and may be preserved in large numbers in oceanic sediments (provided they lie above the lysocline). Studies concerning recent and sub-recent distributions of calcareous dinoflagellate cysts and their corresponding thecae are, to date, extremely limited. The studies being carried out at the University of Bremen focus primarily on the complex, interacting relationships between recent species distributions in the South Atlantic and environmental parameters such as temperature, salinity, light, nutrient content, stratification, etc. A knowledge of these interactions is extremely important for the interpretation of fossil dinoflagellate cyst assemblages in the sedimentary record and they may as such be applicable as proxies in palaeoceanography and palaeoenvironmental modelling. In order to improve our knowledge on the geographic and vertical distribution of individual species and to attempt culturing them for future experimentation, phytoplankton samples were collected during the cruise from variable depths of the water column, ranging from surface waters down to 150 m depth (calcareous dinoflagellates show a variable depth distribution but are generally found within tens of meters below the water surface as they are photosynthetic).

Surface water samples were acquired from a depth of approximately 5 m three times a day using the ship's membrane pump (*ca.* 07:00-11:00; 12:00-16:00 and 18:00-22:00 board time: see Table 10). The water was continuously passed over a 100 μm pre-filter to remove zooplankton and then filtered over a 10 μm gauze, thereby collecting the 10-100 μm particle and organic matter fraction in a 1 liter collecting vessel. The amount of sea water passing through the vessel during filtration was measured accurately. The water samples were concentrated down to *ca.* 150 ml using a 5 μm polycarbonate filter and a vacuum pump system, and were subsequently scanned for living thecate dinoflagellates, calcareous dinoflagellate cysts and *Th. heimii*. Individual specimens were isolated and placed in sterile polyterene Cell Wells™ containing different types of culture media (f/2 35 ‰; K 35 ‰ and 0,2 μm filtered sea water) or mixtures of two of these (ratio 1:1). As such, it was attempted to culture calcareous cyst-producing dinoflagellates under on board conditions using the local day/night cycle at temperatures between 20 and 25°C. Germination experiments and further routine culturing of these dinoflagellates (aimed at investigating various aspects of their ecology, productivity, life cycles, biomineralisation processes and systematics) will be carried out at the University of Bremen. After qualitative analysis, the water samples were transferred into 250 ml NALGENE polycarbonate flasks, fixated with 3-4% formaldehyde and stored in the dark at 4°C.

Table 10 Surface water samples taken for dinoflagellate analyses. Sampling was carried out through 10 μm membrane pump filtration

| **Sample nr.** | **Start and end of filtration (UTC)** | **Latitude (°S) at start and end of filtration** | **Longitude (°W) at start and end of filtration** | **Water depth (m)** | **Water temperature (°C)** | **Salinity (‰)** | **Volume of water filtered (l)** |
|---|---|---|---|---|---|---|---|
| 4/20/a | 10:00 | 27°42,81′ | 40°42,76′ | 3022 | 23,2 | - - | 138 |
| | 13:58 | 28°14,79′ | 40°52,37′ | | | | |
| 4/20/c | 20:56 | 28°31,98′ | 40°51,78′ | 4014 | 23,4 | - - | 250 |
| | 00:56 | 29°10,79′ | 40°30,41′ | | | | |
| 4/21/a | 09:59 | 30°32,60′ | 39°43,22′ | 4587 | 21,0 | 35,67 | 365 |
| | 13:54 | 31°11,19′ | 39°20,58′ | | | | |
| 4/22/a | 10:00 | 31°01,16′ | 39°02,25′ | 4182 | 21,2 | 35,91 | 273,5 |
| | 13:55 | 30°31,60′ | 38°24,85′ | | | | |
| 4/22/b | 15:01 | 30°23,37′ | 38°14,48′ | 3643 | 22,4 | - - | 440 |
| | 19:00 | 29°52,77′ | 37°36,06′ | | | | |
| 4/22/c | 20:56 | 29°39,78′ | 37°19,75′ | 3288 | 21,8 | 36,11 | 460,5 |
| | 00:51 | 29°10,00′ | 36°42,60′ | | | | |
| 4/23/a | 10:00 | 28°01,52′ | 35°17,77′ | 4444 | 23,3 | 35,95 | 538,5 |
| | 13:55 | 27°32,77′ | 34°42,52′ | | | | |
| 4/23/b | 14:50 | 27°25,72′ | 34°33,79′ | 4351 | 23,4 | 35,91 | 396 |
| | 18:50 | 26°56,25′ | 33°57,68′ | | | | |
| 4/24/a | 12:35 | 26°17,99′ | 34°55,99′ | 4350 | 24,1 | 35,95 | 632 |
| | 16:44 | 25°53,99′ | 35°38,90′ | | | | |
| 4/25/a | 10:00 | 25°44,32′ | 34°26,44′ | 4554 | 24,7 | 36,38 | 164,5 |
| | 13:59 | 25°37,58′ | 33°36,02′ | | | | |
| 4/25/b | 14:50 | 25°36,20′ | 33°25,57′ | 4671 | 24,7 | 36,34 | 535 |
| | 18:50 | 25°29,37′ | 32°34,12′ | | | | |
| 4/25/c | 20:59 | 25°25,73′ | 32°06,83′ | 4894 | 23,8 | - - | 669 |
| | 01:02 | 25°18,58′ | 31°13,48′ | | | | |
| 4/26/a | 09:58 | 25°03,74′ | 29°22,20′ | 4984 | 25,7 | 36,72 | 352 |
| | 13:55 | 24°57,32′ | 28°32,97′ | | | | |
| 4/26/b | 14:10 | 24°56,91′ | 28°28,79′ | 5366 | 25,7 | 36,77 | 426 |
| | 18:10 | 24°50,01′ | 27°36,84′ | | | | |
| 4/26/c | 19:52 | 24°47,02′ | 27°14,52′ | 5261 | 24,8 | 36,32 | 511 |
| | 23:59 | 24°40,05′ | 26°22,17′ | | | | |

Table 10 continued

| Sample nr. | Start and end of filtration (UTC) | Latitude (°S) at start and end of filtration | Longitude (°W) at start and end of filtration | Water depth (m) | Water temperature (°C) | Salinity (‰) | Volume of water filtered (l) |
|---|---|---|---|---|---|---|---|
| 4/27/a | 09:20 | 24°24,26′ | 24°24,33′ | 5090 | 26,3 | 37,02 | 246 |
| | 12:46 | 24°21,70′ | 23°55,64′ | | | | |
| 4/27/b | 13:05 | 24°20,71′ | 23°51,86′ | - - | 26,0 | 36,86 | 661 |
| | 17:04 | 24°14,18′ | 23°08,38′ | | | | |
| 4/27/c | 18:45 | 24°11,76′ | 22°50,62′ | 4655 | 25,5 | - - | 531 |
| | 22:30 | 24°06,37′ | 22°10,68′ | | | | |
| 4/28/b | 13:40 | 23°48,97′ | 19°59,76′ | 5233 | 25,4 | 36,82 | 513 |
| | 17:53 | 23°49,75′ | 19°12,89′ | | | | |
| 4/28/c | 18:54 | 23°49,92′ | 19°02,70′ | 4888 | 25,4 | 36,82 | 466 |
| | 23:01 | 23°50,74′ | 18°15,50′ | | | | |
| 4/29/a | 08:50 | 23°50,61′ | 16°24,44′ | 4044 | 24,7 | 36,67 | 260 |
| | 10:07 | 23°49,59′ | 16°16,33′ | | | | |
| 4/29/c | 20:10 | 23°49,55′ | 16°15,43′ | 3835 | 24,9 | 36,73 | 662 |
| | 23:00 | 23°45,83′ | 15°45,44′ | | | | |
| 4/30/a | 07:58 | 23°51,69′ | 14°36,71′ | 3927 | 24,5 | 36,70 | 484 |
| | 11:41 | 24°09,94′ | 13°59,93′ | | | | |
| 5/1/a | 10:30 | 24°10,79′ | 13°21,72′ | 3994 | 24,3 | 36,63 | 856 |
| | 14:32 | 24°10,28′ | 12°34,16′ | | | | |
| 5/2/a | 08:03 | 24°10,15′ | 11°40,74′ | 3676 | 23,8 | 36,50 | 443 |
| | 10:52 | 24°10,28′ | 11°08,08′ | | | | |
| 5/2/c | 18:56 | 24°10,17′ | 10°51,74′ | 4074 | 24,0 | 36,51 | 619 |
| | 22:55 | 24°10,00′ | 10°01,40′ | | | | |
| 5/3/a | 09:55 | 24°09,46′ | 09°00,09′ | 4447 | 23,4 | 36,40 | 475 |
| | 12:55 | 23°34,04′ | 09°00,00′ | | | | |
| 5/3/b | 13:07 | 23°31,29′ | 09°00,03′ | 4573 | 23,7 | 36,46 | 724 |
| | 17:07 | 22°43,90′ | 09°00,01′ | | | | |
| 5/4/a | 10:25 | 20°24,66′ | 09°00,01′ | 4278 | 23,9 | 36,63 | 457 |
| | 12:56 | 20°00,50′ | 09°00,11′ | | | | |
| 5/4/b | 15:35 | 19°59,83′ | 09°00,02′ | 3935 | 23,8 | 36,43 | 564 |
| | 18:49 | 19°28,24′ | 09°24,41′ | | | | |
| 5/4/c | 19:01 | 19°26,15′ | 09°26,04′ | 4155 | 24,0 | 36,60 | 545 |
| | 21:50 | 18°59,99′ | 09°46,25′ | | | | |
| 5/6/c | 15:37 | 19°04,98′ | 10°12,62′ | 3652 | 24,2 | 36,68 | 477 |
| | 17:51 | 19°02,59′ | 10°40,95′ | | | | |
| 5/7/a | 10:15 | 19°26,09′ | 11°03,84′ | 3302 | 23,9 | 36,51 | 685 |
| | 14:03 | 19°24,22′ | 11°49,79′ | | | | |
| 5/7/b | 14:36 | 19°23,93′ | 11°57,00′ | 2671 | 24,2 | 36,69 | 808 |
| | 18:00 | 19°22,14′ | 12°40,25′ | | | | |
| 5/8/a | 09:06 | 19°15,58′ | 13°38,14′ | 3170 | 24,8 | 36,83 | 205 |
| | 13:19 | 19°11,99′ | 14°30,46′ | | | | |
| 5/8/c | 18:32 | 19°11,44′ | 14°39,19′ | 3630 | 24,9 | 36,90 | 635 |
| | 22:19 | 19°04,41′ | 15°26,72′ | | | | |
| 5/9/b | 15:19 | 19°03,12′ | 16°36,75′ | 3660 | 25,1 | 36,83 | 696 |
| | 18:25 | 19°05,89′ | 17°15,11′ | | | | |
| 5/10/b | 11:37 | 18°37,53′ | 18°45,38′ | 4434 | 25,5 | 37,01 | 910 |
| | 17:35 | 18°28,38′ | 19°23,45′ | | | | |
| 5/10/c | 18:56 | 18°16,00′ | 20°08,13′ | 4885 | 25,8 | 37,04 | 719 |
| | 23:00 | 18°03,77′ | 20°52,76′ | | | | |
| 5/11/a | 08:56 | 17°32,78′ | 22°44,84′ | - - | 26,2 | 37,22 | 883 |
| | 13:00 | 17°22,76′ | 23°23,08′ | | | | |
| 5/11/b | 13:50 | 17°19,67′ | 23°32,35′ | - - | 26,5 | 37,24 | 716 |
| | 17:30 | 17°07,73′ | 24°15,34′ | | | | |

Table 10 continued

| Sample nr. | Start and end of filtration (UTC) | Latitude (°S) at start and end of filtration | Longitude (°W) at start and end of filtration | Water depth (m) | Water temperature (°C) | Salinity (‰) | Volume of water filtered (l) |
|---|---|---|---|---|---|---|---|
| 5/11/c | 18:35 | 17°04,23′ | 24°27,96′ | 5483 | 26,6 | 37,25 | 733 |
| | 22:32 | 16°51,36′ | 25°14,20′ | | | | |
| 5/12/a | 08:56 | 16°17,80′ | 27°14,91′ | 5503 | 27,2 | 37,31 | 613 |
| | 12:54 | 16°04,74′ | 28°01,70′ | | | | |
| 5/12/b | 14:02 | 16°00,91′ | 28°15,41′ | 5346 | 27,2 | 37,35 | 736 |
| | 18:00 | 15°47,54′ | 29°03,31′ | | | | |
| 5/12/c | 18:25 | 15°46,47′ | 29°07,27′ | 5183 | 27,2 | 37,41 | 708 |
| | 22:29 | 15°35,82′ | 29°45,41′ | | | | |
| 5/13/a | 10:02 | 15°06,75′ | 31°29,40′ | 4712 | 27,5 | 37,27 | 565 |
| | 14:00 | 14°58,20′ | 31°59,37′ | | | | |
| 5/13/b | 14:10 | 14°57,91′ | 32°01,10′ | -- | 27,9 | 37,44 | 604 |
| | 17:50 | 14°48,46′ | 32°34,42′ | | | | |
| 5/13/c | 18:00 | 14°47,86′ | 32°36,52′ | -- | 27,9 | 37,47 | 595 |
| | 21:40 | 14°38,99′ | 33°08,00′ | | | | |

In addition to acquiring surface water samples, approximately 30-40 l of sea water was collected at 10, 20, 50, 100 m and occasionally at 75, 120 and 150 m water depth using a rosette (Multi Water Sampler MWS, cat. nr. 436918A). Samples were taken at 7 stations (positions and depths are listed in Table 11). In general, three or four 10 l Niskin bottles were filled at each depth. The obtained water was passed over a 100 μm mesh sieve and filtered with 5 μm polycarbonate filters using a vacuum pump. The samples were concentrated to a volume of *ca.* 150 ml and subsequently treated in a similar manner to the surface water samples acquired from the membrane pump. All stored samples will be further analysed at the University of Bremen in order to provide more information on the composition, regional geographic distribution and the vertical distribution of calcareous dinoflagellate communities in the upper 150 m of the regions of the South Atlantic Ocean covered by the cruise.

Motile thecate dinoflagellates and calcareous cysts have been observed, though in relatively low numbers, in almost all the samples taken. Thecae and cysts concentrations were the highest in surface water samples, and were found in considerably lower numbers in the 10-100 m samples. No cysts were found in the 120 and 150 m water samples. The calcareous cyst association was predominated in all water samples by the occurrence of only two cyst species: ?*Sphaerodinella tuberosa* and *Th. heimii*. The calcareous cyst species ?*Sphaerodinella albatrosiana* and *Orthopithonella granifera* occurred sporadically and in very low concentrations. Organic-walled dinoflagellate cysts were not detected, which is not surprising as their corresponding thecae are not, unlike those of calcareous cysts, greatly adapted to oligotrophic (nutrient-depleted) areas. No obvious differences were noticed in cyst composition and quantity between samples taken at different times of the day. Approximately 200 specimens of calcareous dinoflagellate cysts were isolated for cultivation on board. The cells containing these cysts were scanned at regular intervals, in order to register when excystment and reproduction occurred. Those specimens which produced a sufficient number of new cysts and motile thecae were transported to the University of Bremen for experimentation.

Table 11 Water samples taken with the rosette (i.e. 10 l Niskin bottles) at different water depths

| GeoB Station and depth of samples | | Date | Time (UTC) | Water depth (m) | Volume of water filtered (l) | Latitude (°S) | Longitude (°W) | Water temp. (°C) | Salinity (‰) |
|---|---|---|---|---|---|---|---|---|---|
| 5103-2 | 10 m | 21.04.98 | 20:48 | 4611 | 37,5 | 31°12,12′ | 39°23,75′ | 21,007 | 35,735 |
| | 20 m | | | | 38,1 | | | 20,983 | 35,757 |
| | 50 m | | | | 37,8 | | | 20,628 | 35,999 |
| | 100 m | | | | 39,0 | | | 15,707 | 35,642 |
| 5110-2 | 10 m | 24.04.98 | 19:35 | 4198 | - -* | 25°54,00′ | 35°39,01′ | 24,998 | 36,313 |
| | 20 m | | | | 25,8 * | | | 24,951 | 36,343 |
| | 50 m | | | | 32,3 | | | 22,352 | 36,373 |
| | 100 m | | | | 38,5 | | | 19,754 | 36,210 |
| 5112-2 | 10 m | 29.04.98 | 12:48 | 3867 | 28,5 | 23°49,57′ | 16°16,33′ | 25,216 | 36,708 |
| | 20 m | | | | 17,9 * | | | 25,175 | 36,725 |
| | 50 m | | | | 26,4 | | | 25,010 | 36,675 |
| | 100 m | | | | 28,5 | | | 19,945 | 36,170 |
| | 120 m | | | | 30,8 | | | 19,131 | 36,104 |
| | 150 m | | | | 18,2 | | | 18,363 | 35,976 |
| 5119-2 | 10 m | 01.05.98 | 17:39 | 3878 | 38,0 | 24°10,02′ | 12°18,00′ | 24,431 | 36,610 |
| | 20 m | | | | 38,6 | | | 24,429 | 36,631 |
| | 50 m | | | | 37,9 | | | 24,403 | 36,621 |
| | 100 m | | | | 39,0 | | | 20,196 | 36,177 |
| 5129-2 | 10 m | 05.05.98 | 00:59 | 3840 | 28,6 | 18°59,98′ | 09°46,20′ | 24,454 | 36,710 |
| | 20 m | | | | 27,2 | | | 24,452 | 36,710 |
| | 50 m | | | | 27,3 | | | 24,453 | 36,709 |
| | 75 m | | | | 30,5 | | | 21,456 | 36,219 |
| | 100 m | | | | 28,1 | | | 19,370 | 36,026 |
| 5136-3 | 10 m | 07.05.98 | 22:21 | 3227 | 29,5 | 19°21,99′ | 12°42,67′ | 24,691 | 36,721 |
| | 20 m | | | | 29,5 | | | 24,659 | 36,719 |
| | 50 m | | | | 29,1 | | | 24,612 | 36,714 |
| | 75 m | | | | 31,9 | | | 22,524 | 36,400 |
| | 100 m | | | | 28,8 | | | 20,416 | 36,233 |
| 5141-1 | 10 m | 09.05.98 | 18:31 | 3451 | 29,0 | 19°05,75′ | 17°15,12′ | 25,621 | 36,970 |
| | 20 m | | | | 28,8 | | | 25,570 | 36,967 |
| | 50 m | | | | 28,7 | | | 25,543 | 36,968 |
| | 100 m | | | | 29,5 | | | 21,476 | 36,401 |
| | 120 m | | | | 31,1 | | | 20,423 | 36,340 |

* = 1 or more unclosed Niskin bottles.

### 4.4.4 Diatoms

(B. Jahn, T. Lützeler)

During the cruise, plankton was sampled for diatom analysis from surface waters (Table 12). The shipboard clean sea water pump system was used to filter sea water through a net with a mesh size of 10 µm. The amount of water filtered depended on the plankton concentration. The water samples were collected during daylight hours for analysis of the diatom assemblage. The plankton was washed into Kautex bottles, poisoned with formaldehyd solution and stored at 4°C. The net was washed and used again. The plankton material will be investigated for the bulk composition of the biogenic detritus. The material will be further analysed in the laboratories at the University of Bremen.

Table 12 List of pumped net samples for diatom analysis

| No. | Date | Time (UTC) | Start Latitude (S) | Start Longitude (W) | Start Salinity [‰] | Start Temp. [°C] | End Latitude (S) | End Longitude (W) | End Salinity [‰] | End Temp. [°C] | Vol. [m³] |
|---|---|---|---|---|---|---|---|---|---|---|---|
| 1 | 20.04.98 | 13:05 - 18:59 | 28°12,02′ | 40°50,80′ | --- | 24,3 | 28°26,36′ | 40°54,69′ | --- | 23,6 | 1,879 |
| 2 | 21.04.98 | 13:02 - 19:05 | 31°02,83′ | 39°25,54′ | 35,72 | 20,8 | 31°12,09′ | 39°23,75′ | 35,72 | 20,7 | 1,785 |
| 3 | 22.04.98 | 12:57 - 19:02 | 30°38,60′ | 38°33,77′ | 36,17 | 22,5 | 29°53,81′ | 37°37,21′ | 36,16 | 22,1 | 1,717 |
| 4 | 23.04.98 | 12:58 - 18:55 | 27°39,55′ | 34°50,72′ | 35,87 | 23,3 | 26°55,80′ | 33°57,20′ | 36,01 | 23,2 | 3,547 |
| 5 | 24.04.98 | 12:56 - 18:57 | 26°15,98′ | 34°59,63′ | 35,93 | 24,1 | 25°54,02′ | 35°38,98′ | 36,03 | 24,7 | 3,105 |
| 6 | 25.04.98 | 12:58 - 19:39 | 25°39,29′ | 33°48,77′ | 36,45 | 24,9 | 25°28,00′ | 32°23,82′ | 36,16 | 24,6 | 4,016 |
| 7 | 26.04.98 | 12:45 - 18:55 | 24°59,31′ | 28°46,84′ | 36,64 | 25,8 | 24°48,67′ | 27°27,01′ | 36,68 | 25,7 | 2,480 |
| 8 | 27.04.98 | 11:00 - 16:58 | 24°21,60′ | 24°04,18′ | 36,99 | 26,3 | 24°14,29′ | 23°09,29′ | 36,88 | 25,8 | 3,324 |
| 9 | 28.04.98 | 10:56 - 17:13 | 23°48,96′ | 19°59,90′ | 36,78 | 25,4 | 23°49,58′ | 19°21,78′ | 36,80 | 25,4 | 2,589 |
| 10 | 29.04.98 | 10:55 - 15:00 | 23°49,55′ | 16°16,35′ | 36,82 | 24,9 | 23°49,46′ | 16°15,45′ | 36,57 | 25,0 | 1,709 |
| 11 | 30.04.98 | 09:15 - 17:28 | 23°56,53′ | 14°27,04′ | 36,57 | 24,6 | 24°08,64′ | 14°02,58′ | 36,71 | 24,5 | 3,210 |
| 12 | 01.05.98 | 11:21 - 17:20 | 24°10,68′ | 13°12,13′ | 36,56 | 24,2 | 24°10,05′ | 12°18,00′ | 36,60 | 24,1 | 2,607 |
| 13 | 02.05.98 | 11:43 - 17:35 | 24°10,24′ | 11°08,14′ | 36,50 | 24,0 | 24°10,23′ | 11°08,89′ | 36,50 | 24,1 | 1,905 |
| 14 | 03.05.98 | 10:54 - 16:54 | 23°57,94′ | 09°00,09′ | 36,39 | 23,4 | 22°46,62′ | 09°00,01′ | 36,52 | 23,8 | 2,737 |
| 15 | 04.05.98 | 11:11 - 17:15 | 20°15,87′ | 09°00,02′ | 36,73 | 23,7 | 19°43,55′ | 09°12,71′ | 36,50 | 23,9 | 2,824 |
| 16 | 05.05.98 | 11:00 - 17:13 | 19°19,22′ | 09°34,19′ | 36,59 | 24,0 | 19°07,52′ | 09°43,18′ | 36,65 | 24,1 | 3,065 |
| 17 | 06.05.98 | 11:06 - 17:16 | 19°05,11′ | 10°11,58′ | 36,60 | 24,1 | 19°03,31′ | 10°33,94′ | 36,66 | 24,1 | 2,985 |
| 18 | 07.05.98 | 11:11 - 17:11 | 19°25,75′ | 11°14,18′ | 36,51 | 24,0 | 19°22,54′ | 12°30,22′ | 36,67 | 24,4 | 2,790 |
| 19 | 08.05.98 | 11:05 - 17:10 | 19°13,84′ | 14°02,65′ | 36,84 | 24,8 | 19°11,00′ | 14°39,30′ | 36,90 | 24,9 | 3,215 |
| 20 | 09.05.98 | 11:08 - 17:05 | 19°03,14′ | 16°36,87′ | 36,83 | 25,0 | 19°04,69′ | 16°58,70′ | 36,94 | 25,5 | 3,304 |
| 21 | 10.05.98 | 11:13 - 17:01 | 18°38,66′ | 18°43,16′ | 37,05 | 25,5 | 18°22,02′ | 19°46,49′ | 37,07 | 26,0 | 2,925 |
| 22 | 11.05.98 | 11:55 - 18:05 | 17°23,88′ | 23°16,60′ | 37,18 | 26,4 | 17°05,78′ | 24°22,32′ | 37,73 | 26,7 | 3,039 |
| 23 | 12.05.98 | 12:04 - 18:20 | 16°07,53′ | 27°51,79′ | 37,36 | 27,2 | 15°46,60′ | 29°06,80′ | 37,41 | 27,2 | 3,095 |
| 24 | 13.05.98 | 14:08 - 19:47 | 14°57,99′ | 32°00,68′ | 37,42 | 27,6 | 14°43,45′ | 32°52,42′ | 37,49 | 27,9 | 2,974 |

### 4.4.5 Planktic Foraminifera

(H.-S. Niebler)

Sea surface water from about 5 m water depth was pumped using the ship's 'Junker pump'. The water was pumped on 6 days of the cruise for different time intervals of up to 25 hours (Table 13). The sea water was filtered using a plankton hand net (70 µm mesh size), which was tied to the railing at the end of the working deck. Immediately after recovery, planktic foraminifera larger than 150 µm were observed under a binocular and separated from other plankton. The work was focused on the three most abundant species *Globigerinoides trilobus*, *Globigerinoides ruber* (white) and *Globigerinoides ruber* (pink), because in tropical and subtropical regions these species are most important for paleoceanographic research.

Due to very low fertility in the surface water masses of the central Subtropical Gyre only very few foraminifera were found per single sample. The foraminifera were picked and put into Fema-cells, but the amount was absolutely insufficient for oxygen isotope analysis by mass spectrometery (recovery: between 0 and 23 specimens of different species per sample). Therefore, no water samples were taken for reference during plankton sampling. Because of the minimal and unsuccessful recovery the sampling was stopped after 6 days.

Table 13 Locations of sampling profiles and pump intervals for planktic foraminifera

| No. | Pump interval<br>Date / Interval [h] | Latitude<br>(start) | Longitude<br>(start) | Temp.<br>[°C] | Salinity<br>[‰] | Latitude<br>(end) | Lonitude<br>(end) | Temp.<br>[°C] | Salinity<br>[‰] |
|---|---|---|---|---|---|---|---|---|---|
| FP 1 | 21-21.04.98 / 4,50 | 30°47,3'S | 39°34,6'W | 21.0 | 35.73 | 31°12,1'S | 39°23,8'W | 21.4 | 35.68 |
| FP 2 | 22-22.04.98 / 9,25 | 30°44,8'S | 38°41,5'W | 23.2 | 36.17 | 29°42,3'S | 37°22,9'W | 22.2 | 36.11 |
| FP 3 | 23-24.04.98 / 23,0 | 27°39,5'S | 34°50,6'W | 23.6 | 35.87 | 26°18,0'S | 34°56,1'W | 24.3 | 35.97 |
| FP 4 | 24-25.04.98 / 28,0 | 26°18,0'S | 34°56,1'W | 24.3 | 35.97 | 25°35,4'S | 33°19,6'W | 25.0 | 36.37 |
| FP 5 | 25-26.04.98 / 23,0 | 25°35,4'S | 33°19,6'W | 25.0 | 36.37 | 24°58,6'S | 28°41,5'W | 26.1 | 36.66 |
| FP 6 | 26-27.04.98 / 23,5 | 24°58,6'S | 28°41,5'W | 26.1 | 36.66 | 24°22,2'S | 24°00,8'W | 26.5 | 36.98 |

## 4.5 Marine Geology, Sediment Cores

(R. Höppner, B. Jahn, B. Kottke, H. Kuhlmann, T. Lützeler, C. Moos, H.-S. Niebler, S. Rath, F. Schewe, T. Westerhold)

During cruise M 41/3 we used giant box corer (2x), multicorer I (4x), multicorer II (17x) and gravity corer (22x) in order to recover surface sediments and sediment cores from the late Quaternary from the northwestern Vema Channel and from the Mid-Atlantic Ridge on two profiles at 24°S and 19°S. Samples were retrieved from water depths between 2500 and 4200°m The coring locations, water depths, devices used for our sampling program at all stations and the core lengths recovered are given in the station list (Chapter 8, Table 18).

### 4.5.1 Multicorer and Giant Box Corer Sampling

The multicorer is designed to recover undisturbed surface sediment sections and the overlying bottom water. During M 41/3 two models were used. At four stations a large multicorer (see summary station list Chapter 8) with 4 small and 8 large tubes was used, but no cores were recovered. At 17 stations a second multicorer ("MUC II") was used with 4 small and 6 larger plastic tubes (6 and 10 cm in diameter, respectively). At 16 stations 8-10 tubes were filled with the uppermost 11 to 30 cm of sediment and the overlying bottom water. At one station (GeoB 5123-1) the multicorer failed and no samples were recovered. Furthermore, the sandy sediments rich in foraminifera tend to be washed out of the plastic tubes. Depending on the recovery, the tubes were sampled as follows:

- 1 large tube, cut into 1 cm thick slices and frozen for organic carbon (TOC) geochemistry
- 1 large tube, cut into 1 cm thick slices for surveys on dinoflagellates
- 2 large tubes, cut into 1 cm thick slices for investigation of benthic foraminiferal assemblages, stained with rose bengal
- 1 large tube, cut into 1 cm thick slices and frozen for sedimentology
- 1 small tube, cut into 1 cm thick slices for paleomagnetic studies
- 1 small tube, cut into 1 cm thick slices for organic geochemistry, organic matter microscopy and petrology
- 1 large tube, only surface (first cm) for diatom and radiolarian investigations stained with ethanol/methanol
- 1 large tube (without surface) and 2 small tubes were frozen as archive cores
- 50 ml bottom water samples for stable carbon and oxygen isotopes were taken at each station where sediment was recovered

The giant box corer was used at 2 stations (GeoB 5110-5 and 5112-5, see Chapter 8) in order to sample sediments that were expected to be rich in foraminifera. With a surface area of 50x50 cm, the box corer retrieved the uppermost 30 to 46 cm of the sediment column. Once on board, the overlying water was removed, the sediment temperature measured and a surface photograph was taken. Then the sediment surface was sampled according to the following scheme:

- 400 $cm^2$ for foraminiferal analysis stained with rose bengal
- 200 $cm^2$ for radiolaria and diatom analysis preserved with ethanol
- 200 $cm^2$ for organic geochemical analysis frozen at -20°C
- 25 $cm^2$ for diatom analysis preserved with methanol

Afterwards the front lid of the box corer was opened, the sediment cleaned, photographed and described. Two series of 10 ml syringes were taken at 3 cm depth intervals, one for foraminiferal and one for organic geochemical analysis. Furthermore, two archive cores (12 cm diameter) were taken and all sediments were subsampled with one large and three small multicorer tubes, then cut into 1 cm thick slices for paleomagnetic, dinoflagellate and granulometric studies as well as for organic matter microscopy according to the multicorer sampling scheme described above.

### 4.5.2 Gravity Corer Sampling

Using a gravity corer, 22 sediment cores between 30 and 961 cm in length were taken at 19 stations. During M 41/3 a total of 83,5 m of sediments were recovered. Before using the coring tools, the liners were marked with a straight line lengthwise, in order to ensure that later sampling of the core segments be carried out in the same orientation, particularly for paleomagnetic purposes. After the core was retrieved on deck, the liners were cut into 1 m segments, closed with caps at both ends and inscribed (Fig. 22). After the temperature equilibration of the cores was reached, the physical properties were measured (see Chapter 4.6).

Inscription:

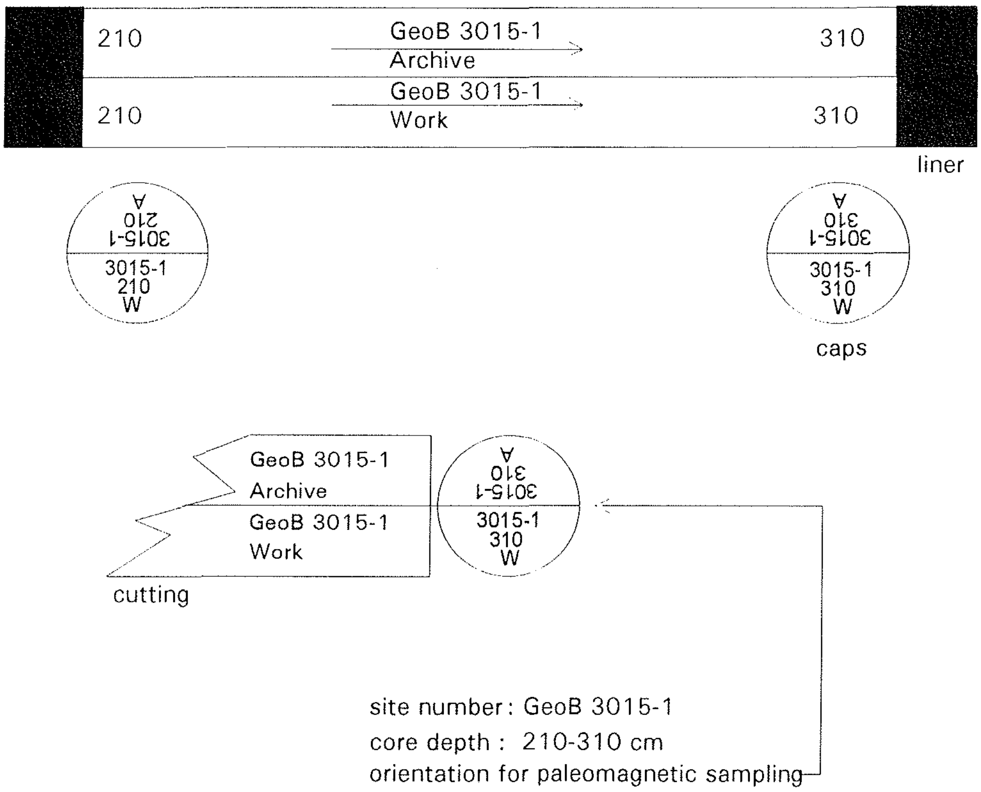


Fig. 22 Scheme of the inscription of gravity core segments

20 of the 22 cores were cut along-core in two halves: one half was kept as 'Archive' material, the other as 'Work' material. The sediments were described, smear-slide samples were prepared from distinctive layers, and spectrophotometric measurements were carried out and a photograph was taken of the 'Archive' half, which was stored in a low temperature room at 4°C.

The surface of every core segment was scraped with a knife to expose a fresh, unsmeared surface for measurements at 5 cm intervals, coinciding with the sampling depths for geochemical and faunal studies. The wet surface of the sediments was covered with a thin, transparent plastic film (Hostaphan) in order to protect the photometer from being soiled. Before measurements, the spectrophotometer was calibrated for white colour reflectance by attaching a white calibration cap. The spectrophotometer readings were transferred to a personal computer and a graphic representation for selected wave band reflection (450, 550, and 700 nm) of each core is given in the following section (Figs. 35 to 56). Finally, electrical conductivity and magnetic susceptibility measurements were carried out in 2 cm intervals (see Chapter 4.6).

From the 'Work' half-core two parallel series of syringe samples (10 $cm^3$) and cube samples (6 $cm^3$) were taken as a routine measure at depth intervals of 5 and 10 cm, respectively. These syringe samples will be used for the measurements and determinations of physical properties, stable isotopes, foraminiferal assemblages, organic geochemistry and paleomagnetic investigations. Additionally, at cores GeoB 5110-4, 5112-4, 5115-1, 5116-2, 5117-1, 5120-2, 5121-1, 5130-2, 5132-3, 5133-1 and 5136-1 syringe samples for an initial shipboard biostratigraphic analysis (10 $cm^3$) were taken at depth intervals of 5 cm in the first 50 cm of the core, and at depth intervals of 20 cm in the rest of the core (see Chapter 4.5.3). Furthermore, at cores GeoB 5115-1 and 5116-2, syringe samples (5 g) were taken at depth intervals of 10 cm for on-board measurements of the carbonate content (see Chapter 4.5.5). The sampling holes were plugged with pieces of polystyrol and both halves of the cores were stored in core tubes (D-tubes).

### 4.5.3 Stratigraphy

(T. Lützeler, H.-S. Niebler)

#### 4.5.3.1 Methods of Biostratigraphic Analysis

An initial shipboard biostratigraphic analysis was made for 11 gravity cores by taking sediment samples at a 5 cm interval in the upper 50 cm of each core and every 20 cm from 50 cm core depth to the core bottom. Depending on sediment facies, 2-8 ml of sediment were washed over a 63 µm mesh sieve, dried in an oven at 70°C and placed into 5 ml glass tubes. The height of the sediment column in the glass tube was used as an indicator for the relative sand content of the sample. The sand content varies depending on the foraminifer fertility in the surface water, but can also be used as an indicator of carbonate dissolution.

The stratigraphic classification was made by determining the abundance of the planktic foraminifer group of *Globorotalia menardii* in the fraction > 150 µm. The *G. menardii* group consists of closely related subspecies (e.g. *G. menardii menardii, G. menardii gibberula, G. tumida, G. tumida flexuosa)*, which occur in the present-day Atlantic Ocean between about 25°N and 30°S. With an OTTO splitter the sample was quantitatively subsampled until about 400 foraminifer specimens were left for binocular investigation. In this split, all foraminifers of the *G. menardii* group were counted and then the total number of *G. menardii* per sample was calculated using the splitting rate.

On the basis of the cyclic appearence and disappearence of the *G. menardi* species group, Ericson and Wollin (1968) defined a biostratigraphic zonation scheme using a letter notation from Z (Holocene) to Q (1.75-2 million years ago), whereby species of the *G. menardi* group are abundant in zone Z, missing in zone Y, abundant in zone X and so on. Up to a certain age the zonal boundaries correlate approximately with stage boundaries of the more precise oxygen isotope stratigraphy. The ages for biostratigraphic boundaries used here are fixed as follows (approximate oxygen isotope stage boundaries in brackets):

| | | |
|---|---|---|
| Z/Y | 12 ka before present | (~1/2) |
| Y/X | 80 ka before present | (~4/5) |
| X/W | 130 ka before present | (~5/6) |
| W/V | 185 ka before present | (~6/7) |
| V/U | 370 ka before present | (~10/11) |
| U/T | 550 ka before present | (~14/15) |

#### 4.5.3.2 Shipboard Results

Planktic foraminifera are abundant in all investigated cores. The cores contain more or less undisturbed Pleistocene sequences. The preliminary biostratigraphic results are summarized in Table 14, listing the estimated sub-bottom depth positions of *G. menardii* zone boundaries. The results are mostly confirmed by an initial stratigraphy using susceptibility data (see Chapter 4.6). The individual biostratigraphies are shown in Figs. 23 to 33 together with the species number of the *G. menardii* group and the down-core variations in sand content.

Table 14 Biostratigraphic summary of sediment cores from cruise M 41/3. Estimated sub-bottom positions (in cm) of identified *G. menardii* zone boundaries

| **Biostratig. Boundaries** | **Z/Y** | **Y/X** | **X/W** | **W/V** | **V/U** | **U/T** |
|---|---|---|---|---|---|---|
| **Core** | **12 ka** | **80 ka** | **130ka** | **185 ka** | **370 ka** | **550 ka** |
| **GeoB 5110-4** | 20 | 295 | 590 | — | — | — |
| **GeoB 5112-4** | -35 | -5 | 50 | 75 | 245 | 395 |
| **GeoB 5115-1** | 5 | 45 | 95 | 120 | — | — |
| **GeoB 5116-2** | 5 | 25 | 115 | 140 | 320 | — |
| **GeoB 5117-1** | 5 | 80 | — | — | — | — |
| **GeoB 5120-2** | 10 | 45 | 145 | 170 | 340 | — |
| **GeoB 5121-1** | 5 | 50 | 75 | 95 | 340 | — |
| **GeoB 5130-2** | 25 | 225 | 510 | — | — | — |
| **GeoB 5132-3** | 10 | 125 | ?315 | — | — | — |
| **GeoB 5133-1** | 10 | 70 | 120 | 140 | 460 | — |
| **GeoB 5136-1** | 15 | 150 | 195 | ?225 | ? | — |

*Northwestern Vema Channel*

GeoB 5110-4 (position 25°54.3'S 35°38.4'W, water depth: 4188 m, length: 961 cm) Fig. 23
The stratigraphic classification in this core is uncertain due to carbonate dissolution (water depth of 4188 m). The carbonate preservation is generally weak, only in a few samples moderate, which is expressed by a very low sand content. The base of the core reaches into zone W. The mean sedimentation rate of core GeoB 5110-4 is 5 cm/ka and varies between 1.5 cm/ka during the Holocene and 6 cm/ka during zone X.

*Mid-Atlantic Ridge, Profile 24°S, Brazil Basin*

GeoB 5112-4 (position 23°49.5'S 16°15.5'W, water depth: 3842 m, length: 559 cm) Fig. 24
The upper 38 cm of this core were recovered from the bomb of the gravity corer, the surface is missing or mixed. Therefore it seems that the Holocene was not fully recovered. The base of the core reaches into zone T and this core reveals the oldest sediments of all recovered cores during this cruise. A further stratigraphic determination is based on a correlation of a diatom ooze layer (e.g. core GeoB 3813-3, see Wefer et al. 1996), which has an age of about 520 ka. The sedimentation rate of core GeoB 5112-4 is generally low in the order of 0.8 cm/ka. The carbonate preservation is generally good, only in a few samples in the zones V and U moderate. The sand contents are higher during zones Z to W, due to a better preservation of larger foraminifera.

GeoB 5115-1 (position 24°08.6'S 14°02.6'W, water depth: 3291 m, length: 406 cm) Fig. 25
The base of the core reaches into zone V. In contrast to the average sedimentation rate of 1.5 cm/ka, the sedimentation rate of the Holocene (zone Z) and isotope stage 6 (zone W) is very low (0.5 cm/ka). In zones Y and X the sedimentation rates are somewhat higher (0.7 cm/ka and 1 cm/ka, respectively). The carbonate preservation is very good, the sand content shows a maximum at the boundary of zones X and V, but becomes low during zone V.

GeoB 5116-1 (position 24°09.5'S 13°46.2'W, water depth: 2550 m, length: 540 cm) Fig. 26
The core reaches into zone U and has an average sedimentation rate of 0.9 cm/ka. As in core GeoB 5115-1 the sedimentation rate of the Holocene (zone Z) is very low, which could also result from a partial loss of the surface sediment. The carbonate preservation is very good. The sand content becomes lower during zones X and U.

GeoB 5117-1 (position 24°08.9′S 13°58.4′W, water depth: 3040 m, length: 139 cm) Fig. 27
Because of its short length this core only penetrates zone X. Thus, the core base is younger than 130 ka. The sedimentation rate is on average 1 cm/ka, whereby the sedimentation rate of the Holocene (zone Z) is again lower. The carbonate preservation is very good. The sand content shows a maximum in zone Y (isotope stages 2-4), but becomes low during warm periods (zone Z and X).

*Mid-Atlantic Ridge, Profile 24°S, Angola Basin*

GeoB 5120-2 (position 24°10.2′S 12°21.8′W, water depth: 3844 m, length: 376 cm) Fig. 28
This core has an average sedimentation rate of 0.9 cm/ka. Sedimentation rates are relatively low in zones Y and Z (0.5 cm/ka), and slightly higher in zones Z, X and V (1 cm/ka, 2 cm/ka and 0.9 cm/ka, respectively). The core ends in zone U. The carbonate preservation is good throughout the core, the sand content becomes higher in zone W.

GeoB 5121-1 (position 24°11.0′S 12°01.3′W, water depth: 3488 m, length: 531 cm) Fig. 29
In this core the identification of zones Z to X is uncertain, but is confirmed by susceptibility data. The sedimentation rates in zones Z to W are low (between 0.4 and 0.7 cm/ka). The sedimentation rate in zone V is higher with 1.3 cm/ka. Core GeoB 5121-1 has an average sedimentation rate of 0.9 cm/ka and is therefore comparable with GeoB 5120-2. Also the carbonate preservation is good. The sand content becomes higher in zone Y, at the boundary of zone W/V and in zone U.

*Mid-Atlantic Ridge, Profile 19°S, Angola Basin*

GeoB 5130-2 (position 19°24.2′S 09°27.6′W, water depth: 3165 m, length: 517 cm) Fig. 30
The base of the core reaches into zone W and therefore this is one of the recovered cores with a higher sedimentation rate. The average sedimentation rate is 4 cm/ka. The sedimentation rate of the Holocene (zone Z) is with 2 cm/ka relatively low, but increases in zones Y (3 cm/ka) and X (6 cm/ka). The carbonate preservation is generally good, but becomes weak at a core depth between 108 and 208 cm (zone Y). The sand content shows a maximum in the Holocene and in the first centimeters of zone Y as well as in zone X.

GeoB 5132-3 (position 19°07.5′S 09°43.1′W, water depth: 3941 m, length: 326 cm) Fig. 31
Core GeoB 5132-3 has an average sedimentation rate of 2.5 cm/ka. The sedimentation rates are relatively low in zones Y and Z (1 cm/ka and 1.7 cm/ka, respectively) and higher in zone X

(4 cm/ka). The core probably ends at zone boundary X/W. The carbonate preservation is good throughout the core. As in core GeoB 5130-2, the sand content shows a maximum in the Holocene and in the first centimeters of zone Y and in zone X.

GeoB 5133-1 (position 19°05.1'S 10°11.6'W, water depth: 3661 m, length: 503 cm) Fig. 32
The stratigraphic classification of this core differs very much from the other two cores from the 19°S Profile in the Angola Basin. Core GeoB 5133-1 reaches into zone U and has an average sedimentation rate of 1.2 cm/ka. The sedimentation rates between the Holocene and isotope stage 5 (zone Z to zone X) are equal with 1 cm/ka. In zone W the sedimentation rate is very low with only 0.4 cm/ka, but becomes higher in zone V (1.7 cm/ka). The carbonate preservation is very good. The sand content is higher in the zones Z to W and becomes lower during zone V.

*Mid-Atlantic Ridge, Profile 19°S, Brazil Basin*

GeoB 5136-1 (position 19°22.2′ S 12°40.2′ W, water depth: 3227 m, length: 529 cm) Fig. 33
This core has an average sedimentation rate of 1.2 cm/ka. Sedimentation rates are relatively high in zones Y and Z (1 cm/ka and 2 cm/ka, respectively), and relatively low in zones X and W (0.9 cm/ka and 0.5 cm/ka, respectively). Core GeoB 5136-1 ends in zone V. The carbonate preservation is very good, but the sand content becomes very low in the lower part of zone Y, which means that foraminifer fragmentation increases.

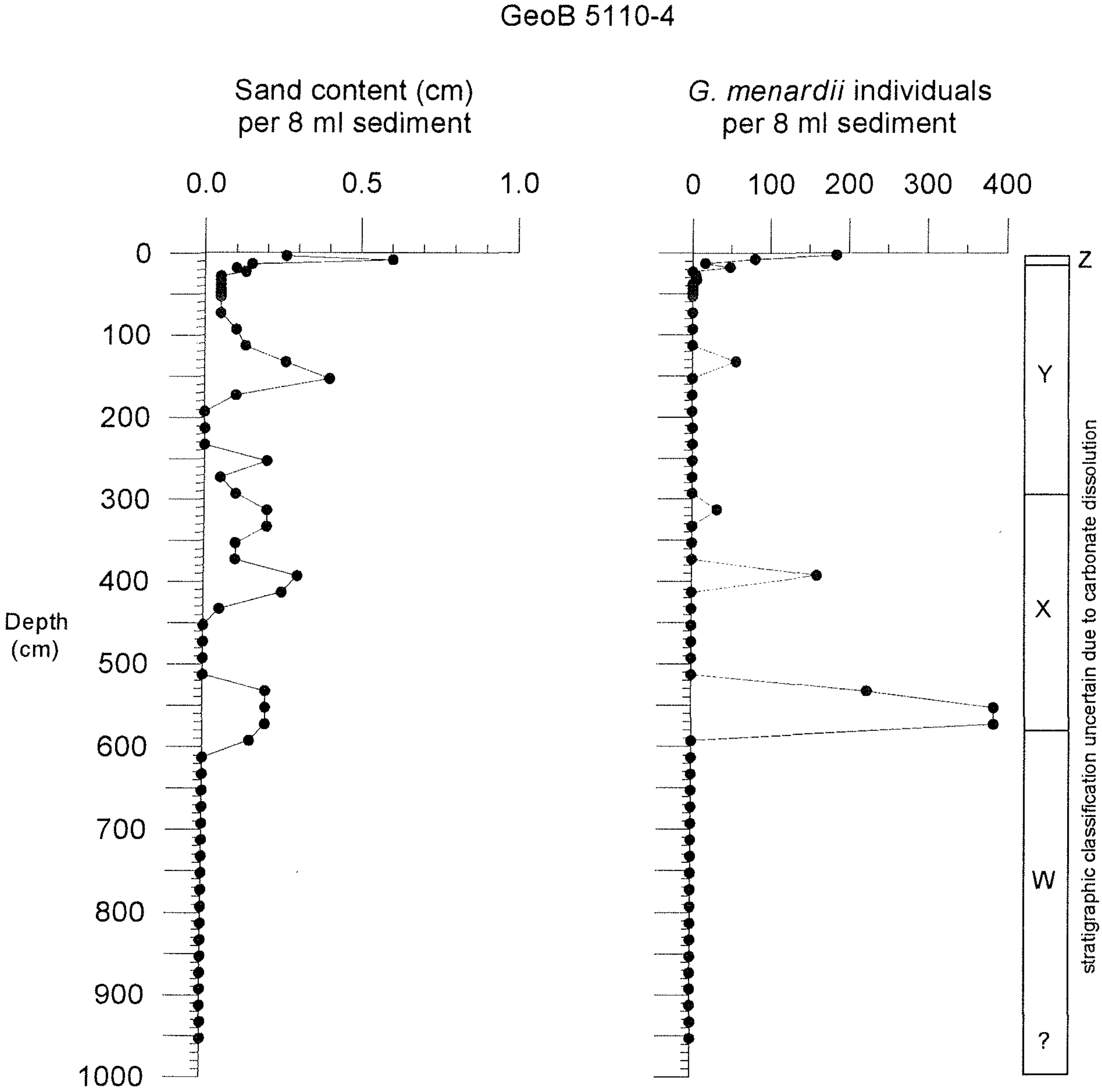


Figure 23 Biostratigraphic analysis and sand content of GeoB 5110-4

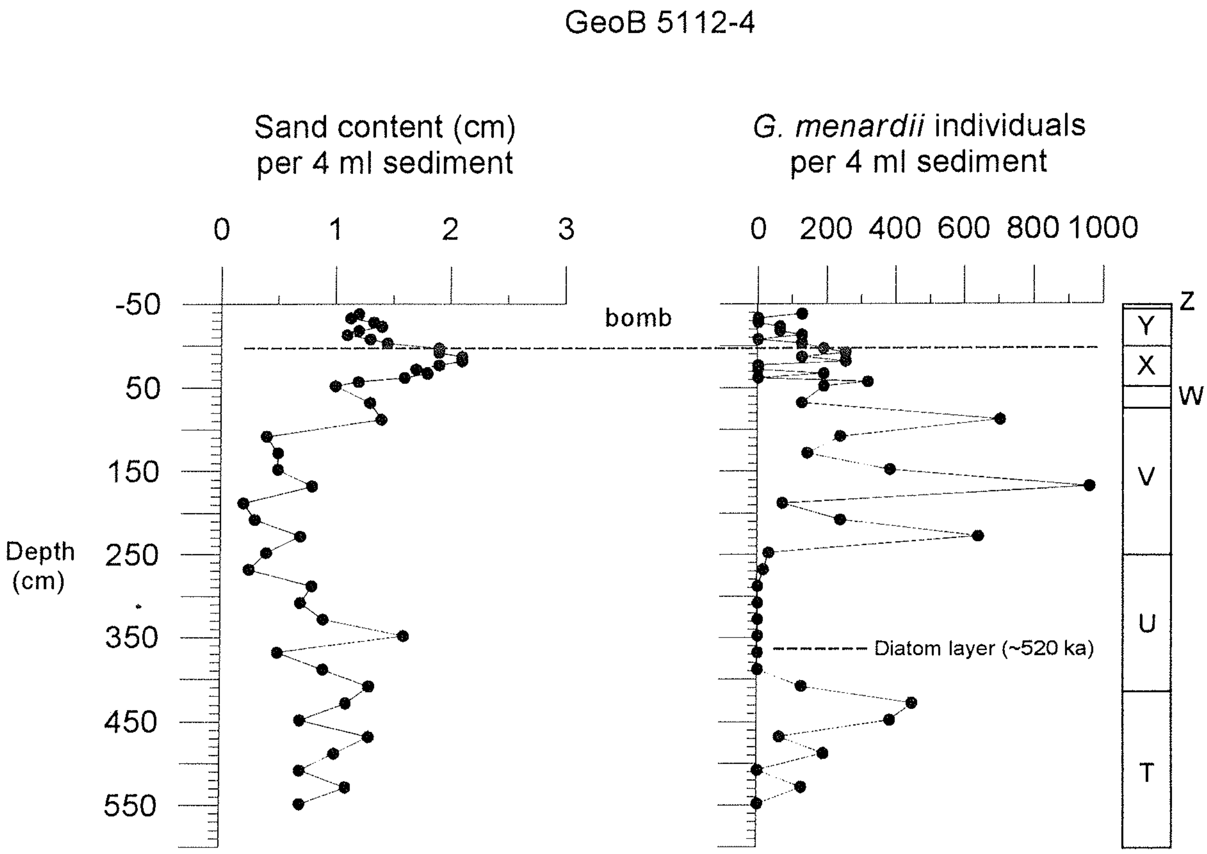


Figure 24 Biostratigraphic analysis and sand content of GeoB 5112-4

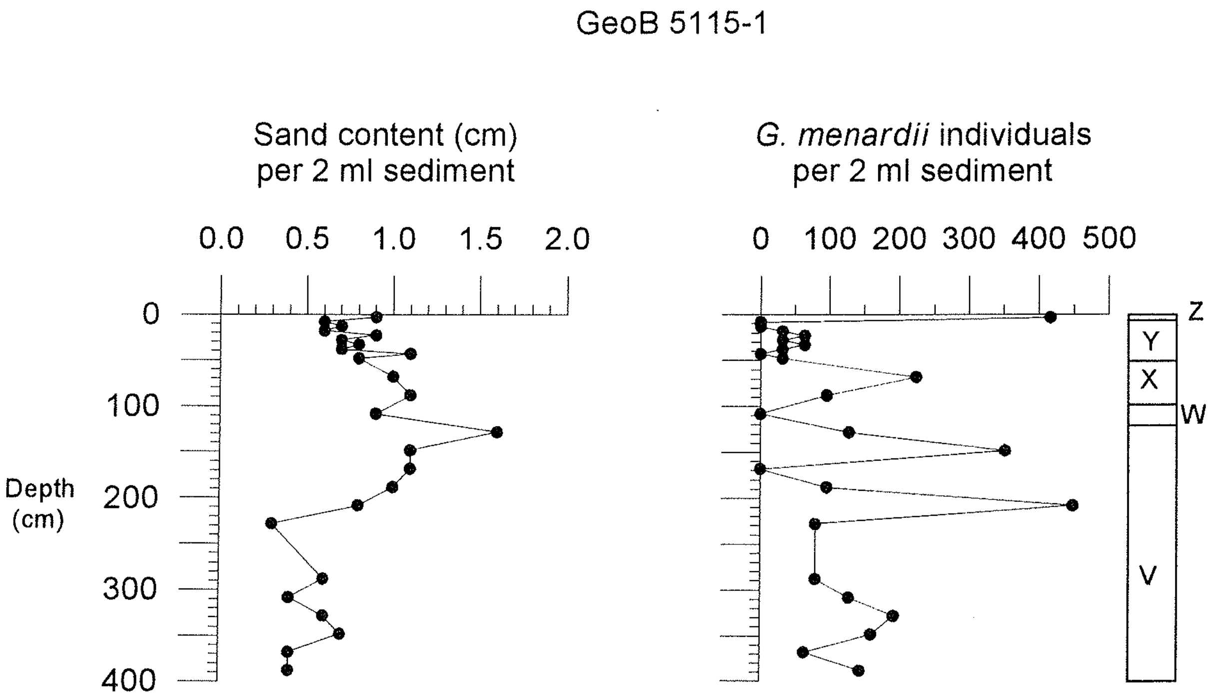


Figure 25 Biostratigraphic analysis and sand content of GeoB 5115-1

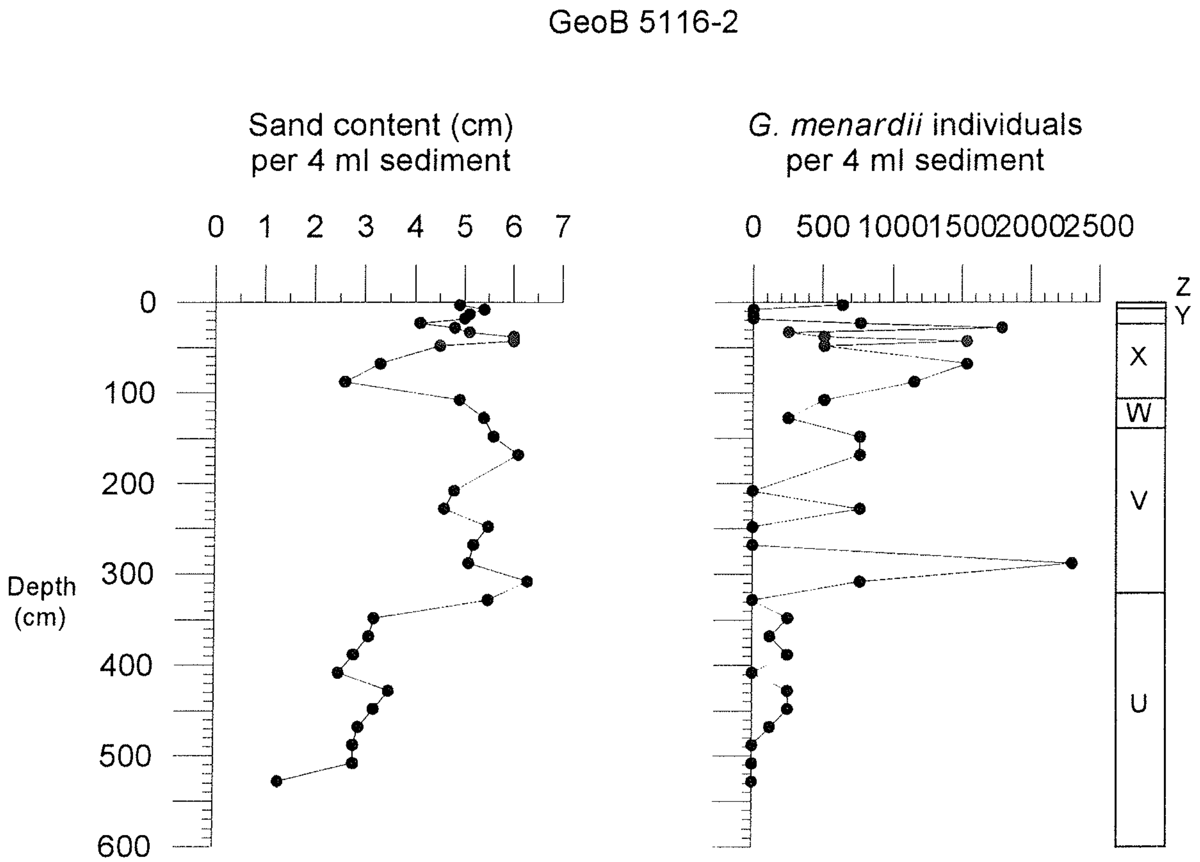


Figure 26 Biostratigraphic analysis and sand content of GeoB 5116-1

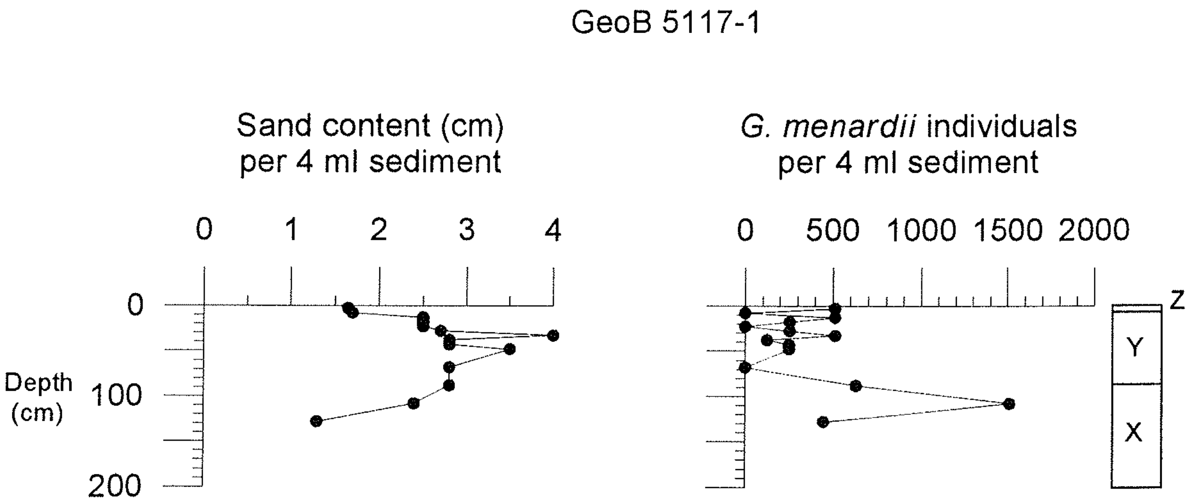


Figure 27 Biostratigraphic analysis and sand content of GeoB 5117-1

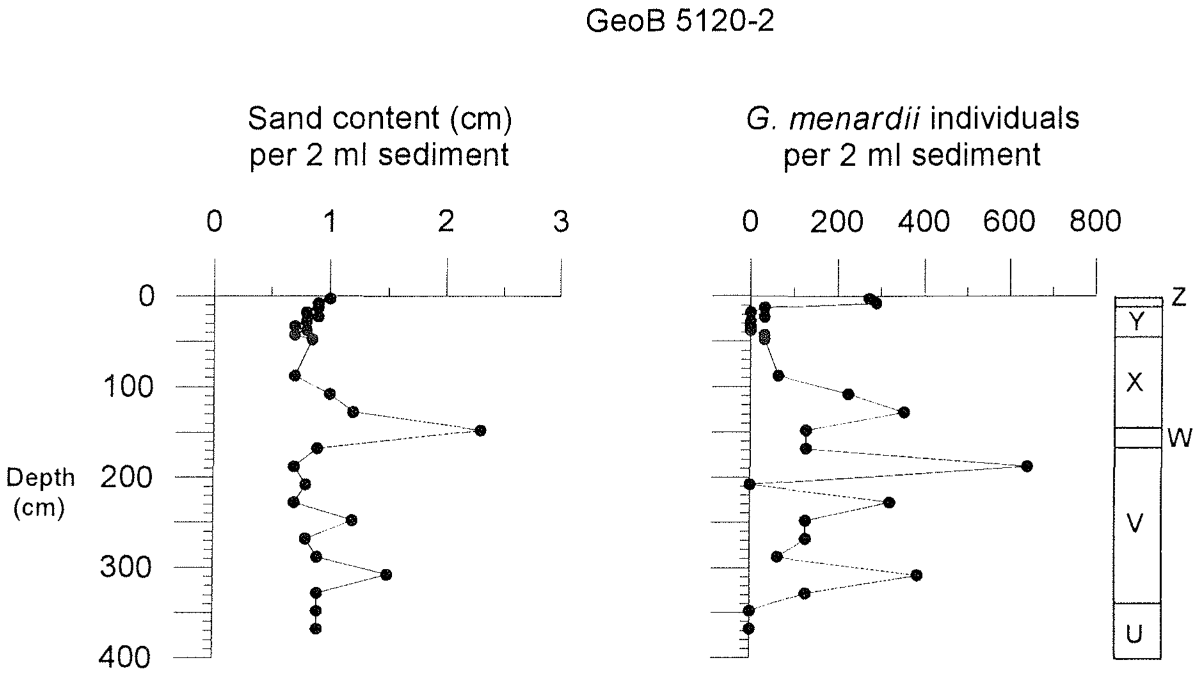


Figure 28 Biostratigraphic analysis and sand content of GeoB 5120-2

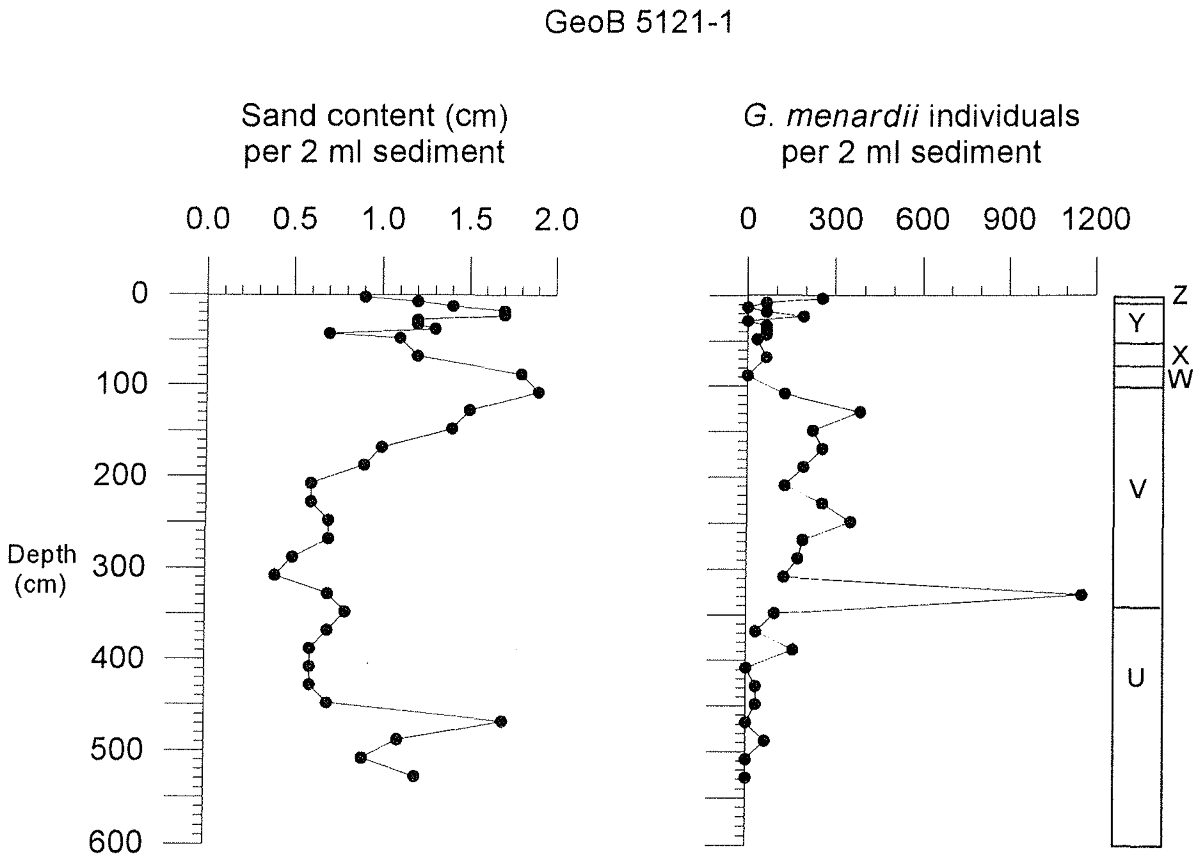


Figure 29 Biostratigraphic analysis and sand content of GeoB 5121-1

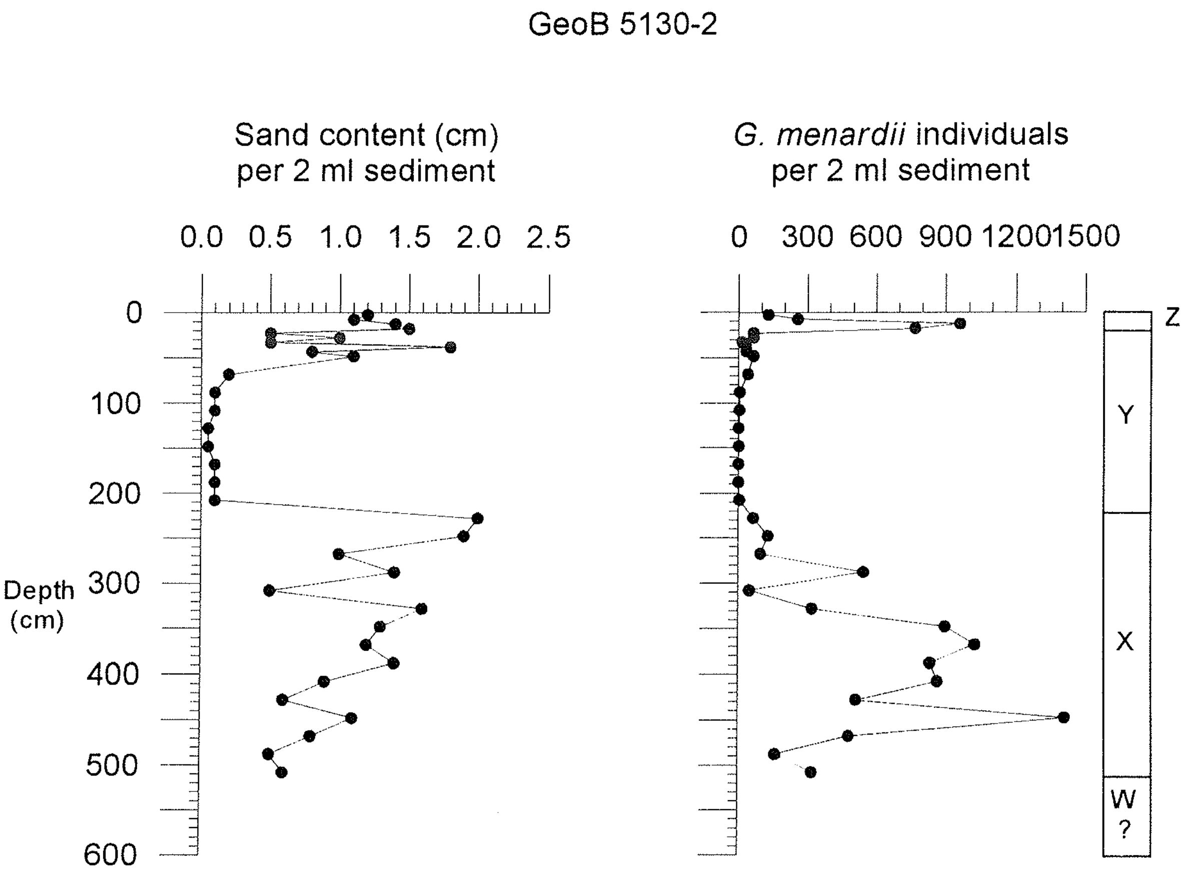


Figure 30 Biostratigraphic analysis and sand content of GeoB 5130-2

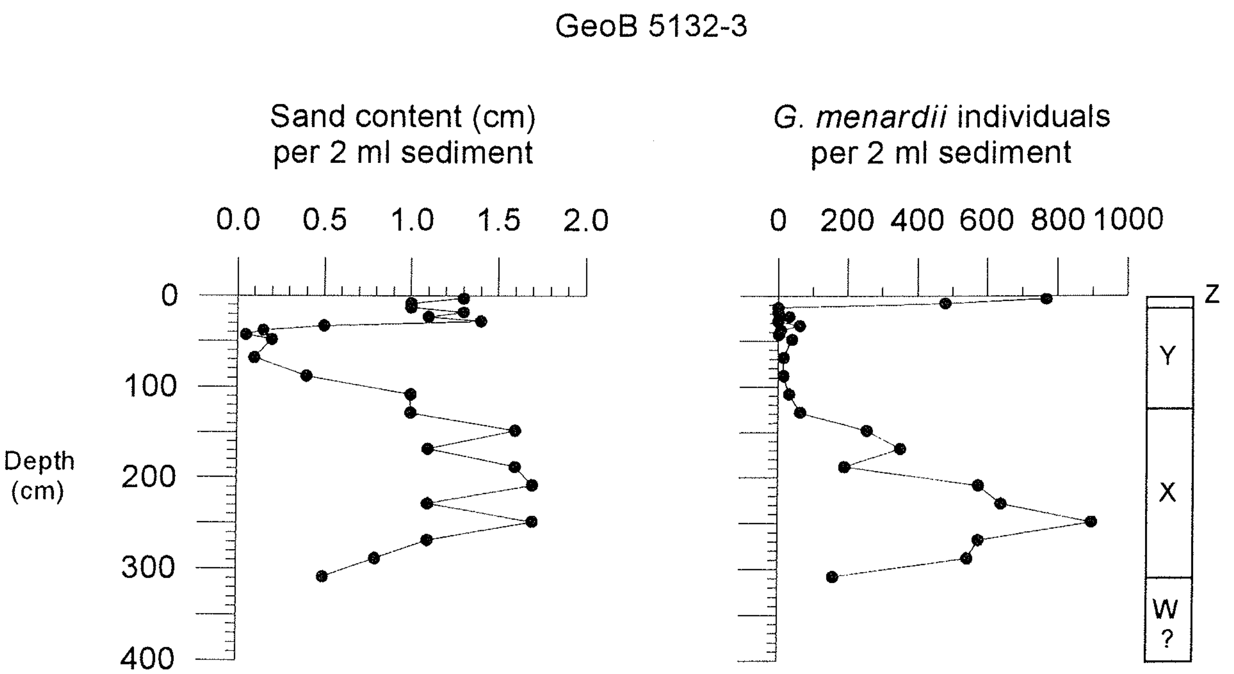


Figure 31 Biostratigraphic analysis and sand content of GeoB 5132-3

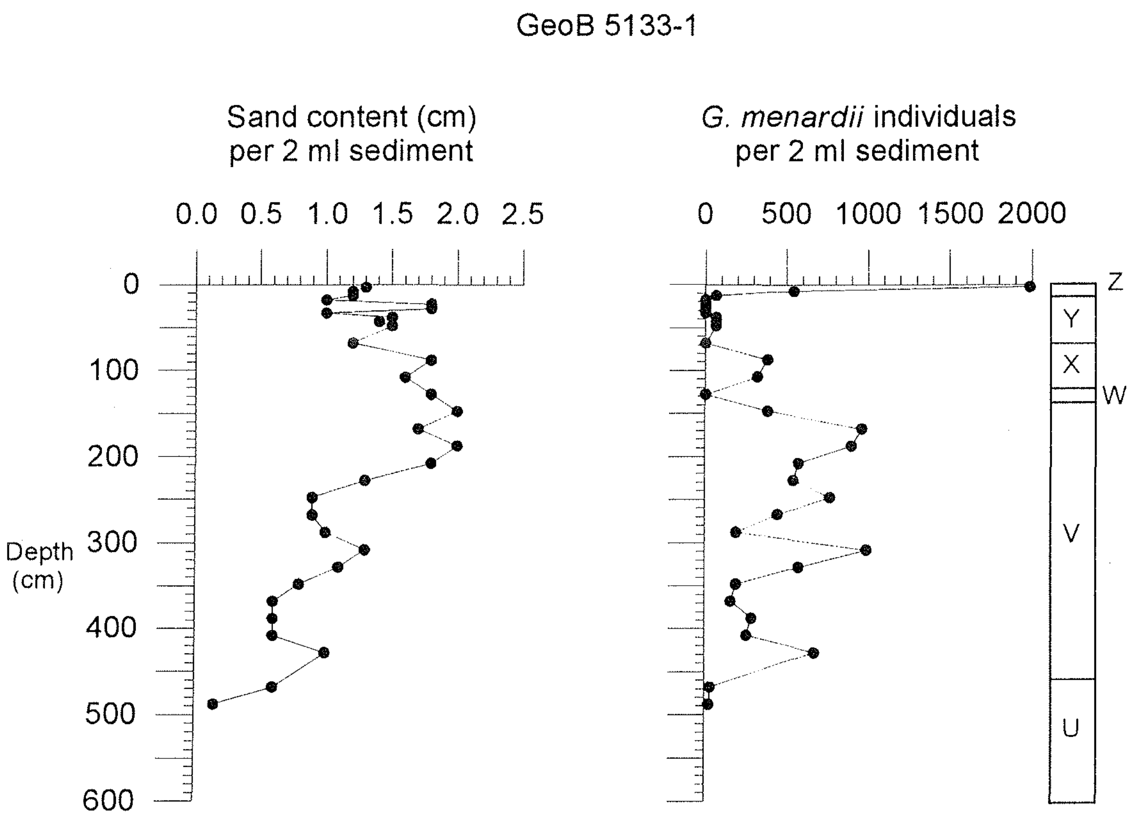


Figure 32 Biostratigraphic analysis and sand content of GeoB 5133-1

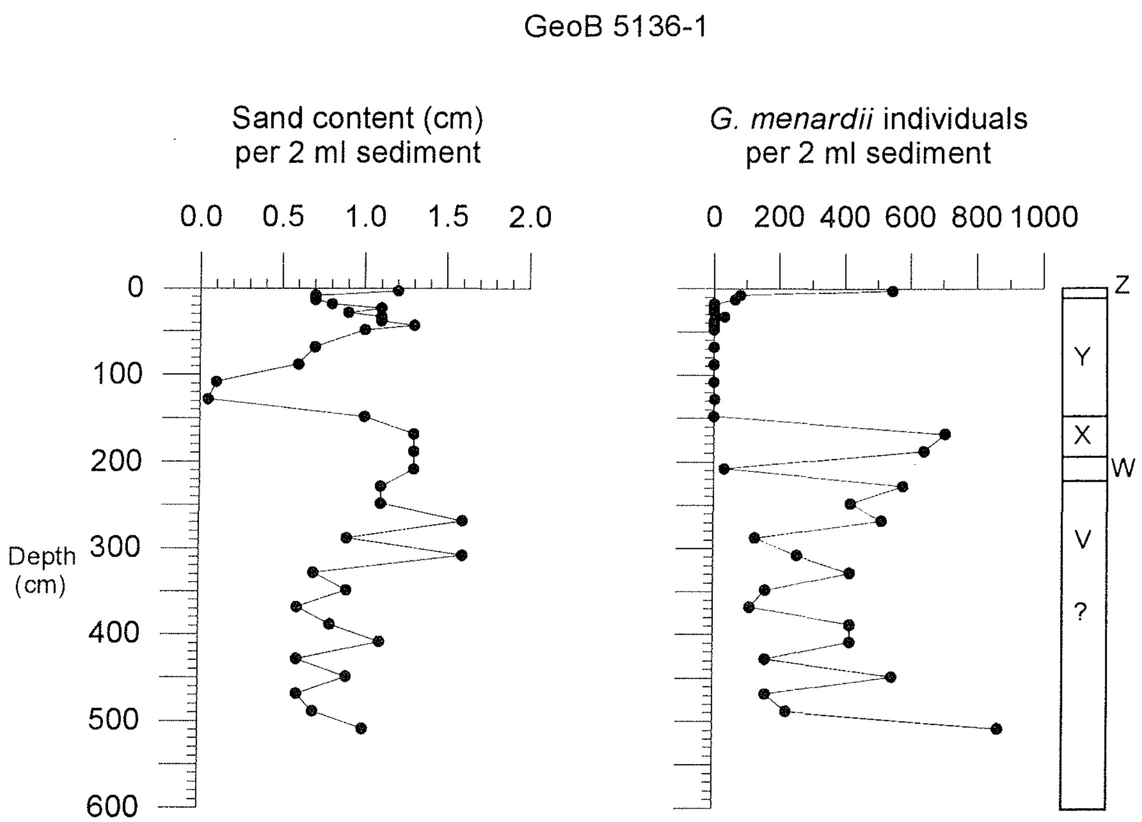


Figure 33 Biostratigraphic analysis and sand content of GeoB 5136-1

### 4.5.4 Lithologic Core Summary

(C. Moos, H.-S. Niebler, T. Westerhold)

This preliminary lithological summary of the sediments retrieved with the gravity corer is based on visual core description and colour scanner readings as well as microscopic observations of the smear slides taken from distinctive sediment horizons. Core descriptions are shown in Figures 35 to 54 (legend for stratigraphic columns is shown in Fig. 34), representing main lithologies, their colour according to the Munsell Soil Color Charts, and sedimentary structures. For correlation, colour scanner readings of distinctive wave length bands (450, 550, 700 nm) are also shown. It is likely, that the colour changes result from variations in the sediment composition - particularly the ratio of carbonate (light and high reflection values) to organic residue and clay mineral (dark or low reflection values) content. The lithological descriptions are primarily based on smear slide analysis. Smear slides were taken from all representative lithological units in all cores and from layers of special interest. The slides were then mounted with „Norland optical adhesive". They were examined on board ship using a transmitted light microscope at 100 to 400x magnification under plane-polarised and cross-polarised light. The sediment classification is based on ODP nomenclature following the terminology defined by Dean et al. (1985). A total of 232 smear slides were prepared and analysed (Table 15). The main purpose of the core description was to characterise all representative lithologies and special or unique layers of particular interest.

To quantify the colour of the sediment a Minolta CM-2002™ hand-held spectrophotometer was used to measure the light reflectance of all gravity cores at 31 wavelength channels in the range of visible light (400 - 700 nm). The readings were taken immediately after splitting the core. The archive halves of the cores were scraped with a knife to expose a fresh, unsmeared surface for the measurements. The core was then covered with a transparent Hostaphan®-film to protect the camera. Measurements were taken every 5 cm, at the same positions as the samples taken from the work half, to resolve small scale colour changes. Before measurements were taken, a white calibration of the spectrophotometer was performed using a white calibration standard and a white reference measurement was included in the data file. The calibration surface was covered with the same plastic film as the core to avoid any bias in the readings.

The reflectance profiles at the three wavelengths (400 nm, 550 nm, 700 nm) are shown next to the core diagrams. These three wavelengths give a good overview of sediment colour spectrum, since they cover most of the spectrum measured. In addition they represent the colours blue, green and red, respectively.

The colour of the sediment is strongly influenced by its carbonate content and terrigenous material. In cores with a carbonate content below approx. 50 wt.% the lightness (L*) of the sediment correlates well with the carbonate content. This correlation can be used as a basis for a preliminary stratigraphy by correlating the lightness of the sediment colour to the carbonate data of other cores from the region. The hue (H) of the sediment colour seems to be strongly influenced by the input of terrigenous material. Low values in lightness and hue are indicators for turbidite and sandy layers. This might be also an effect of porosity. Also air bubbles between the plastic film and the sediment shows same effect.

During M 41/3 sediment cores were mainly recovered from the Mid-Atlantic Ridge except for core GeoB 5110-4, which was retrieved in the northwestern exit of the Vema Channel. The cores from the Mid-Atlantic Ridge, which were recovered on two profiles at about 24°S and 19°S, were underlying the oligotrophic waters of the central Subtropical Gyre. Carbonate, mainly composed of coccolithophorid and foraminiferal shells, is the most abundant biogenic material in these very low productivity waters and constitutes the major sedimentary component. Despite the large distance to the African continent, aeolian transported FeOH-rich terrigenous minerals originating from the Sahara average several wt. % of the sediment. The partly intensive brownish to grey-reddish colours are to some extent caused by the supply of Saharan dust but are probably also a result of deep oxygen penetration depths into the sediment, which are typical for the oligotrophic waters of the pelagic environment. The sediment cores from both profiles are frequently disrupted by turbidite sequences. This may be attributed to the core locations which are mostly situated within small morphological depressions. Most of the cores show similar colour reflectance characteristics which are particularly obvious at the 700 nm wavelength band (red). Colour reflectance and lightness are good indicators to identify turbidites and sandy layers in most of our cores. In most cores lithological units are combined with colour changes and changes in light reflectance.

*Northwestern Vema Channel*

GeoB 5110-4 (position 25°54.3′S 35°38.4′W, water depth: 4188 m, length: 961 cm) Fig. 35
This core was recovered from a depth within the lysocline and therefore selective carbonate dissolution was expected. The selective carbonate dissolution has been observed in high foraminifer fractionation during the initial stratigraphic investigation (see Chapter 4.5.3.2). The upper part of the core is composed of clay bearing nannofossil ooze with foraminifers, whereby the lower part (404-532 cm and below 576 cm) contains clay and only few nannofossils and foraminifera. Minor components are dinoflagellates in depths between 0 to 176 cm. Pyrite occurs between 213 cm and the bottom of the core. The whole core contains sections with mm-thick laminated layers. At 532 cm an erosion surface occurs. Slight bioturbation appears almost in the whole core, but increases at the core top, between 576-680 cm and at 917 cm. Between 632-576 cm worm burrows occur. Brownish colours dominate, but also shades of yellow, gray and olive are abundant.

*Mid-Atlantic Ridge, Profile 24°S, Brazil Basin*

GeoB 5112-4 (position 23°49.5′S 16°15.5′W, water depth: 3842 m, length: 559 cm) Fig. 36
The sediment of this core as well as the 38 cm of sediment recovered from the bomb of the gravity corer are dominated by nannofossil ooze which is foram- and/or dinoflagellate-bearing. The whole core consists of silty to sandy sediments. Colour changes are frequent, varying from yellowish brown and light olive brown to pale yellow. Generally, the core is moderately bioturbated with different sections of worm burrows. Several mm-thick laminated diatom layers occur in the depths between 347-359 cm. These layers are known from other cores further south (e.g. GeoB 3813-3, Wefer et al. 1996) and give the possibility to correlate between cores (see Chapter 4.6).

GeoB 5115-1 (position 24°08.6′S 14°02.6′W, water depth: 3291 m, length: 406 cm) Fig. 38
The core mainly consists of yellow and brown foram-bearing nannofossil ooze. The upper 155 cm of the core are composed of silty dinoflagellate-bearing nannofossil ooze. Below 155 cm the sediment consists of foram-nannofossil ooze with some clayey sections. The core is moderately bioturbated with different sections of worm burrows. In depths between 175-181 cm and 235-270 cm turbidites are found. The turbidites are fine grained and soft, silt content increases towards the base showing graded foram sands.

GeoB 5116-2 (position 24°09.5′S 13°46.2′W, water depth: 2550 m, length: 540 cm) Fig. 39
The dominant lithology is foram bearing nannofossil ooze with dinoflagellates and/or accessory minerals as additional minor components. The upper 510 cm of the moderately bioturbated core contains silt to sand grain sizes. Below 510 cm the sediment becomes clayey to silty. The colours range from very pale brown to light brown and brownish yellow. The boundaries between the colours are diffuse.

GeoB 5117-1 (position 24°08.9′S 13°58.4′W, water depth: 3040 m, length: 139 cm) Fig. 40
During sediment recovery the tube was bent and only 139 cm of sediment were recovered. Foram bearing nannofossil ooze dominates the whole core. The moderately bioturbated light yellowish brown sediment is mainly silty with some more sandy sections. Between 114-139 cm the sediment becomes lighter in colour (pale yellow), is strongly compacted and the grain size changes to clayey silt.

*Mid-Atlantic Ridge, Profile 24°S, Angola Basin*

GeoB 5120-2 (position 24°10.2′S 12°21.8′W, water depth: 3844 m, length: 376 cm) Fig. 41
The upper 65 cm of the core are dominated by moderately bioturbated foram and dinoflagellate bearing nannofossil oozes which are clayey to silty. Between 65-173 cm the lithology changes slightly to silty and sandy grain sizes. In the depths between 65-83 cm and 131-134 cm the core is interrupted by thin turbidites. The turbidites are fine grained, soft sediment, increasingly silty towards their bases and show graded foram sands. Below the second turbidite, three sections with mm-thick laminated layers were found. These layers are interbedded into by clayey-silty nannofossil ooze, which is more or less foram-bearing. This sediment is moderately bioturbated and often contains burrows of worms. Colour changes are frequent, varying from reddish brown to pink and light yellowish brown.

GeoB 5121-1 (position 24°11.0′S 12°01.3′W, water depth: 3488 m, length: 531 cm) Fig. 42
The sediment of this core is dominated by nannofossil ooze which is foram-bearing. The whole core consists of silty to sandy sediments and is moderately bioturbated. Pyrite and glaukonite also occur between in a depth of 463 cm. Different sections of worm burrows can be found throughout the core. In depths between 494-502 cm a turbidite is found, which is fine grained, soft sediment, increasingly silty towards its base and shows graded foram sands. Colour changes are frequent, varying from light yellowish brown to pale yellow, very pale brown and white.

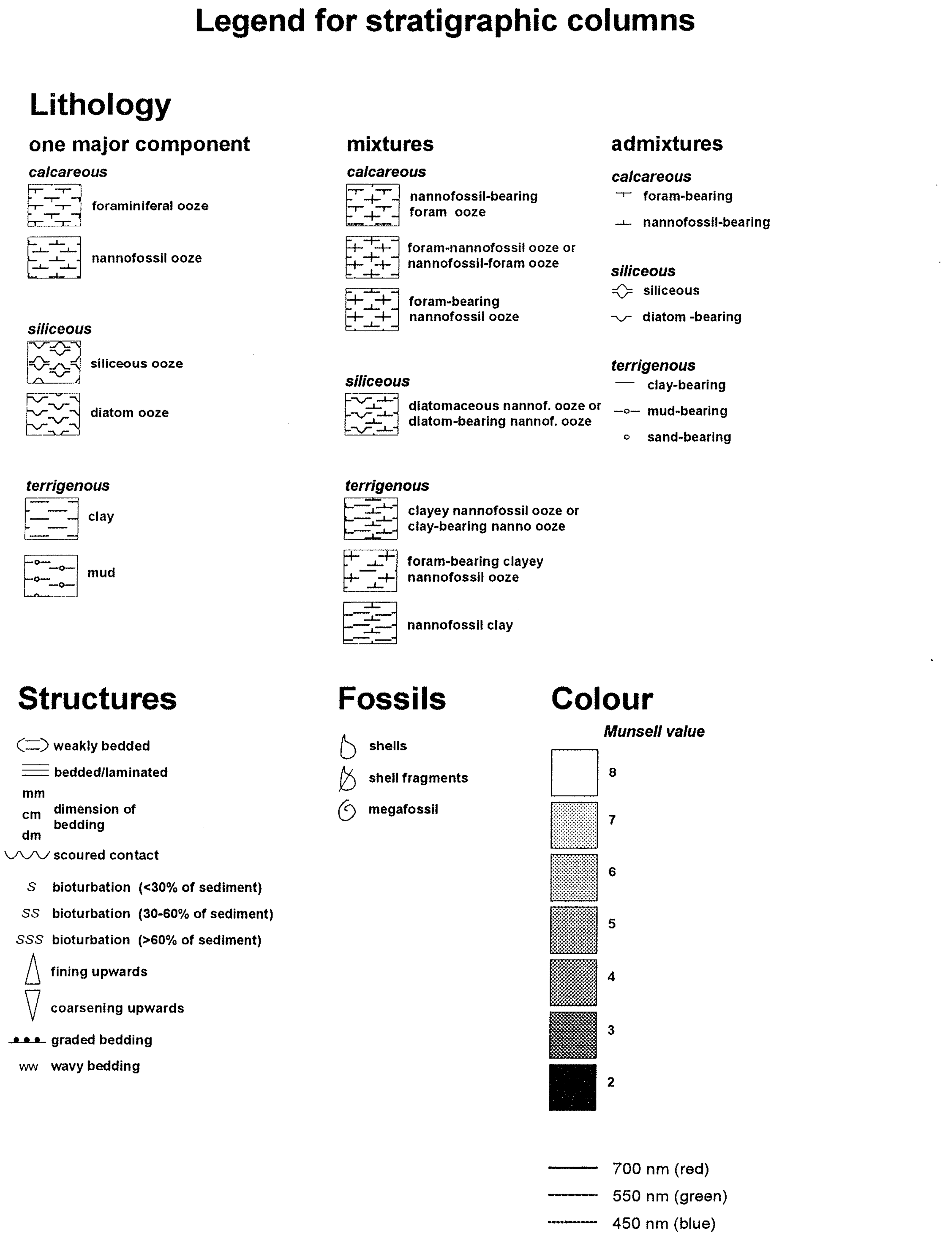


Fig. 34 Legend for stratigraphic columns in Figs. 35 - 56

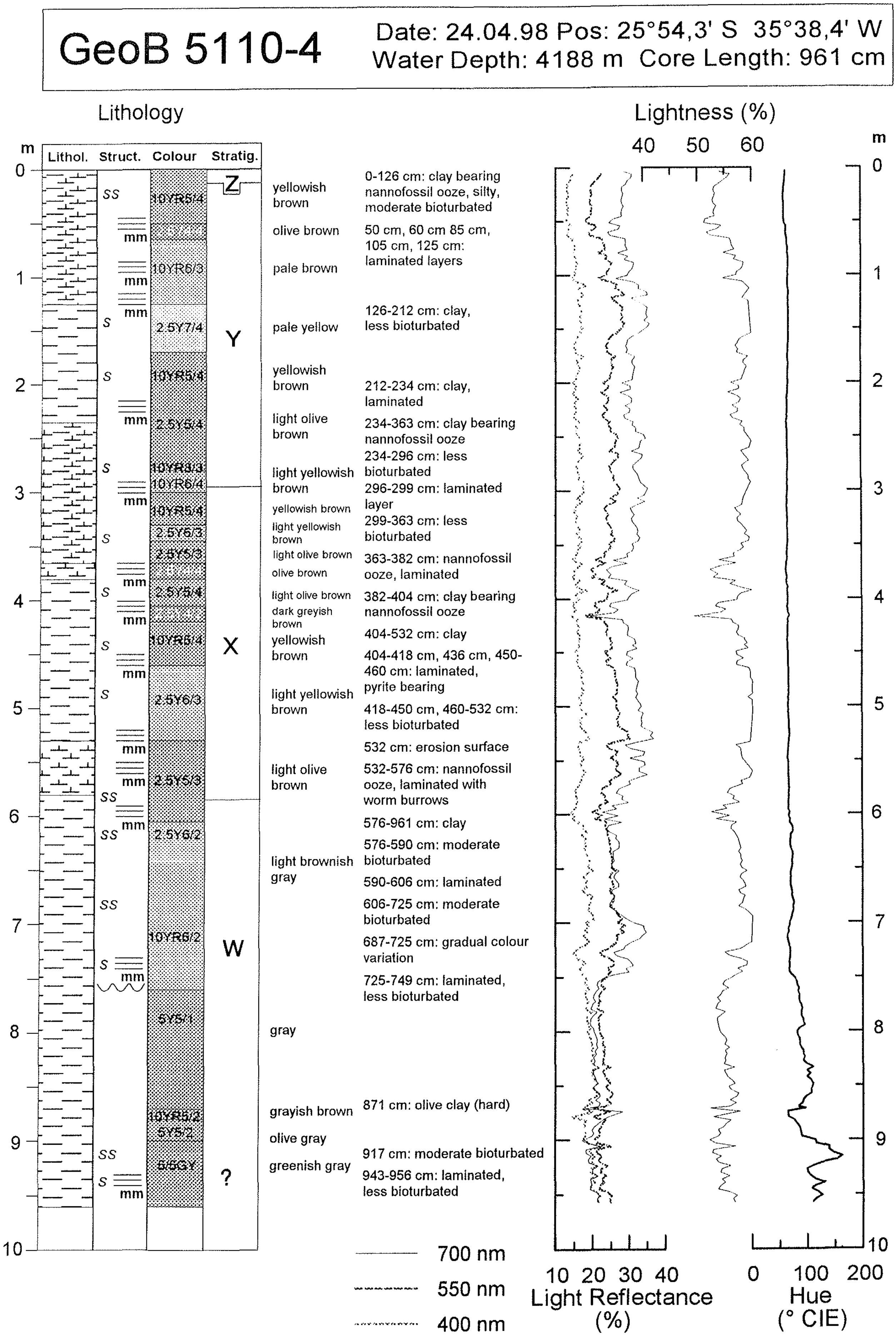


Figure 35a Core description of GeoB 5110-4

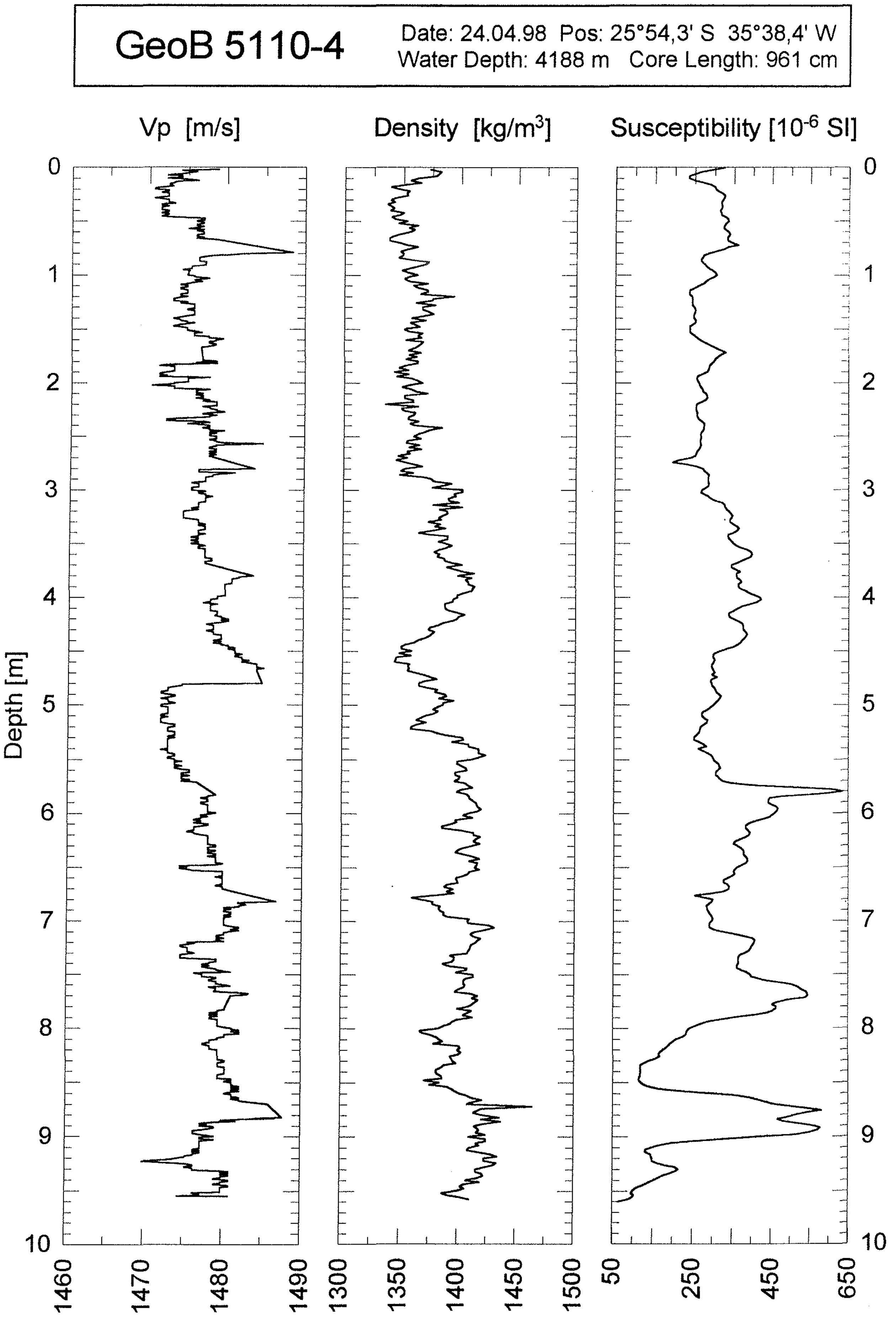


Figure 35b Physical properties data of GeoB 5110-4

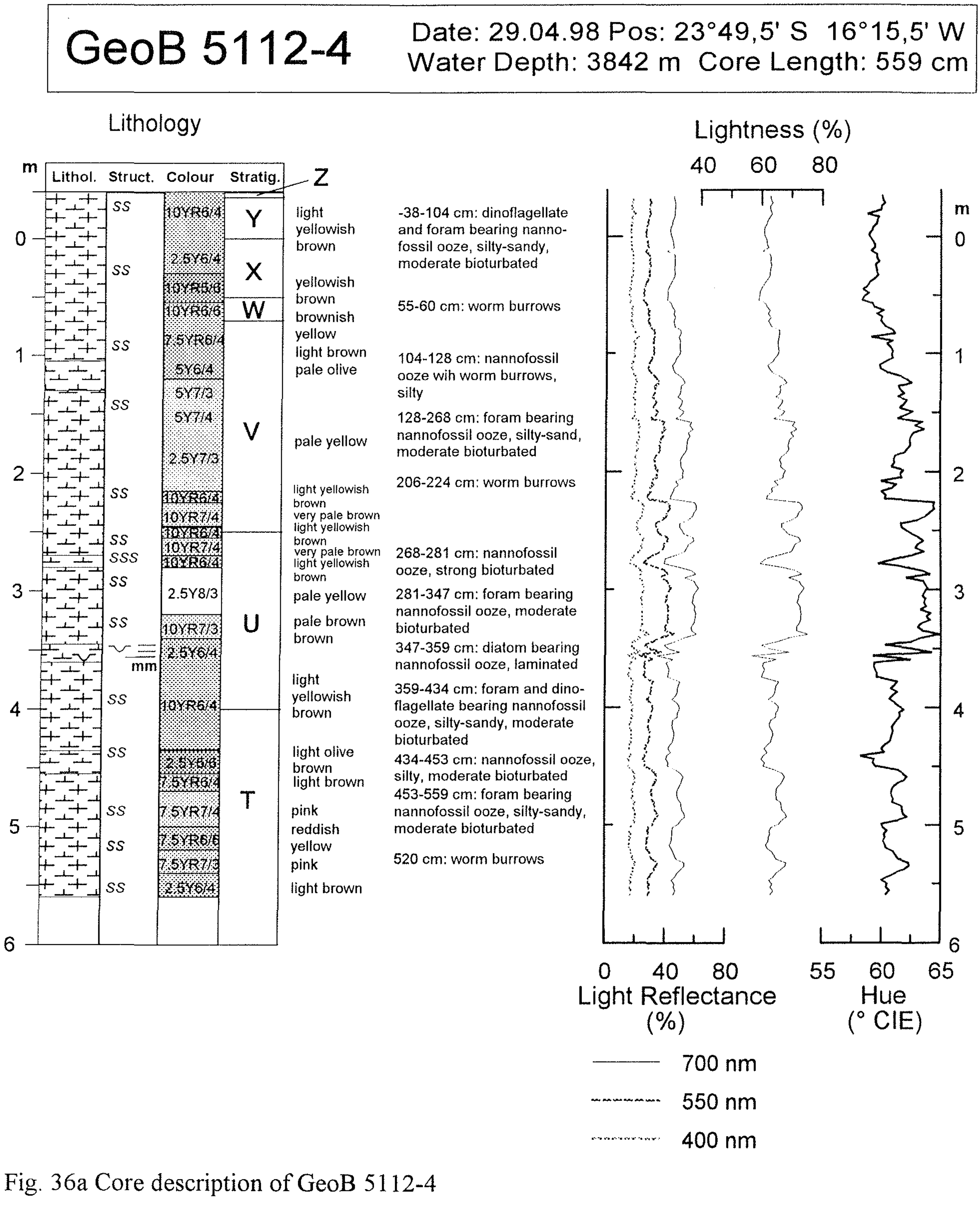


Fig. 36a Core description of GeoB 5112-4

*CORE IS NOT OPENED*

*NO CORE DESCRIPTION AVAILABLE*

Fig. 37a Core description of GeoB 5112-5

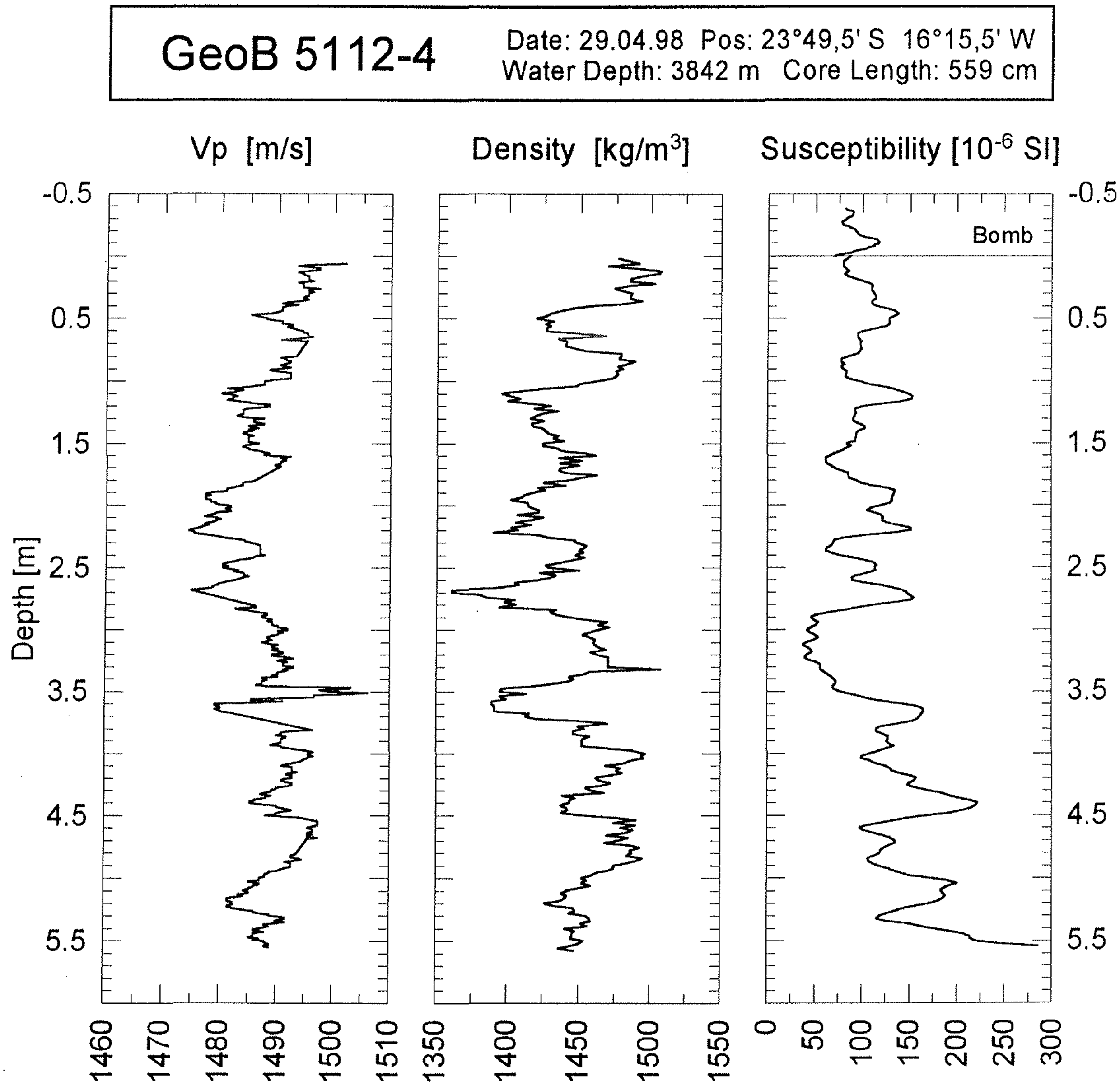


Fig. 36b Physical properties data of GeoB 5112-4

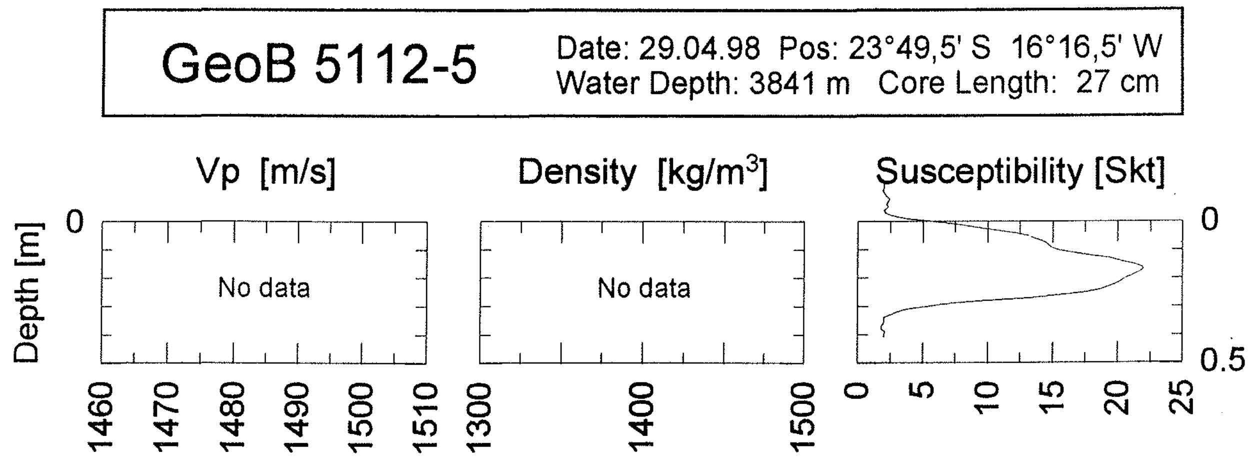


Fig. 37b Physical properties data of GeoB 5112-5

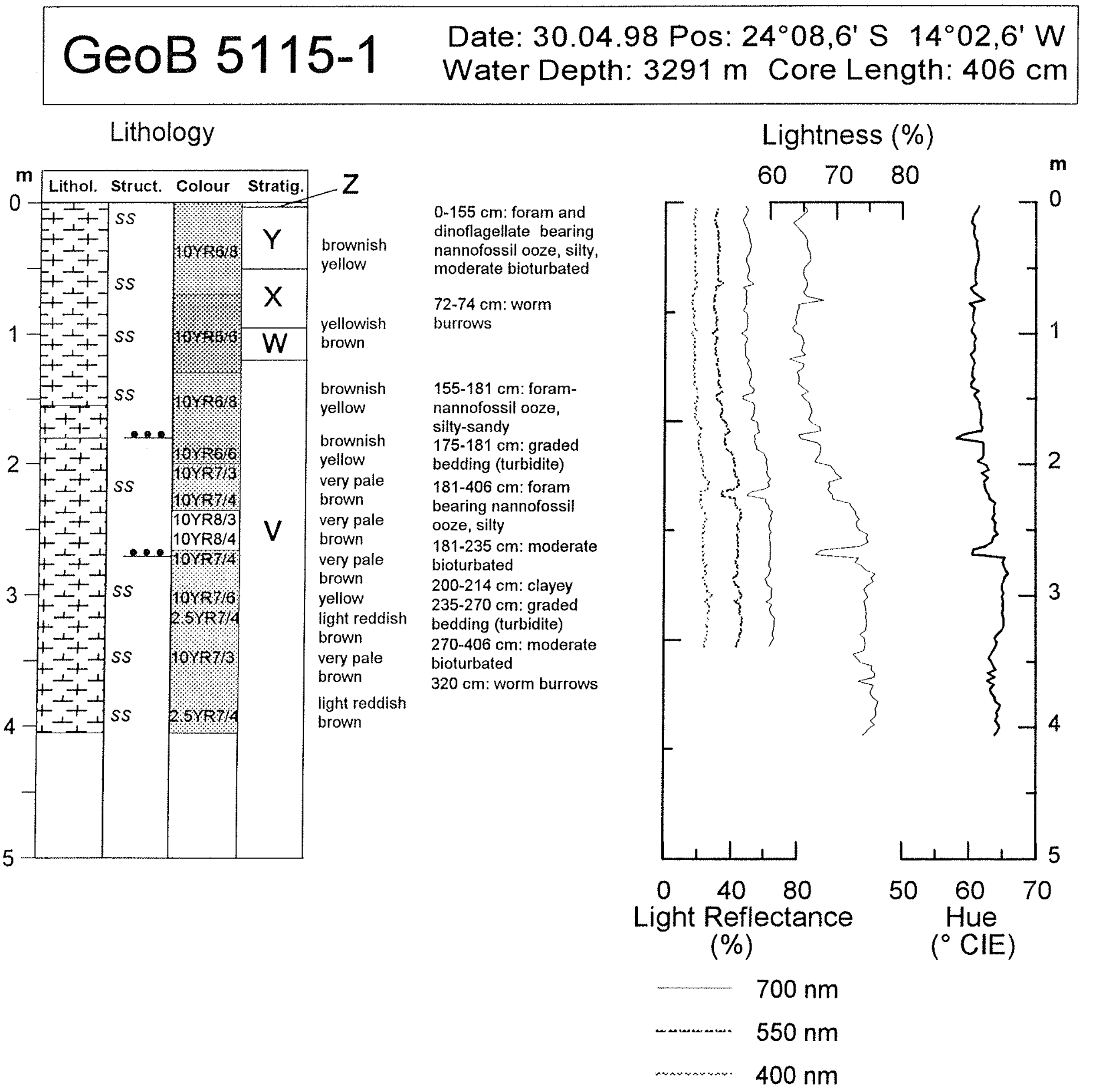


Fig. 38a Core description of GeoB 5115-1

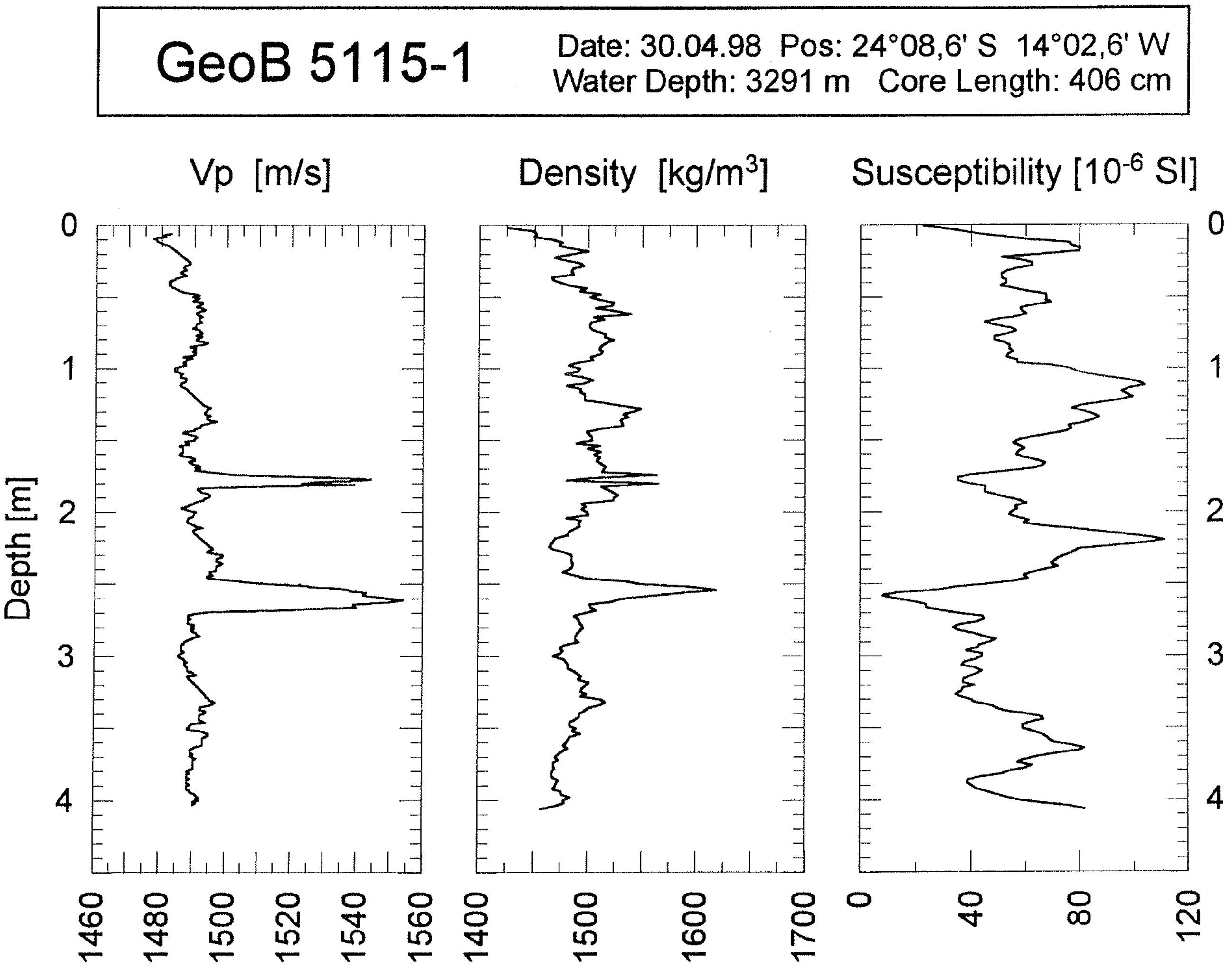


Fig. 38b Physical properties data of GeoB 5115-1

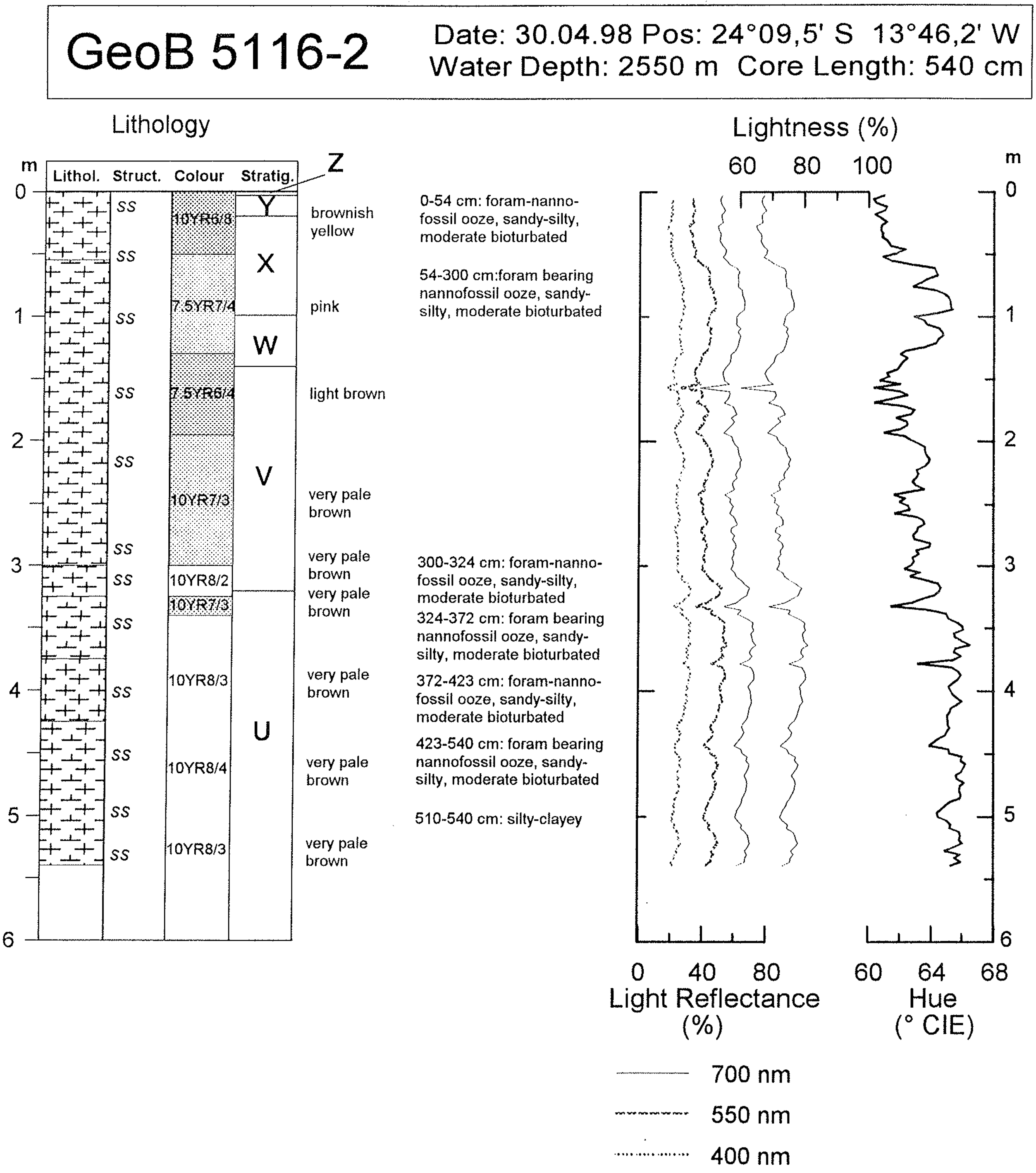


Fig. 39a Core description of GeoB 5116-2

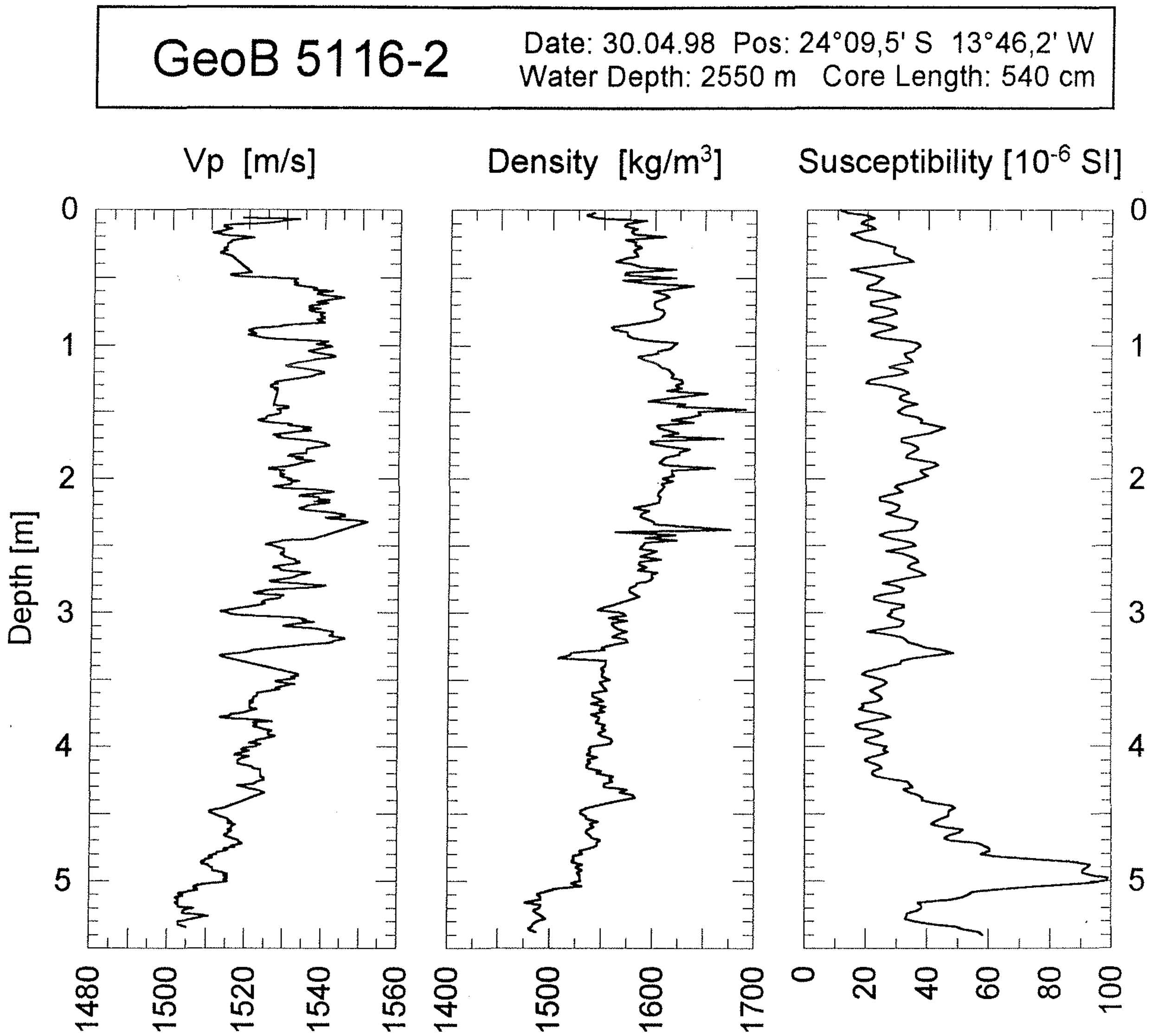


Fig. 39b Physical properties data of GeoB 5116-2

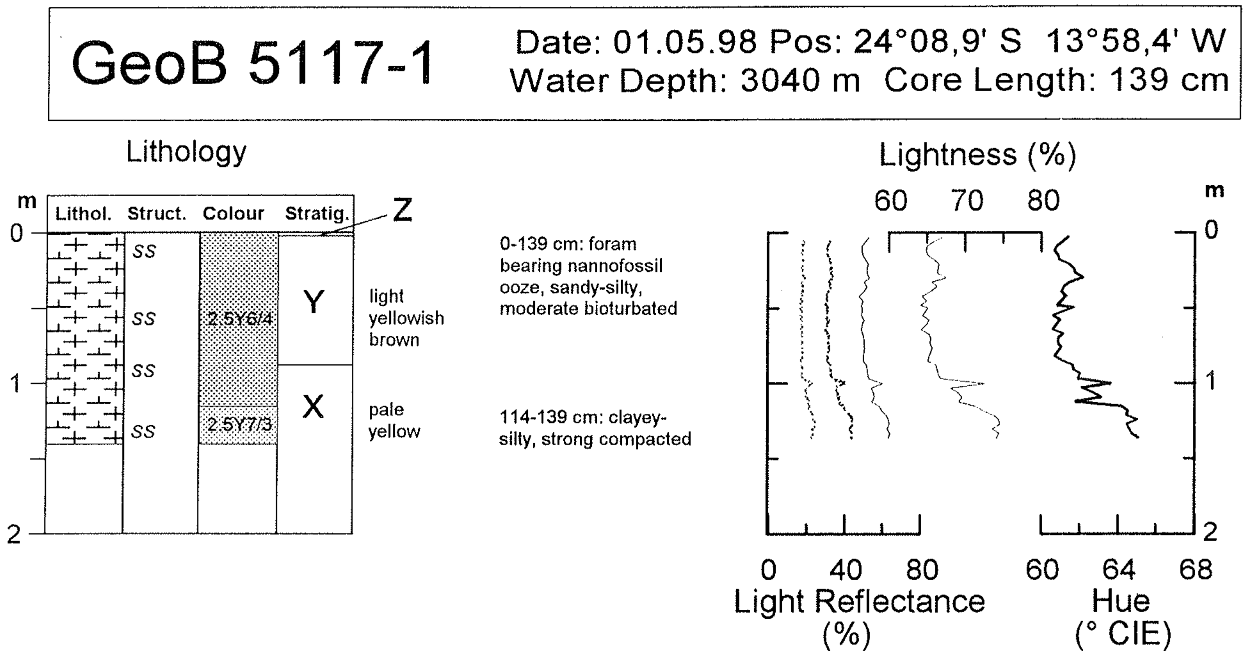


Fig. 40a Core description of GeoB 5117-1

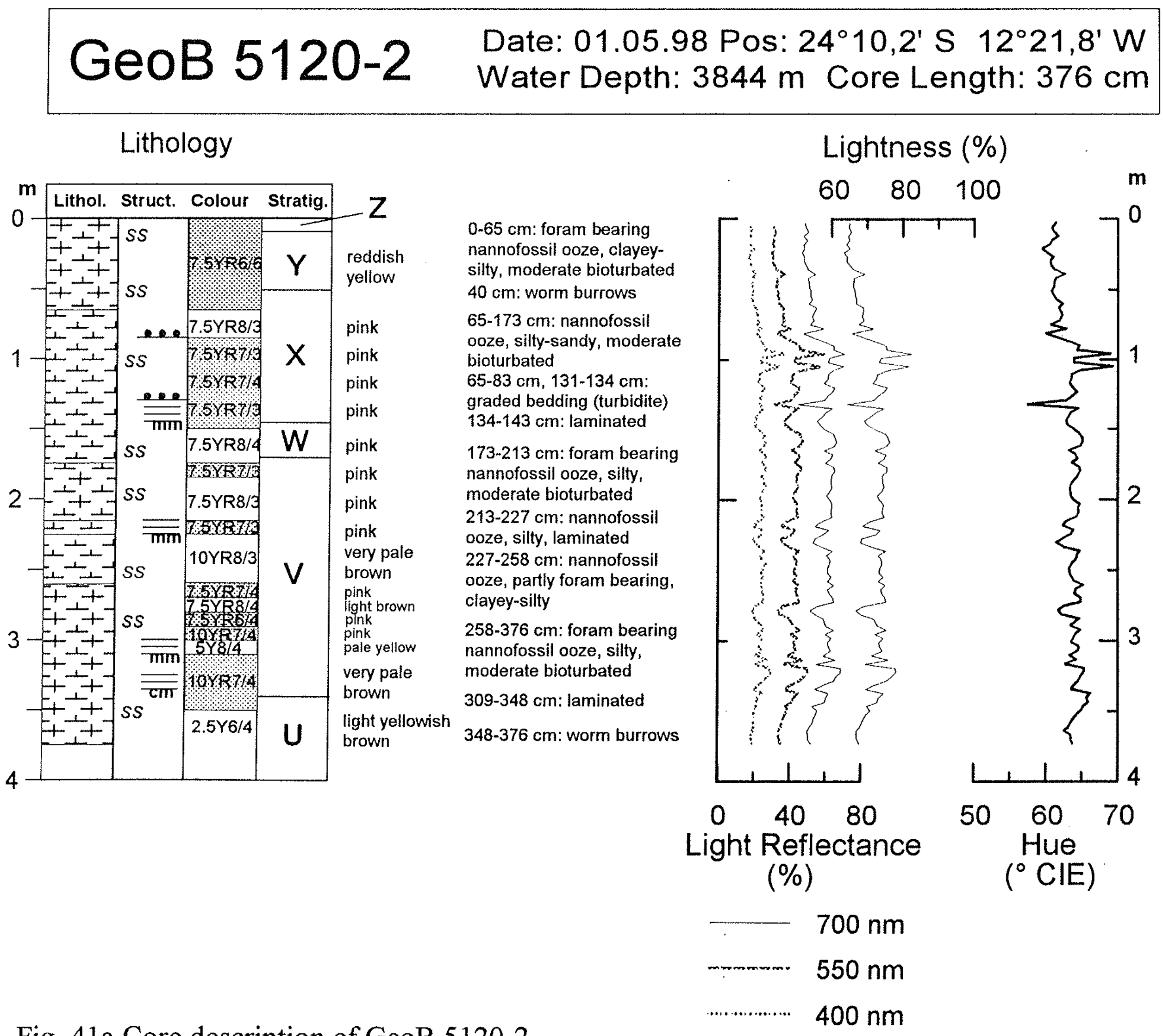


Fig. 41a Core description of GeoB 5120-2

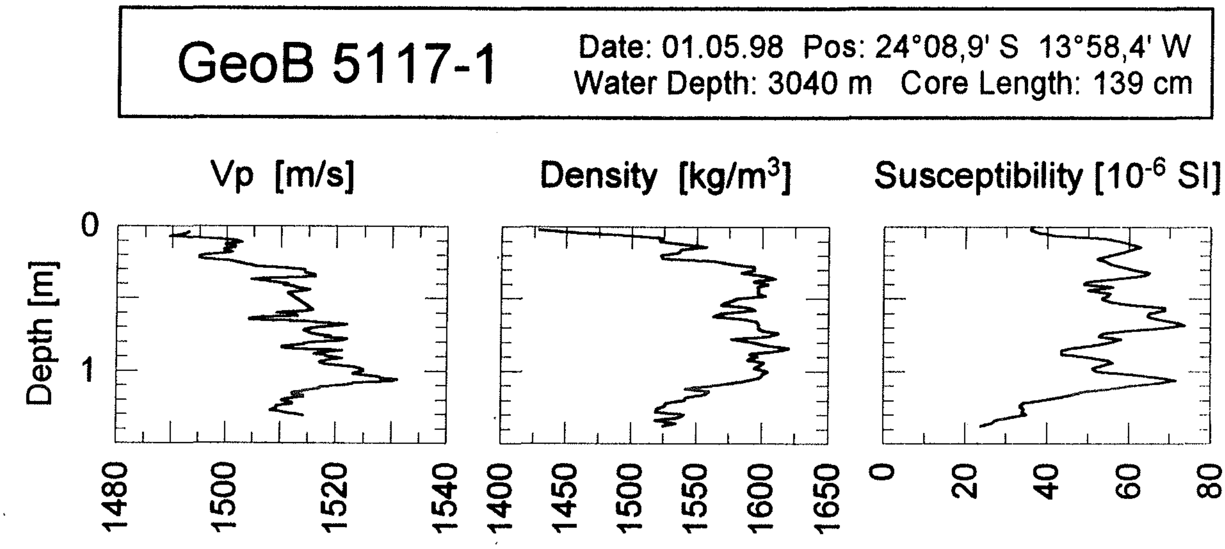


Fig. 40b Physical properties data of GeoB 5117-1

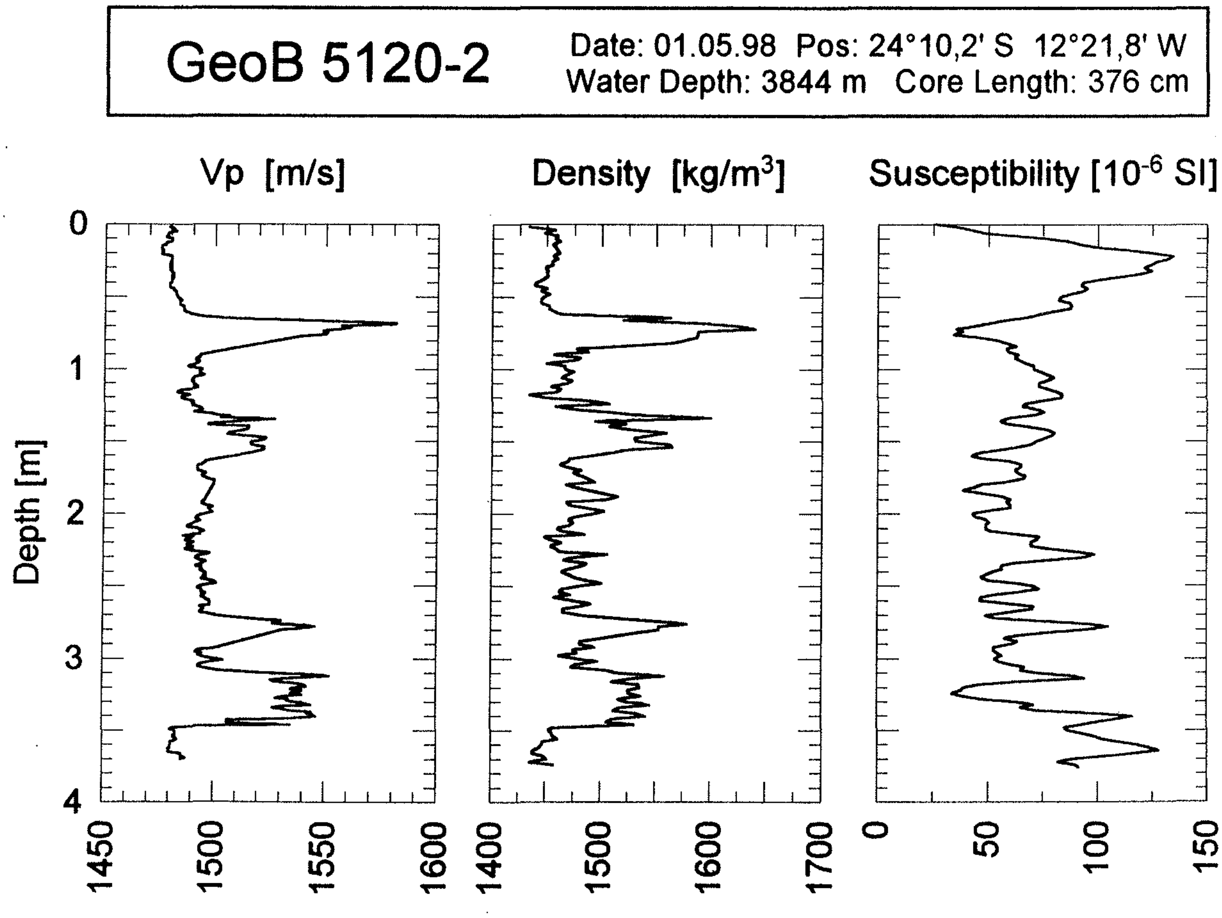


Fig. 41b Physical properties data of GeoB 5120-2

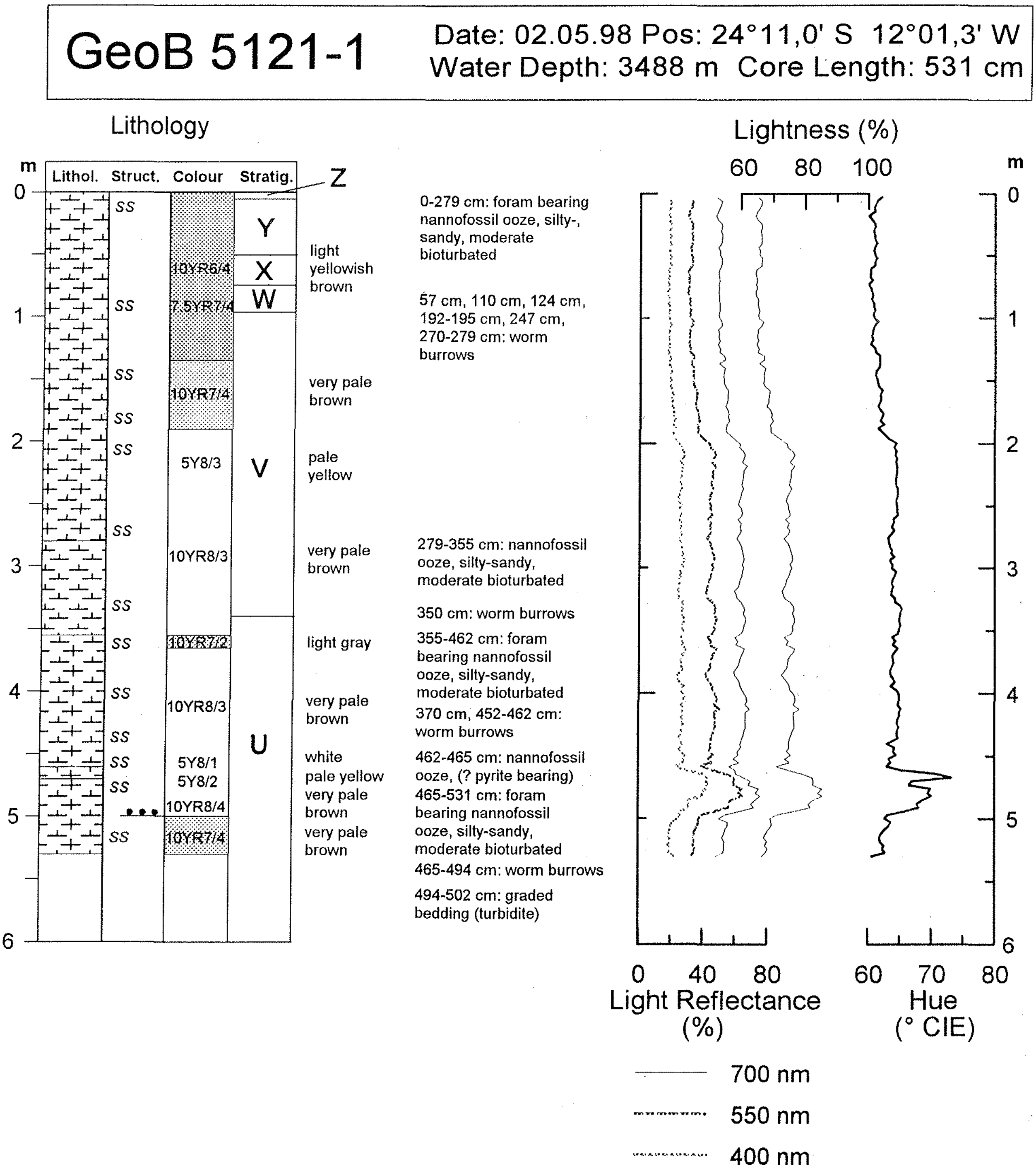


Fig. 42a Core description of GeoB 5121-1

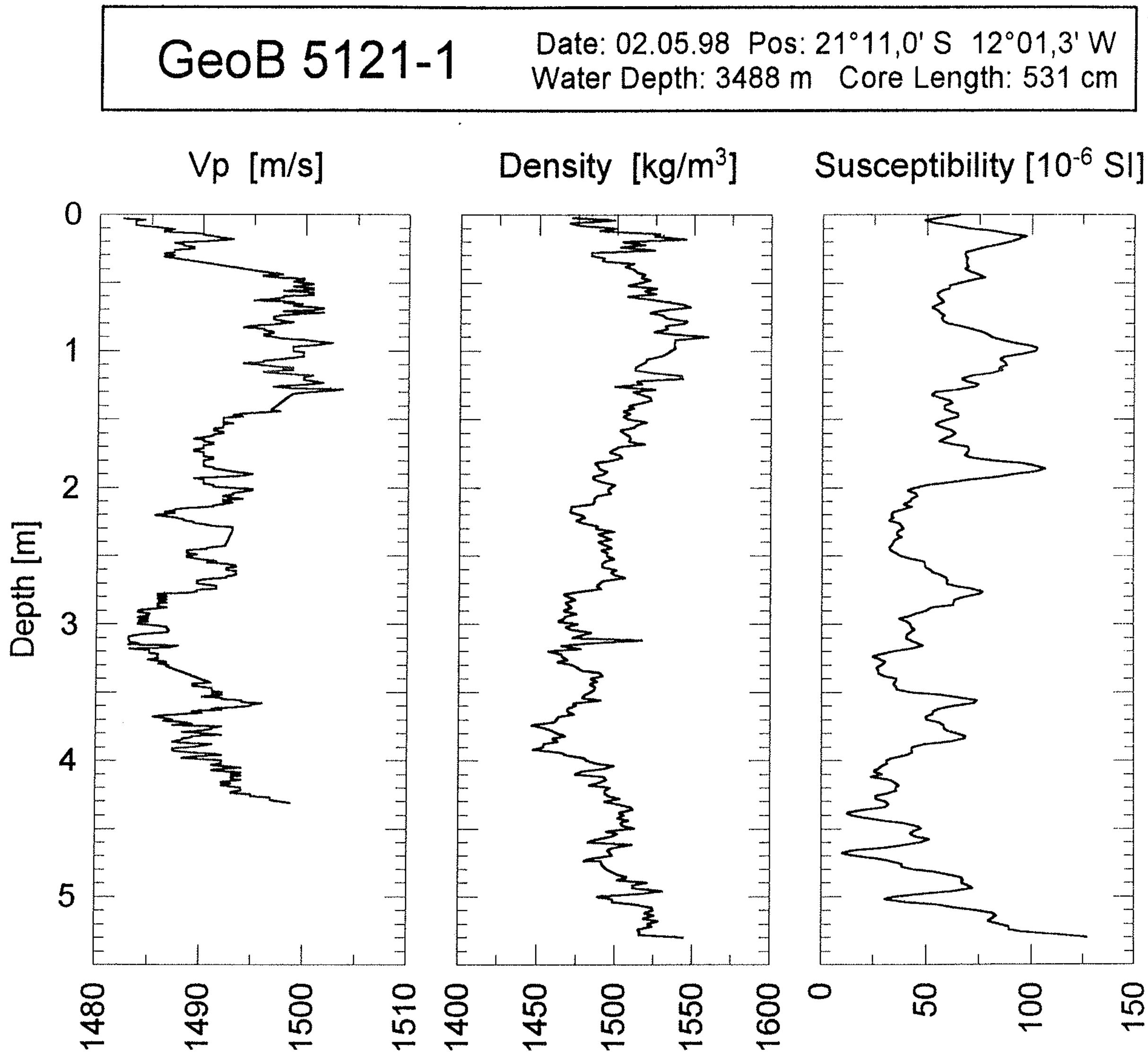


Fig. 42b Physical properties data of GeoB 5121-1

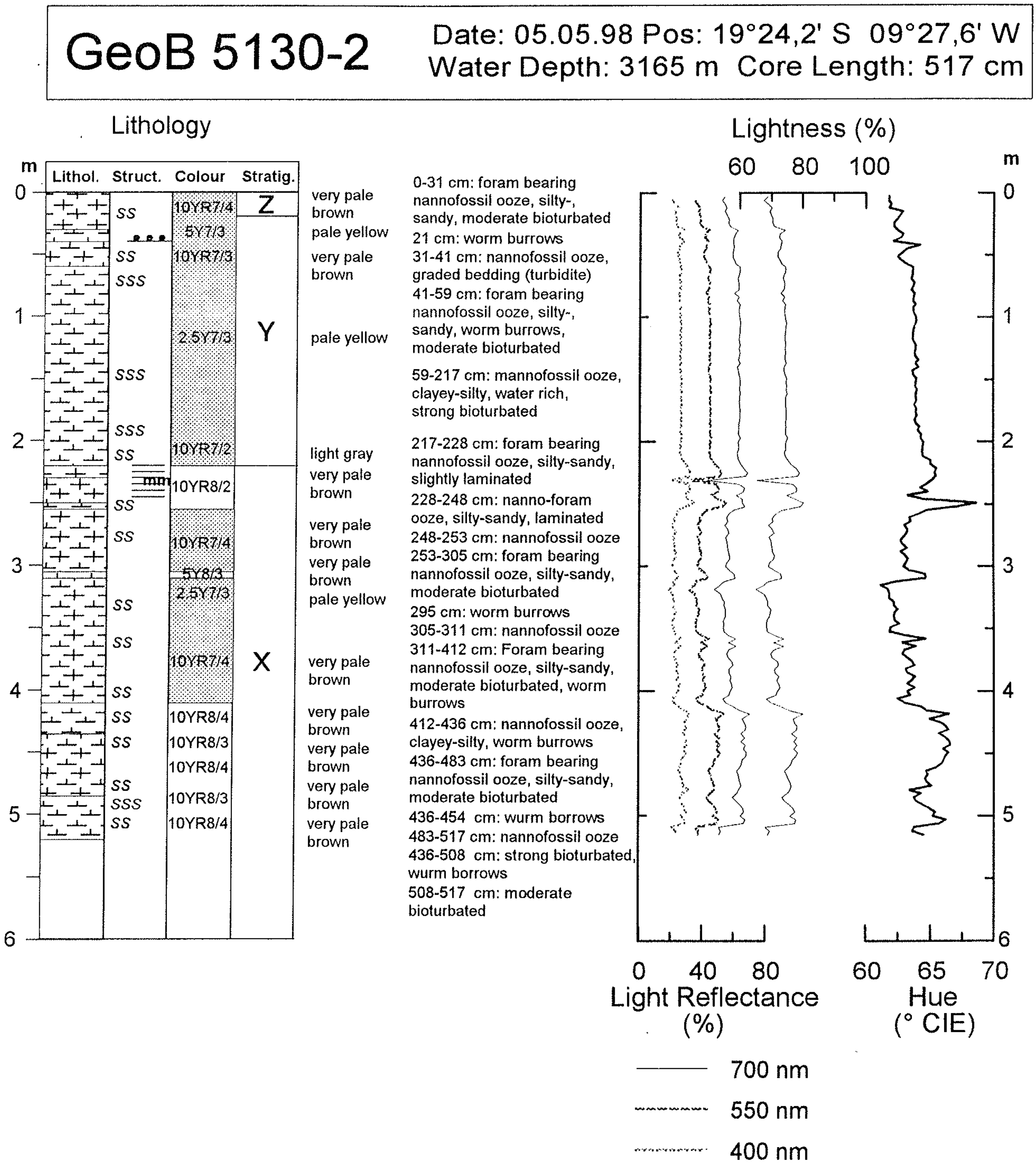


Fig. 43a Core description of GeoB 5130-2

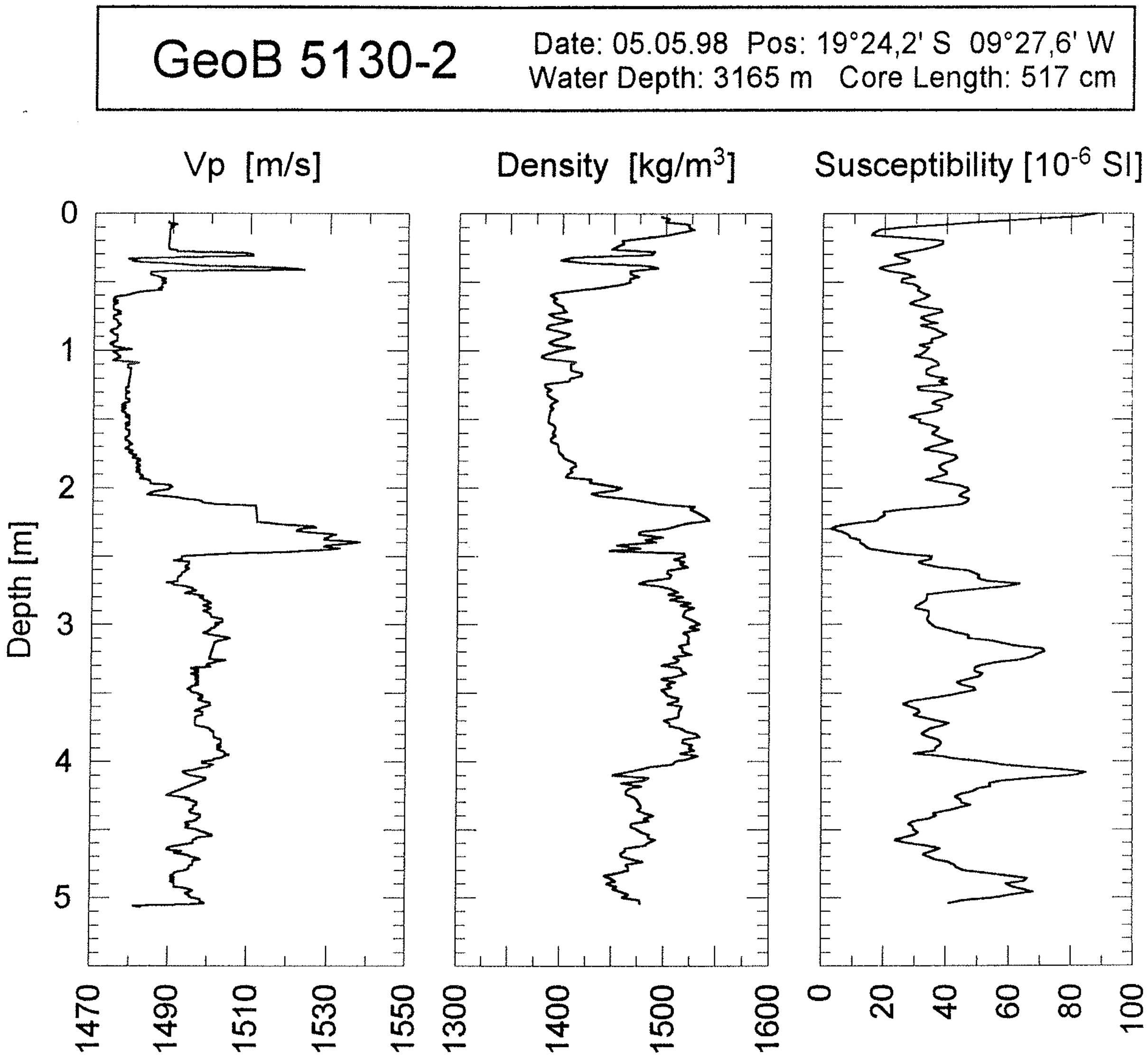


Fig. 43b Physical properties data of GeoB 5130-2

| GeoB 5131-1 | Date: 05.05.98 Pos: 19°02.2' S 09°44.5' W<br>Water Depth: 3886 m Core Length: 216 cm |
|---|---|

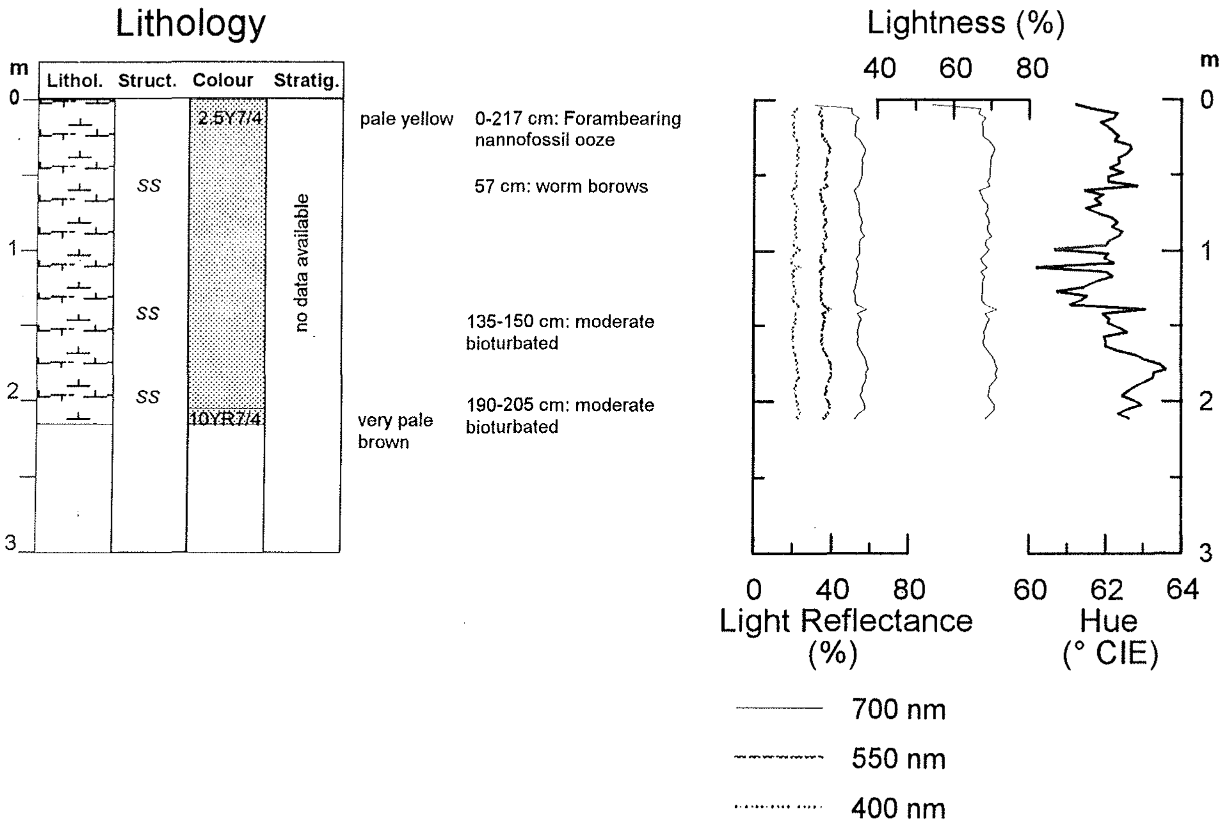


Fig. 44a Core description of GeoB 5131-1

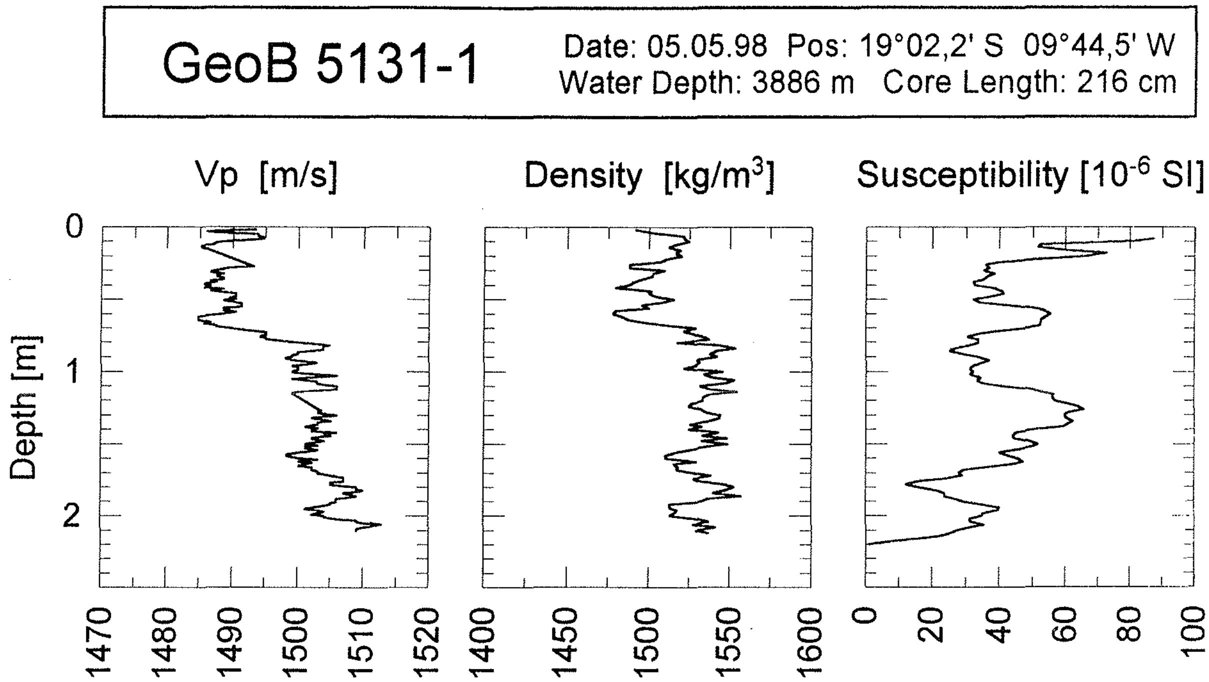


Fig. 44b Physical properties data of GeoB 5131-1

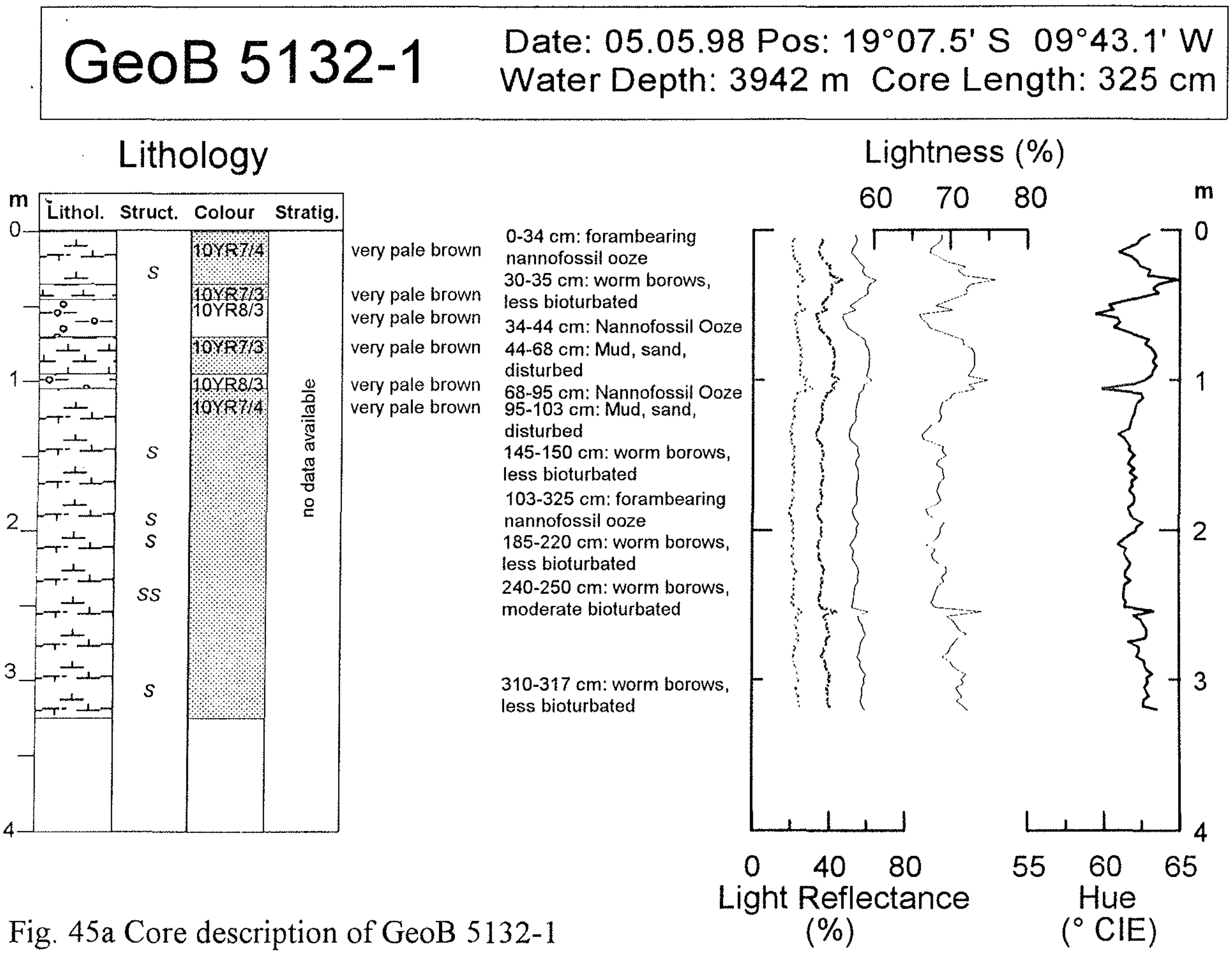


Fig. 45a Core description of GeoB 5132-1

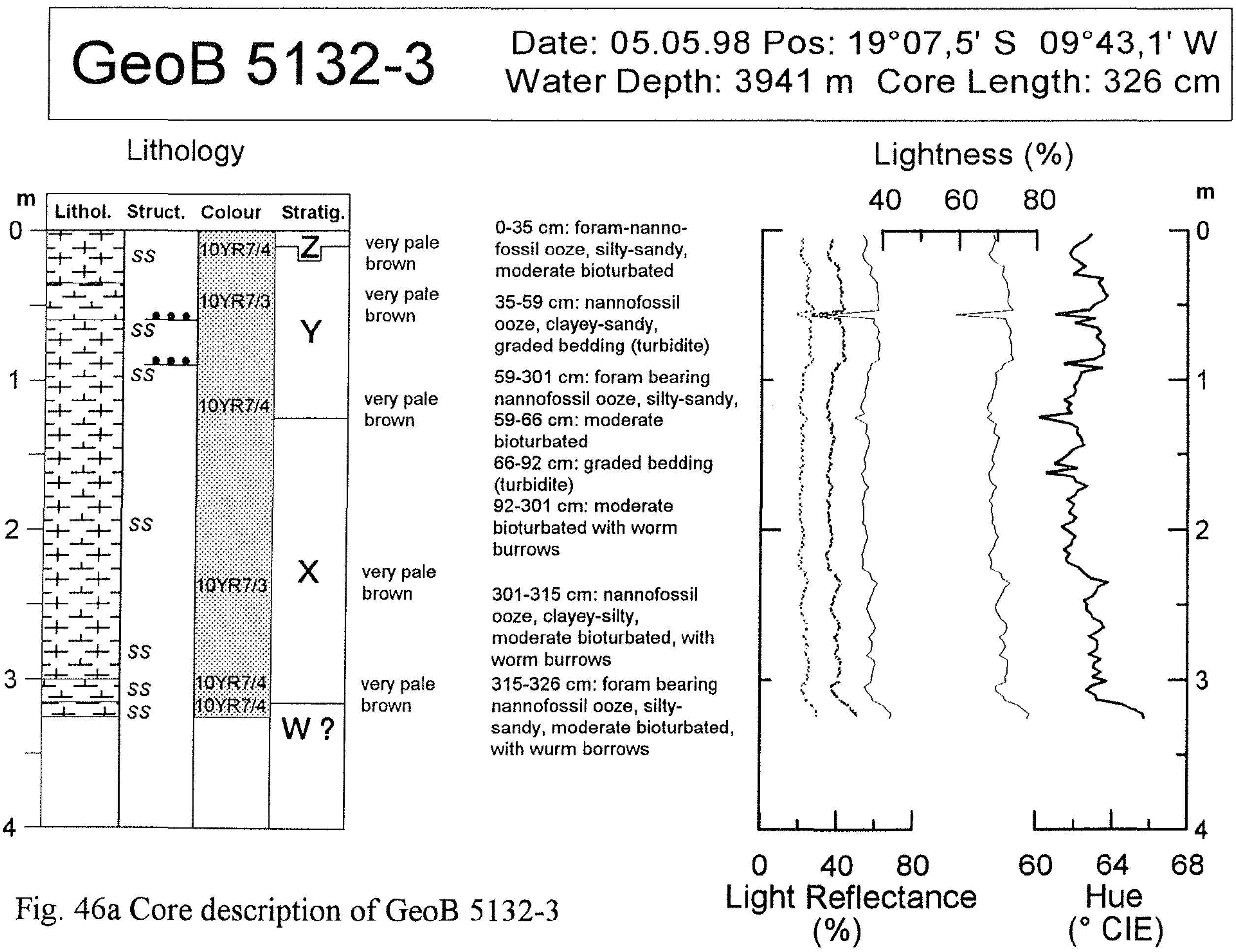


Fig. 46a Core description of GeoB 5132-3

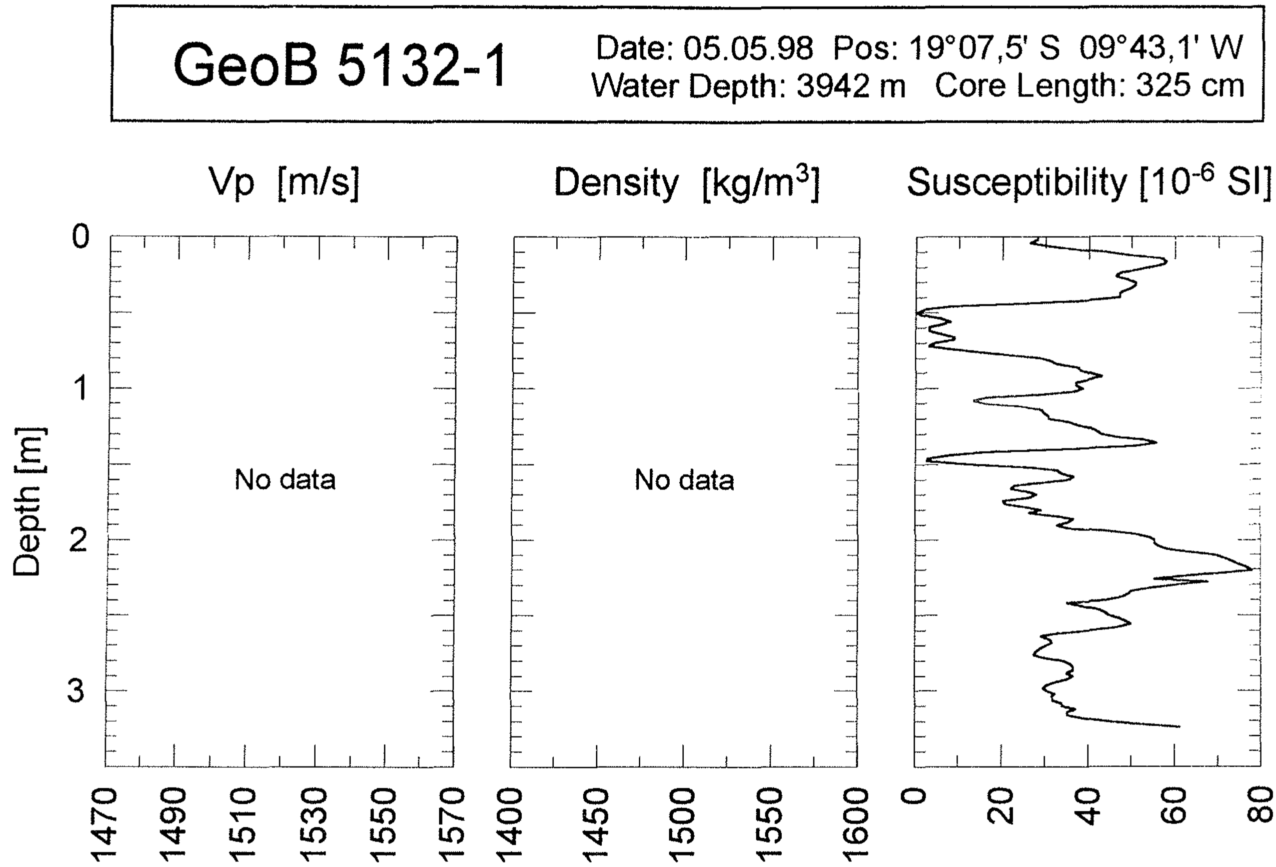


Fig. 45b Physical properties data of GeoB 5132-1

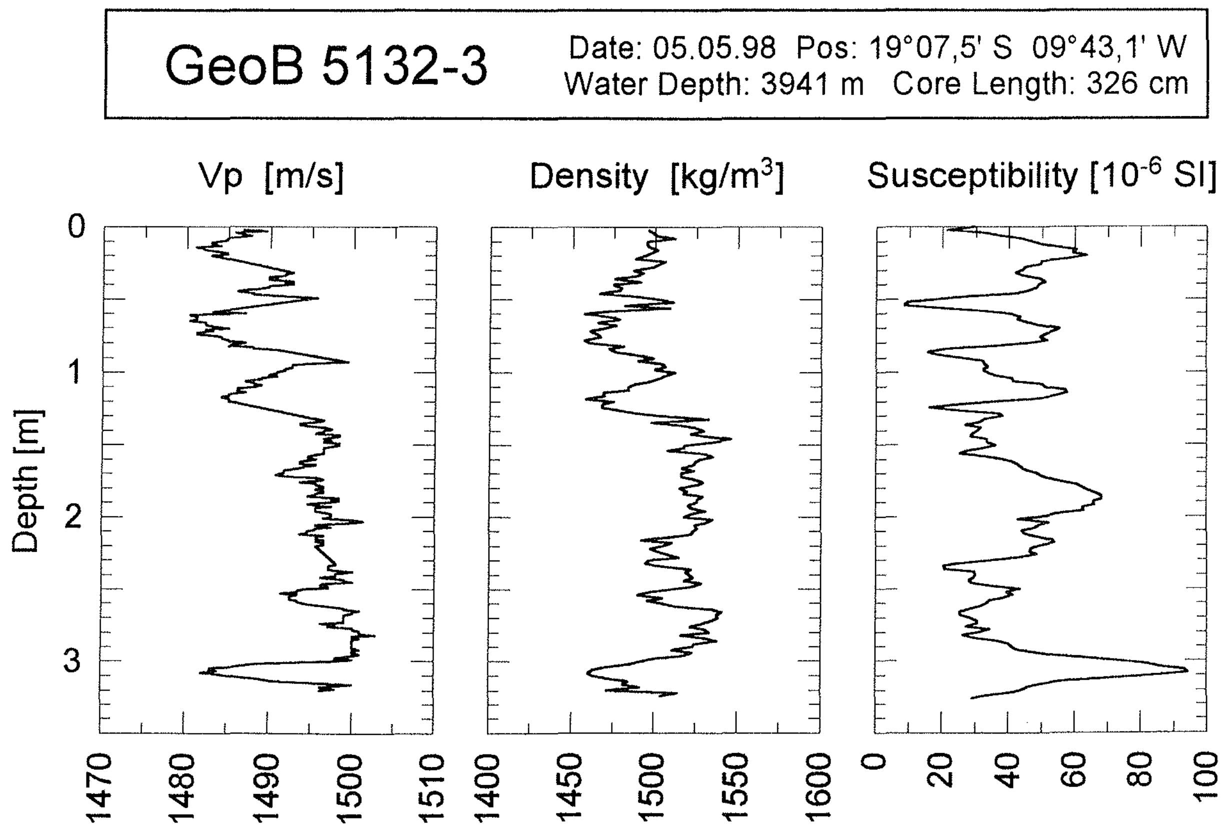


Fig. 46b Physical properties data of GeoB 5132-3

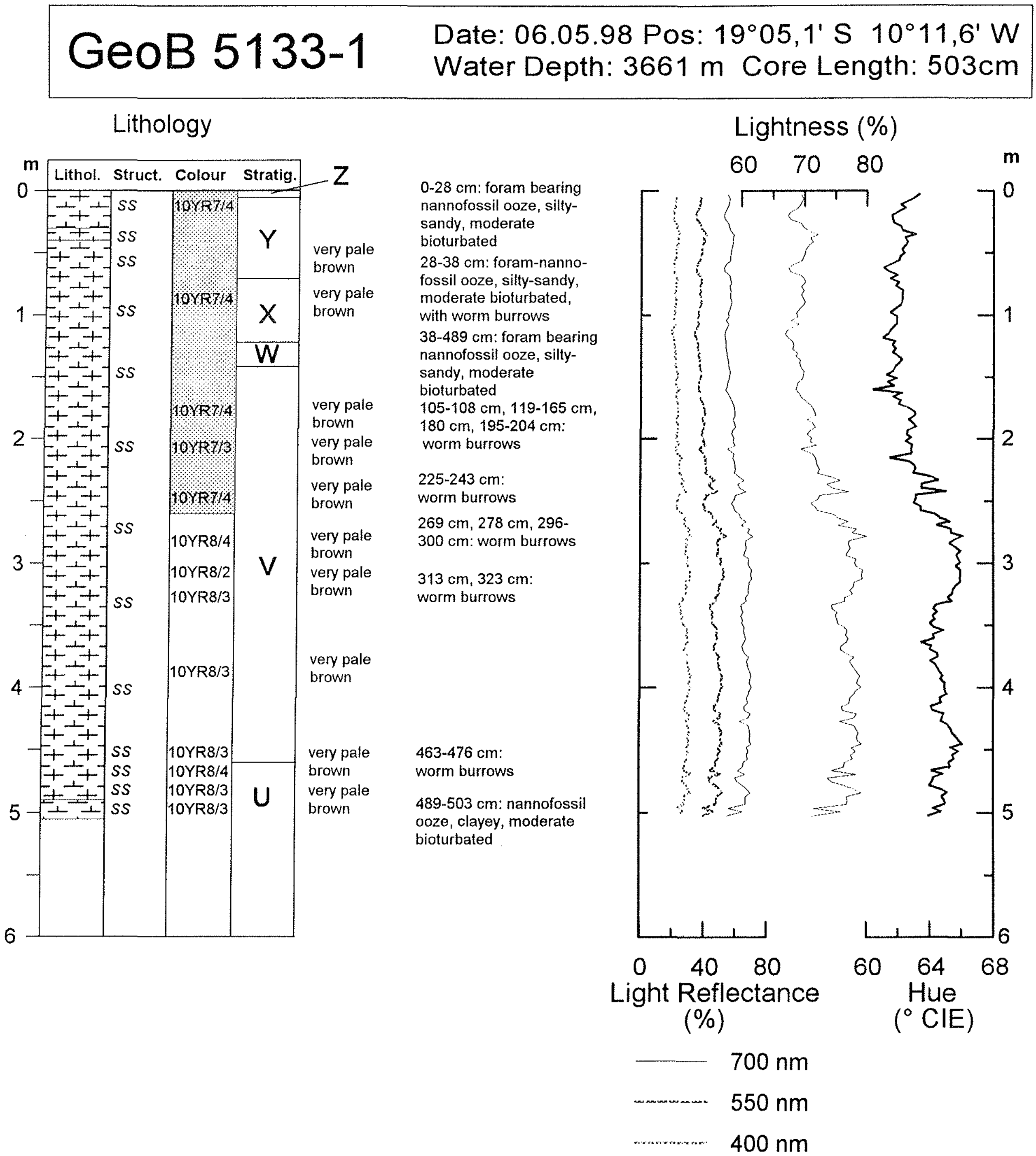


Fig. 47a Core description of GeoB 5133-1

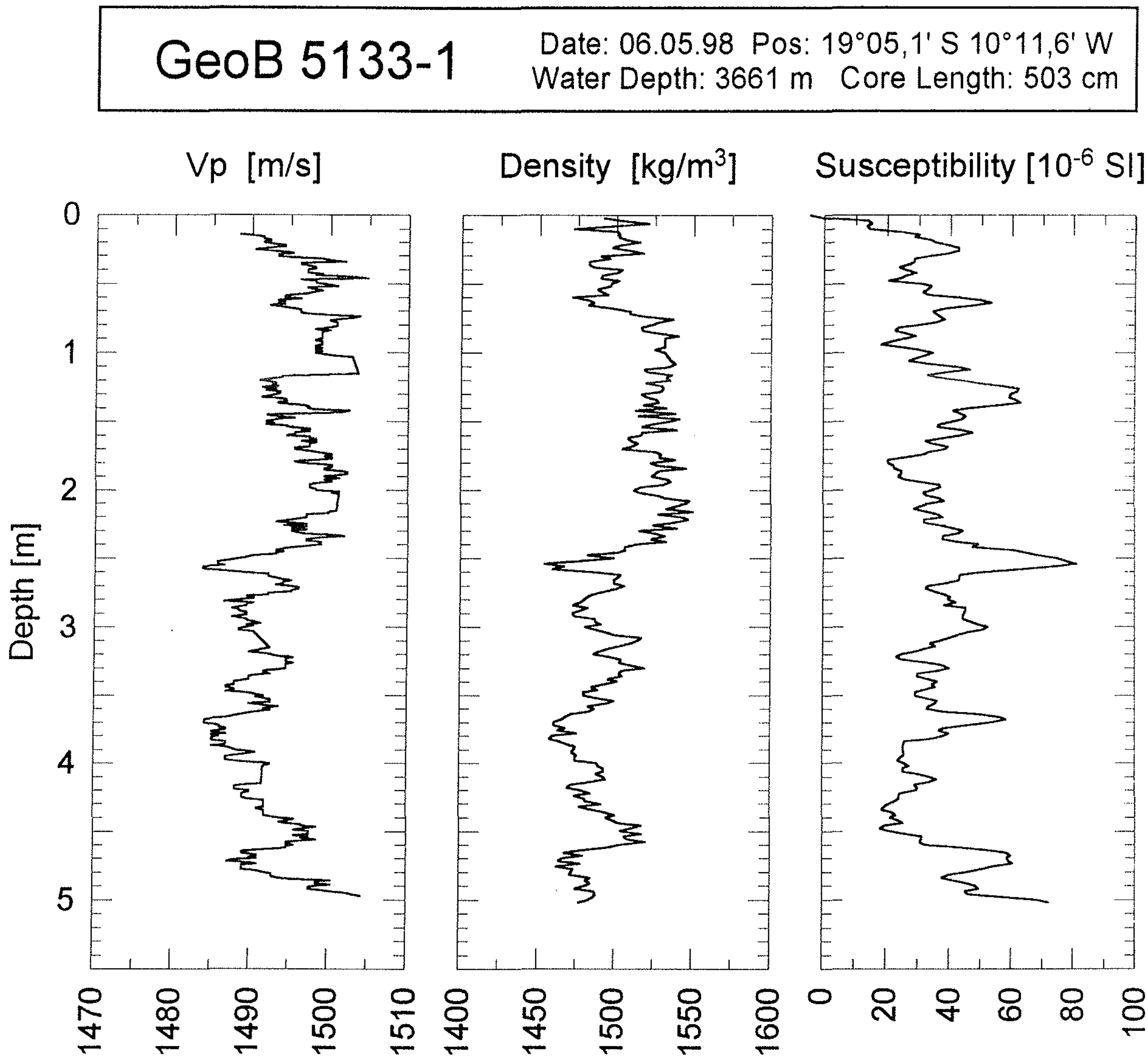


Fig. 47b Physical properties data of GeoB 5133-1

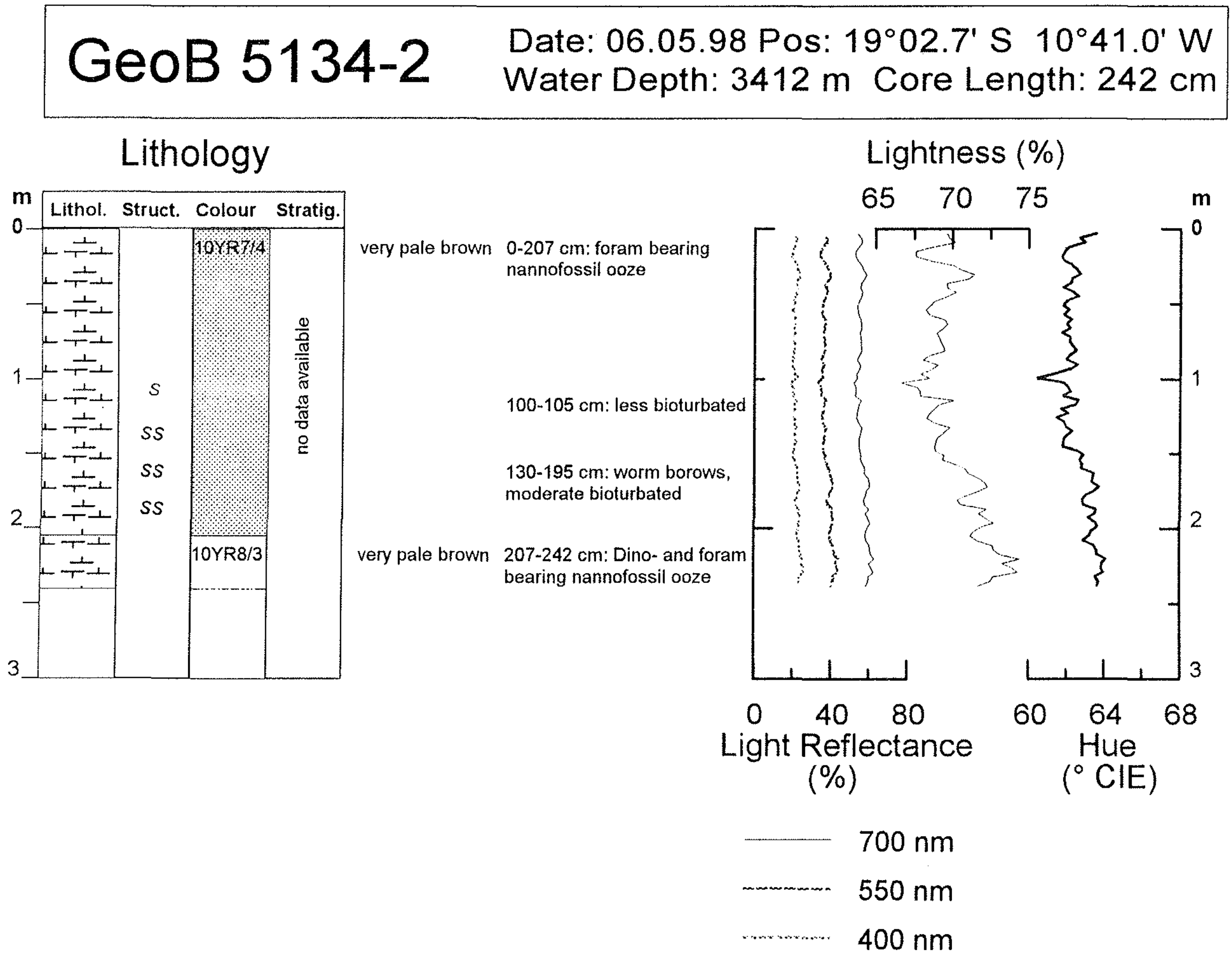


Fig. 48a Core description of GeoB 5134-2

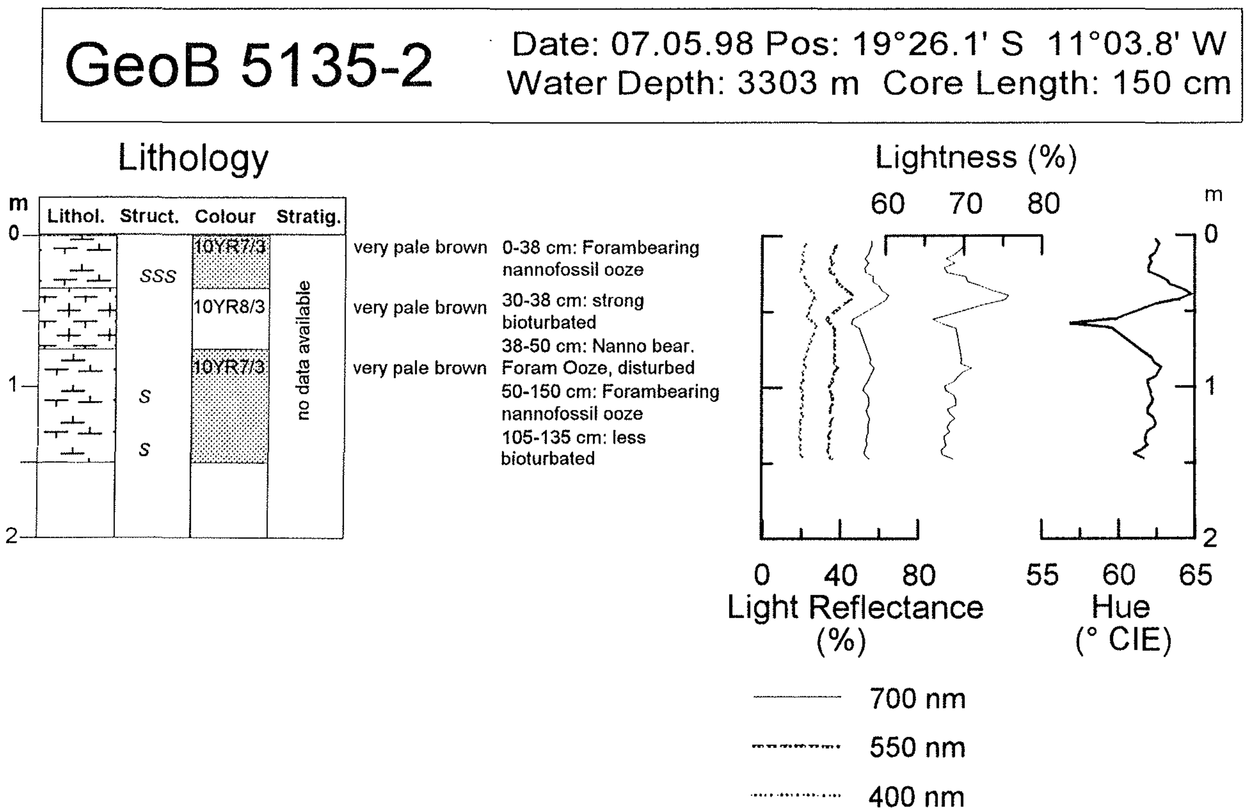


Fig. 49a Core description of GeoB 5135-2

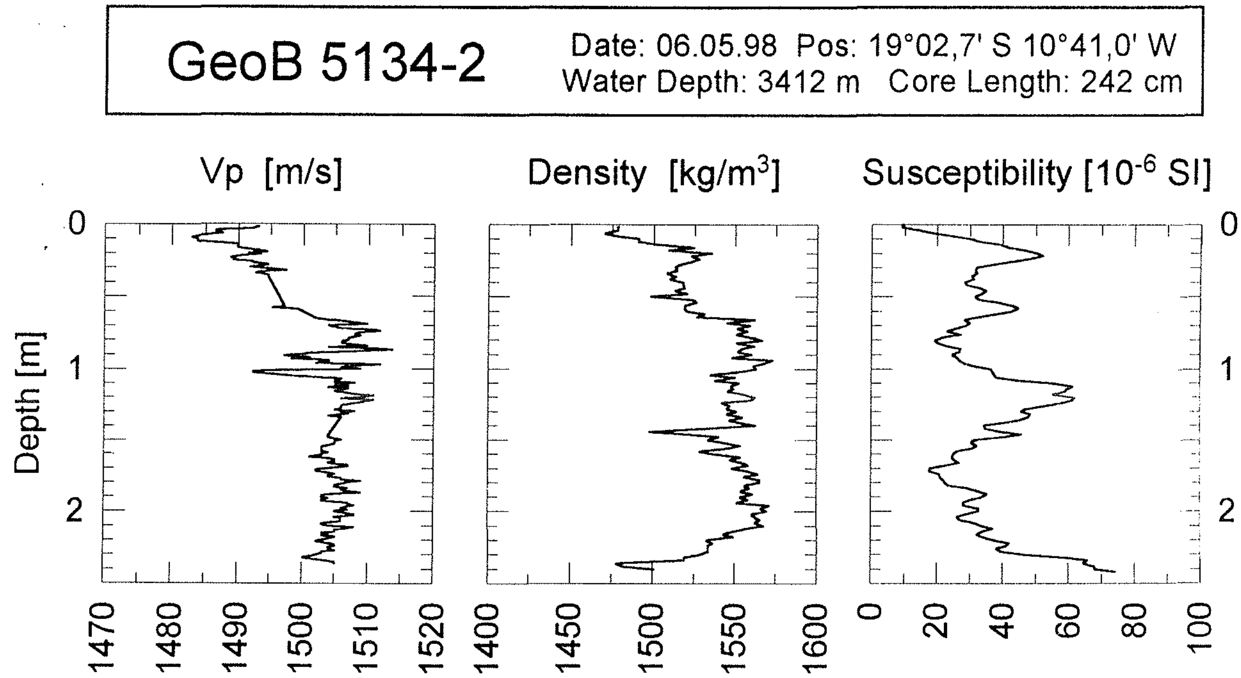


Fig. 48b Physical properties data of GeoB 5134-2

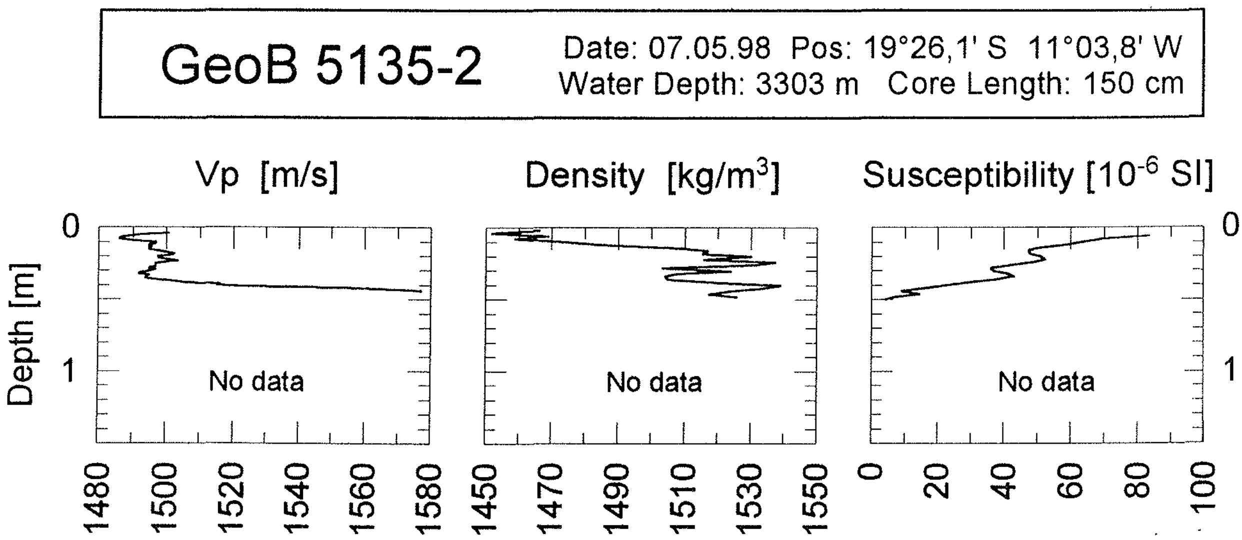


Fig. 49b Physical properties data of GeoB 5135-2

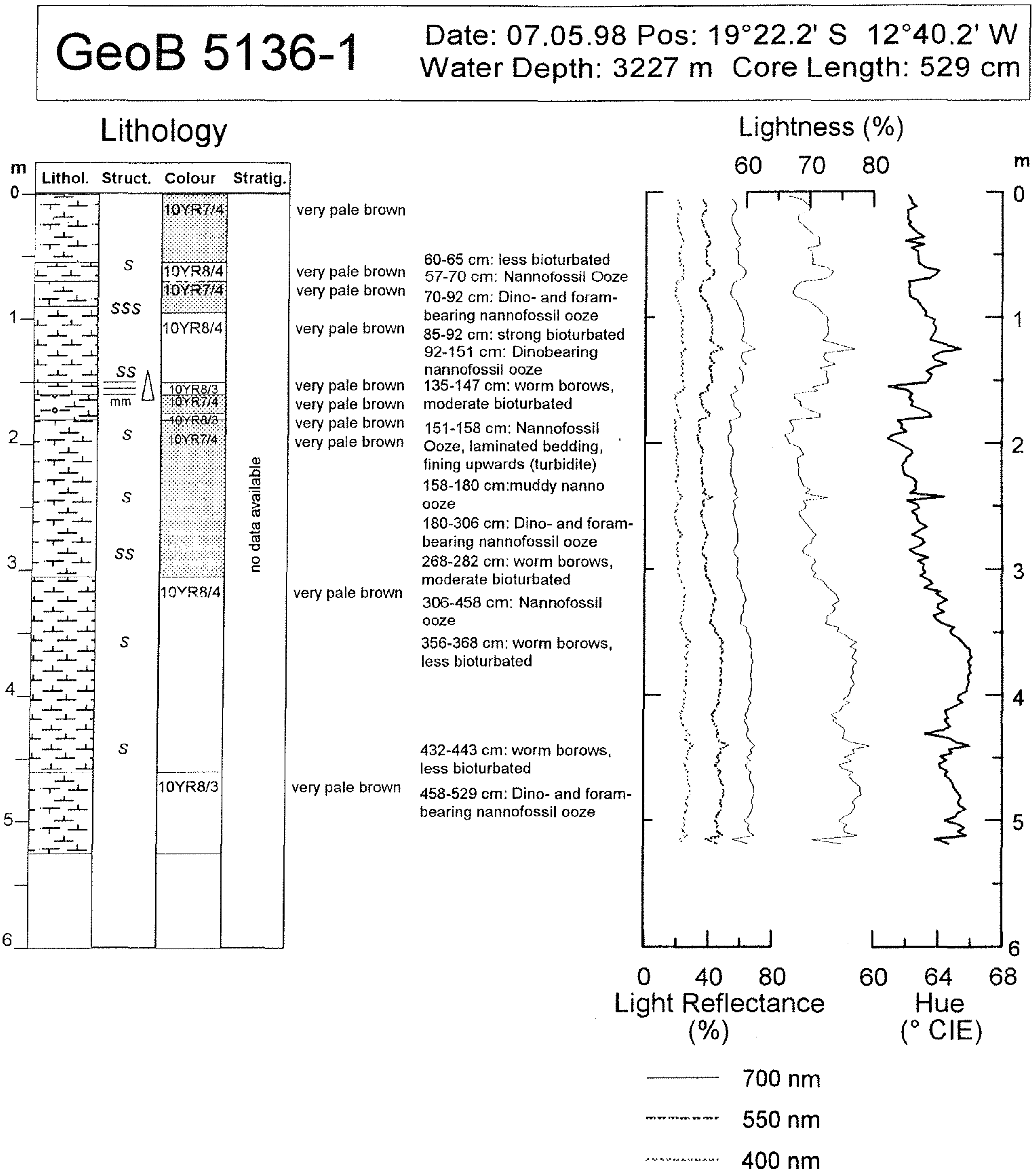


Fig. 50a Core description of GeoB 5136-1

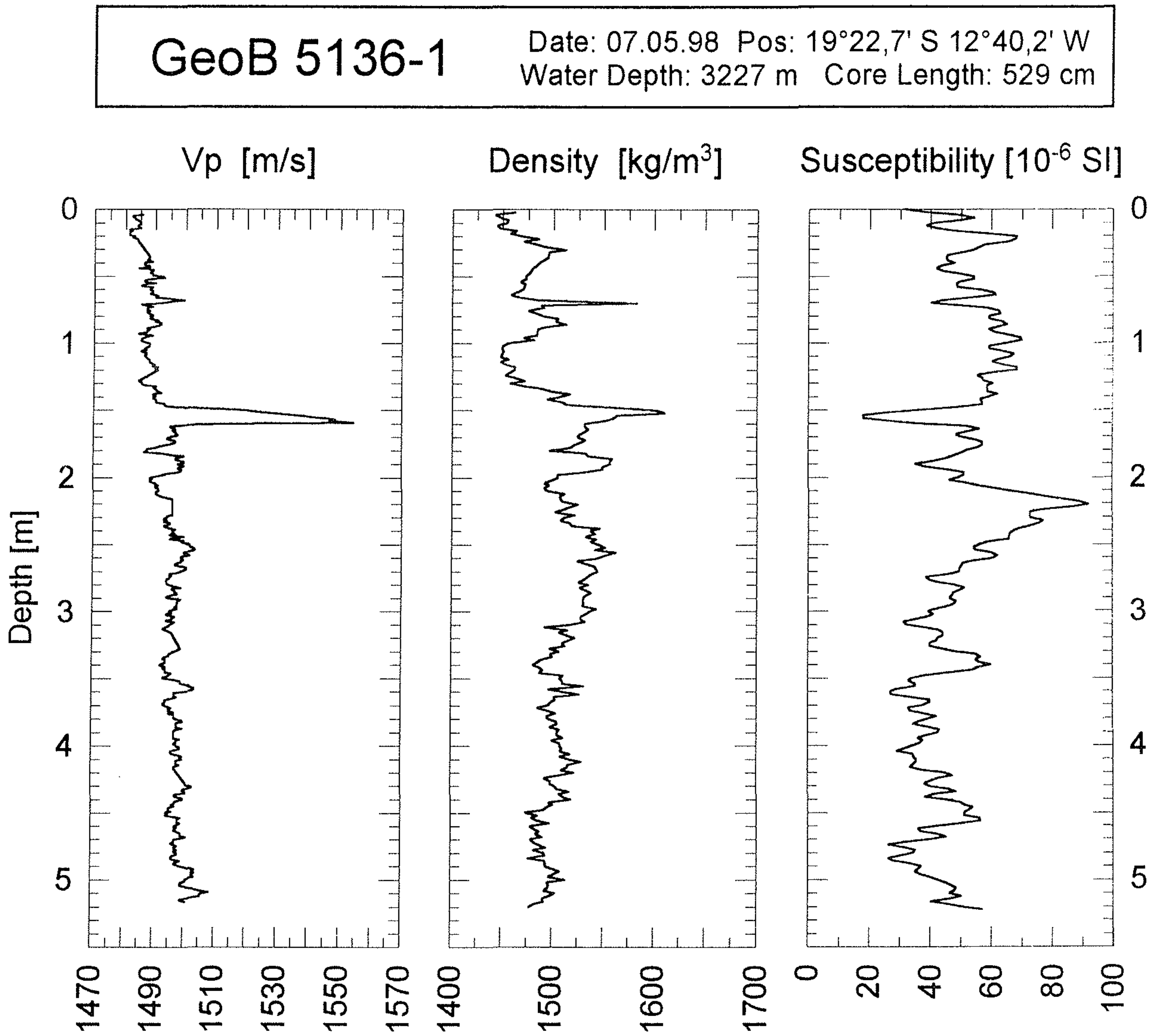


Fig. 50b Physical properties data of GeoB 5136-1

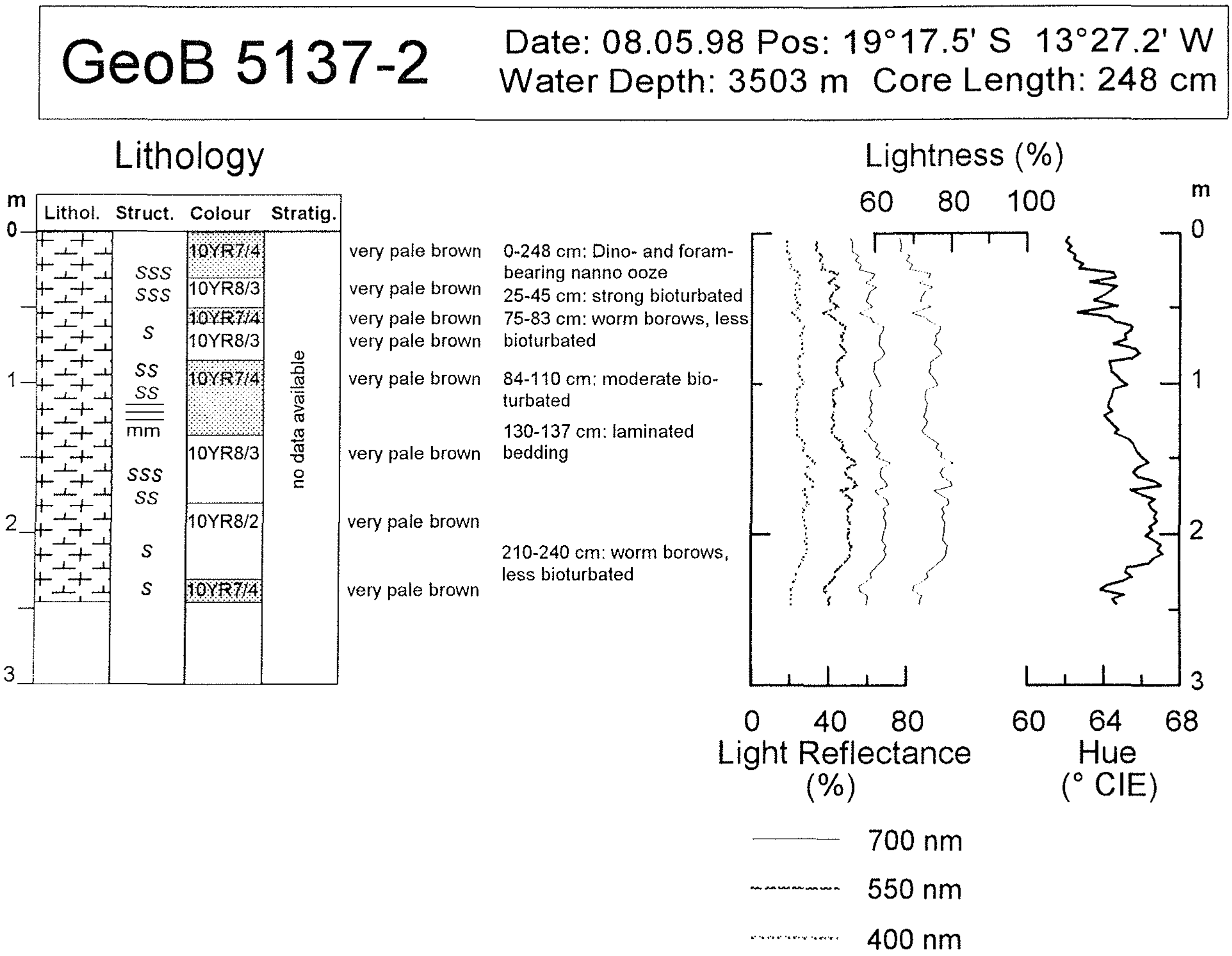


Fig. 51a Core description of GeoB 5137-2

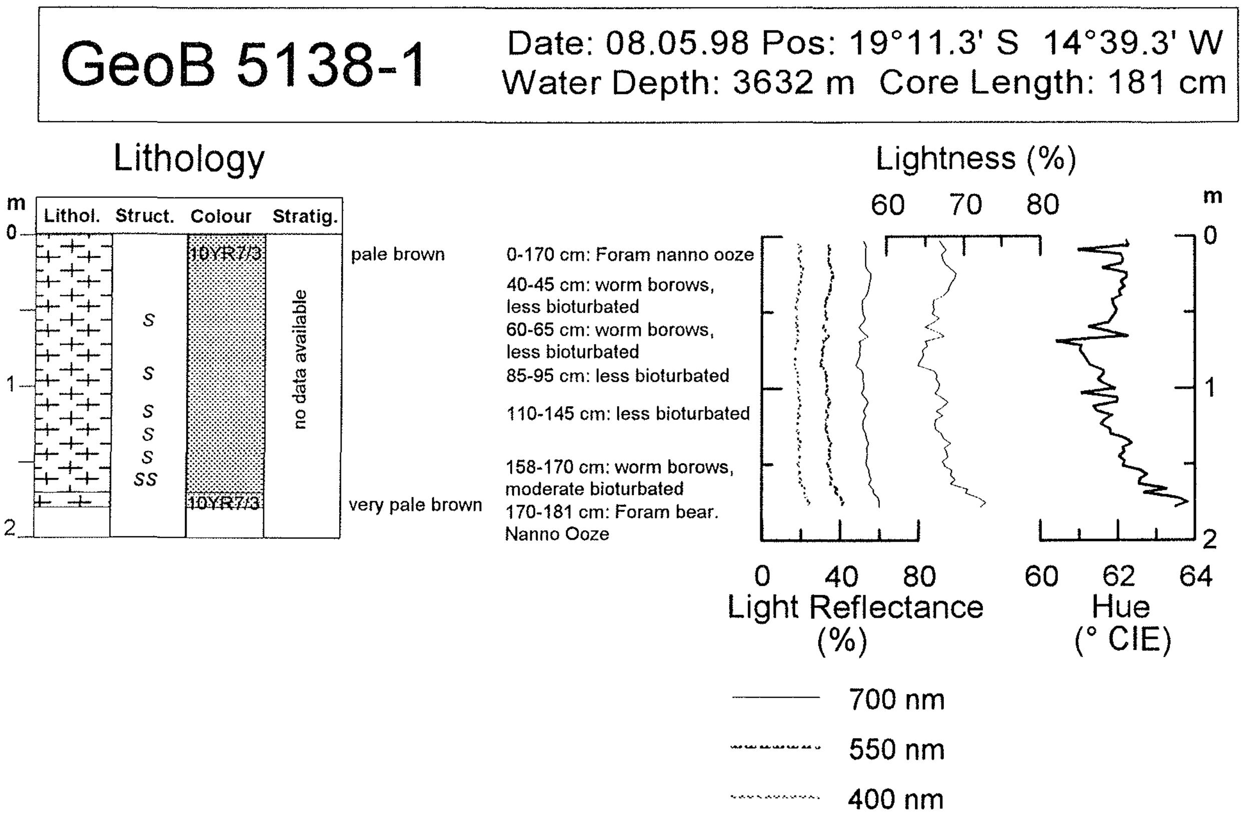


Fig. 52a Core description of GeoB 5138-1

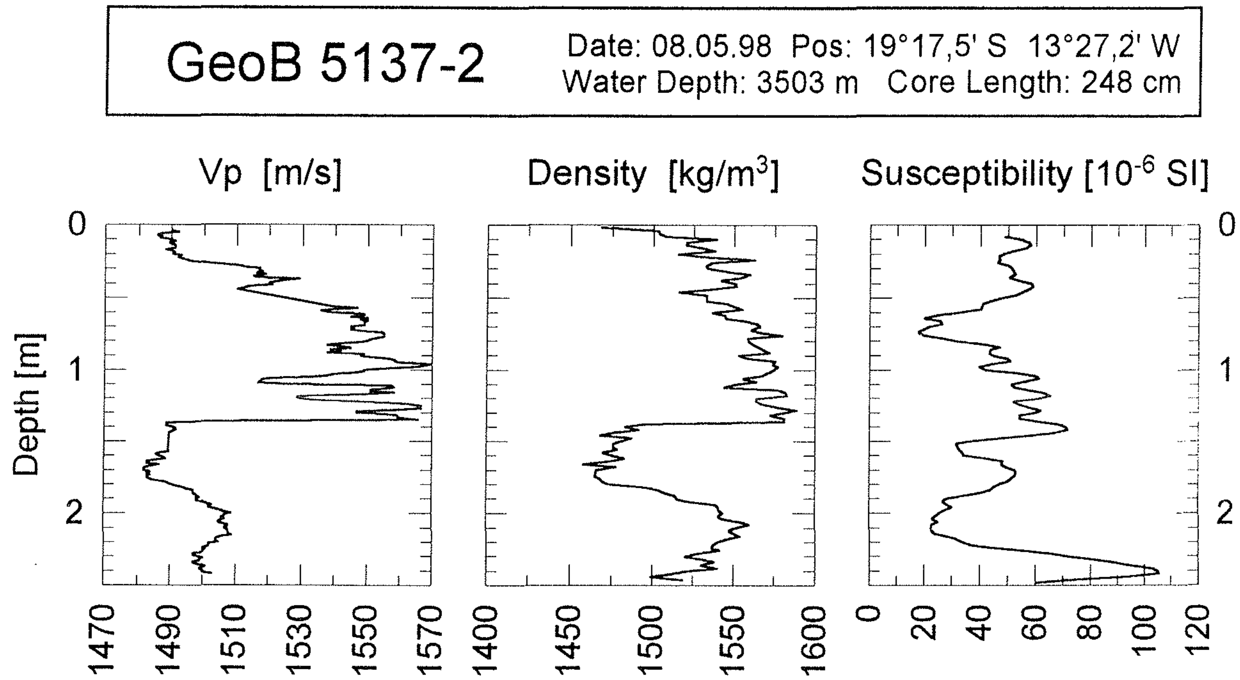


Fig. 51b Physical properties data of GeoB 5137-2

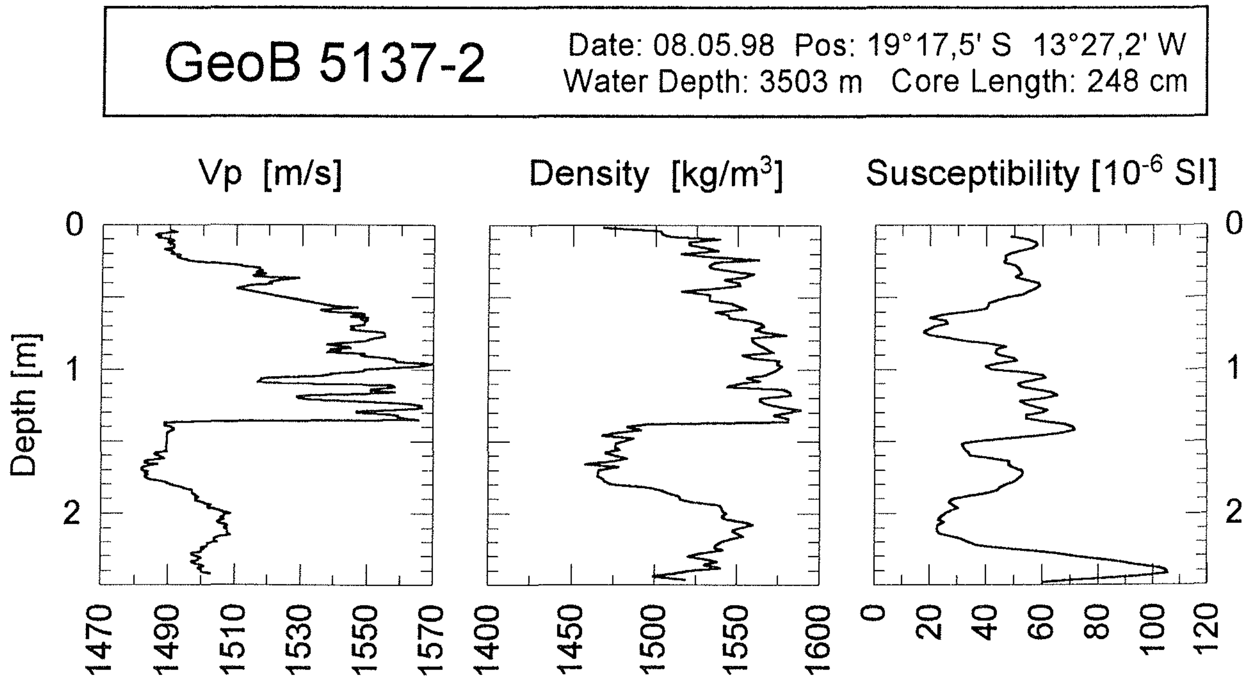


Fig. 52b Physical properties data of GeoB 5138-1

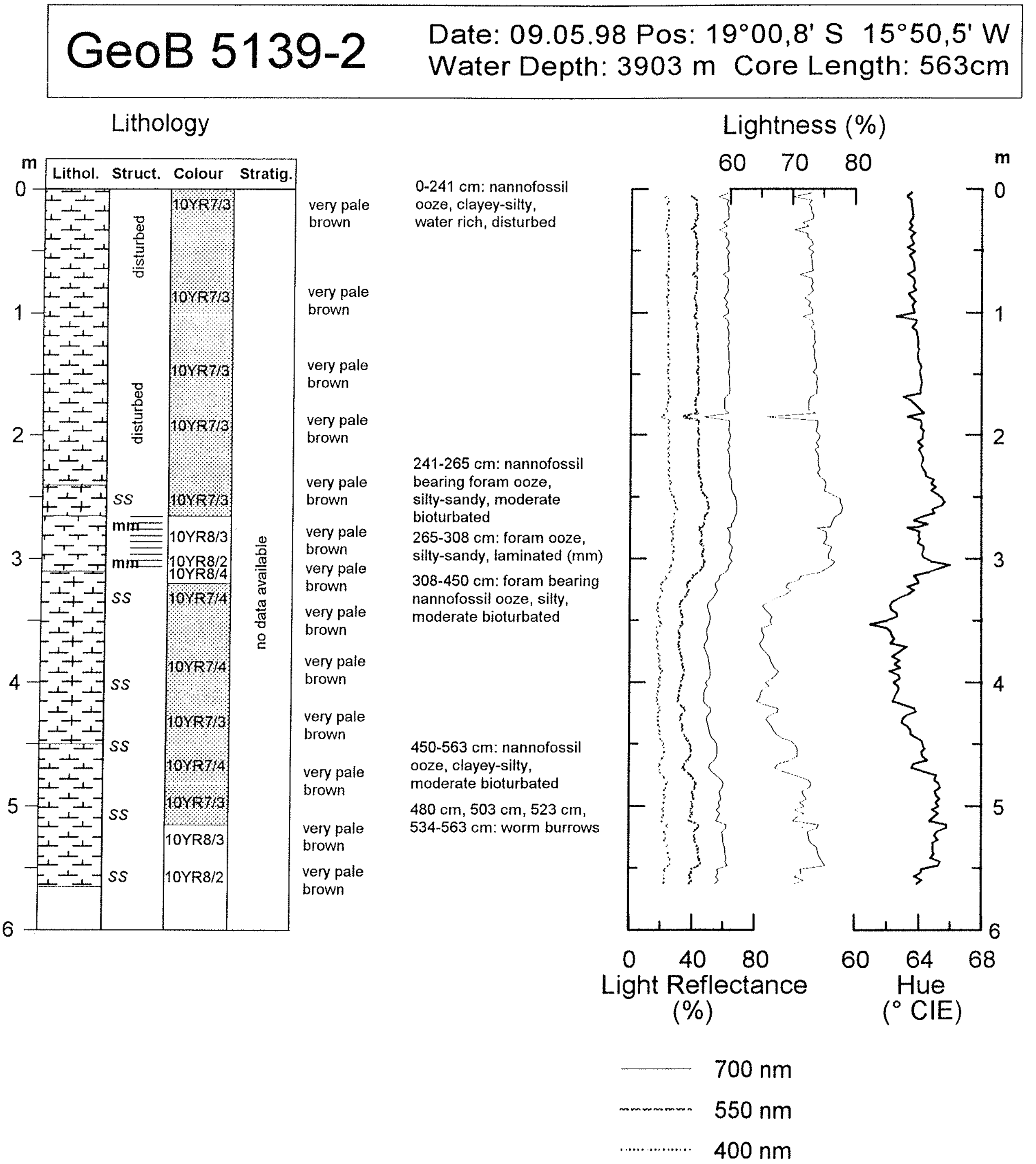


Fig. 53a Core description of GeoB 5139-2

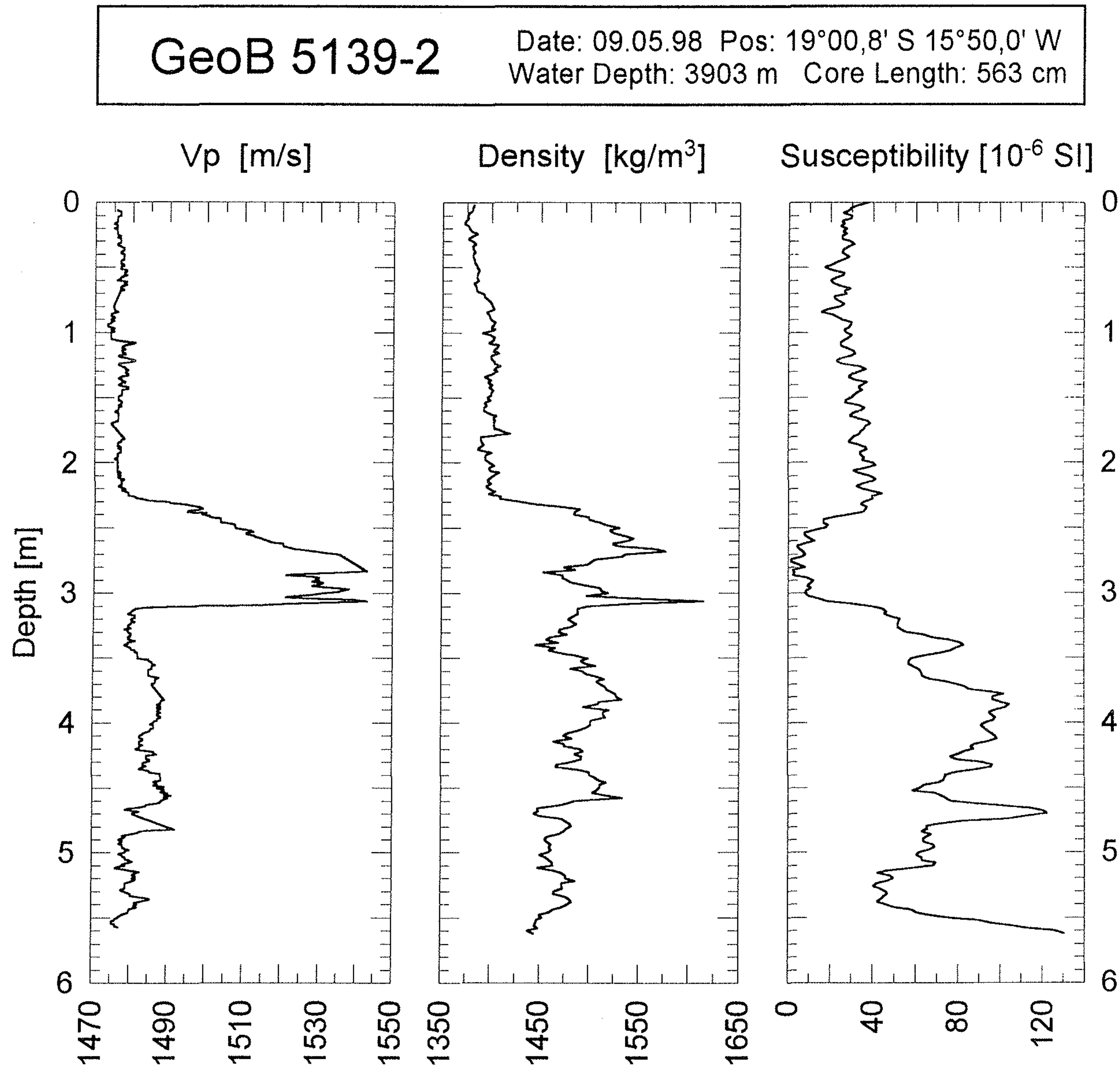


Fig. 53b Physical properties data of GeoB 5139-2

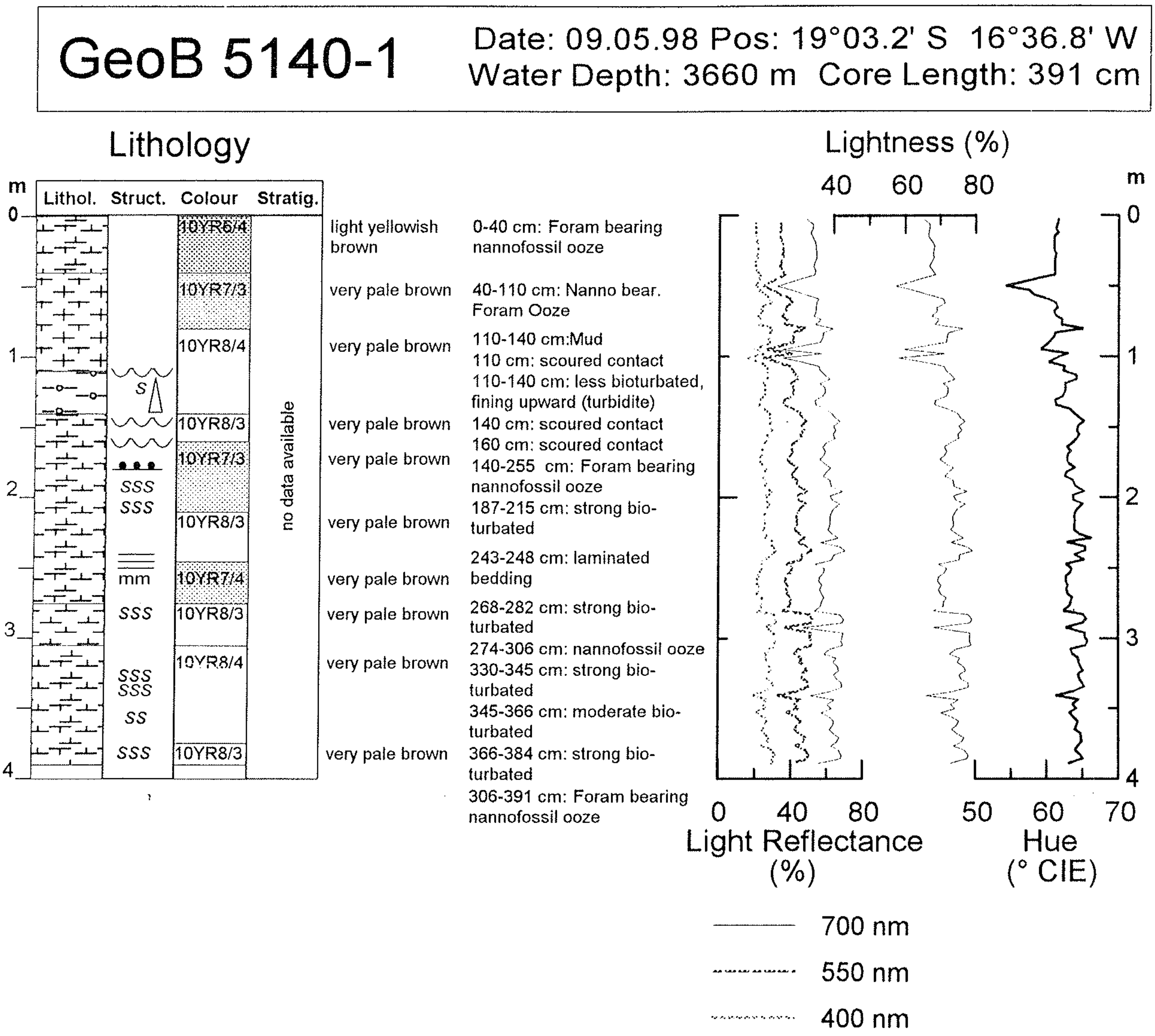


Fig. 54a Core description of GeoB 5140-1

*CORE NOT OPENED*

*NO CORE DESCRIPTION AVAILABLE*

Fig. 55a Core description of GeoB 5140-2

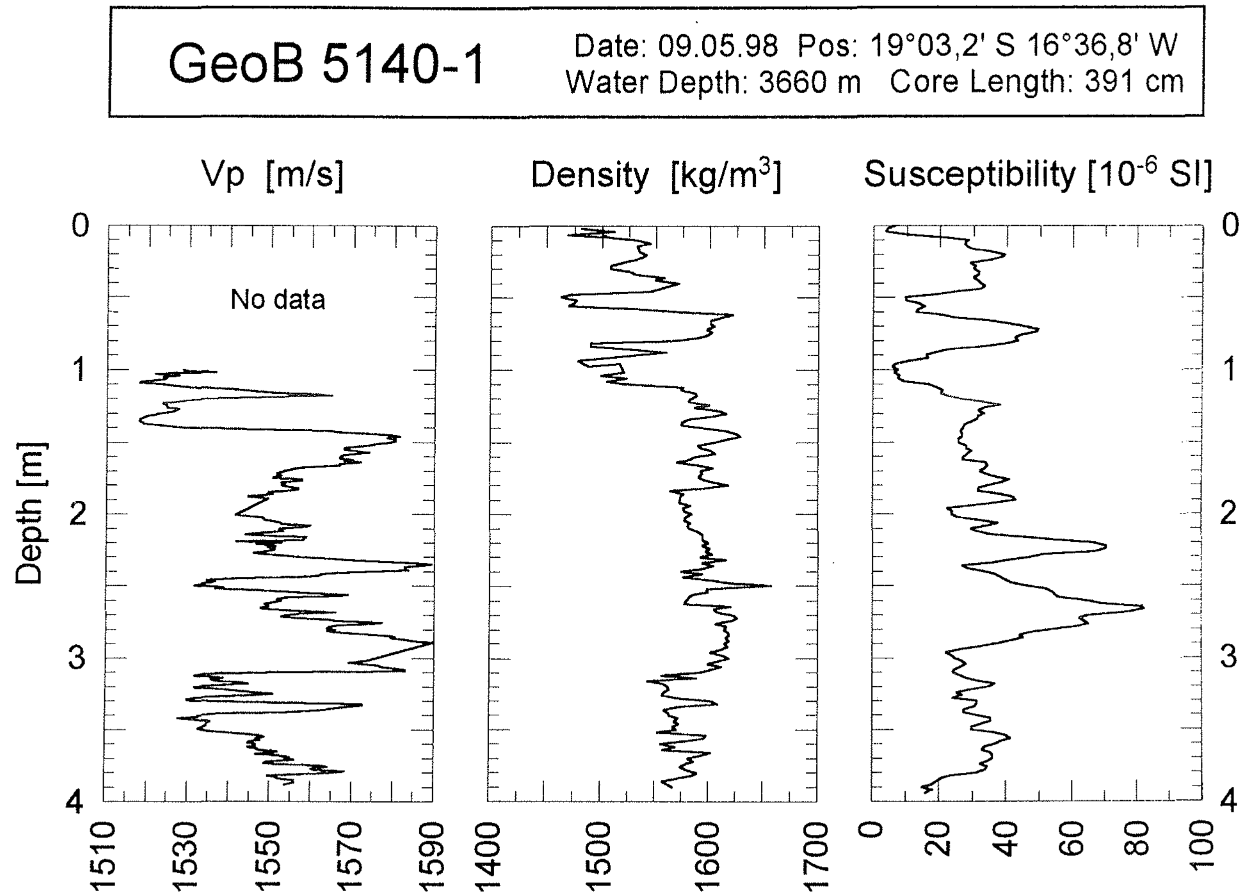


Fig. 54b Physical properties data of GeoB 5140-1

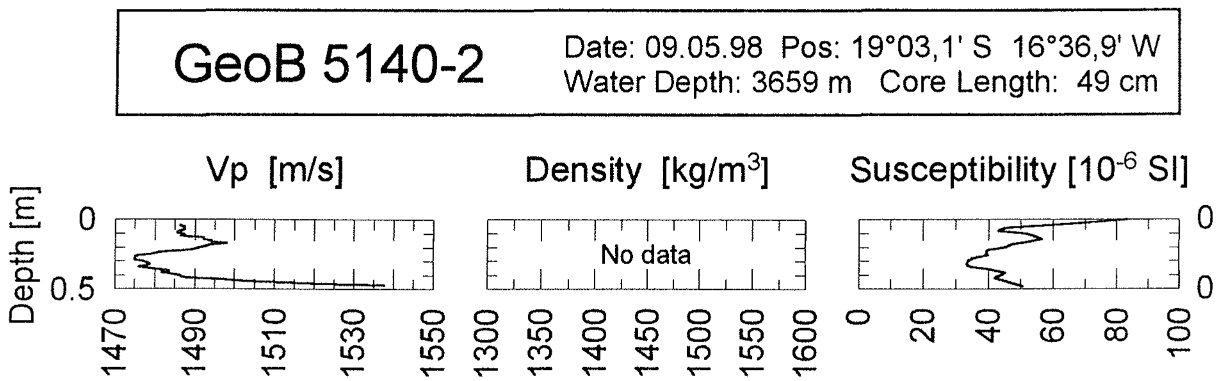


Fig. 55b Physical properties data of GeoB 5140-2

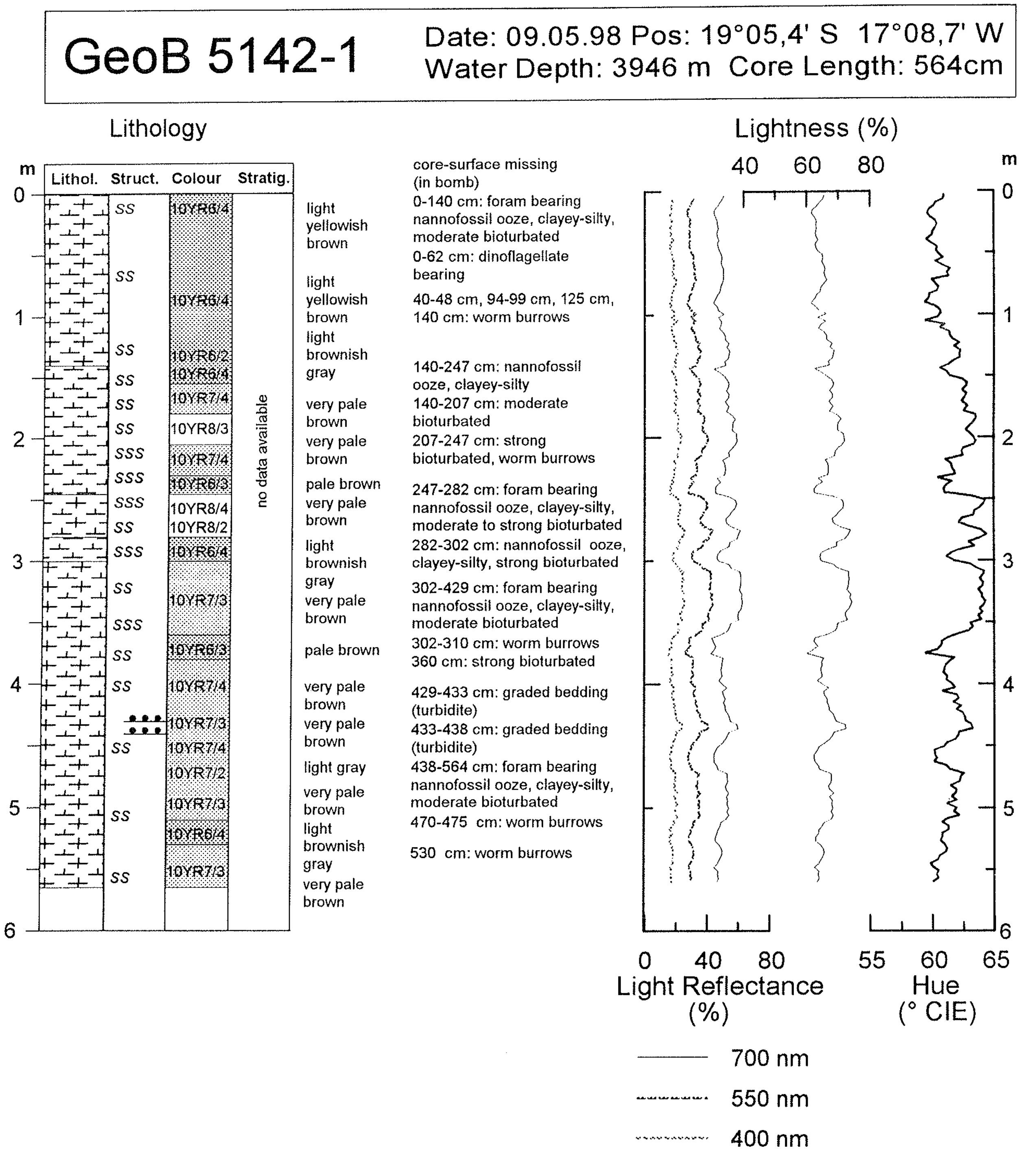


Fig. 56a Core description of GeoB 5142-1

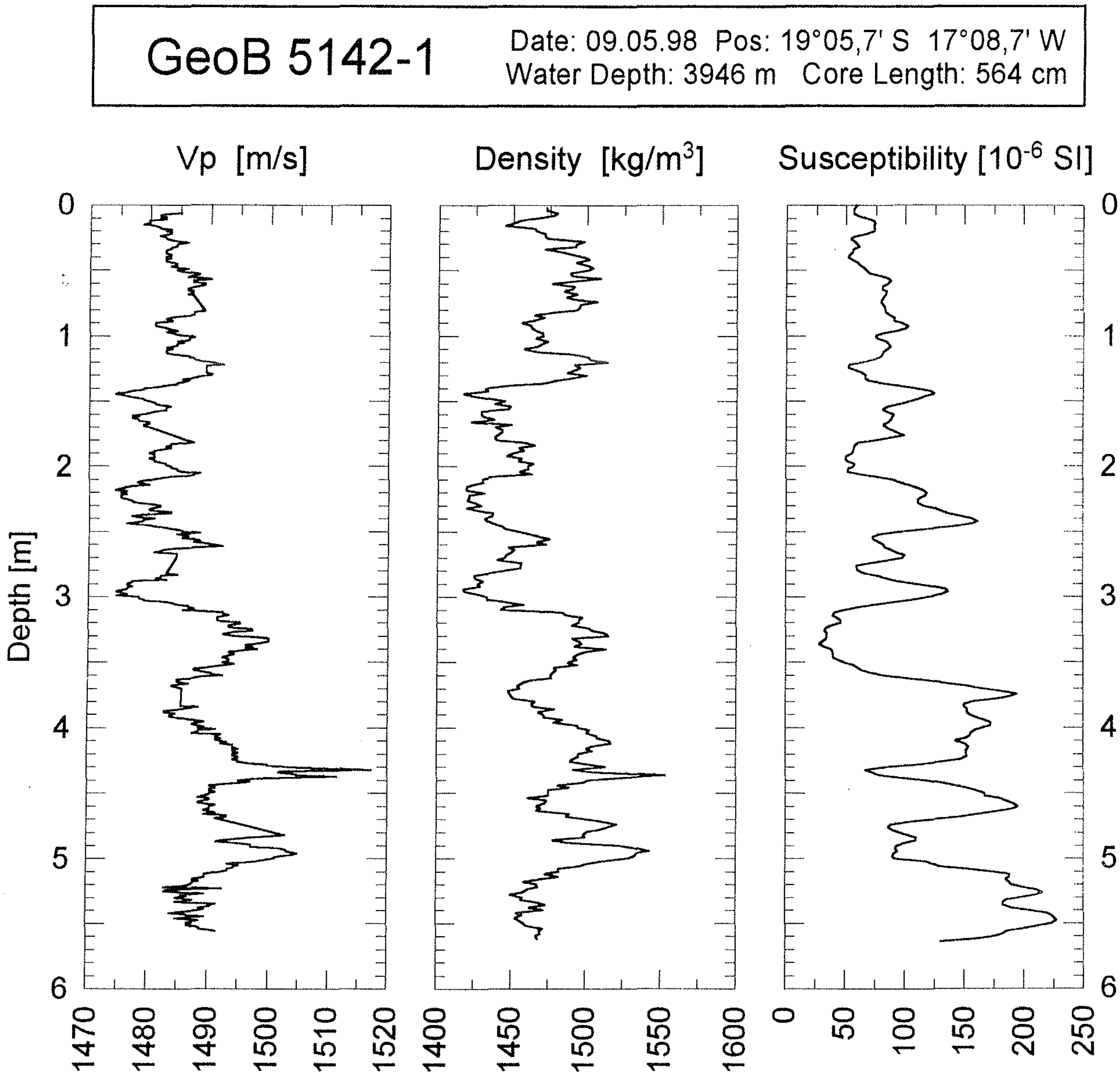


Fig. 56b Physical properties data of GeoB 5142-1

*Mid-Atlantic Ridge, Profil 19°S, Angola Basin*

GeoB 5130-2 (position 19°24.2'S 09°27.6'W, water depth: 3165 m, length: 517 cm) Fig. 43
The core is dominated by nannofossil ooze which is foram- and/or dinoflagellate-bearing. In a depth of 29-31 cm a fine grained foram-sand layer occurs. Between 31 and 41 cm the core is interrupted by a thin turbidite. The turbidite consists of very fine grained, soft sediment increasingly silty towards its base. On the base, a foram-sand layer was found again. A clayey-silty watersaturated layer is situated between 59 and 203 cm. Moderate to strong bioturbation is observed throughout the core, except in depths between 217-248 cm. In these depths, mm thick laminated layers of fine foram-sand were observed. In addition to these laminated layers, the core often contains worm burrows. Colour changes are minor, varying from light gray and pale yellow to very pale brown.

GeoB 5131-1 (position 19°02.2'S 09°44.5'W, water depth: 3886 m, length: 216 cm) Fig. 44
The core consists of foram-bearing nannofossil ooze from 0-216 cm. Bioturbation only takes place at 57 cm, 135-150 cm and from 190-205 cm. Colour changes were only noticed at 200 cm from pale brown to very pale brown.

GeoB 5132-1 (position 19°07.5'S 09°43.1'W, water depth: 3942 m, length: 325 cm) Fig. 45
The core surface as well as sandy layers from 44-68 cm and from 95-103 cm leaked during recovery of the core on board, so the indication of core depths are reconstructed and could include large errors. The rest of the core is dominated by foram-bearing nannofossil ooze. Less bioturbation only takes place from 30-35 cm, 145-150 cm, 185-220 cm, 240-250 cm and 310-317 cm.

GeoB 5132-3 (position 19°07.5'S 09°43.1'W, water depth: 3941 m, length: 326 cm) Fig. 46
This core was taken at the same location as GeoB 5132-1. The upper 35 cm are dominated by moderate bioturbated foram and dinoflagellate bearing nannofossil ooze which is silty to sandy. In depths between 35-59 and 66-92 cm, the core is interrupted by two turbidites. The turbidites are fine grained, soft clayey sediment increasingly silty towards their bases, which show graded fine foram sands. Between and below the two turbidites, a moderate bioturbated nannofossil ooze with worm burrows is observed. Between 301-315 cm the lithology changes slightly to clayey grain sizes, but from 315 cm down to the core bottom again silty-sandy grain sizes occur. A very pale brown colour dominates throughout the core.

GeoB 5133-1 (position 19°05.1′S 10°11.6′W, water depth: 3661 m, length: 503 cm) Fig. 46
The core mainly consists of very pale brown foram and dinoflagellate-bearing nannofossil ooze. The sediment between 28-38 cm is composed of silty-sandy foram-nannofossil ooze, whereby here worm burrows occur. Below 38 cm until 489 cm, the core contains an equal sequence of silty-sandy foram- and dinoflagellate-bearing nannofossil ooze. At 489 cm, the nannofossil ooze becomes more clayey. The whole core is moderately bioturbated with high worm burrow density reaching a maximum between 105-323 cm.

GeoB 5134-2 (position 19°02.7′ S 10°41.0′ W, water depth: 3412 m, length: 242 cm) Fig. 47
The Sediment of core 5134-2 is described in the smear slide analysis as foram-bearing nannofossil ooze. The core is undisturbed and only in the second meter less or moderately bioturbated. Light reflectance shows only small variations.

GeoB 5135-2 (position 19°26.1′ S 11°03.8′ W, water depth: 3303 m, length: 150 cm) Fig. 48
The core shows a layer of clayey foram-bearing nannofossil ooze from 0-38 cm and 50-150 cm and nanno-bearing foram ooze (38-50 cm). These units are also represented in colour changes. Between 38 and 50 cm the core is disturbed. Lightness and hue are good indicators for disturbed parts.

*Mid-Atlantic Ridge, Profil 19°S, Brazil Basin*

GeoB 5136-1 (position 19°22.2′ S 12°40.2′ W, water depth: 3227 m, length: 529 cm) Fig. 49
This core consists of nannofossil ooze, in some layers foram- and/or dinoflagellate-bearing. Between 151 and 158 cm a thin turbidite layer is included. From 158-180 cm, the sediment is a silty carbonate mud. Worms burrows only take place in a few parts of the core. The core is only less bioturbated below the turbitide layer and only the upper part between 85 and 92 cm is strongly bioturbated.

GeoB 5137-2 (position 19°17.5′ S 13°27.2′ W, water depth: 3503 m, length: 248 cm) Fig. 50
The core shows cyclic changing lithological units of clay and carbonate rich sediments, described in the smear slide as dino- and foram-bearing nannofossil ooze. Between 130 and 137 cm the sediment shows laminated bedding. Most parts are moderately or strongly bioturbated.

GeoB 5138-1 (position 19°11.3′ S 14°39.3′ W, water depth: 3632 m, length: 181 cm) Fig. 52
The core 5138-1 is dominated by foram nannofossil ooze and in some depths only less bioturbated. Also light reflectance only changes within a very small range.

GeoB 5139-2 (position 19°00.8′S 15°50.0′W, water depth: 3903 m, length: 563 cm) Fig. 53
The first 60 cm sediment of core GeoB 5139-2 were recovered as a disturbed mass sample from the bomb. The first 241 cm of the core show a disturbed sequence of equal, extremely fine and soft sediment of clay texture, described in the smear slide as nannofossil ooze. The sediment between 241-265 cm is composed of silty-sandy moderately bioturbated nannofossi-bearing foram ooze. Between 265-308 cm, mm thick laminated layers of light fine foram-sand were observed. Below 308 cm until 450 cm, the core contains a silty-sandy foram-bearing nannofossil ooze, which is moderately bioturbated. At 450 cm, the nannofossil ooze becomes more clayey and different sections of worm burrows are observed. A very pale brown colour dominates throughout this core.

GeoB 5140-1 (position 19°03.2′S 16°36.8′W, water depth: 3660 m, length: 391 cm) Fig. 54
The core is dominated by foram-bearing nannofossil ooze. Some sandy layers between one and two m are disturbed or lost. Most layers are rich in clay and moderately or strongly bioturbated with several worm burrows. From 110-140 cm, the core is interrupted by a turbidite layer.

GeoB 5142-1 (position 19°05.4′S 17°08.7′W, water depth: 3946 m, length: 564 cm) Fig. 56
The core-surface is missing because the first 30 cm sediment of this core were recovered from the bomb. The core description starts on this sub-surface level. Core GeoB 5142-1 is dominated by nannofossil ooze which is foram- and/or dinoflagellate-bearing. This sediment is clayey-silty and in the upper 207 cm moderately bioturbated. Between 208 and 360 cm, a strong bioturbation with worm burrows is often observed. From 360 to 429 cm the sediment is moderately bioturbated. In depths between 429-433 cm and 433-438 cm the core is interrupted by very thin turbidites. The turbidites are fine grained, soft sediment, in a very few cm increasingly silty towards their bases, and show small bands of graded foram-sands. Below the second turbidite, foram-bearing nannofossil ooze of ‘normal’ pelagic sedimentation is found. Again this nannofossil ooze is moderately bioturbated and often contains worm burrows. The whole sediment is dominated by brownish colours with lighter and darker shades.

Table 15 Smear slide analysis on sediment cores from M 41/3

| Station | depth [cm] | Qz | C | F | NF | D | Type |
|---|---|---|---|---|---|---|---|
| 5110-4 | 1 | 2 | 15 | | 75 | 1 | CbNFO |
| 5110-4 | 39 | | 12 | | 82 | 1 | CbNFO |
| 5110-4 | 79 | | 15 | | 74 | 1 | CbNFO |
| 5110-4 | 112 | | 15 | 1 | 81 | | CbNFO |
| 5110-4 | 176 | 5 | 88 | | 2 | | C |
| 5110-4 | 213 | 2 | 88 | | 3 | | C |
| 5110-4 | 262 | 3 | 20 | | 77 | | CbNFO |
| 5110-4 | 294 | 3 | 12 | | 82 | | CbNFO |
| 5110-4 | 370 | | 2 | | 9 | | NFO |
| 5110-4 | 393 | 1 | 15 | | 80 | | CbNFO |
| 5110-4 | 416 | | 90 | | | | C |
| 5110-4 | 468 | | 97 | | | | C |
| 5110-4 | 510 | | 94 | | | | C |
| 5110-4 | 534 | | 3 | | 91 | | NFO |
| 5110-4 | 571 | | 1 | | 96 | | NFO |
| 5110-4 | 596 | 1 | 94 | | | | C |
| 5110-4 | 656 | | 97 | | | | C |
| 5110-4 | 715 | | 99 | | | | C |
| 5110-4 | 764 | 3 | 95 | | | | C |
| 5110-4 | 803 | 2 | 96 | | | | C |
| 5110-4 | 870 | 5 | 92 | | | | C |
| 5110-4 | 893 | 6 | 93 | | | | C |
| 5110-4 | 950 | 4 | 95 | | | | C |
| 5112-4 | -28 | | 3 | 15 | 63 | | NbFO |
| 5112-4 | -3 | | 2 | 15 | 70 | | NbFO |
| 5112-4 | 12 | | 2 | 13 | 67 | | NbFO |
| 5112-4 | 48 | | 3 | 10 | 71 | | NbFO |
| 5112-4 | 77 | | 1 | 20 | 67 | | FbNFO |
| 5112-4 | 112 | | 1 | 8 | 76 | | NFO |
| 5112-4 | 149 | | | 15 | 75 | | FbNFO |
| 5112-4 | 171 | | | 10 | 79 | | FbNFO |
| 5112-4 | 191 | | | 10 | 80 | | NFO |
| 5112-4 | 219 | | | 15 | 74 | | FbNFO |
| 5112-4 | 238 | | | 15 | 75 | | FbNFO |
| 5112-4 | 274 | | | 9 | 82 | | NFO |
| 5112-4 | 311 | | | 17 | 72 | | FbNFO |
| 5112-4 | 347 | | | 5 | 30 | 55 | NDO |
| 5112-4 | 352 | | | 5 | 55 | 37 | DNFO |
| 5112-4 | 367 | | | 15 | 73 | | FbNFO |
| 5112-4 | 414 | | | 15 | 70 | | NbFO |
| 5112-4 | 445 | | | 5 | 80 | | NFO |
| 5112-4 | 468 | | | 20 | 70 | | FbNFO |
| 5112-4 | 513 | | | 12 | 79 | | FbNFO |
| 5112-4 | 529 | | | 10 | 80 | | FbNFO |
| 5112-4 | 556 | | | 11 | 78 | | FbNFO |
| 5115-1 | 10 | | | 15 | 72 | | NbFO |
| 5115-1 | 42 | | | 12 | 77 | | FbNFO |
| 5115-1 | 73 | | | 10 | 73 | | NbFO |
| 5115-1 | 110 | | | 15 | 72 | | NbFO |
| 5115-1 | 136 | | | 12 | 74 | | NbFO |
| 5115-1 | 165 | | | 25 | 63 | | FbNFO |
| 5115-1 | 172 | | | 70 | 30 | | NFO |
| 5115-1 | 202 | | | 14 | 75 | | FbNFO |
| 5115-1 | 218 | | | 18 | 72 | | FbNFO |
| 5115-1 | 249 | | | 20 | 72 | | FbNFO |
| 5115-1 | 275 | | | 10 | 83 | | FbNFO |
| 5115-1 | 318 | | | 10 | 86 | | FbNFO |
| 5115-1 | 332 | | | 12 | 76 | | FbNFO |
| 5115-1 | 389 | | | 11 | 82 | | FbNFO |
| 5116-2 | 20 | | 1 | 30 | 63 | | FNFO |
| 5116-2 | 91 | | | 20 | 69 | | FbNFO |
| 5116-2 | 189 | | | 20 | 72 | | FbNFO |
| 5116-2 | 262 | | | 20 | 74 | | FbNFO |
| 5116-2 | 316 | | 2 | 25 | 61 | | FbNFO |
| 5116-2 | 338 | | | 18 | 75 | | FbNFO |
| 5116-2 | 389 | | | 25 | 68 | | FNFO |
| 5116-2 | 433 | | | 15 | 80 | | FbNFO |
| 5116-2 | 474 | | | 15 | 81 | | FbNFO |
| 5116-2 | 520 | | | 10 | 85 | | FbNFO |
| 5117-1 | 2 | | | 15 | 72 | | FbNFO |
| 5117-1 | 42 | | | 12 | 82 | | FbNFO |
| 5117-1 | 76 | | | 17 | 74 | | FbNFO |
| 5117-1 | 113 | | | 20 | 68 | | FbNFO |
| 5117-1 | 131 | | | 10 | 82 | | FbNFO |
| 5120-2 | 8 | | | 12 | 78 | | FbNFO |
| 5120-2 | 60 | | | 10 | 81 | | FbNFO |
| 5120-2 | 90 | | | 9 | 83 | | NFO |
| 5120-2 | 116 | | | 5 | 90 | | NFO |
| 5120-2 | 135 | | | 5 | 92 | | NFO |
| 5120-2 | 162 | | | 9 | 88 | | NFO |
| 5120-2 | 195 | | | 15 | 75 | | FbNFO |
| 5120-2 | 220 | | | 9 | 82 | | NFO |
| 5120-2 | 229 | | | 15 | 78 | | FbNFO |
| 5120-2 | 253 | | | 9 | 84 | | NFO |
| 5120-2 | 284 | | | 17 | 74 | | FbNFO |
| 5120-2 | 309 | | | 15 | 77 | | FbNFO |
| 5120-2 | 320 | | | 10 | 85 | | FbNFO |
| 5120-2 | 347 | | 2 | 11 | 82 | | FbNFO |
| 5120-2 | 372 | | | 10 | 80 | | FbNFO |
| 5121-1 | 20 | | | 20 | 68 | | FbNFO |
| 5121-1 | 74 | | | 20 | 70 | | FbNFO |
| 5121-1 | 126 | | | 20 | 70 | | FbNFO |
| 5121-1 | 165 | | | 20 | 72 | | FbNFO |
| 5121-1 | 225 | | | 20 | 77 | | FbNFO |
| 5121-1 | 265 | | | 21 | 75 | | FbNFO |
| 5121-1 | 316 | | | 9 | 87 | | NFO |
| 5121-1 | 358 | | | 10 | 85 | | FbNFO |
| 5121-1 | 378 | | | 10 | 81 | | FbNFO |
| 5121-1 | 427 | | | 20 | 76 | | FbNFO |
| 5121-1 | 456 | | | 20 | 71 | | FbNFO |
| 5121-1 | 463 | | | 25 | 64 | | FNFO |
| 5121-1 | 480 | | | 12 | 80 | | FbNFO |
| 5121-1 | 491 | | | 15 | 79 | | FbNFO |
| 5121-1 | 519 | | | 10 | 78 | | NbFO |
| 5130-2 | 10 | | | 27 | 65 | | FNFO |
| 5130-2 | 23 | | | 9 | 82 | | NFO |
| 5130-2 | 34 | | | 9 | 85 | | NFO |
| 5130-2 | 48 | | | 15 | 78 | | FbNFO |
| 5130-2 | 80 | | | 8 | 86 | | NFO |
| 5130-2 | 116 | | | 3 | 94 | | NFO |
| 5130-2 | 158 | | | 8 | 83 | | NFO |
| 5130-2 | 210 | | | 7 | 86 | | NFO |
| 5130-2 | 218 | | | 17 | 73 | | FbNFO |
| 5130-2 | 238 | | | 50 | 42 | | FNFO |
| 5130-2 | 251 | | | 9 | 83 | | NFO |
| 5130-2 | 290 | | | 21 | 73 | | FbNFO |
| 5130-2 | 308 | | | 9 | 87 | | NFO |
| 5130-2 | 352 | | | 13 | 76 | | FbNFO |

Table 15 continued

| Station | depth [cm] | Qz | C | F | NF | D | Type |
|---|---|---|---|---|---|---|---|
| 5130-2 | 402 | | | 12 | 83 | | FbNFO |
| 5130-2 | 418 | | | 9 | 85 | | NFO |
| 5130-2 | 447 | | | 10 | 82 | | FbNFO |
| 5130-2 | 495 | | | 9 | 88 | | NFO |
| 5130-2 | 516 | | | 8 | 87 | | NFO |
| 5131-1 | 12 | | | 20 | 74 | | FbNFO |
| 5131-1 | 81 | | | 18 | 74 | | FbNFO |
| 5131-1 | 210 | | | 21 | 71 | | FbNFO |
| 5132-1 | 20 | | | 15 | 78 | | FbNFO |
| 5132-1 | 40 | | | 9 | 83 | | NFO |
| 5132-1 | 80 | | | 5 | 86 | | NFO |
| 5132-1 | 193 | | | 10 | 79 | | NbFO |
| 5132-2 | 11 | | | 25 | 63 | | FNFO |
| 5132-2 | 45 | | | 5 | 87 | | NFO |
| 5132-2 | 61 | | | 10 | 85 | | FbNFO |
| 5132-2 | 78 | | | 10 | 85 | | FbNFO |
| 5132-2 | 112 | | | 20 | 75 | | FbNFO |
| 5132-2 | 171 | | | 12 | 81 | | FbNFO |
| 5132-2 | 211 | | | 20 | 76 | | FbNFO |
| 5132-2 | 254 | | | 10 | 85 | | FbNFO |
| 5132-2 | 306 | | | 3 | 91 | | NFO |
| 5132-2 | 322 | | | 15 | 83 | | FbNFO |
| 5133-1 | 4 | | | 20 | 73 | | FbNFO |
| 5133-1 | 29 | | | 25 | 67 | | FNFO |
| 5133-1 | 78 | | | 20 | 74 | | FbNFO |
| 5133-1 | 139 | | | 17 | 75 | | FbNFO |
| 5133-1 | 186 | | | 15 | 76 | | FbNFO |
| 5133-1 | 225 | | | 20 | 76 | | FbNFO |
| 5133-1 | 254 | | | 12 | 78 | | FbNFO |
| 5133-1 | 289 | | | 10 | 86 | | FbNFO |
| 5133-1 | 334 | | | 10 | 84 | | FbNFO |
| 5133-1 | 392 | | | 12 | 84 | | FbNFO |
| 5133-1 | 440 | | | 14 | 81 | | FbNFO |
| 5133-1 | 467 | | | 12 | 81 | | FbNFO |
| 5133-1 | 483 | | | 10 | 83 | | FbNFO |
| 5133-1 | 500 | | | 3 | 95 | | NFO |
| 5134-2 | 103 | | | 11 | 79 | | FbNFO |
| 5134-2 | 224 | | | 10 | 79 | | FbNFO |
| 5135-2 | 10 | | | 20 | 70 | | FbNFO |
| 5135-2 | 45 | | | 75 | 15 | | NbFO |
| 5135-2 | 113 | | | 15 | 76 | | FbNFO |
| 5136-1 | 17 | | | 10 | 78 | | FbNFO |
| 5136-1 | 107 | | | 5 | 79 | | NFO |
| 5136-1 | 174 | | | 10 | 74 | | FbNFO |
| 5136-1 | 208 | | | 12 | 72 | | FbNFO |
| 5136-1 | 274 | | | 12 | 72 | | FbNFO |
| 5136-1 | 380 | | | 6 | 88 | | NFO |
| 5136-1 | 500 | | | 10 | 77 | | NbFO |

| Station | depth [cm] | Qz | C | F | NF | D | Type |
|---|---|---|---|---|---|---|---|
| 5137-2 | 12 | | | 25 | 49 | | FNFO |
| 5137-2 | 89 | | | 15 | 72 | | NbFO |
| 5137-2 | 144 | | | 10 | 78 | | NbFO |
| 5137-2 | 205 | | | 10 | 78 | | NbFO |
| 5137-2 | 243 | | | 11 | 78 | | NbFO |
| 5138-1 | 53 | | | 25 | 65 | | FNFO |
| 5138-1 | 175 | | | 13 | 79 | | FbNFO |
| 5139-2 | 8 | | | 8 | 82 | | NFO |
| 5139-2 | 62 | | | 8 | 82 | | NFO |
| 5139-2 | 200 | | | 9 | 81 | | NFO |
| 5139-2 | 262 | | | 60 | 30 | | NbFO |
| 5139-2 | 290 | | | 90 | 5 | | FO |
| 5139-2 | 350 | | | 15 | 73 | | FbNFO |
| 5139-2 | 408 | | | 12 | 78 | | FbNFO |
| 5139-2 | 455 | | | 9 | 80 | | NFO |
| 5139-2 | 468 | | | 7 | 87 | | NFO |
| 5139-2 | 496 | | | 3 | 92 | | NFO |
| 5139-2 | 542 | | | 7 | 88 | | NFO |
| 5140-1 | 16 | | | 20 | 69 | | FbNFO |
| 5140-1 | 71 | | | 55 | 35 | | NbFO |
| 5140-1 | 88 | | | 50 | 43 | | NbFO |
| 5140-1 | 143 | | | 20 | 73 | | FbNFO |
| 5140-1 | 177 | | | 25 | 68 | | FNFO |
| 5140-1 | 215 | | | 23 | 69 | | FbNFO |
| 5140-1 | 228 | | | 18 | 77 | | FbNFO |
| 5140-1 | 255 | | | 14 | 81 | | FbNFO |
| 5140-1 | 287 | | | 9 | 86 | | NFO |
| 5140-1 | 337 | | | 21 | 74 | | FbNFO |
| 5140-1 | 275 | | | 10 | 83 | | FbNFO |
| 5140-1 | 382 | | | 15 | 80 | | FbNFO |
| 5142-1 | 8 | | | 23 | 60 | | NbFO |
| 5142-1 | 62 | | | 15 | 73 | | NbFO |
| 5142-1 | 84 | | | 10 | 80 | | FbNFO |
| 5142-1 | 129 | | | 17 | 73 | | FbNFO |
| 5142-1 | 144 | | | 9 | 90 | | NFO |
| 5142-1 | 164 | | | 8 | 87 | | NFO |
| 5142-1 | 195 | | | 8 | 84 | | NFO |
| 5142-1 | 222 | | | 5 | 90 | | NFO |
| 5142-1 | 239 | | | 8 | 87 | | NFO |
| 5142-1 | 259 | | | 10 | 81 | | FbNFO |
| 5142-1 | 278 | | | 11 | 83 | | FbNFO |
| 5142-1 | 297 | | | 9 | 80 | | NFO |
| 5142-1 | 337 | | | 10 | 82 | | FbNFO |
| 5142-1 | 372 | | | 10 | 85 | | FbNFO |
| 5142-1 | 402 | | | 10 | 80 | | FbNFO |
| 5142-1 | 435 | | | 15 | 81 | | FbNFO |
| 5142-1 | 460 | | | 15 | 77 | | FbNFO |
| 5142-1 | 516 | | | 12 | 83 | | FbNFO |
| 5142-1 | 548 | | | 10 | 80 | | FbNFO |

| | | | | | |
|---|---|---|---|---|---|
| Quartz | Qz | Nannofossilooze | NFO | Nannofossil bearing FO | NbFO |
| Clay | C | Foraminiferooze | FO | Nannofossil Diatomooze | NDO |
| Ooze | O | Clay bearing NFO | CbNFO | Nannofossil Foraminiferooze | N-FO |
| Foraminifers | F | Diatom-Nannofossilooze | DNFO | NF bearing Foraminiferooze | NbFO |
| Diatoms | D | Foraminifer bearing NFO | FbNFO | | |
| Nannofossils | NF | Foraminifer NFO | FNFO | | |

### 4.5.5 Carbonate Content Measuring

(R. Höppner, B. Kottke, S. Rath)

Variations in carbonate content mainly reflect changes between marine, carbonate-dominated sedimentation during high sea-level (interglacials) and terrigenous, carbonate-impoverished sedimentation during low sea-level (glacials). The carbonate mainly origins from skeletons of marine phytoplankton (Coccolithophores, Dinoflagellates) and zooplankton (benthic and planktonic foraminifera, pteropods). Periodical changes can be interpreted as orbital variations (precession, obliquity, eccentricity). The reliability of carbonate content measuring can be tested by various parameters investigated on board (magnetic susceptibility - see Chapter "4.6 Physical properties", light reflectance - see Chapter 4.5.4 "Lithologic Core Summary"). Carbonate contents were measured on board using a "carbonate-bomb". Sediment cores GeoB 5115-1 and GeoB 5116-2 were measured for their carbonate content:

Samples were taken in 10 cm intervals, oven dried at 40°C, weighed in 1 g portions and finally treated with HCl (25 %). The $CaCO_3$ content in percent of each sample was ascertained by measuring the $CO_2$ pressure passing a photovoltaic cell. The absolute error of a single determination is given as about 1 % calcium carbonate (Müller and Gastner 1971). Comparisons with other carbonate investigation methods (e.g. LECO) show that the bias of the "carbonate bomb" is always less than 0.5 %.

Generally the sediments are rich in carbonate. Both of the cores were taken at water depths which are above the recent carbonate compensation depth (CCD) from the western part of the Mid-Atlantic Ridge. Although some parts obviously show a disturbed sedimentation pattern (turbidites), all samples were investigated. In general carbonate values vary from 65 wt % up to more than 96 wt % (see Table 16 ). The deeper core (GeoB 5115-1) shows a slight pattern of alternating higher and lower carbonate contents, indicating interglacial and glacial variations (see Fig. 57).

Table 16 Carbonate content of the gravity cores GeoB 5115-1 and 5116-2

| No. | Sample weight | Depth | GeoB 5115-1 CaCO3 content [wt %] | GeoB 5116-2 CaCO3 content [wt %] |
|---|---|---|---|---|
| 1 | 1,0 | 3 | 66,6 | 82,7 |
| 2 | 1,0 | 13 | 64,9 | 90,4 |
| 3 | 1,0 | 23 | 71,7 | 92,6 |
| 4 | 1,0 | 33 | 67,5 | 90,0 |
| 5 | 1,0 | 43 | 65,3 | 91,3 |
| 6 | 1,0 | 53 | 69,3 | 91,8 |
| 7 | 1,0 | 63 | 73,0 | 93,1 |
| 8 | 1,0 | 73 | 73,7 | 93,1 |
| 9 | 1,0 | 83 | 74,1 | 94,4 |
| 10 | 1,0 | 93 | 74,4 | 93,4 |
| 11 | 1,0 | 103 | 71,0 | 90,0 |
| 12 | 1,0 | 113 | 69,5 | 92,6 |
| 13 | 1,0 | 123 | 74,1 | 93,1 |
| 14 | 1,0 | 133 | 80,0 | 91,3 |
| 15 | 1,0 | 143 | 81,4 | 90,6 |
| 16 | 1,0 | 153 | 81,9 | 90,9 |
| 17 | 1,0 | 163 | 81,7 | 92,9 |
| 18 | 1,0 | 173 | 86,5 | 93,6 |
| 19 | 1,0 | 183 | 85,9 | 92,4 |
| 20 | 1,0 | 193 | 81,9 | 92,5 |
| 21 | 1,0 | 203 | 84,9 | 92,8 |
| 22 | 1,0 | 213 | 82,4 | 91,2 |
| 23 | 1,0 | 223 | 82,8 | 92,4 |
| 24 | 1,0 | 233 | 88,2 | 92,1 |
| 25 | 1,0 | 243 | 91,4 | 86,6 |
| 26 | 1,0 | 253 | 93,3 | 92,1 |
| 27 | 1,0 | 263 | 92,8 | 90,1 |
| 28 | 1,0 | 273 | 90,5 | 94,8 |
| 29 | 1,0 | 283 | 89,6 | 93,4 |
| 30 | 1,0 | 293 | 89,7 | 89,1 |
| 31 | 1,0 | 303 | 88,0 | 93,5 |
| 32 | 1,0 | 313 | 87,5 | 94,0 |
| 33 | 1,0 | 323 | 88,7 | 94,2 |
| 34 | 1,0 | 333 | 89,3 | 90,7 |
| 35 | 1,0 | 343 | 80,0 | 95,9 |
| 36 | 1,0 | 353 | 88,2 | 94,3 |
| 37 | 1,0 | 363 | 88,5 | 96,7 |
| 38 | 1,0 | 373 | 87,6 | 95,4 |
| 39 | 1,0 | 383 | 87,9 | 92,5 |
| 40 | 1,0 | 393 | 87,4 | 97,8 |
| 41 | 1,0 | 403 | 88,9 | 95,8 |
| 42 | 1,0 | 413 | | 95,4 |
| 43 | 1,0 | 423 | | 95,2 |
| 44 | 1,0 | 433 | | 87,9 |
| 45 | 1,0 | 443 | | 86,7 |
| 46 | 1,0 | 453 | | 89,1 |
| 47 | 1,0 | 463 | | 91,3 |
| 48 | 1,0 | 473 | | 93,7 |
| 49 | 1,0 | 483 | | 90,7 |
| 50 | 1,0 | 493 | | 92,3 |
| 51 | 1,0 | 503 | | 92,1 |
| 52 | 1,0 | 513 | | 92,4 |
| 53 | 1,0 | 523 | | 91,2 |
| 54 | 1,0 | 533 | | 90,9 |

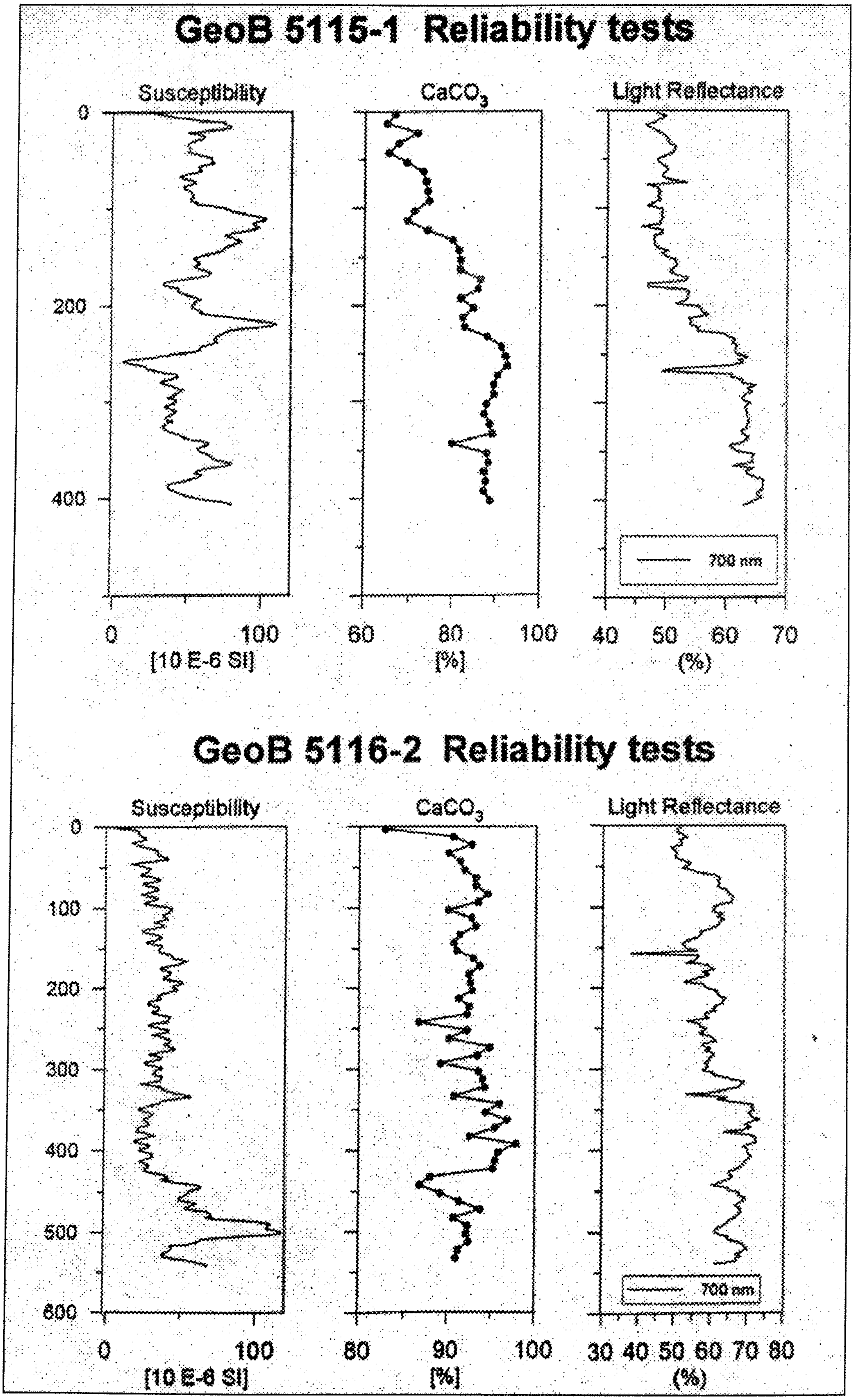


Fig. 57 Reliability tests of the gravity cores GeoB 5115-1 and GeoB 5116-2

### 4.5.6 Particle Size Distribution

(R. Höppner, B. Kottke, S. Rath)

The circulation of water masses plays an essential role in oceanographic exploration and the reconstruction of material transfer in marine systems. Information on flow conditions is preserved in characteristic sediment distributions. These distributions reflect regional circulation patterns and sea floor morphology. Large parts of the deep ocean basins and the nearby continental margins are characterised by geostrophic currents moving with speeds of 5-20 cm/s (McCave et al. 1980). These regional variable flow velocities lead to the formation of typical sediment associations and special particle distribution patterns.

Coarse grain sizes reflect high velocity currents, thereby washing out the fine fraction. Uniform steady flows (e.g. contourites) lead to the deposition of well- to medium-sorted grain sizes, transporting a defined range of sediment particles. Accumulative sediment patterns are produced by low velocity currents, which are responsible for the sedimentation of finer grain sizes. Therefore, the silt fraction is sensitive to speed variations of marine currents (Ledbetter 1984, 1986).

During cruise M 41/3, 18 multicorer (MUC) and giant box corer (GKG) samples were collected (see Chapter 8). The undisturbed sediment cores were cut into 1 cm slices and deep-frozen at -20°C. At Bremen University, these samples will be wet-sieved, splitted into sand-, silt- and clay-sized particles, dried and decarbonated with HCl. Afterwards the settling velocity of each non-biogenic sample will be measured with a silt-settling-tube and a particle-size-analyser (Sedigraph) in order to evaluate the grain size distribution and the mean particle sizes. These sediment parameters, in combination with the hydrosphere data (salinity, pressure, temperature, etc.), will provide a better understanding of regional circulation patterns and local marine current systems.

### 4.5.7 Organic Petrology and Geochemistry

(R. Höppner, B. Kottke, S. Rath)

The quantitative assessment of the marine versus terrigenous fraction of particulate organic matter in marine sediments is of fundamental importance to discuss sedimentary organic carbon records with regard to climate-induced changes in paleoproductivity and the supply of terrigenous matter. To calibrate modern climatic and oceanographic conditions in the South Atlantic to surface sediments, organic petrologic studies are performed. Evaluation of factors controlling organic matter sedimentation during late Quaternary climatic cycles are deduced from selected glacial-interglacial core sections. These studies concentrate on the continental margins of South and West Africa and South America as well as the Equatorial Atlantic. Presumably, C4 organic material input as a part of the dust injection leads to a significant bias of the $\delta^{13}$Corg signal in marine sediments.

On every sediment station (see Table 17) samples were taken from multicorer or box corer cores. The cores were cut in slices of 1 cm and were immediately stored at -20°C in the deep-freeze room. At Bremen University further investigations, e.g. organic microscopy and mazerale analysis, will be carried out.

Table 17 Positions of all samples taken with respect to organic investigations

| Core GeoB | Coretype | Latitude | Longitude | Depth [m] | Recovery [cm] | Particle size distribution | Organic petrol. and geochem. |
|---|---|---|---|---|---|---|---|
| **5110-5** | GKG | 25°54,30'S | 35°38,40'W | 4206 | 45 | x | x |
| **5112-5** | GKG | 23°49,54'S | 16°15,56'W | 3841 | 27 | x | x |
| **5115-2** | MUC | 24°08,66'S | 14°02,57'W | 3292 | 24 | x | x |
| **5116-1** | MUC | 24°09,58'S | 13°46,24'W | 2256 | 26 | x | x |
| **5117-2** | MUC | 24°08,84'S | 13°58,43'W | 3039 | 16 | x | x |
| **5120-1** | MUC | 24°10,20'S | 12°21,69'W | 3847 | 16 | x | x |
| **5121-2** | MUC | 24°10,98'S | 12°01,26'W | 3488 | 16 | x | x |
| **5130-1** | MUC | 19°24,26'S | 09°27,56'W | 4165 | 16 | x | x |
| **5132-2** | MUC | 19°07,48'S | 09°43,17'W | 3941 | 14 | x | x |
| **5133-3** | MUC | 19°05,18'S | 10°11,54'W | 3661 | 15 | x | x |
| **5134-1** | MUC | 19°02,70'S | 10°41,04'W | 3411 | 19 | x | x |
| **5135-1** | MUC | 19°26,17'S | 11°03,78'W | 3303 | 20 | x | x |
| **5136-2** | MUC | 19°22,15'S | 12°40,21'W | 3227 | 18 | x | x |
| **5137-1** | MUC | 19°17,41'S | 13°27,22'W | 3500 | 17 | x | x |
| **5138-2** | MUC | 19°11,40'S | 14°39,27'W | 3631 | 20 | x | x |
| **5139-1** | MUC | 19°00,80'S | 15°49,97'W | 3903 | 10 | x | |
| **5140-3** | MUC | 19°03,21'S | 16°36,76'W | 3660 | 13 | x | x |
| **5142-2** | MUC | 19°05,40'S | 17°08,60'W | 3946 | 12 | x | x |

## 4.6 Physical Properties Studies

(T. Frederichs, K. Fabian, J. Funk)

The complete sediment series recovered during METEOR Cruise M 41/3 with the gravity corer were subject to laboratory geophysical studies. Shipboard measurements on the segmented cores routinely comprised three basic physical parameters:

- compressional (p-) wave velocity $v_p$,
- electric resistivity $R_s$ (as a measure of density and porosity), and,
- magnetic volume susceptibility $\kappa$.

These properties are closely related to lithology and grain size of the sediments and provide high-resolution core logs (spacing 1 cm for p-wave velocity, 2 cm for electric resistivity and magnetic volume susceptibility) available prior to all other detailed investigations. In addition, oriented samples for subsequent shore-based rock and paleomagnetic studies were taken at routine intervals of 5 cm.

### 4.6.1 Physical Background and Experimental Techniques

The experimental setups for the shipboard measurements were basically identical to those of previous cruises. Their descriptions are therefore kept brief here. A more detailed treatment of the experimental procedures are given in Wefer et al. (1991) for $R_s$ and Schulz et al. (1991) for $v_p$.

*P-Wave Velocity*

The p-wave velocity $v_p$ is derived from digitally processed ultrasonic transmission seismograms recorded perpendicular to the core axis with a fully automated logging system. First arrivals are picked using a cross-correlation algorithm based on the 'zero-offset' signal of the piezoelectric wheel probes. Combined with the core diameter d, the travel time of the first arrivals t yields a p-wave velocity profile with an accuracy of 1 to 2 m/s

$$v_p = (d - d_L) / (t - t_0 - t_L)$$

where $d_L$ is the thickness of the liner walls, $t_L$ the travel time through the liner walls and $t_0$ the 'zero-offset' travel time.

Following Schultheiss and McPhail (1989), a temperature calibration of $v_p$ is effected using the equation

$$v_{20} = v_T + 3 \cdot (20 - T)$$

where $v_{20}$ is the p-wave velocity at 20 °C and T the temperature (in °C) of the core segment when logged. Simultaneously, the maximum peak-to-peak amplitudes of the transmission seismograms are evaluated to estimate attenuation variations along the sediment core. P-wave profiles can be used for locating strong as well as fine-scale lithological changes, e.g., turbidite layers or gradual changes in the sand, silt or clay content.

*Electrical Resistivity, Porosity, and Density*

The electrical sediment resistivity $R_s$ was determined using a handhold sensor with a miniaturized four-electrodes-in-line ('Wenner') configuration (electrode spacing: 4 mm). A rectangular alternating current signal is fed to the sediment about 1 cm below the split core surface by the two outer electrodes. Assuming a homogeneously conducting medium, the potential difference at the inner two electrodes will be directly proportional to the sediment resistivity $R_s$. An integrated fast resistance thermometer simultaneously provides data for a temperature correction.

According to the empirical ARCHIE's equation, the ratio of sediment resistivity $R_s$ and pore water resistivity $R_w$ can be approximated by a power function of porosity $\phi$

$$R_s/R_w = k \cdot \phi^{-m}$$

Following a recommendation by Boyce (1968), suitable for sea water saturated clay-rich sediments, values of 1.30 and 1.45 were used for the constants k and m, respectively. The calculated porosity $\phi$ is subsequently converted to wet bulk density $\rho_{wet}$ using the equation (Boyce 1976)

$$\rho_{wet} = \phi \cdot \rho_f + (1 - \phi) \cdot \rho_m$$

with a pore water density $\rho_f$ of 1030 kg/m$^3$ and a matrix density $\rho_m$ of 2670 kg/m$^3$. For the sake of an unbiased uniform treatment of all cores, these empirical coefficients were not adapted to individual sediment lithologies at this stage. Nevertheless, at least relative density changes should be well documented.

*Magnetic Volume Susceptibility*

The magnetic volume susceptibility $\kappa$ is defined by the equations

$$B = \mu_0 \cdot \mu_r \cdot H = \mu_0 \cdot (1 + \kappa) \cdot H = \mu_0 \cdot H + \mu_0 \cdot \kappa \cdot H = B_0 + M$$

with the magnetic induction B, the absolute and relative permeabilities $\mu_0$ and $\mu_r$, the magnetizing field H, the magnetic volume susceptibility $\kappa$ and the volume magnetization M. As can be seen from the third term, $\kappa$ is a dimensionless physical quantity. It records the amount to which a material is magnetized by an external magnetic field.

For marine sediments the magnetic susceptibility may vary from an absolute minimum value of around $-15 \cdot 10^{-6}$ (diamagnetic minerals such as pure carbonate or silicate) to a maximum of some $10.000 \cdot 10^{-6}$ for basaltic debris rich in (titano-) magnetite. In most cases $\kappa$ is primarily determined by the concentration of ferrimagnetic minerals, while paramagnetic matrix components such as clays are of minor importance. High magnetic susceptibilities indicate high concentrations of lithogenic compounds / high iron (bio-)mineraliztion or low carbonate / opal productivity and vice versa. This relation may serve for the mutual correlation of sedimentary sequences which were deposited under similar global or regional conditions.

The measuring equipment consists of a commercial BARTINGTON M.S.2 susceptibility meter with a 125 mm loop sensor and a non-magnetic core conveyor system. Due to the sensor's size, its sensitivity extends over a core interval of about 8 cm. Consequently, sharp susceptibility changes in the sediment column will appear smoothed in the $\kappa$ core log and, e.g., thin layers such as ashes cannot appropriately be resolved by whole-core susceptibility measurement.

### 4.6.2 Shipboard Results

*Sampling Sites and Recovery*

The gravity coring program of Cruise M 41/3 concentrated primarily on two transects across the mid-Atlantic Ridge. One from the Brazil Basin into the Angola Basin at 24°S (about 16 to 12°W), including cores GeoB 5112-4, 5115-1, 5116-2, 5117-1, 5120-2, 5121-1 covering water depths between 2550 and 3844 m. A reversed profile from the Angola Basin into the Brazil Basin at 19°S (about 9 to 17°W) comprises of cores from water depths between 3227 and 4165 m (GeoB 5130-2, 5131-1, 5132-1/3, 5133-1, 5134-2, 5135-2/3, 5136-1, 5137-2, 5138-1, 5139-2, 5140-1/2, 5142-1). Some of the sites had to be sampled twice due to the difficult morphological and lithological environment of the Mid-Atlantic Ridge area. One gravity core was recovered at the northwestern extension of the Vema Channel (26°S / 36°W) at a water depth of 4188 m (GeoB 5110-4).

The recovery varied between 30 (core GeoB 5135-3) and 961 cm (core GeoB 5110-4). A total of 22 sediment cores with a cumulative length of 84 m was investigated (see upper part of Figure 58). Additionally electric resistivity measurements of seven cores from cruise M 41/1 (GeoB 4903-4, 4910-2, 4913-6, 4915-4, 4916-2, 4917-8, 4918-5) and two more cores from cruise M 41/2 (GeoB 5007-2 and 5008-2), which were opened during M 41/3, were performed. The results of these cores are presented in the cruise reports of M 41/1 and M 41/2, respectively.

*General Results*

The general characteristics of the physical properties are compiled in the lower part of Figure 58. Dots mark the mean values of compressional wave velocity, density and magnetic susceptibility for the individual cores, vertical bars denote their standard deviations. Each diagram is divided into three sections according to the three working areas, separating data sets from the Vema Channel, the 24°S and the 19°S profile through the Brazil Basin (BB) and the Angola Basin (AB).

The average p-wave velocities range from 1477 to 1552 m/s. The data of the 24°S profile show increasing velocities with decreasing water depth, which might be due to stronger water currents at the top of the mid-Atlantic Ridge resulting in a winnowing of finer particles. Another possible explanation is a different conservation status of foraminifera shells, which

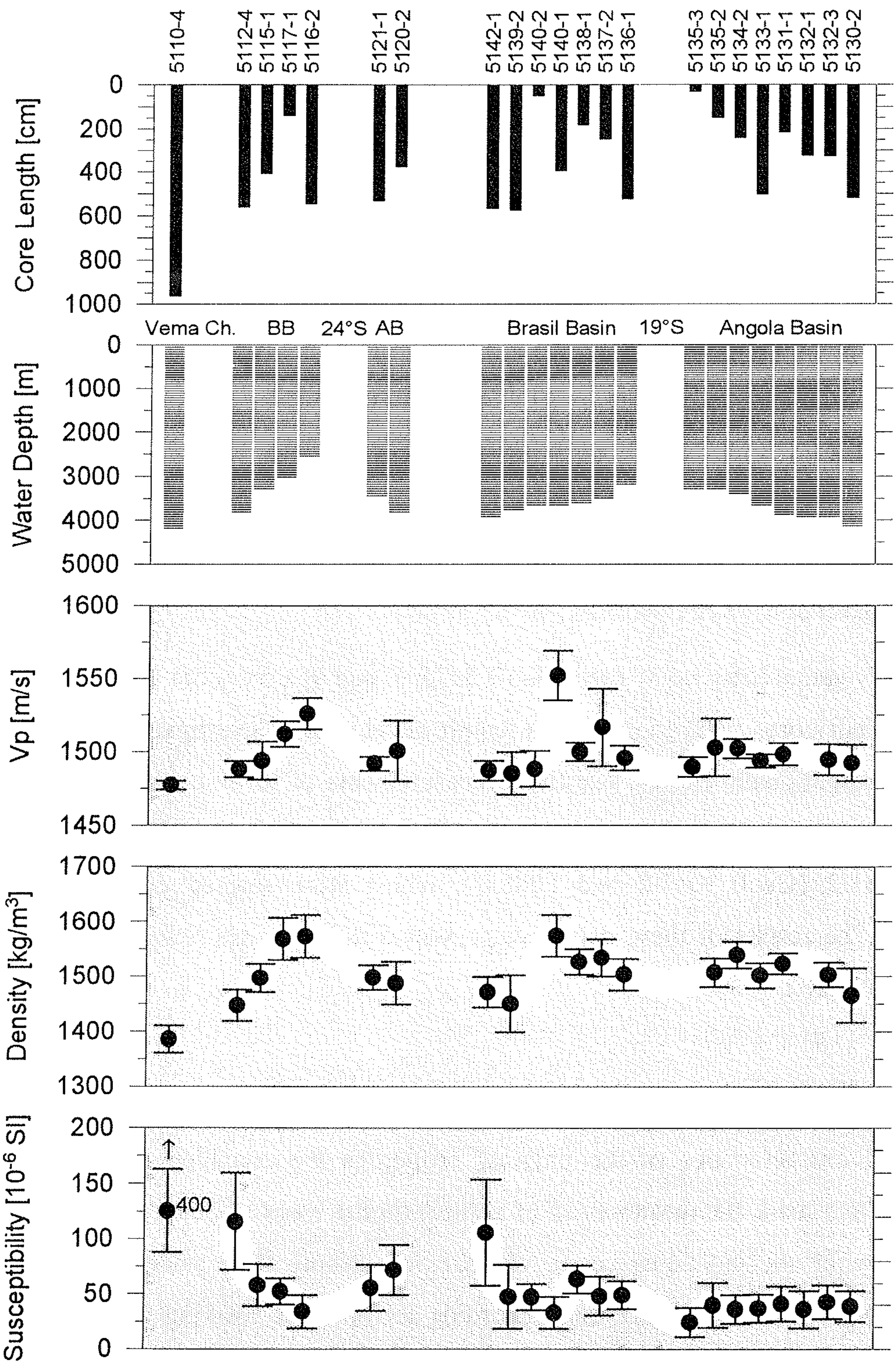


Fig. 58 Mean compressional wave velocities, densities and magnetic susceptibilities of cores GeoB 5110-4 through 5142-1 as compared with variations in water depth at the sampling sites and core recovery. The vertical bars denote standard deviations. Data sets are classified according to the three working areas, the Vema Channel, the 24°S profile from the Brazil Basin (BB) into the Angola Basin (AB) and the reversed profile at 19°S

might be more dissolved in deeper water leading to smaller particle sizes and therefore lower p-wave velocities. $V_p$ values of cores from the 19°S transect exhibit no well developed trends in relation to water depth. The high velocities of core GeoB 5140-1, the highest values of all cores, are quite remarkable. Core GeoB 5110-4, from the Vema Channel, shows the lowest velocity data, reflecting the quite different depositional regime at this site.

Overall, average densities (1385 to 1574 $kg/m^3$) parallel the results of p-wave velocity measurements of increasing density with decreasing water depth for the 24°S profile. The data of the 9°S profile shows only weak variations with no consistent relationship to water depth.

As for p-wave velocity, the lowest mean density (1385 $kg/m^3$) was found for the sediments from the Vema Channel (GeoB 5110-4).

Mean susceptibilities vary from 24 to $116 \cdot 10^{-6}$ SI for the entire core collection, except for core GeoB 5110-4 (Vema Channel) which mean value is three times higher ($313 \cdot 10^{-6}$ SI). In the case of the 24°S profile, it decreases with decreasing water depth. The lower concentration of magnetominerals on bathymetric highs may support the suggestion of winnowing of finer grain sizes by enforced water currents, considering the fact that magnetic minerals are constituents of the finest grain size fraction. The mean susceptibilities of the cores from the 19°S transect through the Brazil Basin show no uniform weak variations whereas mean susceptibilities of cores from the Angola Basin are almost of the same value regardless of water depth.

Physical property logs for the individual cores are shown in Figs. 35 to 56 together with the visual core descriptions.

*Special Features*

*Vema Channel (Core GeoB 5110-4)*

This core, consisting mainly of clay bearing nannofossil ooze, differs from all the other cores in all of its physical properties, reflecting a totally different depositional environment. These sediments from the northwestern outlet of the Vema Channel bear distinctly higher concentrations of fine-grained terrigenous material resulting in high magnetic susceptibility (mean $313 \cdot 10^{-6}$ SI), low compressional wave velocities (mean 1477 m/s) and densities (mean 1385 $kg/m^3$). The core base may be of a similar age as cores GeoB 3822-3 and 3823-1 recovered during METEOR cruise M 34/3 according to their susceptibility logs.

*24°S Profile Brazil Basin (Cores GeoB 5112-4, 5115-1, 5116-2, 5117-1)*

Mean susceptibilities range from 34 to $116 \cdot 10^{-6}$ SI, densities from 1447 to 1573 kg/m$^3$, and p-wave velocities from 1488 to 1526 m/s. Susceptibility patterns of cores from water depths below 3000 m can be correlated to a well dated curve of stacked susceptibilities of cores recovered on a transect at about 30°S during METEOR M 34/3 (Schmieder, in prep.) This 'susceptibility stratigraphy' (Schmieder 1996) gives a maximum sediment age of 780 ka for core GeoB 5112-4. Sedimentation rates can be calculated to 0.7 to 1.0 cm/ky for cores GeoB 5112-4, 5115-1, 5117-1. A thin peak of $v_p$ in core GeoB 5112-4 can be attributed to a laminated diatom bearing nannofossil ooze, perhaps the same feature which was found during METEOR cruise M34/3 in cores GeoB 3801-6 and 3813-3. High $v_p$-values in core GeoB 5115-1 at 175 to 181 cm and 35 to 275 cm are correlated to turbidites.

*24°S Profile Angola Basin (Cores GeoB 5120-2, 5121-1)*

Sediments from the Angola Basin at 24°S consisting mainly of foram bearing nannofossil ooze show cyclic variations in their magnetic susceptibility (mean values 56 to $72 \cdot 10^{-6}$ SI). Mean densities range from 1488 to 1498 kg/m$^3$, p-wave velocities from 1492 to 1500 m/s. Peak values of compressional wave velocities in core GeoB 5120-2 in depths of 65 to 83, 134 to 155, and 309 to 348 cm correlate with turbidites and laminated sequences, respectively. The quite obvious correlation of the magnetic susceptibility pattern of core GeoB 5121-1 to the stacked susceptibility of 30°S cores (Schmieder, 1996) results in a core base age of around 750 ky and a corresponding sedimentation rate of 0.7 cm/ky.

*19°S Profile Brazil Basin (Cores GeoB 5136-1, 5137-2, 5138-1, 5139-2, 5140-1, 5142-1)*

Sediments from the Brazil Basin at 24°S yield p-wave velocities of 1485 to 1552 m/s, densities of 1450 to 1574 kg/m$^3$ and magnetic susceptibilities of 33 to $105 \cdot 10^{-6}$ SI. It is remarkable that $v_p$ and density on the one hand and magnetic susceptibility on the other correlate negatively in cores GeoB 5136-1, 5139-2, and 5142-1, but positively in cores GeoB 5137-2, 5138-1, and 5140-1. The last three cores were recovered from intermediate water depths of around 3500 to 3700 m, whereas the first three originate from a more shallow water depth (GeoB 5136-1, 3227 m) as well as from deeper water depths of about 3900 m. The most prominent feature in core GeoB 5139-2 is a 80 cm thick turbidite from 220 to 319 cm. A thin turbidite also occurs in core GeoB 5136-1 at 250 to 260 cm depth. Core GeoB 5142-1 exhibits cyclic variations in all three physical parameters without any turbidites. According to the 'susceptibility stratigraphy' mentioned before, which can be applied to all cores except core GeoB 5139-2 whose magnetic susceptibility shows no characteristic variations in the upper three meters, sedimentation rates can be calculated to values of 0.7 (GeoB 5137-2) to 1.0 cm/ky (GeoB 5140-2). The oldest sediments with an age of about 690 ka were recovered in core GeoB 5142-1 which shows a well developed cyclic susceptibility signal.

*19°S Profile Angola Basin (Cores GeoB 5130-2, 5131-1, 5132-3, 5133-1, 5134-2, 5135-2)*

Mean densities of 1502 to 1538 kg/m$^3$, compressional wave velocities of 1492 to 1503 m/s and magnetic susceptibilities of 24 to $43 \cdot 10^{-6}$ SI were found for sediments from the Angola Basin at 19°S. High p-wave velocities and densities of core GeoB 5130-2 at 31 to 41 cm and 217 to 248 cm are correlated with a turbidite and a laminated silty-sandy foram bearing nannofossil ooze. Variations in the magnetic susceptibility of the upper two meters are very weak, whereas the lower sediment sequences show clearly developed cyclic patterns. These cyclic variations can be found throughout the whole sediment column of core GeoB 5132-3. Peaks of magnetic susceptibility are correlated with minima in p-wave velocity and density. Using the technique of 'susceptibility stratigraphy', the oldest sediments with an age of 630 ka were recovered in core GeoB 5133-2. Mean sedimentation rates of 0.5 (GeoB 5132-3) to 0.9 cm/ky (GeoB 5134-2) can be calculated by this method.

## 4.7 Underway Geophysics

(B.Laser and Shipboard Scientific Party)

*Introduction*

During METEOR Cruise M 41/3 the shipboard acoustical systems HYDROSWEEP and PARASOUND were used on a 24 hour schedule to record continuous high resolution bathymetric and sediment echosounding profiles. The digitization and storage of the echosounding seismograms were realized using the software package PARADIGMA (Spieß, 1993).

The underway geophysical program along several profiles in the Southern Brazil Basin, Santos Plateau, Rio Grande Rise, Vema Channel, the Mid-Atlantic Ridge and finally the central Brazil Basin is part of the long term research program Sonderforschungsbereich 261, the complete coverage of the South Atlantic Ocean with a net of sampling stations and geophysical profiles. The data recorded along the profiles provided valuable information for finding suitable coring stations from different sedimental environments of the Mid-Atlantic Ridge.

*Recording Parameters and Preliminary Data Processing*

The shipboard sediment echosounder PARASOUND and the multibeam echosounder HYDROSWEEP were operated by the scientific crew during a 24 hour watch. Both systems worked without severe technical problems.

The registration and recording system HYDROMAP ONLINE (STN-Atlas-Elektronik,1994) which was installed on RV METEOR in December, 1996, allowed an increased online control of the swath-data quality by permitting the display of several different survey data sets at one time in a windowed screen layout. Rough sea bottom topography, as found at the Mid-Atlantic Ridge, caused problems to the system. Some profiles in such areas suffer from a poor coverage of the bottom topography. The raw data recording was performed continuously.

The multibeam sounder provides bathymetric data with a swath width of twice the water depth and, in combination with the sediment echosounder PARASOUND, proved to be a very efficient aid for the selection of suitable coring stations. The precise knowledge of the local topography is essential to select suitable sites and to evaluate the impact of morphology, slope angles and sediment instabilities on the continuity of sedimentation.

The sediment echosounding data were routinely registered as analogue paper recordings with the DESO 25 device and at the same time digitally by means of the PARADIGMA 4.02 system (Spieß 1992). The data were stored directly on 6250 bpi, 1/2" magnetic tapes using the standard, industry-compatible SEGY-format.

The seismograms were sampled at 40 kHz with a typical registration length of 266 ms for a depth window of ~200 m. The source signal was a non band limited sinusoidal wavelet of 4 kHz dominant frequency with a duration of 2 periods.

A preprocessed profile plot was produced online with a vertical depth scale of several hundred meters to eliminate most of the changes in window depth. To improve the signal to noise ratio, the seismogram sections were filtered with a steep band-pass filter of 2.5 - 6 kHz. In addition the data were normalized to a constant value much smaller than the maximum average amplitude. In particular, deeper and often weaker reflections could thereby be amplified. These plots provided a first impression of variations in sea floor morphology, sediment coverage and sediment patterns along the ships track.

*Shipboard Results*

During cruise METEOR M 41/3 two profiles of sediment cores were taken across the Mid-Atlantic Ridge at 24° and 19° South. An additional core was taken in the Southern Brazil Basin, north of the Vema Channel. These coring locations were found by the aid of the PARASOUND and HYDROSWEEP systems on this cruise. The PARASOUND data provided information about the the physical state of the sea bottom as well as about sediment structures up to a depth of 50m below the sea floor. The penetration of the PARASOUND signal depends on the density of the uppermost sediment layers and the impedance contrasts between these layers and at the sea floor. Thus, the penetration was used as a first indication of the quality of a coring location.

Due to the limitation of the PARASOUND system to sea bottom slopes less than 6° profiles in ridge areas and fracture zones show a generally lesser quality. At the Mid-Atlantic Ridge signal, typical penetration was not higher than a few meters. However, it was possible to identify sediments in more even areas or in relatively small basins.

The sediments in the western work area, in and north of the Vema Channel, showed the influence of relatively strong currents. In the deep channels, the reflection patterns of PARASOUND indicate almost none, or to a high degree sorted sediments. Mostly, only a strong, elongated sea bottom reflector could be observed. On the Santos Plateau and in the Southern Brazil Basin north of the Vema Channel, sediment waves were found in water depths between ~3700 m and ~4200 m.

The cruise M 41/3 led the ship to extremely different sedimentary environments including ridges and fracture zones, deep sea basins and the strongly current influenced area of the Vema Channel. More than 12 Gbyte of data were recorded during the long steaming times between the work areas and during the search for suitable coring locations. The following examples are intended to give a short overview of the sediment structures which were found. The complete track of RV METEOR cruise 41/3 with indicated sampling locations and PARASOUND profiles shown in this chapter is given in Fig. 59.

### *Vema Channel and Southern Brazil Basin*

Fig. 60 shows an enlarged map of the south-western investigation area where the PARASOUND profiles presented in Figs. 61 through 64 are indicated.

Mud waves are a prominent feature of the current controlled sedimentation around the Rio Grande Rise, Santos Plateau and north of the Vema Channel. The first occurence of mud waves during cruise M 41/3 was on the Santos Plateau between 28°30.1'S / 40°52.7'W and 29°20.3'S / 40°29.7'W. The profile shown in Fig. 61 ranges from 3750 m water depth to 4100 m water depth. The mud waves are symmetrical and vary in length and amplitude along the profile. In the upper part of the profile, the mud waves seem to be superimposed on an also wavy underlying topography. Due to the high speed of the vessel, only the morphology of the mud-wave field is imaged in the PARASOUND record, while its inner structure is not resolved.

Another example of symmetrical mud waves is given in Fig. 62. These mudwaves were observed north of the Vema Channel in ~4200m water depth between 26°36.9'S / 34°22.9'W and 25°40.1'S / 33°54.7'W. The waves are irregular in length and height, they partly superimpose each other and grow together. The irregular geometry of the mud waves may be due to the two-dimensional character of the echosounder record. Only a suitable processing of the HYDROSWEEP data collected along the same track can reveal more information about these mud-wave fields such as the striking direction and lateral extension of the sediment structures.

Another effect of water currents on sediments is erosion and the re-deposition of eroded sediments. The Figs. 63 and 64 show PARASOUND recordings from the northern slope of the Rio Grande Rise and the southernmost Brazil Basin. The first example (Fig. 63) illustrates erosion and/or slumping at the northern slope of the Rio Grande Rise in a water depth of 4250 m to 4350 m. Further to the North-West (Fig. 64), well-layered, but not completely undisturbed sediments were found. The relatively high penetration of the PARASOUND signal indicates soft sediments and possibly high sedimentation rates. Therefore, these sediments may have been transported by deep currents to this location.

### *Mid-Atlantic Ridge*

The sediments found on the Mid-Atlantic Ridge (MAR) area mainly vary with water depth. In greater depth, softer sediments are expected and the signal penetration should be higher.

Between ~20°S and ~25°S the MAR has the smallest longitudinal extension in the South-Atlantic and many transform faults found in this latitude further complicate the sea floor morphology. Thus, most of the the topograhy and sediment structures could not be imaged by the PARASOUND system, which does not receive useful echoes at slope angles of more than 2°. The coring positions at 19°S and 24°S were determined by using both the PARASOUND and HYDROSWEEP information.

*Central Brazil Basin*

The first PARASOUND profile crossing the central Brazil Basin between 15°S and 20°S was recorded during the RV METEOR cruise 41/3. On the larger part of this profile we observed the same reflection pattern consisting of three prominent reflector groups (Figs. 65, 66, 67). Each of the two upper reflector groups are formed by three distinct reflectors which seem to mark discordant layering. This assumption is very speculative, because the reflection patterns within and between these reflector groups is certainly difficult to interpret and seems to change along the profile (Fig. 66). If the pattern is caused by discontinuities in sedimentation it would reflect large scale changes in bottom water circulation in the central deep Brazil Basin. In any case these data reflect some kind of 'events' with influence within the entire central deep Brazil Basin at these latitudes.

The reflection pattern described above was first observed at ~25°30'W (Fig. 65) and can be identified well as far as ~29°40'W. The PARASOUND record along this track is interrupted by several local highs caused by buried ridges parallel to the MAR. Between these highs the reflection pattern can be correlated well. West of ~29°40'W, the sedimentation changes with slowly decreasing water depth. However, structures similar to those in the deep basin can be observed until ~32°30'W, where the sub-bottom image delivered by the PARASOUND system completely changes due to the changing morphology while approaching the South-American continental margin.

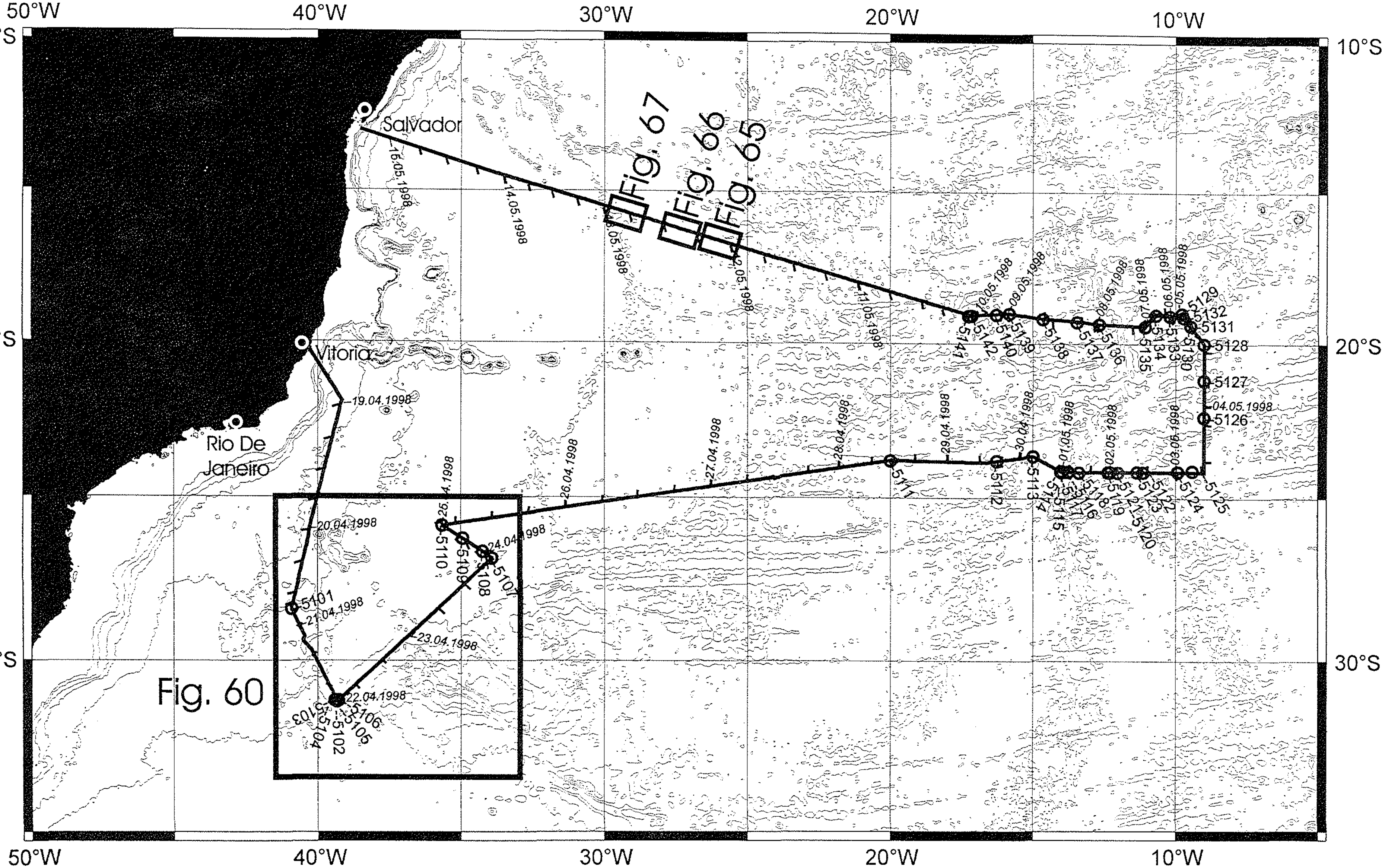


Fig. 59 RV METEOR Cruise M 41/3. Track annotation interval is 6 hours, dates are set at 0 hours. Sampling locations are annotated as well as locations of Figs. 60 and 65 to 67

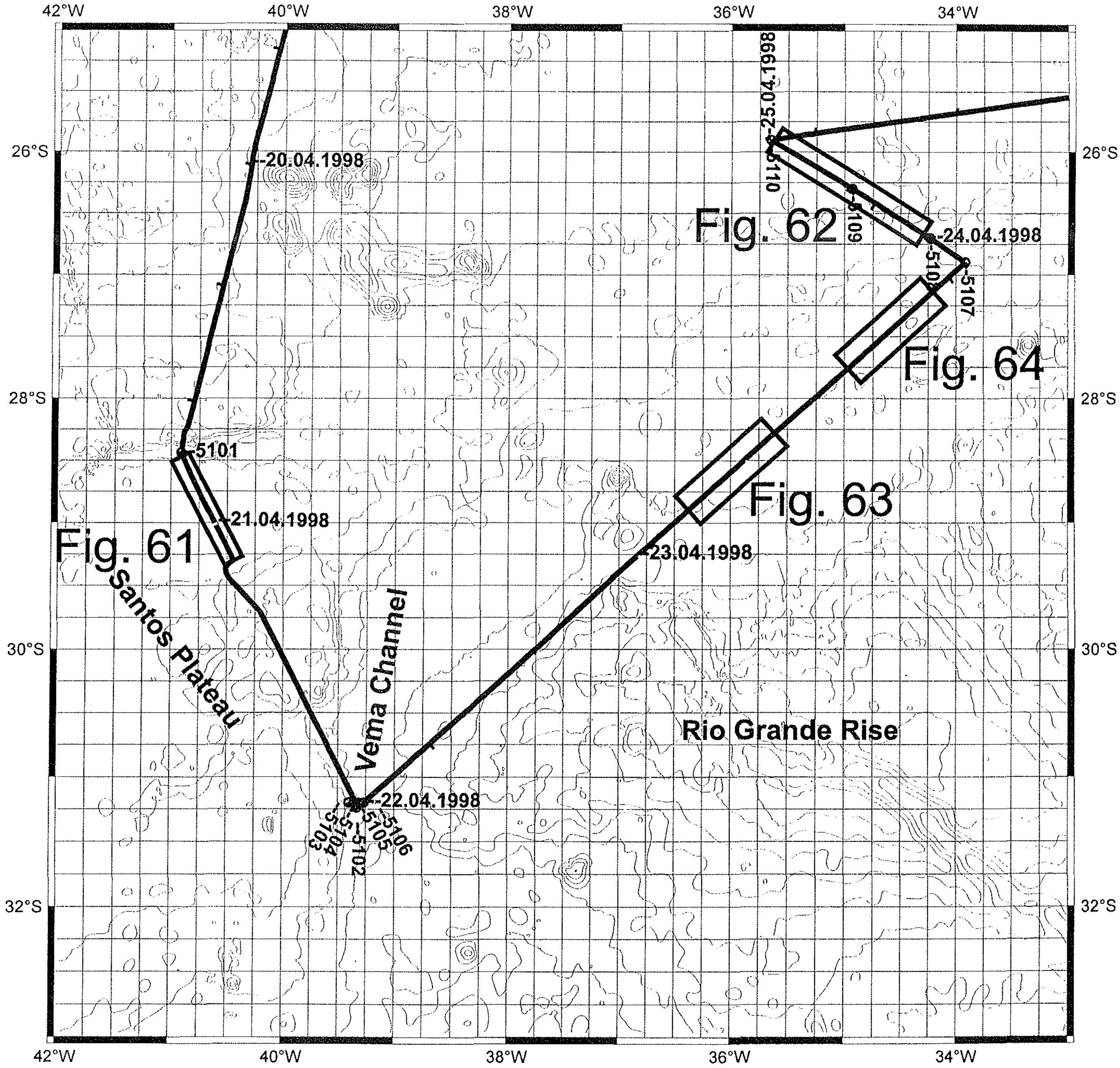


Fig. 60 Track of RV METEOR Cruise M 41/3 in the Vema Channel research area. Sampling locations and PARASOUND profiles shown in Figs. 61 to 64 are annotated

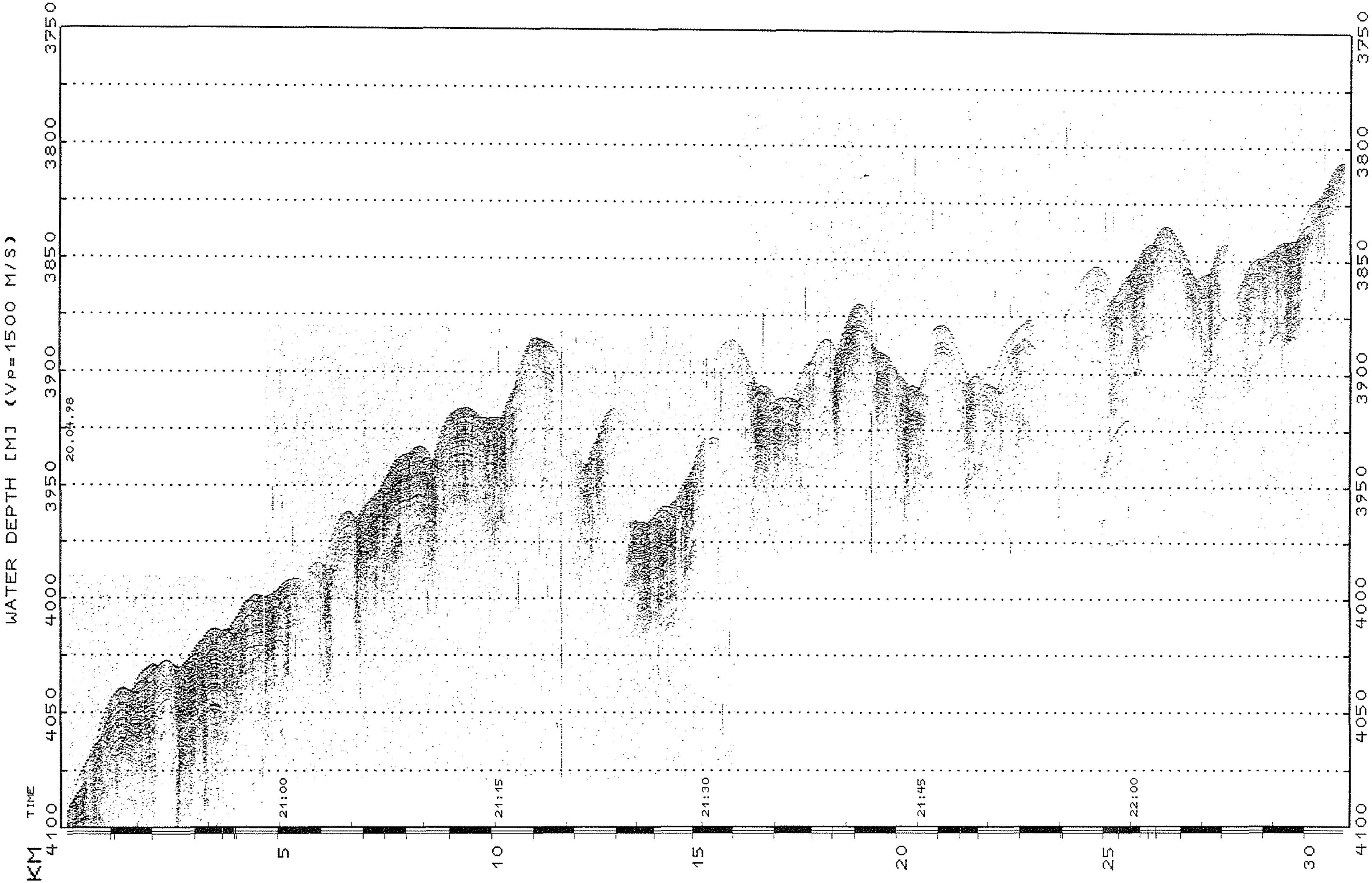


Fig. 61 Digital PARASOUND profile from the Santos Plateau at the western flank of the Vema Channel. The profile shows symmetric but irregularly sized and distributed mud waves.The geometry and character of a suggested mud wave field

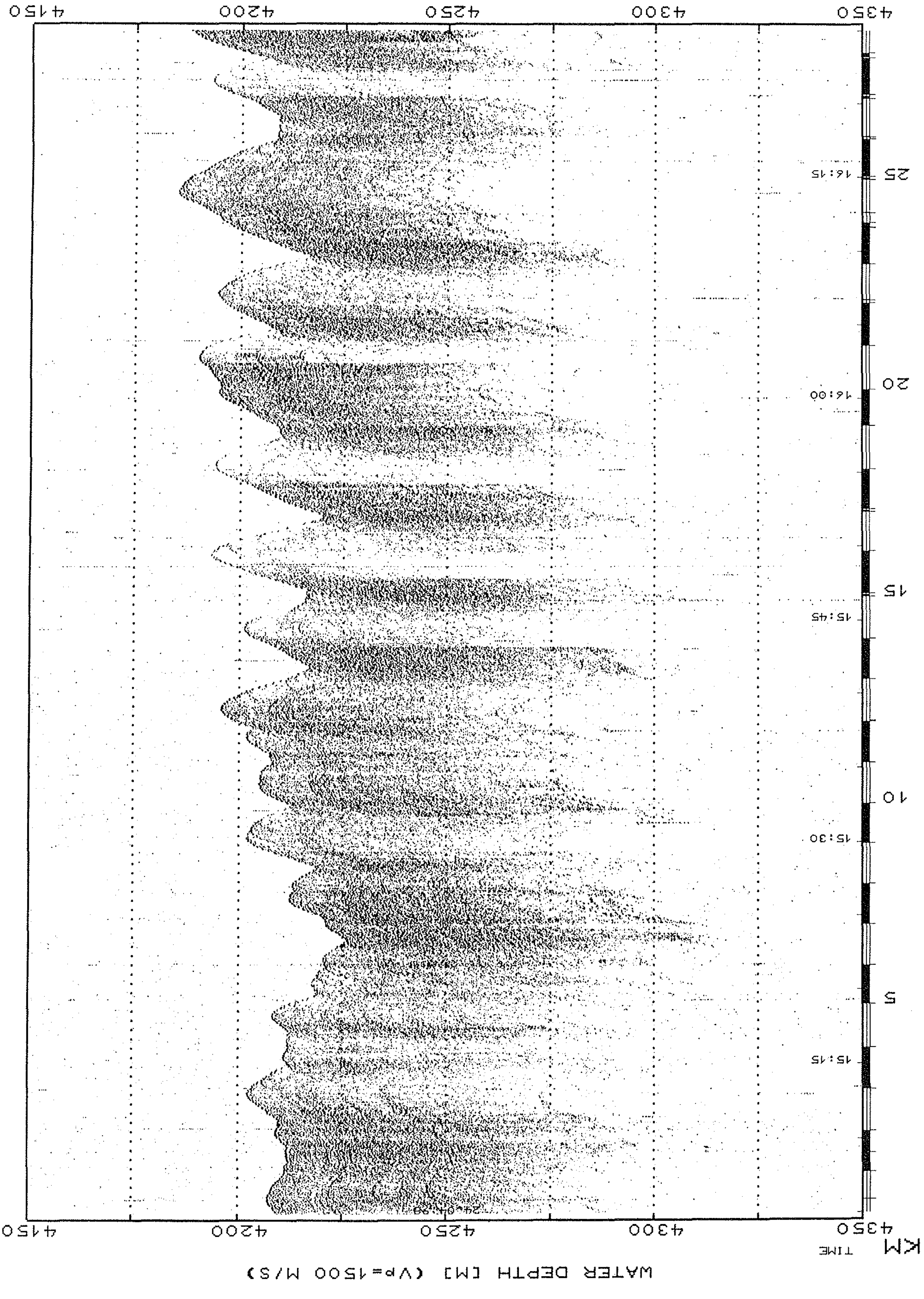


Fig. 62 Digital PARASOUND profile showing mud waves. The profile was recorded on the western slope north of Vema Channel (see Fig. 59)

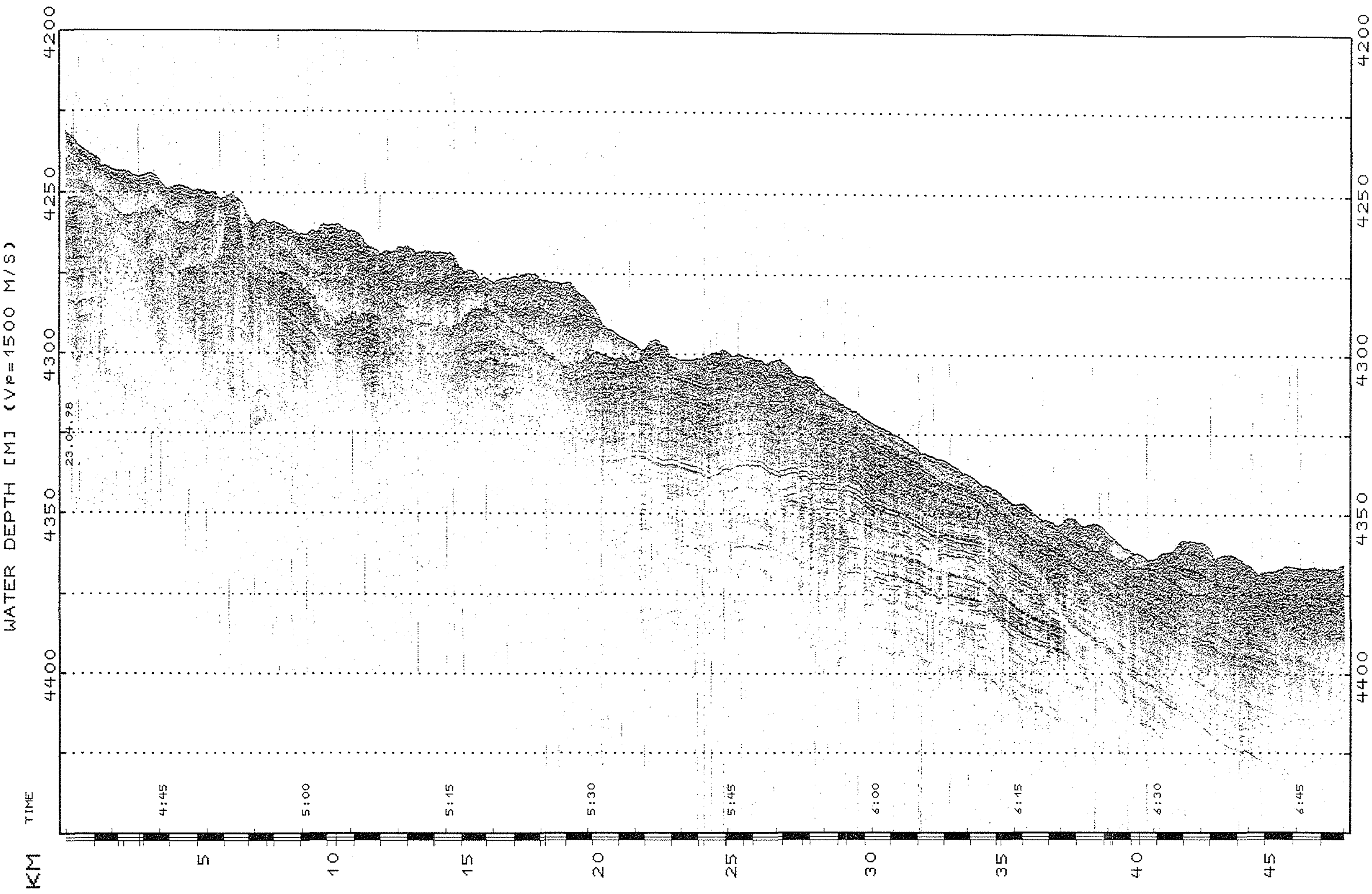


Fig. 63 Digital PARASOUND profile from the northern slope of Rio Grande Rise. Slumps can be observed on top of a layered but erosionally truncated sediment body in the lower part of the profile. The upper part also shows a more complex seismic discordance separating slumps or younger sediments from the underlying sequence

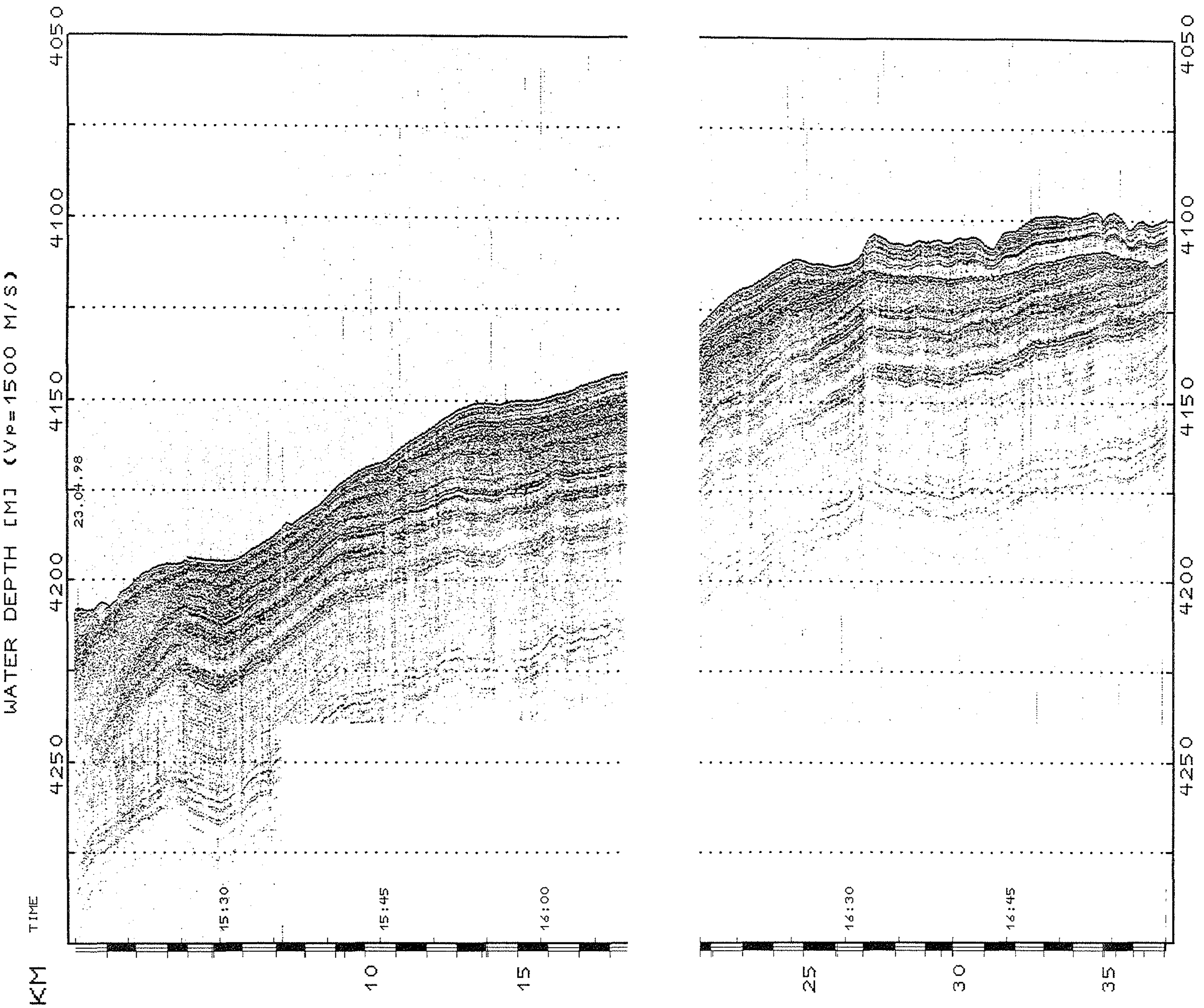


Fig. 64 Digital PARASOUND profile from the southernmost Brazil Basin north of Rio Grande Rise. The deep penetration of the PARASOUND signal and the fine layering suggest soft sediments and relatively high sedimentation rates for the area. The sediments at this location may have been transported by deep currents

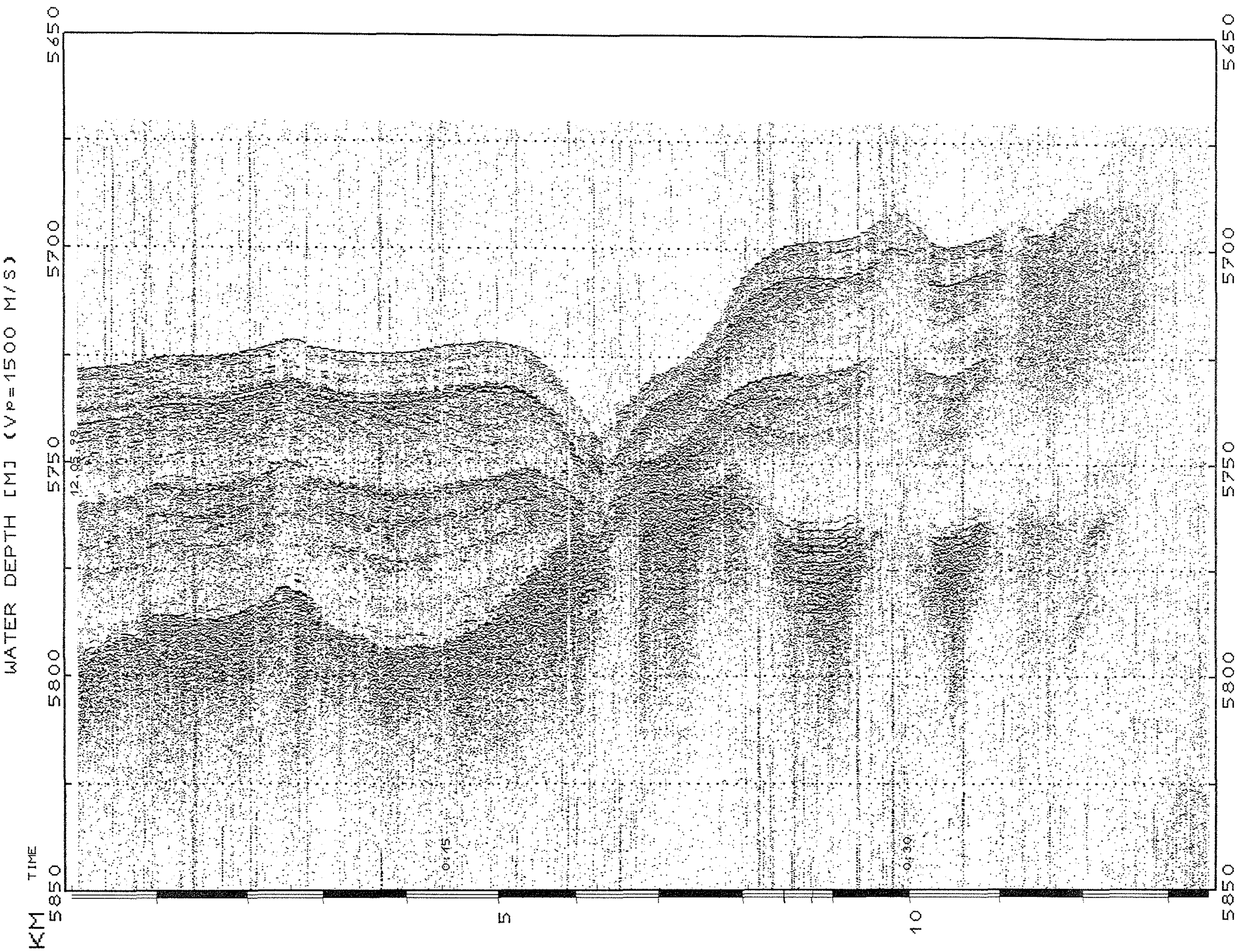


Fig. 65 Digital PARASOUND profile from the deep central Brazil Basin. The profile shows the first recorded occurence of a reflection pattern which could be identified from ~25°W to ~29°W (see text)

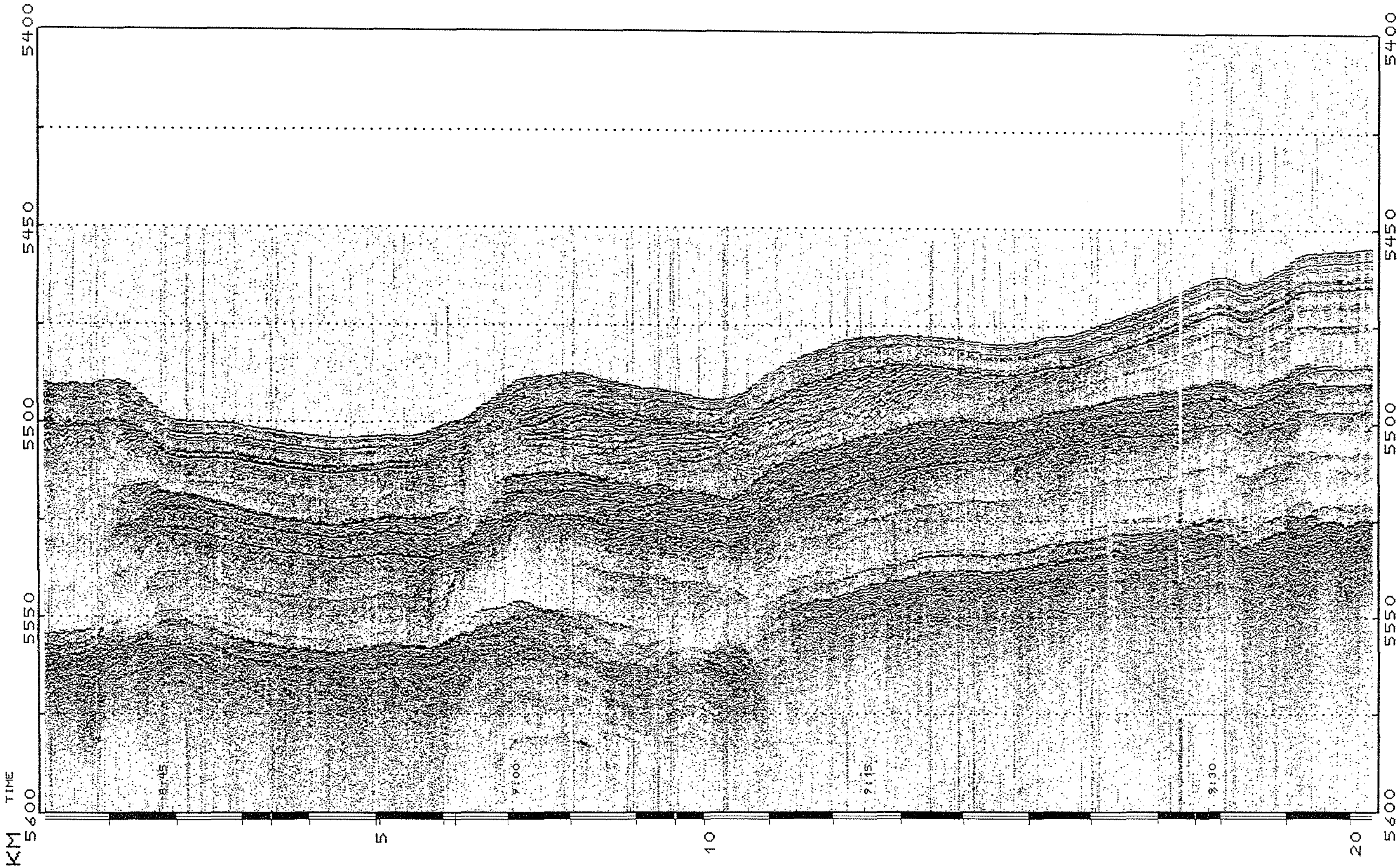


Fig. 66 Digital PARASOUND profile from the deep central Brazil Basin. The profile shows the best resolution of the reflection pattern found throughout the deep part of the basin (see text)

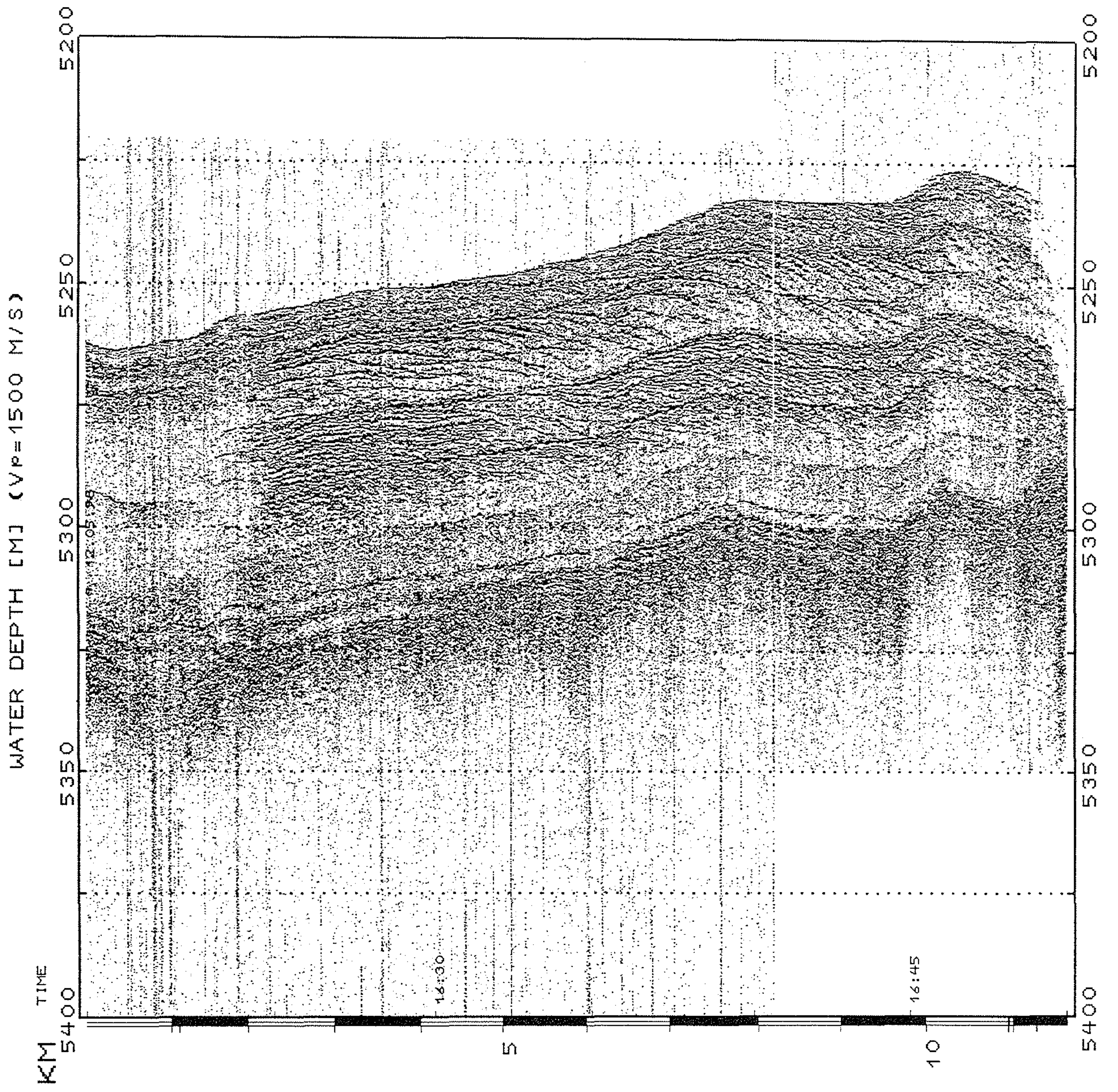


Fig. 67 Digital PARASOUND profile from the deep central Brazil Basin. The profile is located close to the easternmost clear occurence of the typical reflection pattern for this area (see text). In the center of the figure the reflection pattern suggests a seismically discordant layering

## 5 Ship's Meteorological Station

(C. Knaack, D. Bassek)

The 3rd leg of RV METEOR cruise no. 41 began on April 18, 1998 at 08:15 local time in Vitória (Espirito Santo). The ship set out on a southerly course. A northerly wind of force 5, occasionally 6 was blowing, caused by an intense subtropical high lying over the eastern South Atlantic. During the first night, the cold front of a low off the south Brasilian coast crossed our route with thunderstorms and gusts.

On April 20 at noon, the first waypoint near 2°S / 41°W (Vema Channel) was reached. An upper trough brought some intense rain showers with gusts during the morning, later the weather was rather calm. A southwestern swell of about 3 m height did not affect the scientific work considerably. The next day RV METEOR reached the southernmost point of the cruise at 31.3°S / 39.3°W. High pressure influence favoured our research work, which included the deployment of a near bottom mooring. Course was then set northeastwards to the operational area in the northern part of the Vema Channel. The weather pattern during the next days was as follows: an anticyclone between Tristan da Cunha and South Africa connected by a high pressure ridge with another anticyclone over the western part of the ocean causing an easterly flow of approximately force 5. In front of a south Brasilian low which moved eastwards, the wind backed to the north on April 24 and to the northwest on April 25. A cold front caused increasing winds of force 6 to 7 and passed us with heavy rain showers accompanied by gusts. On the rear side of this "lull front" the wind abated.

On April 28 a zonal section across the Mid-Atlantic Ridge began at 24°S / 20°W. The dominant high moved from a southwestern position to the east, causing mostly easterly winds between forces 1 and 5. Now and then, the typical calmness of the horse latitudes was observed. The southerly swell of 1.5 to 2.5 m height temporarily made the navigation during stations difficult, as its direction differed from that of the wind. The high pressure influence lasted during the meridional section at 9°E and also during the final zonal section at 19°S from 9°W to 17°W.

With the help of our radio soundings during this time, the characteristic trade wind inversion was observed. From the surface up to 1200 - 1500 m height the temperature dropped from about 23°C to 11 - 13°C, reaching a maximum relative humidity. In the next layer of only a few hundred meters, the temperature increased up to 17 - 20°C. Above this level, temperature decreased with the tropospheric lapse rate of 0,65 K/100 m. Below the inversion, mostly flat cu clouds were observed, although almost overcast sc layers also appeared. From time to time humidity and instability caused convection with towering cu clouds and some rain showers. On April 29 a water spout occurred.

On May 10, 1998 the scientific work on board was completed. Over the last days of the cruise, rear winds of force 4 - 5 accompanied RV METEOR during the northwesterly route to Salvador (Bahia), where we arrived safely in the morning of May 15, 1998.

## 6 Acknowledgements and Concluding Remarks

The goals of the research program of RV METEOR cruise 41/3 were fully achieved. All measuring systems functioned flawlessly. One mooring was successfully deployed in the central Vema Channel. 42 stations were covered using different equipment 75 times. 22 gravity cores, 21 multicores and 2 box cores were taken, at 25 stations CTD profiles were measured and water samples were taken with both the CTD/rosette and the rosette. In addition, plankton samples taken from the ship's pumps. PARASOUND and HYDROSWEEP recordings were performed during 600 nm between 20.04.1998 09:00 UTC and 14.05.1998 09:00 UTC.

The success of the cruise was made possible by the exemplary performance of the crew. In work at deck and in maneuvering of the ship, the highest competence was displayed. Throughout the cruise there was outstanding teamwork and friendly companionship between the crew and the scientists. For this we sincerely thank Captain M. Kull and the entire crew.

The work was funded by the Deutsche Forschungsgemeinschaft (DFG) within the scope of the Sonderforschungsbereich 261 („The South Atlantic in the Late Quaternary: Reconstruction of material budget and current systems") at Bremen University.

## 7 References

Boebel, O., C. Schmid and W. Zenk (1997) Flow and recirculation of Antarctic Intermediate Water across the Rio Grande Rise. J. Geophys. Res., 102 (C9), 20,967-20,986.

Boyce, R.E. (1968) Electrical resistivity of modern marine sediments from the Bering Sea. J. Geophys. Res. 73: 4759-4766.

Boyce, R.E. (1976) Sound velocity - density parameters of sediment and rock from DSDP Drill Sites 315 - 318 on the Line Islands Chain, Manihiki Plateau, and Tuamotu Ridge in the Pacific Ocean. In: S.O. Schlanger, E.D. Jackson et al., Init. Repts. DSDP 33: 695-728.

Fischer, J. and M. Visbeck (1993) Deep velocity profiling with self-contained ADCPs. J. Atm. Ocean Techn., 10, 764-773.

Haq, B.U. and A. Boersma (1978) Introduction to Marine Micropaleontology. pp. 376, Elsevier, New York - Oxford.

Heimdal, B.R. (1993) Modern Coccolithophorids. In: C.R. JOMAS (ed.) - Marine Phythoplankton - A Guide to Naked Flagellates and Coccolithophorids. pp 180, Academic Press Inc.; San Diego, New York.

Hogg, N. and W. Zenk (1997) Long-period changes in the bottom water flowing through Vema Channel. J. Geophys. Res. 102 (C7) 15,639-15,646.

Hogg, N., G. Siedler and W. Zenk (1998) Circulation and variability at the southern boundary of the Brazil Basin. J. Phys. Oceanogr. (in press)

Hogg, N.G., P. Biscaye, W. Gardner and W.J. Schmitz, jr. (1982) On the transport and modification of Antarctic Bottom Water in the Vema Channel. J. Mar. Res., 40 (suppl.), 231–263.

Hogg, N.G., W. Brechner Owens, G. Siedler and W. Zenk (1996) Circulation in the Deep Brazil Basin. In: Wefer, G., W.H. Berger, G. Siedler and D.J. Webb (Eds.): The South Atlantic: Present and Past Circulation. Springer Verlag, Berlin, Heidelberg, 249-260.

Jungclaus, J.H. and M. Vanicek (1998) Frictionally modified flow in a deep ocean channel: Application to the Vema Channel. J. Geophys. Res. (in press)

Ledbetter, M.T. (1984) Bottom current speed in the Vema Channel during the Late Quaternary based on particle size analyses. Mar. Geol., 58: 137-149.

Ledbetter, M.T. (1986) Bottom-current pathways in the Argentine Basin revealed by mean silt particle size. Nature, 321: 423-425.

McCave, I.N., P.F. Lonsdale, C.D. Hollister and W.D. Gardner (1980) Sediment transport over the Hattan and Gardar contourite drifts. J. Sed. Petrol., 50: 1049-1062.

Mercier, H. and K. Speer (1997) Transport of bottom water in the Romanche Fracture Zone and the Chain Fracture Zone. J. Phys. Oceanogr. (accepted).

Müller; G. and M. Gastner (1971) The "Karbonat-Bombe", a single device for the determination of the carbonate content in sediments, soils and other materials. Neues Jahrb. Min., Monatsh., 10: 466-469.

Reid, J.L., W.D. Nowlin and W.C. Patzert (1977) On the characteristics and circulation in the southwestern Atlantic Ocean. J. Phys. Oceanogr., 7, 62–91.

Schmieder, F. (1996) Susceptibility Stratigraphy. In: G. Wefer et al., M 16/1. Berichte, Fachbereich Geowissenschaften, Universität Bremen 79: 139-143.

Schmieder, F., T. v. Dobeneck and U. Bleil (1998) Cycles, trends and events of Quaternary sedimentation in the oligotrophic subtropical South Atlantic Ocean derived from high-resolution magnetic chronostratigraphies (submitted).

Schultheiss, P.J. and S.D. McPhail (1989) An automated p-wave logger for recording fine-scale compressional wave velocity structures in sediments. In: W. Ruddiman, M. Sarnthein et al., Proc. ODP, Sci. Results 108: 407-413.

Schulz, H.D. et al. (1991) Bericht und erste Ergebnisse der METEOR-Fahrt M16/2. Berichte, Fachbereich Geowissenschaften, Universität Bremen 19: 149 p.

Siedler, G. and W. Zenk (1992) WOCE Südatlantik 1991, Reise Nr. 15, 30. Dezember 1990 - 23. März 1991. METEOR-Berichte, Univeristät Hamburg, 92-1, 126 S.

Siedler, G., T.J. Müller, R. Onken, M. Arhan, H. Mercier, B.A. King and P.M. Saunders (1996) The zonal WOCE sections in the South Atlantic. In: Wefer, G., W.H. Berger, G. Siedler and D.J. Webb (Eds.): The South Atlantic: Present and Past Circulation. Springer Verlag, Berlin, Heidelberg, 83-104.

Smith, W.H.F. and D.T. Sandwell (1997) Global sea floor topography from satellite altimetry and ship depth soundings. Science, 277, 1956-1962.

Speer, K.G. and W. Zenk (1993) The flow of Antarctic Bottom Water into the Brazil Basin. J. Phys. Oceanogr. 23, 2667-2682.

Speer, K.G., G. Siedler and L. Talley (1995) The Namib Col Current. Deep-Sea Res. I, 42 (11/12), 1933-1950.

Spiess, V. (1993) Digitale Sedimentechographie - Neue Wege zu einer hochauflösenden Akustostratigraphie, Berichte, Fachbereich Geowissenschaften, Universität Bremen, Nr. 35, Bremen, 1993

Wefer, G. et al. (1991) Bericht und erste Ergebnisse über die METEOR-Fahrt M 16/1. Berichte, Fachbereich Geowissenschaften, Universität Bremen 18: 120 p.

Zangenberg, N. and G. Siedler (1998) Path of the North Atlantic Deep Water in the Brazil Basin. J. Geophys. Res., 103 (C3), 5419-5428.

Zenk, W. and N.G. Hogg (1996) Warming trend in Antarctic Bottom Water flowing into the Brazil Basin. Deep-Sea Res. I, 43 (9), 1461-1473.

Zenk, W., G. Siedler, B. Lenz and N.G. Hogg (1998) Antarctic Bottom Water Flow through the Hunter Channel. J. Phys. Oceanogr. (submitted).

Zenk, W., K.G. Speer and N.G. Hogg (1993) Bathymetry at the Vema Sill. Deep-Sea Res., 40 (9), 1925-1933.

# 8 Station List and Standard CTD Data

## 8.1 Station List

Table 18 Station list of RV METEOR Cruise M 41/3

| Meteor No. 1998 | GeoB No. | Date 1998 | Equipment | Time Seafloor (UTC) | Position Latitude | Longitude | Water Depth (m) | Samples/ Sediment recovery (cm) | Remarks |
|---|---|---|---|---|---|---|---|---|---|
| **Lower Santos Plateau, Rio Grande Fracture Zone** | | | | | | | | | |
| 208 | 5101-1 | 20.04. | CTD/Ro | 18:06 | 28°26.3´S | 40°54.7´W | 4388 | 21x10 l | CTD station for calibration, water samples from 4421, 4300, 4000, 3500, 3000, 2500, 2000, 1500, 1250, 1000, 750, 500, 300, 200, 150, 125, 100, 70, 50, 25, 10 dbar ($\delta^{13}C$, $\delta^{18}O$, $PO_4$) |
| | 5101-2 | | Ro II | 20:01 | 28°26.5´S | 40°54.7´W | 4387 | 18x10 l | Station for calibration |
| **Central Vema Channel** | | | | | | | | | |
| 209 | 5102-1 | 21.04. | Mooring | 16:58 | 31°14.3´S | 39°20.0´W | 4602 | | Mooring No. V389-01 put out |
| 210 | 5103-1 | | CTD/Ro | 19:10 | 31°12.1´S | 39°23.7´W | 4614 | 21x10 l | CTD station, water samples from 4659, 4610, 4500, 4250, 4000, 3750, 3500, 3250, 3000, 2600, 2300, 2000, 1500, 1000, 750,500, 300, 200, 100, 2x10 dbar ($\delta^{13}C$, $\delta^{18}O$, $PO_4$, He, $^3H$, CFC) |
| | 5103-2 | | Ro II | 20:53 | 31°12.1´S | 39°27.7´W | 4612 | 18x10 l | Water samples from 200, 150, 4x100, 4x50, 4x20, 4x10 m depth ($\delta^{13}C$, $\delta^{18}O$, $PO_4$, dino-flagellates, coccolithophorids) |
| 211 | 5104-1 | | CTD/Ro | 23:26 | 31°12.1´S | 39°21.0´W | 4571 | | CTD station, tracer oceano-graphy (samples for He, CFC) |
| 212 | 5105-1 | 22.04. | CTD/Ro | 03:12 | 31°12.0´S | 39°19.1´W | 4487 | 21x10 l | CTD station, water samples from 4520, 4500, 4400, 4300, 4150, 4000, 3750, 3500, 3250, 3000, 2600, 2300, 2000, 1500, 1000, 750, 500, 300, 200, 50, 10 dbar ($\delta^{13}C$, $\delta^{18}O$, $PO_4$, He, $^3H$, CFC) |
| 213 | 5106-1 | | CTD/Ro | 07:15 | 31°12.0´S | 39°16.0´W | 4066 | | CTD station, tracer oceano-graphy (samples for He, CFC) |
| **Northwestern Vema Channel** | | | | | | | | | |
| 214 | 5107-1 | 23.04. | CTD/Ro | 20:33 | 26°54.0´S | 33°55.0´W | 3786 | | CTD station, tracer oceano-graphy (samples for He, CFC) |
| 215 | 5108-1 | 24.04. | CTD/Ro | 01:30 | 26°42.0´S | 34°14.0´W | 4784 | 21x10 l | CTD station, water samples from 4853, 4800, 4499, 4250, 3999, 3751, 3500, 3250, 3000, 2601, 2300, 2000, 1500, 1001, 749, 500, 300, 200, 100, 2x10, dbar ($\delta^{13}C$, $\delta^{18}O$, $PO_4$, He, $^3H$, CFC) |

Table 18 continued

| Meteor No. 1998 | GeoB No. | Date 1998 | Equipment | Time Seafloor (UTC) | Position Latitude | Longitude | Water Depth (m) | Samples/ Sediment recovery (cm) | Remarks |
|---|---|---|---|---|---|---|---|---|---|
| 216 | 5109-1 | 24.04. | CTD/Ro | 08:30 | 26°18.0´S | 34°56.2´W | 4353 | | CTD station, tracer oceanography (samples for He, $^3$H, CFC) |
| | 5109-2 | | MUC I | 11:25 | 26°18.0´S | 34°56.5´W | 4353 | -- | did not close, no core recovery |
| 217 | 5110-1 | | CTD/Ro | 18:05 | 25°54.1´S | 35°39.0´W | 4190 | | CTD station, tracer oceanography (samples for He, $^3$H, CFC) |
| | 5110-2 | | Ro II | 19:41 | 25°53.9´S | 35°39.0´W | 4203 | 18x10 l | Water samples from 200, 150 4x100, 4x50, 4x20, 4x10 m depth ($\delta^{13}$C, $\delta^{18}$O, $PO_4$, dinoflagellates, coccolithophorids) |
| 217 | 5110-3 | 24.04. | MUC I | 21:28 | 25°54.3´S | 35°38.4´W | 4184 | 16 | Did not close all tubes, 3 big tubes filled: nannofossil ooze, dark brown |
| | 5110-4 | | SL12 | 23:55 | 25°54.3´S | 35°38.4´W | 4188 | 961 | cc: Clay, greenish grey |
| | 5110-5 | 25.05. | GKG | 02:43 | 25°54.3´S | 35°38.4´W | 4182 | 46 | Nannofossil ooze, dark brown |
| **Mid-Atlantic Ridge, Profile 24°S, Brazil Basin** | | | | | | | | | |
| 218 | 5111-1 | 28.04. | CTD/Ro | 11:54 | 23°48.9´S | 19°59.8´W | 5215 | 21x10 l | CTD station, water samples from 5285, 5202, 5000, 4750, 4502, 4252, 4002, 3602, 3002, 2602, 2302, 2001, 1501, 1001, 750, 503, 301, 201, 50, 11 dbar ($\delta^{13}$C, $\delta^{18}$O, $PO_4$, He, $^3$H, CFC) |
| 219 | 5112-1 | 29.04. | CTD/Ro | 11:22 | 23°49.6´S | 16°16.3´W | 3881 | 21x10 l | CTD station, water samples from 3890, 3750, 3600, 3400, 3200, 3000, 2750, 2500, 2250, 2000, 1600, 1300, 1000, 800, 600, 500, 300, 200, 100, 50, 10 dbar ($\delta^{13}$C, $\delta^{18}$O, $PO_4$, He, $^3$H, CFC) |
| | 5112-2 | | Ro II | 12:52 | 23°49.6´S | 16°16.3´W | 3879 | 17x10 l | Water samples from 200, 2x150, 3x120, 3x100, 3x50, 3x20, 3x10 m depth ($\delta^{13}$C, $\delta^{18}$O, $PO_4$, dinoflagellates, coccolithophorids) |
| | 5112-3 | | MUC I | 14:28 | 23°49.6´S | 16°15.6´W | 3844 | -- | No recovery |
| | 5112-4 | | SL6 | 16:32 | 23°49.5´S | 16°15.5´W | 3842 | 559 | 38 cm sediment recovered from the bomb, cc: foram bearing nannofossil ooze, silty, light brown |
| | 5112-5 | | GKG | 18:50 | 23°49.5´S | 16°15.5´W | 3841 | 27 | foram-nannofossil ooze, light yellowish brown |
| 220 | 5113-1 | 30.04. | CTD/Ro | 04:13 | 23°40.3´S | 15°00.0´W | 3855 | 21x10 l | CTD station, water samples from 3880, 3800, 3600, 3400, 3200, 3000, 2750, 2500, 2250, 2000, 1600, 1300, 1000, 800, 600, 500, 300, 200, 100, 50, 10 dbar ($\delta^{13}$C, $\delta^{18}$O, $PO_4$, He, CFC) |
| 221 | 5114-1 | 30.04. | CTD/Ro | 12:49 | 24°10.0´S | 13°59.7´W | 3182 | 21x10 l | CTD station, water samples from 3200, 3100, 3000, 2750, 2500, 2250, 2000, 1750, 1500, 1250, 1000, 800, 700, 600, 500, 400, 300, 200, 100, 50, 10 dbar ($\delta^{13}$C, $\delta^{18}$O, $PO_4$, He, CFC) |

Table 18 continued

| Meteor No. 1998 | GeoB No. | Date 1998 | Equipment | Time Seafloor (UTC) | Position Latitude | Longitude | Water Depth (m) | Samples/ Sediment recovery (cm) | Remarks |
|---|---|---|---|---|---|---|---|---|---|
| 222 | 5115-1 | 30.04. | SL12 | 15:19 | 24°08.6'S | 14°02.6'W | 3291 | 406 | cc: Foram bearing nannofossil ooze, silty, light reddish brown |
| | 5115-2 | | MUC II | 17:24 | 24°08.6'S | 14°02.6'W | 3291 | 25 | 6 big, 4 small tubes filled, foram-nannofossil ooze, light yellowish brown - brownish yellow |
| 223 | 5116-1 | | MUC II | 21:38 | 24°09.6'S | 13°46.2'W | 2556 | 28 | 6 big, 4 small tubes filled, foram-nannofossil ooze with pteropods, light yellowish brown - pale yellow |
| | 5116-2 | | SL9 | 23:13 | 24°09.5'S | 13°46.2'W | 2550 | 540 | cc: Foram bearing nannofossil ooze, sandy-silty, very pale brown |
| 224 | 5117-1 | 01.05. | SL9 | 02:11 | 24°08.9'S | 13°58.4'W | 3040 | 139 | Tube bent, cc: Foram bearing nannofossil ooze, clayey-silty, pale yellow |
| | 5117-2 | | MUC II | 04:07 | 24°08.8'S | 13°58.4'W | 3039 | 15 | 6 big, 4 small tubes filled, foram bearing nannofossil ooze |
| 225 | 5118-1 | | CTD/Ro | 09:12 | 24°10.8'S | 13°23.0'W | 2734 | 20x10 l | CTD station, water samples from 2780, 2730, 2500, 2250, 2000, 1750, 1500, 1250, 2x1000, 900, 800, 700, 600, 400, 300, 200, 100, 50, 10 dbar ($\delta^{13}C$, $\delta^{18}O$, $PO_4$, He, $^3H$, CFC) |
| **<u>Mid-Atlantic Ridge, Profile 24°S, Angola Basin</u>** | | | | | | | | | |
| 226 | 5119-1 | 01.05. | CTD/Ro | 17:14 | 24°10.0'S | 12°18.0'W | 3865 | 21x10 l | CTD station, water samples from 4000, 3900, 3600, 3400, 3200, 3000, 2750, 2500, 2250, 2000, 1600, 1300, 1000, 800, 600, 500, 300, 200, 100, 50, 10 dbar ($\delta^{13}C$, $\delta^{18}O$, $PO_4$, He, CFC) |
| | 5119-2 | | Ro II | 17:39 | 24°10.0'S | 12°17.9'W | 3732 | 18x10 l | Water saples from 200, 150, 4x100, 4x50, 4x20, 4x10 m depth ($\delta^{13}C$, $\delta^{18}O$, $PO_4$, dino-flagellates, coccolithophorids) |
| 227 | 5120-1 | | MUC II | 20:30 | 24°10.2'S | 12°21.8'W | 3844 | 21 | 6 big, 4 small tubes filled, foram-nannofossil ooze, light yellowish brown |
| | 5120-2 | | SL6 | 22:45 | 24°10.2'S | 12°21.8'W | 3844 | 376 | cc: foram bearing nannofossil ooze, silty, light yellowish brown |
| 228 | 5121-1 | 02.05. | SL6 | 03:03 | 24°11.0'S | 12°01.3'W | 3488 | 531 | cc: foram bearing nannofossil ooze, silty-sandy, very pale brown |
| | 5121-2 | | MUC II | 05:02 | 24°11.0'S | 12°01.3'W | 3486 | 19 | 6 big, 4 small tubes filled, foram-nannofossil ooze, light yellowish brown |
| 229 | 5122-1 | | CTD/Ro | 12:16 | 24°10.2'S | 11°08.1'W | 3741 | 20x10 l | CTD station, water samples from 3750, 3700, 3400, 3200, 3000, 2750, 2500, 2250, 2000, 1600, 1300, 1000, 2x750, 500, 300, 200, 100, 50, 10 dbar ($\delta^{13}C$, $\delta^{18}O$, $PO_4$, He, CFC) |
| 230 | 5123-1 | 02.05. | MUC II | 15:37 | 24°09.9'S | 11°20.3'W | 3190 | -- | No recovery |

Table 18 continued

| Meteor No. 1998 | GeoB No. | Date 1998 | Equipment | Time Seafloor (UTC) | Position Latitude | Longitude | Water Depth (m) | Samples/ Sediment recovery (cm) | Remarks |
|---|---|---|---|---|---|---|---|---|---|
| 231 | 5124-1 | 03.05. | CTD/Ro | 01:00 | 24°10.0´S | 09°54.0´W | 4320 | 20x10 l | CTD station, water samples from 4375, 4300, 4200, 4000, 3800, 3500, 3250, 3000, 2600, 2300, 2000, 1500, 1000, 750, 500, 300, 200, 100, 50, 10 dbar ($\delta^{13}C$, $\delta^{18}O$, $PO_4$, CFC) |
| **Angola Basin, Profile 9°W** | | | | | | | | | |
| 232 | 5125-1 | 03.05. | CTD/Ro | 08:20 | 24°10.0´S | 9°00.0´W | 4463 | 21x10 l | CTD station, water samples from 4520, 4300, 4000, 3500, 3000, 2500, 2000, 1500, 1250, 1000, 750, 500, 300, 200, 150, 125, 100, 75, 50, 25, 10 dbar ($\delta^{13}C$, $\delta^{18}O$, $PO_4$, He, $^3H$, CFC) |
| 233 | 5126-1 | 03.05. | CTD/Ro | 20:15 | 22°23.9´S | 9°00.0´W | 4196 | 21x10 l | CTD station, water samples from 4230, 4100, 4000, 3745, 3500, 3252, 3000, 2600, 2300, 2000, 1600, 1300, 1000, 800, 600,400, 300, 200, 100, 50, 10 dbar ($\delta^{13}C$, $\delta^{18}O$, $PO_4$, He, $^3H$, CFC) |
| 234 | 5127-1 | 04.05. | CTD/Ro | 05:04 | 21°11.9´S | 8°59.9´W | 3949 | 21x10 l | CTD station, water samples from 3860, 3800, 3600, 3400, 3200, 3000, 2750, 2500, 2250, 2000, 1600, 1300, 1000, 800, 600, 500, 300, 200, 100, 50, 1 10 dbar($\delta^{13}C$, $\delta^{18}O$, $PO_4$, CFC) |
| 235 | 5128-1 | | CTD/Ro | 14:14 | 19°59.9´S | 9°00.1´W | 3948 | 21x10 l | CTD station, water samples from 3950, 3900, 3700, 3400, 3200, 3000, 2750, 2500, 2250, 2000, 1600, 1300, 1000, 750, 500, 300, 200, 100, 50, 10 dbar ($\delta^{13}C$, $\delta^{18}O$, $PO_4$, He, $^3H$, CFC) |
| **Mid-Atlantic Ridge, Profile 19°S, Angola Basin** | | | | | | | | | |
| 236 | 5129-1 | 04.05. | CTD/Ro | 22:59 | 19°00.0´S | 9°46.2´W | 3841 | 20x10 l | CTD station, water samples from 3857, 3750, 3600, 3400, 3200, 2750, 2500, 2250, 2000, 1600, 1300, 1000, 800, 600, 500, 300, 200, 100, 50, 10 dbar ($\delta^{13}C$, $\delta^{18}O$, $PO_4$, $^3H$, CFC) |
| | 5129-2 | 05.05. | CTD/Ro | 01:03 | 19°00.0´S | 9°46.2´W | 3838 | 18x10 l | Water samples from 250, 230, 200, 170, 150, 120, 3x100, 3x75, 3x50, 3x20, 3x10 depth ($\delta^{13}C$, $\delta^{18}O$,$PO_4$, dinoflagel-lates, coccolithophorids) |
| 237 | 5130-1 | | MUC II | 06:20 | 19°24.2´S | 09°27.5´W | 3166 | 18 | 6 big, 4 small tubes filled, foram-nannofossil ooze, grey-beige |
| | 5130-2 | | SL12 | 08:48 | 19°24.2´S | 09°27.6´W | 3165 | 517 | cc: nannofossil ooze, silty, very pale brown |
| 238 | 5131-1 | | SL12 | 14:02 | 19°02.2´S | 9°44.5´W | 3886 | 216 | Tube bent, cc: foram bearing nannofossil ooze, silty, very pale brown |

Table 18 continued

| Meteor No. 1998 | GeoB No. | Date 1998 | Equipment | Time Seafloor (UTC) | Position Latitude | Position Longitude | Water Depth (m) | Samples/ Sediment recovery (cm) | Remarks |
|---|---|---|---|---|---|---|---|---|---|
| 239 | 5132-1 | 05.05. | SL6 | 16:39 | 19°07.5´S | 09°43.1´W | 3942 | 325 | Core surface leaked, cc: nannofossil ooze, very pale brown |
| | 5132-2 | | MUC II | 18:49 | 19°07.5´S | 09°43.2´W | 3941 | 14 | 6 big, 3 small tubes filled, foram-nannofossil ooze, very pale brown |
| | 5132-3 | | SL6 | 21:07 | 19°07.5´S | 09°43.1´W | 3941 | 326 | cc: nannofossil ooze, very pale brown |
| 240 | 5133-1 | 06.05. | SL6 | 10:02 | 19°05.1´S | 10°11.6´W | 3661 | 503 | cc: nannofossil ooze, clayey, very pale brown |
| | 5133-2 | | MUC I | 12:08 | 19°05.1´S | 10°11.5´W | 3670 | -- | No recovery |
| | 5133-3 | | MUC II | 14:21 | 19°05.2´S | 10°11.5´W | 3660 | 19 | 6 big, 4 small tubes filled, foram-Nannofossil ooze, very pale brown |
| 241 | 5134-1 | | MUC II | 18:50 | 19°02.7´S | 10°41.0´W | 3411 | 19 | 6 big, 4 small tubes filled, foram-nannofossil ooze, very pale brown |
| | 5134-2 | 06.05. | SL6 | 20:51 | 19°02.7´S | 10°41.0´W | 3412 | 242 | cc: foram-nannofossil ooze, silty, very pale brown |
| 242 | 5135-1 | 07.05. | MUC II | 05:21 | 19°26.2´S | 11°03.8´W | 3304 | 20 | 5 big, 4 small tubes filled, foram-nannofossil ooze, very pale brown |
| | 5135-2 | | SL6 | 07:17 | 19°26.1´S | 11°03.8´W | 3303 | 150 | Tube bent, cc: foram-nanno-fossil ooze, very pale brown |
| | 5135-3 | | SL3 | 09:15 | 19°26.0´S | 11°03.8´W | 3303 | 30 | cc: foram-nannofossil ooze, silty, very pale brown |
| **<u>Mid-Atlantic Ridge, Profile 19°S, Brazil Basin</u>** | | | | | | | | | |
| 243 | 5136-1 | 07.05. | SL6 | 18:59 | 19°22.2´S | 12°40.2´W | 3227 | 529 | cc: foram-nannofossil ooze, very pale brown |
| | 5136-2 | | MUC II | 20:52 | 19°22.2´S | 12°40.2´W | 3227 | 20 | 6 big, 4 small tubes filled, foram-nannofossil ooze, very pale brown |
| | 5136-3 | | CTD/Ro | 22:51 | 19°21.9´S | 12°42.7´W | 3227 | 21x10 l | CTD station, water samples from 1500, 1250, 1000, 750, 200, 150, 3x100, 3x75, 3x50 3x20, 3x10 dbar ($\delta^{13}C$, $\delta^{18}O$, $PO_4$) |
| 244 | 5137-1 | 08.05. | MUC II | 04:57 | 19°17.5´S | 13°27.2´W | 3502 | 19 | 5 big, 4 small tubes filled, foram-nannofossil ooze, very pale brown |
| | 5137-2 | | SL12 | 07:00 | 19°17.5´S | 13°27.2´W | 3503 | 248 | Tube bent, cc: foram-nanno-fossil ooze, silty, very pale brown |
| 245 | 5138-1 | | SL6 | 15:12 | 19°11.3´S | 14°39.3´W | 3632 | 181 | cc: foram-nannofossil ooze, silty-sandy, very pale brown |
| | 5138-2 | | MUC II | 17:15 | 19°11.4´S | 14°39.3´W | 3631 | 21 | 6 big, 4 small tubes filled, foram-nannofossil ooze, very pale brown |
| 246 | 5139-1 | 09.05. | MUC II | 01:29 | 19°00.8´S | 15°50.0´W | 3903 | 13 | 5 big, 2 small tubes filled, 2 big tubes partly leaked, foram-nannofossil ooze, very pale brown |
| | 5139-2 | | SL6 | 03:36 | 19°00.8´S | 15°50.0´W | 3903 | 563 | 60 cm sediment recovered from the bomb (mass sample), cc: nannofossil ooze, clayey, very pale brown |

Table 18 continued

| Meteor No. 1998 | GeoB No. | Date 1998 | Equipment | Time Seafloor (UTC) | Position Latitude | Water Longitude | Samples/ Depth (m) | Remarks Sediment recovery (cm) | |
|---|---|---|---|---|---|---|---|---|---|
| 247 | 5140-1 | 09.05. | SL12 | 09:53 | 19°03.2´S | 16°36.8´W | 3660 | 391 | Tube bent, cc: foram-nanno-fossil ooze, silty, very pale brown |
| | 5140-2 | | SL6 | 12:08 | 19°03.1´S | 16°36.9´W | 3659 | 49 | Tube bent, cc: foram-nanno-fossil ooze, silty, very pale brown |
| | 5140-3 | | MUC II | 14:06 | 19°03.1´S | 16°36.8´W | 3660 | 15 | 6 big, 4 small tubes filled, foram-nannofossil ooze, very pale brown |
| 248 | 5141-1 | | CTD/Ro | 18:59 | 19°05.8´S | 17°15.0´W | 3460 | 21x10 l | CTD station, water samples from 1200, 900, 700, 500, 200 150, 3x120, 3x100, 3x50, 3x20, 3x10 dbar ($\delta^{13}C$, $\delta^{18}O$, $PO_4$) |
| 249 | 5142-1 | | SL6 | 21:05 | 19°05.4´S | 17°08.7´W | 3946 | 564 | 30 cm sediment recovered from the bomb and 25 cm sediment recovered from the core catcher, cc: nannofossil ooze, silty, very pale brown |
| | 5142-2 | | MUC II | 23:22 | 19°05.3´S | 17°08.7´W | 3946 | 18 | 5 big, 4 small tubes filled, foram-nannofossil ooze, very pale brown |

| | |
|---|---|
| CTD/Ro | CTD/Rosette water samples, 21 NISKIN bottles with 10 l |
| GKG | Large box corer (Großkastengreifer) |
| MUC I | Multicorer with 8 big and 4 small tubes |
| MUC II | Multicorer with 6 big and 4 small tubes |
| Ro II | Rosette water samples, 18 NISKIN bottles with 10 l |
| SL3/6/9/12 | Gravity corer with 3, 6, 9 and 12 m pipe length, resp. |

## 8.2 Standard CTD Data

Table 19 Distribution of hydrographic parameters on standard pressure levels from all CTD stations taken during cruise M 41/3. Columns represent pressure (p), *in situ* temperature (T), potential temperature (θ) and salinity (S) for each station. Considerations on data accuracies are given in the text (see Chapter 4.1)

**Station 208 Profil 01**
**40° 54.59 W 28° 26.25 S**
**20.04.1998 UTC 16:44 4388 m**

| p dbar | T °C | θ °C | S |
|---|---|---|---|
| 2.0 | 23.911 | 23.911 | 36.554 |
| 10.0 | 23.912 | 23.910 | 36.551 |
| 20.0 | 23.908 | 23.904 | 36.551 |
| 50.0 | 22.920 | 22.910 | 36.393 |
| 75.0 | 19.622 | 19.608 | 36.159 |
| 100.0 | 18.548 | 18.531 | 36.083 |
| 150.0 | 16.836 | 16.811 | 35.830 |
| 200.0 | 15.487 | 15.456 | 35.569 |
| 250.0 | 14.667 | 14.630 | 35.467 |
| 300.0 | 14.590 | 14.545 | 35.534 |
| 350.0 | 13.504 | 13.454 | 35.337 |
| 400.0 | 12.769 | 12.714 | 35.222 |
| 450.0 | 11.689 | 11.631 | 35.051 |
| 500.0 | 10.307 | 10.247 | 34.855 |
| 600.0 | 8.122 | 8.060 | 34.598 |
| 700.0 | 6.434 | 6.370 | 34.426 |
| 800.0 | 5.302 | 5.235 | 34.349 |
| 900.0 | 4.436 | 4.366 | 34.329 |
| 1000.0 | 3.830 | 3.756 | 34.338 |
| 1500.0 | 3.014 | 2.906 | 34.628 |
| 2000.0 | 3.528 | 3.368 | 34.922 |
| 2500.0 | 3.202 | 2.998 | 34.944 |
| 3000.0 | 2.878 | 2.630 | 34.928 |
| 3500.0 | 1.186 | 0.927 | 34.769 |
| 4000.0 | 0.504 | 0.214 | 34.698 |
| 4430.0 | 0.364 | 0.032 | 34.682 |

**Station 210 Profil 02**
**39° 23.86 W 31° 11.84 S**
**21.04.1998 UTC 17:42 4614 m**

| p dbar | T °C | θ °C | S |
|---|---|---|---|
| 4.0 | 21.070 | 21.070 | 35.754 |
| 10.0 | 21.027 | 21.025 | 35.760 |
| 20.0 | 20.983 | 20.979 | 35.767 |
| 50.0 | 20.628 | 20.619 | 36.008 |
| 75.0 | 17.265 | 17.252 | 35.763 |
| 100.0 | 16.030 | 16.014 | 35.669 |
| 150.0 | 15.043 | 15.020 | 35.589 |
| 200.0 | 14.338 | 14.309 | 35.490 |
| 250.0 | 13.936 | 13.900 | 35.427 |
| 300.0 | 13.551 | 13.508 | 35.386 |
| 350.0 | 12.725 | 12.678 | 35.228 |
| 400.0 | 11.484 | 11.433 | 35.024 |
| 450.0 | 10.298 | 10.244 | 34.868 |
| 500.0 | 9.136 | 9.080 | 34.714 |
| 600.0 | 6.501 | 6.452 | 34.397 |
| 700.0 | 5.154 | 5.097 | 34.281 |
| 800.0 | 4.579 | 4.516 | 34.279 |
| 900.0 | 4.005 | 3.938 | 34.281 |
| 1000.0 | 3.701 | 3.628 | 34.325 |
| 1500.0 | 2.859 | 2.753 | 34.626 |
| 2000.0 | 3.240 | 3.084 | 34.886 |
| 2500.0 | 3.112 | 2.910 | 34.936 |
| 3000.0 | 2.751 | 2.506 | 34.922 |
| 3500.0 | 2.140 | 1.856 | 34.869 |
| 4000.0 | 0.950 | 0.646 | 34.727 |
| 4500.0 | 0.207 | -0.128 | 34.675 |
| 4666.0 | 0.220 | -0.133 | 34.673 |

Table 19 continued

**Station 211 Profil 03**
**39° 21.02 W 31° 12.04 S**
**21.04.1998 UTC 21:59 4574 m**

| p dbar | T °C | θ °C | S |
|---|---|---|---|
| 2.0 | 21.183 | 21.183 | 35.768 |
| 10.0 | 21.177 | 21.175 | 35.764 |
| 20.0 | 21.056 | 21.052 | 35.757 |
| 50.0 | 20.703 | 20.694 | 36.009 |
| 75.0 | 17.446 | 17.433 | 35.753 |
| 100.0 | 16.247 | 16.231 | 35.708 |
| 150.0 | 15.126 | 15.103 | 35.597 |
| 200.0 | 14.533 | 14.503 | 35.521 |
| 250.0 | 13.975 | 13.939 | 35.441 |
| 300.0 | 13.476 | 13.433 | 35.370 |
| 350.0 | 12.539 | 12.492 | 35.198 |
| 400.0 | 11.342 | 11.292 | 35.010 |
| 450.0 | 10.324 | 10.270 | 34.867 |
| 500.0 | 9.292 | 9.235 | 34.720 |
| 600.0 | 6.939 | 6.882 | 34.459 |
| 700.0 | 5.461 | 5.402 | 34.314 |
| 800.0 | 4.550 | 4.487 | 34.262 |
| 900.0 | 4.086 | 4.018 | 34.292 |
| 1000.0 | 3.712 | 3.639 | 34.330 |
| 1500.0 | 2.877 | 2.770 | 34.616 |
| 2000.0 | 3.211 | 3.055 | 34.879 |
| 2500.0 | 3.096 | 2.895 | 34.938 |
| 3000.0 | 2.776 | 2.530 | 34.923 |
| 3500.0 | 2.188 | 1.903 | 34.874 |
| 4000.0 | 1.275 | 0.962 | 34.772 |
| 4500.0 | 0.205 | -0.129 | 34.674 |
| 4630.0 | 0.217 | -0.132 | 34.674 |

**Station 212 Profil 04**
**39° 18.90 W 31° 12.02 S**
**22.04.1998 UTC 01:42 4475 m**

| p dbar | T °C | θ °C | S |
|---|---|---|---|
| 2.0 | 21.129 | 21.128 | 35.780 |
| 10.0 | 21.143 | 21.141 | 35.773 |
| 20.0 | 21.069 | 21.066 | 35.762 |
| 50.0 | 20.679 | 20.670 | 35.985 |
| 75.0 | 17.478 | 17.466 | 35.833 |
| 100.0 | 15.957 | 15.941 | 35.673 |
| 150.0 | 15.117 | 15.094 | 35.597 |
| 200.0 | 14.572 | 14.542 | 35.541 |
| 250.0 | 14.141 | 14.105 | 35.476 |
| 300.0 | 13.504 | 13.462 | 35.376 |
| 350.0 | 12.560 | 12.513 | 35.203 |
| 400.0 | 11.507 | 11.455 | 35.039 |
| 450.0 | 10.421 | 10.367 | 34.879 |
| 500.0 | 8.749 | 8.695 | 34.640 |
| 600.0 | 6.665 | 6.609 | 34.408 |
| 700.0 | 5.354 | 5.295 | 34.322 |
| 800.0 | 4.477 | 4.415 | 34.269 |
| 900.0 | 4.118 | 4.050 | 34.298 |
| 1000.0 | 3.673 | 3.600 | 34.322 |
| 1500.0 | 2.877 | 2.771 | 34.613 |
| 2000.0 | 3.165 | 3.010 | 34.862 |
| 2500.0 | 3.098 | 2.896 | 34.936 |
| 3000.0 | 2.777 | 2.531 | 34.919 |
| 3500.0 | 2.223 | 1.938 | 34.873 |
| 4000.0 | 1.378 | 1.062 | 34.781 |
| 4500.0 | 0.198 | -0.137 | 34.672 |
| 4528.0 | 0.201 | -0.136 | 34.674 |

**Station 213 Profil 05**
**39° 16.02 W 31° 12.03 S**
**22.04.1998 UTC 05:56 4066 m**

| p dbar | T °C | Θ °C | S |
|---|---|---|---|
| 2.0 | 21.412 | 21.412 | 35.772 |
| 10.0 | 21.419 | 21.417 | 35.764 |
| 20.0 | 21.233 | 21.229 | 35.754 |
| 50.0 | 20.857 | 20.848 | 35.957 |
| 75.0 | 17.798 | 17.785 | 35.786 |
| 100.0 | 16.425 | 16.409 | 35.754 |
| 150.0 | 15.241 | 15.218 | 35.623 |
| 200.0 | 14.635 | 14.605 | 35.548 |
| 250.0 | 14.030 | 13.993 | 35.437 |
| 300.0 | 13.494 | 13.451 | 35.367 |
| 350.0 | 12.650 | 12.602 | 35.212 |
| 400.0 | 11.802 | 11.750 | 35.083 |
| 450.0 | 10.464 | 10.410 | 34.889 |
| 500.0 | 9.098 | 9.042 | 34.703 |
| 600.0 | 6.836 | 6.779 | 34.449 |
| 700.0 | 5.380 | 5.322 | 34.326 |
| 800.0 | 4.577 | 4.515 | 34.288 |
| 900.0 | 4.169 | 4.101 | 34.316 |
| 1000.0 | 3.643 | 3.571 | 34.330 |
| 1500.0 | 3.109 | 3.000 | 34.664 |
| 2000.0 | 3.176 | 3.021 | 34.870 |
| 2500.0 | 3.093 | 2.892 | 34.934 |
| 3000.0 | 2.786 | 2.540 | 34.924 |
| 3500.0 | 2.288 | 2.001 | 34.882 |
| 4000.0 | 1.378 | 1.062 | 34.786 |
| 4096.0 | 1.247 | 0.925 | 34.771 |

**Station 214 Profil 06**
**33° 54.96 W 26° 53.99 S**
**23.04.1998 UTC 19:16 3798 m**

| p dbar | T °C | Θ °C | S |
|---|---|---|---|
| 2.0 | 23.566 | 23.565 | 36.051 |
| 10.0 | 23.569 | 23.567 | 36.046 |
| 20.0 | 23.565 | 23.560 | 36.040 |
| 50.0 | 22.402 | 22.392 | 36.006 |
| 75.0 | 20.422 | 20.407 | 36.249 |
| 100.0 | 18.757 | 18.739 | 36.061 |
| 150.0 | 16.584 | 16.559 | 35.784 |
| 200.0 | 15.157 | 15.126 | 35.553 |
| 250.0 | 14.602 | 14.564 | 35.556 |
| 300.0 | 14.257 | 14.213 | 35.515 |
| 350.0 | 13.643 | 13.593 | 35.406 |
| 400.0 | 12.363 | 12.310 | 35.172 |
| 450.0 | 11.192 | 11.136 | 34.979 |
| 500.0 | 10.308 | 10.248 | 34.865 |
| 600.0 | 7.704 | 7.643 | 34.560 |
| 700.0 | 6.150 | 6.088 | 34.409 |
| 800.0 | 4.847 | 4.782 | 34.324 |
| 900.0 | 4.099 | 4.031 | 34.325 |
| 1000.0 | 3.601 | 3.529 | 34.364 |
| 1500.0 | 2.872 | 2.765 | 34.687 |
| 2000.0 | 2.834 | 2.684 | 34.852 |
| 2500.0 | 2.903 | 2.705 | 34.927 |
| 3000.0 | 2.673 | 2.430 | 34.922 |
| 3500.0 | 2.262 | 1.976 | 34.886 |
| 3820.0 | 1.605 | 1.302 | 34.815 |

Table 19 continued

**Station 215 Profil 07**
**34° 14.02 W 26° 41.97 S**
**23.04.1998 UTC 23:53 4783 m**

| p | T | θ | S |
|---|---|---|---|
| 2.0 | 23.629 | 23.629 | 36.075 |
| 10.0 | 23.632 | 23.630 | 36.076 |
| 20.0 | 23.633 | 23.628 | 36.075 |
| 50.0 | 22.641 | 22.631 | 36.237 |
| 75.0 | 20.524 | 20.510 | 36.221 |
| 100.0 | 19.303 | 19.285 | 36.155 |
| 150.0 | 17.544 | 17.518 | 35.864 |
| 200.0 | 16.135 | 16.103 | 35.663 |
| 250.0 | 14.920 | 14.882 | 35.490 |
| 300.0 | 14.927 | 14.881 | 35.588 |
| 350.0 | 13.621 | 13.571 | 35.327 |
| 400.0 | 12.716 | 12.661 | 35.199 |
| 450.0 | 11.631 | 11.573 | 35.038 |
| 500.0 | 10.656 | 10.594 | 34.914 |
| 600.0 | 8.254 | 8.191 | 34.615 |
| 700.0 | 6.374 | 6.310 | 34.430 |
| 800.0 | 5.005 | 4.940 | 34.326 |
| 900.0 | 4.210 | 4.141 | 34.329 |
| 1000.0 | 3.601 | 3.529 | 34.359 |
| 1500.0 | 2.910 | 2.803 | 34.685 |
| 2000.0 | 3.277 | 3.120 | 34.929 |
| 2500.0 | 3.002 | 2.802 | 34.939 |
| 3000.0 | 2.755 | 2.509 | 34.927 |
| 3500.0 | 2.362 | 2.073 | 34.892 |
| 4000.0 | 1.351 | 1.036 | 34.785 |
| 4500.0 | 0.505 | 0.161 | 34.694 |
| 4862.0 | 0.278 | -0.098 | 34.676 |

**Station 216 Profil 08**
**34° 56.16 W 26° 17.99 S**
**24.04.1998 UTC 07:06 4341 m**

| p | T | θ | S |
|---|---|---|---|
| 2.0 | 24.313 | 24.312 | 36.004 |
| 10.0 | 24.327 | 24.325 | 36.016 |
| 20.0 | 24.323 | 24.319 | 36.013 |
| 50.0 | 22.340 | 22.330 | 36.384 |
| 75.0 | 20.277 | 20.263 | 36.264 |
| 100.0 | 19.045 | 19.027 | 36.091 |
| 150.0 | 17.066 | 17.041 | 35.784 |
| 200.0 | 16.044 | 16.012 | 35.632 |
| 250.0 | 14.994 | 14.956 | 35.493 |
| 300.0 | 14.322 | 14.277 | 35.428 |
| 350.0 | 13.415 | 13.366 | 35.280 |
| 400.0 | 12.337 | 12.283 | 35.118 |
| 450.0 | 11.551 | 11.493 | 35.013 |
| 500.0 | 10.404 | 10.344 | 34.862 |
| 600.0 | 7.900 | 7.838 | 34.570 |
| 700.0 | 5.961 | 5.899 | 34.387 |
| 800.0 | 4.701 | 4.638 | 34.319 |
| 900.0 | 4.169 | 4.100 | 34.337 |
| 1000.0 | 3.740 | 3.667 | 34.378 |
| 1500.0 | 3.192 | 3.082 | 34.727 |
| 2000.0 | 3.380 | 3.222 | 34.938 |
| 2500.0 | 3.051 | 2.850 | 34.941 |
| 3000.0 | 2.754 | 2.509 | 34.924 |
| 3500.0 | 2.291 | 2.004 | 34.885 |
| 4000.0 | 1.114 | 0.806 | 34.759 |
| 4388.0 | 0.303 | -0.023 | 34.680 |

**Station 217 Profil 09**
**35° 38.89 W 25° 53.88 S**
**24.04.1998 UTC 16:45 4215 m**

| p | T | θ | S |
|---|---|---|---|
| 2.0 | 25.065 | 25.065 | 36.244 |
| 10.0 | 24.988 | 24.986 | 36.273 |
| 20.0 | 24.951 | 24.947 | 36.352 |
| 50.0 | 24.597 | 24.586 | 36.525 |
| 75.0 | 21.502 | 21.487 | 36.470 |
| 100.0 | 20.511 | 20.493 | 36.332 |
| 150.0 | 18.227 | 18.201 | 35.978 |
| 200.0 | 16.792 | 16.759 | 35.747 |
| 250.0 | 15.415 | 15.376 | 35.529 |
| 300.0 | 14.396 | 14.351 | 35.379 |
| 350.0 | 13.369 | 13.320 | 35.269 |
| 400.0 | 12.432 | 12.378 | 35.125 |
| 450.0 | 11.223 | 11.166 | 34.963 |
| 500.0 | 10.217 | 10.157 | 34.834 |
| 600.0 | 8.166 | 8.103 | 34.609 |
| 700.0 | 6.361 | 6.297 | 34.441 |
| 800.0 | 5.083 | 5.017 | 34.364 |
| 900.0 | 4.157 | 4.089 | 34.350 |
| 1000.0 | 3.811 | 3.737 | 34.401 |
| 1500.0 | 3.699 | 3.583 | 34.727 |
| 2000.0 | 3.950 | 3.783 | 34.952 |
| 2500.0 | 2.950 | 2.751 | 34.937 |
| 3000.0 | 2.286 | 2.051 | 34.892 |
| 3500.0 | 1.636 | 1.366 | 34.820 |
| 4000.0 | 0.794 | 0.494 | 34.728 |
| 4240.0 | 0.415 | 0.102 | 34.689 |

**Station 218 Profil 10**
**20° 00.03 W 23° 48.81 S**
**28.04.1998 UTC 10:14 5215 m**

| p | T | θ | S |
|---|---|---|---|
| 4.0 | 25.685 | 25.684 | 36.793 |
| 10.0 | 25.685 | 25.683 | 36.799 |
| 20.0 | 25.696 | 25.691 | 36.806 |
| 50.0 | 25.701 | 25.689 | 36.807 |
| 75.0 | 23.416 | 23.400 | 36.404 |
| 100.0 | 21.480 | 21.461 | 36.303 |
| 150.0 | 18.158 | 18.132 | 35.920 |
| 200.0 | 15.772 | 15.741 | 35.546 |
| 250.0 | 14.493 | 14.456 | 35.349 |
| 300.0 | 13.376 | 13.333 | 35.203 |
| 350.0 | 12.332 | 12.285 | 35.080 |
| 400.0 | 11.110 | 11.060 | 34.937 |
| 450.0 | 10.240 | 10.187 | 34.831 |
| 500.0 | 9.068 | 9.013 | 34.698 |
| 600.0 | 7.181 | 7.123 | 34.519 |
| 700.0 | 5.495 | 5.436 | 34.402 |
| 800.0 | 4.515 | 4.452 | 34.388 |
| 900.0 | 3.965 | 3.898 | 34.410 |
| 1000.0 | 3.628 | 3.555 | 34.470 |
| 1500.0 | 3.129 | 3.019 | 34.758 |
| 2000.0 | 3.138 | 2.984 | 34.916 |
| 2500.0 | 2.929 | 2.730 | 34.934 |
| 3000.0 | 2.700 | 2.455 | 34.920 |
| 3500.0 | 2.305 | 2.017 | 34.883 |
| 4000.0 | 1.634 | 1.310 | 34.811 |
| 4500.0 | 1.227 | 0.860 | 34.767 |
| 5000.0 | 0.927 | 0.512 | 34.734 |
| 5282.0 | 0.893 | 0.445 | 34.726 |

Table 19 continued

**Station 219 Profil 11**
**16° 16.34 W 23° 49.59 S**
**29.4.1998 UTC 10:07 3874 m**

| p | T | θ | S |
|---|---|---|---|
| 2.0 | 25.167 | 25.167 | 36.679 |
| 10.0 | 25.170 | 25.168 | 36.722 |
| 20.0 | 25.175 | 25.170 | 36.734 |
| 50.0 | 25.156 | 25.145 | 36.728 |
| 75.0 | 20.837 | 20.822 | 36.219 |
| 100.0 | 19.614 | 19.596 | 36.169 |
| 150.0 | 18.363 | 18.337 | 35.985 |
| 200.0 | 16.071 | 16.039 | 35.610 |
| 250.0 | 14.656 | 14.619 | 35.375 |
| 300.0 | 13.465 | 13.423 | 35.214 |
| 350.0 | 12.245 | 12.198 | 35.072 |
| 400.0 | 10.778 | 10.729 | 34.899 |
| 450.0 | 9.532 | 9.481 | 34.760 |
| 500.0 | 8.831 | 8.777 | 34.685 |
| 600.0 | 7.020 | 6.962 | 34.519 |
| 700.0 | 5.493 | 5.433 | 34.413 |
| 800.0 | 4.563 | 4.500 | 34.386 |
| 900.0 | 3.938 | 3.871 | 34.414 |
| 1000.0 | 3.527 | 3.455 | 34.459 |
| 1500.0 | 3.240 | 3.129 | 34.806 |
| 2000.0 | 3.217 | 3.061 | 34.938 |
| 2500.0 | 2.888 | 2.690 | 34.930 |
| 3000.0 | 2.604 | 2.362 | 34.907 |
| 3500.0 | 2.231 | 1.945 | 34.867 |
| 3900.0 | 1.937 | 1.616 | 34.838 |

**Station 220 Profil 12**
**15° 00.02 W 23° 40.12 S**
**30.04.1998 UTC 02:58 3853 m**

| p | T | θ | S |
|---|---|---|---|
| 4.0 | 24.989 | 24.988 | 36.728 |
| 10.0 | 24.992 | 24.990 | 36.739 |
| 20.0 | 24.993 | 24.989 | 36.757 |
| 50.0 | 24.989 | 24.978 | 36.756 |
| 75.0 | 21.944 | 21.929 | 36.318 |
| 100.0 | 21.158 | 21.139 | 36.302 |
| 150.0 | 19.166 | 19.139 | 36.128 |
| 200.0 | 17.149 | 17.116 | 35.780 |
| 250.0 | 15.009 | 14.971 | 35.427 |
| 300.0 | 13.424 | 13.382 | 35.205 |
| 350.0 | 12.463 | 12.416 | 35.093 |
| 400.0 | 11.484 | 11.433 | 34.976 |
| 450.0 | 10.188 | 10.135 | 34.830 |
| 500.0 | 8.732 | 8.677 | 34.675 |
| 600.0 | 7.171 | 7.113 | 34.541 |
| 700.0 | 5.778 | 5.717 | 34.420 |
| 800.0 | 4.571 | 4.508 | 34.370 |
| 900.0 | 4.014 | 3.947 | 34.393 |
| 1000.0 | 3.603 | 3.530 | 34.453 |
| 1500.0 | 3.088 | 2.979 | 34.759 |
| 2000.0 | 3.197 | 3.042 | 34.933 |
| 2500.0 | 2.766 | 2.571 | 34.906 |
| 3000.0 | 2.654 | 2.411 | 34.908 |
| 3500.0 | 2.446 | 2.155 | 34.887 |
| 3888.0 | 2.136 | 1.811 | 34.857 |

**Station 221 Profil 13**
**13° 59.86 W 24° 09.95 S**
**30.04.1998 UTC 11:46 3171 m**

| p dbar | T °C | θ °C | S |
|---|---|---|---|
| 4.0 | 24.725 | 24.724 | 36.740 |
| 10.0 | 24.728 | 24.725 | 36.740 |
| 20.0 | 24.730 | 24.726 | 36.739 |
| 50.0 | 24.723 | 24.712 | 36.736 |
| 75.0 | 22.406 | 22.391 | 36.307 |
| 100.0 | 20.866 | 20.847 | 36.233 |
| 150.0 | 19.339 | 19.312 | 36.153 |
| 200.0 | 16.756 | 16.724 | 35.719 |
| 250.0 | 14.673 | 14.636 | 35.377 |
| 300.0 | 13.215 | 13.173 | 35.180 |
| 350.0 | 11.684 | 11.638 | 34.997 |
| 400.0 | 10.849 | 10.800 | 34.899 |
| 450.0 | 9.994 | 9.941 | 34.805 |
| 500.0 | 8.744 | 8.690 | 34.671 |
| 600.0 | 6.995 | 6.938 | 34.506 |
| 700.0 | 5.632 | 5.572 | 34.411 |
| 800.0 | 4.790 | 4.726 | 34.398 |
| 900.0 | 4.191 | 4.122 | 34.424 |
| 1000.0 | 3.877 | 3.803 | 34.471 |
| 1500.0 | 3.178 | 3.067 | 34.741 |
| 2000.0 | 2.864 | 2.713 | 34.871 |
| 2500.0 | 2.739 | 2.544 | 34.897 |
| 3000.0 | 2.616 | 2.374 | 34.891 |
| 3200.0 | 2.608 | 2.345 | 34.892 |

**Station 225 Profil 14**
**13° 23.07 W 24° 10.81 S**
**01.05.1998 UTC 08:17 2741 m**

| p dbar | T °C | θ °C | S |
|---|---|---|---|
| 4.0 | 24.584 | 24.583 | 36.668 |
| 10.0 | 24.594 | 24.592 | 36.668 |
| 20.0 | 24.598 | 24.593 | 36.670 |
| 50.0 | 24.608 | 24.597 | 36.670 |
| 75.0 | 23.072 | 23.057 | 36.485 |
| 100.0 | 20.861 | 20.842 | 36.281 |
| 150.0 | 18.768 | 18.742 | 36.061 |
| 200.0 | 16.094 | 16.062 | 35.611 |
| 250.0 | 14.747 | 14.709 | 35.391 |
| 300.0 | 13.659 | 13.616 | 35.240 |
| 350.0 | 12.359 | 12.312 | 35.082 |
| 400.0 | 11.038 | 10.988 | 34.924 |
| 450.0 | 10.100 | 10.046 | 34.819 |
| 500.0 | 9.021 | 8.966 | 34.687 |
| 600.0 | 7.093 | 7.035 | 34.525 |
| 700.0 | 5.474 | 5.415 | 34.415 |
| 800.0 | 4.709 | 4.646 | 34.411 |
| 900.0 | 4.242 | 4.173 | 34.430 |
| 1000.0 | 3.909 | 3.834 | 34.463 |
| 1500.0 | 3.170 | 3.060 | 34.741 |
| 2000.0 | 2.870 | 2.720 | 34.889 |
| 2500.0 | 2.761 | 2.565 | 34.894 |
| 2774.0 | 2.713 | 2.491 | 34.895 |

Table 19 continued

**Station 226 Profil 15**
**12° 18.11 W 24° 10.08 S**
**01.05.1998 UTC 15:57 3910 m**

| p | T | θ | S |
|---|---|---|---|
| 4.0 | 24.432 | 24.431 | 36.637 |
| 10.0 | 24.432 | 24.430 | 36.637 |
| 20.0 | 24.429 | 24.425 | 36.640 |
| 50.0 | 24.403 | 24.392 | 36.644 |
| 75.0 | 21.050 | 21.036 | 36.194 |
| 100.0 | 19.853 | 19.834 | 36.189 |
| 150.0 | 17.491 | 17.465 | 35.810 |
| 200.0 | 15.543 | 15.512 | 35.511 |
| 250.0 | 14.514 | 14.476 | 35.350 |
| 300.0 | 13.638 | 13.595 | 35.231 |
| 350.0 | 12.554 | 12.507 | 35.099 |
| 400.0 | 11.287 | 11.236 | 34.952 |
| 450.0 | 10.094 | 10.041 | 34.815 |
| 500.0 | 8.905 | 8.851 | 34.688 |
| 600.0 | 7.077 | 7.019 | 34.517 |
| 700.0 | 5.416 | 5.357 | 34.407 |
| 800.0 | 4.728 | 4.665 | 34.403 |
| 900.0 | 4.127 | 4.058 | 34.434 |
| 1000.0 | 3.818 | 3.744 | 34.478 |
| 1500.0 | 3.144 | 3.034 | 34.738 |
| 2000.0 | 2.665 | 2.518 | 34.832 |
| 2500.0 | 2.511 | 2.321 | 34.874 |
| 3000.0 | 2.478 | 2.239 | 34.881 |
| 3500.0 | 2.489 | 2.197 | 34.880 |
| 4000.0 | 2.487 | 2.139 | 34.879 |
| 4006.0 | 2.487 | 2.139 | 34.880 |

**Station 229 Profil 16**
**11° 07.95 W 24° 10.25 S**
**02.05.1998 UTC 10:56 3737 m**

| p | T | θ | S |
|---|---|---|---|
| 2.0 | 24.273 | 24.273 | 36.540 |
| 10.0 | 24.288 | 24.286 | 36.538 |
| 20.0 | 24.293 | 24.288 | 36.537 |
| 50.0 | 24.270 | 24.260 | 36.534 |
| 75.0 | 23.752 | 23.737 | 36.372 |
| 100.0 | 19.784 | 19.766 | 35.925 |
| 150.0 | 16.207 | 16.183 | 35.570 |
| 200.0 | 14.233 | 14.203 | 35.299 |
| 250.0 | 13.320 | 13.285 | 35.183 |
| 300.0 | 12.411 | 12.371 | 35.082 |
| 350.0 | 11.293 | 11.249 | 34.952 |
| 400.0 | 10.116 | 10.068 | 34.813 |
| 450.0 | 9.446 | 9.395 | 34.739 |
| 500.0 | 8.616 | 8.563 | 34.652 |
| 600.0 | 6.754 | 6.698 | 34.483 |
| 700.0 | 5.162 | 5.105 | 34.372 |
| 800.0 | 4.331 | 4.270 | 34.403 |
| 900.0 | 3.893 | 3.826 | 34.437 |
| 1000.0 | 3.604 | 3.531 | 34.475 |
| 1500.0 | 3.168 | 3.058 | 34.758 |
| 2000.0 | 2.661 | 2.514 | 34.838 |
| 2500.0 | 2.511 | 2.321 | 34.874 |
| 3000.0 | 2.434 | 2.195 | 34.880 |
| 3500.0 | 2.400 | 2.110 | 34.880 |
| 3764.0 | 2.410 | 2.091 | 34.881 |

**Station 231 Profil 17**
**09° 53.92 W 24° 09.96 S**
**02.05.1998 UTC 23:35 4322 m**

| p | T | θ | S |
|---|---|---|---|
| 4.0 | 23.874 | 23.873 | 36.566 |
| 10.0 | 23.873 | 23.871 | 36.570 |
| 20.0 | 23.871 | 23.867 | 36.574 |
| 50.0 | 23.876 | 23.865 | 36.573 |
| 75.0 | 22.069 | 22.054 | 36.189 |
| 100.0 | 19.430 | 19.412 | 36.037 |
| 150.0 | 17.559 | 17.534 | 35.791 |
| 200.0 | 15.069 | 15.038 | 35.436 |
| 250.0 | 13.735 | 13.699 | 35.242 |
| 300.0 | 12.954 | 12.913 | 35.145 |
| 350.0 | 11.884 | 11.838 | 35.025 |
| 400.0 | 11.118 | 11.068 | 34.935 |
| 450.0 | 9.964 | 9.912 | 34.801 |
| 500.0 | 8.367 | 8.315 | 34.633 |
| 600.0 | 6.375 | 6.320 | 34.455 |
| 700.0 | 5.312 | 5.254 | 34.391 |
| 800.0 | 4.365 | 4.304 | 34.380 |
| 900.0 | 3.894 | 3.827 | 34.420 |
| 1000.0 | 3.701 | 3.628 | 34.483 |
| 1500.0 | 3.332 | 3.220 | 34.755 |
| 2000.0 | 2.750 | 2.601 | 34.848 |
| 2500.0 | 2.541 | 2.350 | 34.873 |
| 3000.0 | 2.429 | 2.191 | 34.880 |
| 3500.0 | 2.384 | 2.094 | 34.880 |
| 4000.0 | 2.395 | 2.050 | 34.885 |
| 4374.0 | 2.428 | 2.038 | 34.886 |

**Station 232 Profil 18**
**09° 00.19 W 24° 09.91 S**
**03.05.1998 UTC 06:55 4462 m**

| p | T | θ | S |
|---|---|---|---|
| 2.0 | 23.715 | 23.715 | 36.423 |
| 10.0 | 23.726 | 23.724 | 36.424 |
| 20.0 | 23.735 | 23.731 | 36.427 |
| 50.0 | 23.662 | 23.652 | 36.425 |
| 75.0 | 20.946 | 20.932 | 35.978 |
| 100.0 | 19.052 | 19.034 | 35.929 |
| 150.0 | 17.125 | 17.100 | 35.733 |
| 200.0 | 15.455 | 15.424 | 35.488 |
| 250.0 | 14.211 | 14.174 | 35.309 |
| 300.0 | 12.922 | 12.881 | 35.138 |
| 350.0 | 11.959 | 11.913 | 35.031 |
| 400.0 | 10.862 | 10.813 | 34.902 |
| 450.0 | 9.573 | 9.522 | 34.758 |
| 500.0 | 8.912 | 8.857 | 34.676 |
| 600.0 | 7.260 | 7.201 | 34.544 |
| 700.0 | 5.364 | 5.306 | 34.392 |
| 800.0 | 4.445 | 4.383 | 34.373 |
| 900.0 | 4.127 | 4.058 | 34.427 |
| 1000.0 | 3.786 | 3.712 | 34.474 |
| 1500.0 | 3.470 | 3.356 | 34.765 |
| 2000.0 | 2.737 | 2.589 | 34.835 |
| 2500.0 | 2.510 | 2.319 | 34.873 |
| 3000.0 | 2.399 | 2.161 | 34.878 |
| 3500.0 | 2.361 | 2.072 | 34.884 |
| 4000.0 | 2.393 | 2.047 | 34.887 |
| 4500.0 | 2.438 | 2.033 | 34.887 |
| 4522.0 | 2.441 | 2.033 | 34.887 |

Table 19 continued

**Station 233 Profil 19**
**08° 59.96 W 22° 23.96 S**
**03.05.1998 UTC 19:00 4192 m**

| p | T | θ | S |
|---|---|---|---|
| 2.0 | 24.105 | 24.105 | 36.497 |
| 10.0 | 24.031 | 24.029 | 36.552 |
| 20.0 | 24.018 | 24.013 | 36.580 |
| 50.0 | 24.002 | 23.992 | 36.612 |
| 75.0 | 23.018 | 23.003 | 36.397 |
| 100.0 | 20.287 | 20.268 | 36.003 |
| 150.0 | 17.878 | 17.853 | 35.818 |
| 200.0 | 15.852 | 15.820 | 35.536 |
| 250.0 | 14.185 | 14.148 | 35.302 |
| 300.0 | 12.934 | 12.893 | 35.140 |
| 350.0 | 11.835 | 11.790 | 35.018 |
| 400.0 | 10.389 | 10.341 | 34.830 |
| 450.0 | 9.211 | 9.161 | 34.721 |
| 500.0 | 8.096 | 8.044 | 34.603 |
| 600.0 | 6.102 | 6.048 | 34.446 |
| 700.0 | 4.872 | 4.816 | 34.395 |
| 800.0 | 4.184 | 4.124 | 34.414 |
| 900.0 | 3.867 | 3.801 | 34.450 |
| 1000.0 | 3.646 | 3.573 | 34.512 |
| 1500.0 | 3.473 | 3.359 | 34.810 |
| 2000.0 | 3.058 | 2.905 | 34.890 |
| 2500.0 | 2.589 | 2.397 | 34.878 |
| 3000.0 | 2.441 | 2.203 | 34.878 |
| 3500.0 | 2.364 | 2.075 | 34.883 |
| 4000.0 | 2.382 | 2.037 | 34.888 |
| 4236.0 | 2.401 | 2.028 | 34.889 |

**Station 234 Profil 20**
**09° 00.15 W 21° 12.10 S**
**04.05.1998 UTC 03:51 3941 m**

| p | T | θ | S |
|---|---|---|---|
| 4.0 | 24.325 | 24.324 | 36.693 |
| 10.0 | 24.328 | 24.326 | 36.693 |
| 20.0 | 24.333 | 24.328 | 36.693 |
| 50.0 | 24.336 | 24.326 | 36.691 |
| 75.0 | 21.873 | 21.858 | 36.273 |
| 100.0 | 20.422 | 20.403 | 36.141 |
| 150.0 | 17.202 | 17.177 | 35.765 |
| 200.0 | 15.492 | 15.461 | 35.504 |
| 250.0 | 14.056 | 14.020 | 35.286 |
| 300.0 | 13.295 | 13.253 | 35.187 |
| 350.0 | 11.710 | 11.665 | 34.996 |
| 400.0 | 10.229 | 10.182 | 34.829 |
| 450.0 | 9.126 | 9.076 | 34.716 |
| 500.0 | 8.037 | 7.986 | 34.611 |
| 600.0 | 6.378 | 6.323 | 34.501 |
| 700.0 | 5.088 | 5.030 | 34.424 |
| 800.0 | 4.329 | 4.268 | 34.434 |
| 900.0 | 3.947 | 3.880 | 34.468 |
| 1000.0 | 3.736 | 3.663 | 34.519 |
| 1500.0 | 3.439 | 3.326 | 34.816 |
| 2000.0 | 3.036 | 2.883 | 34.898 |
| 2500.0 | 2.654 | 2.461 | 34.894 |
| 3000.0 | 2.441 | 2.203 | 34.882 |
| 3500.0 | 2.368 | 2.079 | 34.881 |
| 3876.0 | 2.381 | 2.050 | 34.882 |

**Station 235 Profil 21**
**09° 00.09 W 20° 00.03 S**
**04.05.1998 UTC 13:03 3959 m**

| p | T | Θ | S |
|---|---|---|---|
| 2.0 | 23.967 | 23.967 | 36.466 |
| 10.0 | 23.943 | 23.941 | 36.461 |
| 20.0 | 23.890 | 23.886 | 36.459 |
| 50.0 | 23.846 | 23.836 | 36.455 |
| 75.0 | 21.581 | 21.566 | 36.252 |
| 100.0 | 20.324 | 20.305 | 36.206 |
| 150.0 | 18.076 | 18.050 | 35.881 |
| 200.0 | 15.206 | 15.176 | 35.431 |
| 250.0 | 13.364 | 13.329 | 35.196 |
| 300.0 | 11.904 | 11.865 | 35.028 |
| 350.0 | 10.750 | 10.707 | 34.906 |
| 400.0 | 9.552 | 9.506 | 34.775 |
| 450.0 | 8.259 | 8.212 | 34.644 |
| 500.0 | 7.205 | 7.157 | 34.552 |
| 600.0 | 5.883 | 5.830 | 34.486 |
| 700.0 | 5.030 | 4.973 | 34.450 |
| 800.0 | 4.329 | 4.268 | 34.458 |
| 900.0 | 4.001 | 3.934 | 34.494 |
| 1000.0 | 3.840 | 3.765 | 34.541 |
| 1500.0 | 3.642 | 3.527 | 34.824 |
| 2000.0 | 3.092 | 2.938 | 34.903 |
| 2500.0 | 2.643 | 2.450 | 34.891 |
| 3000.0 | 2.454 | 2.216 | 34.884 |
| 3500.0 | 2.388 | 2.099 | 34.883 |
| 3962.0 | 2.396 | 2.055 | 34.889 |

**Station 236 Profil 22**
**09° 46.23 W 18° 59.98 S**
**04.05.1998 UTC 21:48 3838 m**

| p | T | Θ | S |
|---|---|---|---|
| 4.0 | 24.448 | 24.448 | 36.733 |
| 10.0 | 24.452 | 24.450 | 36.732 |
| 20.0 | 24.458 | 24.454 | 36.733 |
| 50.0 | 24.412 | 24.401 | 36.720 |
| 75.0 | 21.409 | 21.394 | 36.228 |
| 100.0 | 19.608 | 19.590 | 36.066 |
| 150.0 | 17.286 | 17.261 | 35.756 |
| 200.0 | 14.320 | 14.291 | 35.323 |
| 250.0 | 12.773 | 12.739 | 35.124 |
| 300.0 | 11.544 | 11.506 | 34.986 |
| 350.0 | 10.058 | 10.017 | 34.821 |
| 400.0 | 9.351 | 9.306 | 34.753 |
| 450.0 | 8.538 | 8.490 | 34.676 |
| 500.0 | 7.379 | 7.330 | 34.567 |
| 600.0 | 5.785 | 5.734 | 34.484 |
| 700.0 | 4.723 | 4.668 | 34.452 |
| 800.0 | 4.236 | 4.175 | 34.464 |
| 900.0 | 3.936 | 3.869 | 34.499 |
| 1000.0 | 3.824 | 3.750 | 34.567 |
| 1500.0 | 3.668 | 3.551 | 34.836 |
| 2000.0 | 3.172 | 3.017 | 34.904 |
| 2500.0 | 2.706 | 2.512 | 34.896 |
| 3000.0 | 2.466 | 2.227 | 34.886 |
| 3500.0 | 2.404 | 2.114 | 34.883 |
| 3856.0 | 2.428 | 2.098 | 34.884 |

Table 19 continued

**Station 236 Profil 23**
**09° 46.20 W 18° 59.98 S**
**05.05.1998 UTC 00:57 3840 m**

| p | T | θ | S |
|---|---|---|---|
| 2.0 | 24.431 | 24.430 | 36.740 |
| 10.0 | 24.447 | 24.445 | 36.738 |
| 20.0 | 24.434 | 24.430 | 36.738 |
| 50.0 | 24.434 | 24.423 | 36.735 |
| 75.0 | 22.587 | 22.572 | 36.388 |
| 100.0 | 19.317 | 19.299 | 36.047 |
| 150.0 | 17.077 | 17.052 | 35.730 |
| 200.0 | 14.577 | 14.547 | 35.365 |
| 248.0 | 13.174 | 13.140 | 35.178 |

**Station 243 Profil 24**
**12° 42.67 W 19° 22.00 S**
**07.05.1998 UTC 22:22 4536 m**

| p | T | θ | S |
|---|---|---|---|
| 4.0 | 24.677 | 24.676 | 36.697 |
| 10.0 | 24.673 | 24.671 | 36.715 |
| 20.0 | 24.674 | 24.670 | 36.730 |
| 50.0 | 24.630 | 24.619 | 36.739 |
| 75.0 | 22.372 | 22.357 | 36.394 |
| 100.0 | 20.598 | 20.579 | 36.252 |
| 150.0 | 18.568 | 18.542 | 36.046 |
| 200.0 | 16.025 | 15.993 | 35.612 |
| 250.0 | 14.194 | 14.158 | 35.316 |
| 300.0 | 12.601 | 12.560 | 35.108 |
| 350.0 | 11.131 | 11.087 | 34.959 |
| 400.0 | 9.763 | 9.717 | 34.798 |
| 450.0 | 8.568 | 8.520 | 34.671 |
| 500.0 | 7.347 | 7.298 | 34.567 |
| 600.0 | 5.764 | 5.712 | 34.472 |
| 700.0 | 4.829 | 4.773 | 34.446 |
| 800.0 | 4.267 | 4.206 | 34.457 |
| 900.0 | 3.825 | 3.759 | 34.500 |
| 1000.0 | 3.700 | 3.626 | 34.548 |
| 1498.0 | 3.482 | 3.368 | 34.849 |

**Station 248 Profil 25**
**17° 15.12 W 19° 05.75 S**
**09.05.1998 UTC 18:30 3453 m**

| p | T | θ | S |
|---|---|---|---|
| 2.0 | 25.829 | 25.829 | 36.947 |
| 10.0 | 25.567 | 25.564 | 36.971 |
| 20.0 | 25.541 | 25.536 | 36.993 |
| 50.0 | 25.523 | 25.512 | 37.005 |
| 75.0 | 23.108 | 23.093 | 36.537 |
| 100.0 | 21.152 | 21.132 | 36.413 |
| 150.0 | 19.127 | 19.100 | 36.152 |
| 200.0 | 16.246 | 16.214 | 35.637 |
| 250.0 | 14.339 | 14.302 | 35.352 |
| 300.0 | 12.869 | 12.828 | 35.167 |
| 350.0 | 11.445 | 11.401 | 35.000 |
| 400.0 | 10.030 | 9.983 | 34.841 |
| 450.0 | 8.928 | 8.879 | 34.728 |
| 500.0 | 7.941 | 7.890 | 34.636 |
| 600.0 | 6.127 | 6.073 | 34.497 |
| 700.0 | 4.823 | 4.767 | 34.431 |
| 800.0 | 4.213 | 4.153 | 34.437 |
| 900.0 | 3.847 | 3.781 | 34.467 |
| 1000.0 | 3.713 | 3.640 | 34.508 |
| 1500.0 | 3.651 | 3.535 | 34.847 |